UNIVERSITA' VITA-SALUTE SAN RAFFAELE

CORSO DI DOTTORATO DI RICERCA INTERNAZIONALE IN MEDICINA MOLECOLARE

CURRICULUM IN NEUROSCIENZE E NEUROLOGIA SPERIMENTALE

MAPPING STRUCTURAL AND FUNCTIONAL MRI CORRELATES OF CLINICAL DISABILITY AND COGNITIVE IMPAIRMENT IN PEDIATRIC MS

DoS: Prof.ssa Maria Assunta Rocca

Second Supervisor: Prof.ssa Eluen Ann Yeh

Tesi di DOTTORATO di RICERCA di:

Ermelinda De Meo matr. 013876

Ciclo di dottorato: XXIV

SSDs: MED 26/ MED 37/ MED 39

Anno Accademico 2020/2021

UNIVERSITA' VITA-SALUTE SAN RAFFAELE

CORSO DI DOTTORATO DI RICERCA INTERNAZIONALE IN MEDICINA MOLECOLARE

CURRICULUM IN NEUROSCIENZE E NEUROLOGIA SPERIMENTALE

MAPPING STRUCTURAL AND FUNCTIONAL MRI CORRELATES OF CLINICAL DISABILITY AND COGNITIVE IMPAIRMENT IN PEDIATRIC MS

DoS: Prof.ssa Maria Assunta Rocca

Second Supervisor: Prof.ssa Eluen Ann-Yeh

Tesi di DOTTORATO di RICERCA di:

Ermelinda De Meo matr. 013876

Ciclo di dottorato: XXIV

SSDs: MED 26/ MED 37/ MED 39

Anno Accademico 2020/2021

THESIS CONSULTATION AUTHORISATION

I	Ermelinda De Meo
Registration number	013876
born at	Naples
on	29th April 1989

Author of the PhD Thesis titled "ADVANCES IN PEDIATRIC MULTIPLE SCLEROSIS FROM CLINICAL AND MRI PERSPECTIVES"

DOES NOT AUTHORIZE *the public release of the thesis for* 12 *months from the PhD thesis date, specifically*

From 27/11/2021 *to* 27/11/2022

because:

Parts of the thesis have been or are being submitted to a publisher or are in press.

Copyright the contents of the thesis in whole or in part is forbidden

Date 27.11.2021 Firma /Signature

DECLARATION

This thesis has been composed by myself and has not been used in any previous application for a degree. Throughout the text I use both ‘I’ and ‘We’ interchangeably.

All the results presented here were obtained by myself.

All sources of information are acknowledged by means of reference.

ACKNOWLEDGEMENTS

I would like to thank Prof. Filippi, who gave me the possibility to complete this PhD course, thus improving my researcher attitude.

Then, I would like to thank Prof. Amato, who gave me the opportunity to realize different projects.

Finally, I have to thank my DoS Prof. Rocca, who has guided me during my time at the Neuroimaging Research Unit.

My greatest acknowledgment is for Raffi who supported me during this PhD course more than anyone else.

ACRONYMS AND ABBREVIATIONS

AAL	automated anatomical labelling
ACC	anterior cingulate cortex
AD	axial diffusivity
ADC	apparent diffusion coefficient
ADEM	acute disseminated encephalomyelitis
ADS	acquired demyelinating syndromes
ARR	annualized relapse rate
AQP4	anti-aquaporin 4 antibodies
BAEP	brainstem auditory evoked potential
BDNF	brain derived neurotrophic factor
BOLD	blood-oxygenation level dependent
BRB	Rao's Brief Repeatable Battery
CA	cornus ammonis
CADSIL	cerebral autosomal dominant arteriopathy with subcortical infarcts and leukoencephalopathy
CCPT	Conners Continuous Performance Test
CI	cognitively impaired
CIS	clinically isolated syndrome
CLs	cortical lesions
CLTR	Consistent Long-Term Retrieval
CMV	Cytomegalovirus
CNS	central nervous system
CP	cognitively preserved
CSF	cerebrospinal fluid
CSTs	corticospinal tracts
D	delayed recall
DARTEL	Diffeomorphic Anatomical Registration using Exponentiated Lie algebra
DG	dentate gyrus
DE	dual-echo
DIR	double inversion recovery
DIS	dissemination in space
DIT	dissemination in time
DMF	dimethyl fumarate
DMN	default mode network
DMT	disease modifying therapies
DTI	Diffusion Tensor Imaging

EBV	Epstein-Barr virus
EDSS	Expanded Disability Status Scale
EEG	electroencephalography
EMA	European Medicines Agency
EP	evoked potentials
EPI	echo-planar imaging
FA	fractional anisotropy
FC	functional connectivity
FDA	Food and Drug Admninstration
FFE	fast field echo
FLAIR	fluid attenuation inversion recovery
fMRI	functional MRI
FSS	Fatigue Severity Scale
FWE	family-wise error
GA	Glatiramer Acetate
GCIPL	ganglion cell and inner plexiform layer
GCL	granule cell layer
GM	grey matter
HATA	Hippocampus-amygdala transitional area
HC	healthy controls
HLA	human leukocyte antigen
^{1}H-MRS	Proton magnetic resonance spectroscopy
HR	hazard ratio
HSR	Hospital San Raffaele
HSV	herpes simplex virus
IFG	inferior frontal gyrus
IFN-β	interferon-β
IPL	inferior parietal lobule
IPMSSG	International Pediatric Multiple Sclerosis Study Group
IPS	information processing speed
IQ	intelligence quotient
ISI	interstimulus intervals
ITG	inferior temporal gyrus
IVIG	intravenous immunoglobulin
JCV	John Cunningham virus
KSADS	Schedule for Affective Disorders and Schizophrenia for School- Age Children-Present and Lifetime Version
L	Left

LETM	longitudinally extensive transverse myelitis
LMEM	linear mixed-effects model
LPA	latent profile analysis
LTP	long-term potentiation
LTS	Long-Term Storage
LV	lesion volumes
MADRS	Montgomery-Asberg Depression Scale
MAG	myelin-associated glycoprotein
MD	mean diffusivity
MDEM	multiphasic disseminated encephalomyelitis
MBP	myelin basic protein
MFG	middle frontal gyrus
MFS	magnetic field strength
MOG	myelin oligodendrocyte glycoprotein
MRI	magnetic resonance imaging
MS	multiple sclerosis
MTG	middle temporal gyrus
MTR	magnetization transfer ratio
NAA	N-acetylaspartate
NAWM	normal appearing white matter
NBV	normalized brain volume
NcGMV	normalized cortical gray matter volume
NEDA	no evidence of disease activity
NGMV	normalized gray matter volume
NMO	neuromyelitis optica
NMOSD	NMO spectrum disorder
NWMV	normalized white matter volume
OCBs	oligoclonal bands
OCT	optical coherence tomography
ON	optic neuritis
OR	odds ratio
PASAT	Paced Auditory Serial Addition Test
PML	progressive multifocal leukoencephalitis
PoCG	postcentral gyrus
PP	primary progressive
RCTs	randomized controlled trials
RD	radial diffusivity
RIS	radiologically isolated syndrome
RNFL	retinal nerve fiber layer

ROI	regions of interest
R	Right
RR	relapsing-remitting
RS	resting-state
RT	reaction times
SCWT	Stroop Color and Word Test
SDMT	Symbol Digit Modalities Test
SEP	sensitive evoked potential
SFG	superior frontal gyrus
SLE	Systemic Lupus Erythematosus
SMA	supplementary motor area
sNfL	serum neurofilament level
SNPs	single nucleotide polymorphisms
SP	secondary progressive
SPART	Spatial Recall Test
SRT	Selective Reminding Test
STG	superior temporal gyrus
STIR	short tau inversion recovery
TBM	tensor-based morphometry
TBSS	tract-based spatial statistics
TM	transverse myelitis
TMT	Trail Making Test
TSE	turbo spin-echo
VBM	voxel-based morphometry
VEP	visual evoked responses
WISC-R	Wechsler Intelligence Scale for children
WLG	Word List Generation
WM	white matter
95% CI	95% confidence interval

LIST OF FIGURES AND TABLES

	Figures
Figure 3.1.1	**fMRI patterns of activation and deactivation during CCPT in HC and pediatric MS patients.** Brain regions showing linearly increasing functional magnetic resonance imaging (fMRI) activations (A, B) and deactivations (C, D) with increasing Conner's Continuous Performance Test (CCPT) difficulty in healthy controls (HC) (A, C) and pediatric patients with multiple sclerosis (MS) (B, D) (one-sample t-tests, $p < 0.001$ uncorrected). Areas showing increased activation with increasing CCPT load in pediatric MS patients versus healthy controls are shown in E, while brain areas showing reduced activation are shown in F. Images are displayed with the neurological convention (De Meo *et al*, 2017).
Figure 3.1.2	**fMRI patterns of activation and deactivation during CCPT in CP and CI pediatric MS patients.** Brain regions showing significantly different fMRI activations and deactivations with increasing Conner's Continuous Performance Test (CCPT) difficulty in cognitively preserved (CP) and cognitively impaired (CI) patients with multiple sclerosis (MS). Results are shown at $p < 0.001$, uncorrected. Images are displayed with the neurological convention (De Meo *et al.*, 2017).
Figure e-3.1.1	**Box plots of correct responses in pediatric MS patients.** Correct responses at Conner's Continuous Performance Test (CCPT) were reported as percentages. The light gray box plot represents cognitively preserved (CP) pediatric multiple sclerosis (MS) patients' percentage of correct responses; the dark gray box plot represents the percentage of correct responses in cognitively impaired (CI) pediatric MS patients (De Meo *et al.*, 2017).
Figure 3.2.1	**Gray matter developmental trajectories estimation and assessment of deviations from them in pediatric multiple sclerosis patients.** (A.1) Left thalamus gray matter (GM) developmental trajectories are represented as estimated in the whole group of HC (means are represented by solid lines and 95% confidence interval by dashed lines). The model was estimated, for illustrative purpose, from average relative GM volumes (representing the amount of GM relative to the voxel size) within the left thalamus mask from Automatic Anatomical Labelling (AAL) atlas (Tzourio-Mazoyer et al., 2002). Spaghetti

	lines for each participant's measurements over time are also shown. (A.2) Graphical representation for the pediatric multiple sclerosis (MS) patients of deviations from the sex- and age-specific GM developmental trajectories. One male and one female MS patient whose longitudinal scans were available, were taken as examples to show their deviation from the expected values (vertical solid arrows) as assessed at baseline and at follow-up. From magnetic-field-strength-adjusted measurements obtained for each MS patient at each time point, z-scores were computed by subtracting and dividing by the normative sex- and age-specific estimated mean (solid line) and standard deviation (SD) respectively. Mean ± 1 SD reference lines are also represented (dotted lines) for comparison. (B) GM volume deviations from the expected values in pediatric MS patients (represented in terms of mean z-scores) at baseline (one sample t-test, $p<0.05$ FWE corrected). Brain regions experiencing significantly greater loss of GM are highlighted on the blue-light blue scale. (C) Longitudinal changes (expressed as mean estimated z-score changes) in GM volume deviations from the expected values in pediatric MS patients (one-sample t-test, adjusted for follow-up duration, baseline EDSS and disease duration, $p<0.001$ uncorrected). Brain regions experiencing GM damage progression are highlighted using the blue/light blue scale, while those experiencing reduced deviation from the expected values are highlighted using the red/yellow scale. Images are presented in neurological convention (De Meo *et al*, 2019).
Figure 3.2.2	**Gray matter growth rate in the whole group of healthy controls.** Relative gray matter (GM) volume change per year in healthy controls at each age decile, shown separately for males and females. Brain regions showing a significant increase of relative GM volume per year are red-yellow, while brain regions showing a significant negative GM volume change per year are represented in blue-light blue (linear mixed-effects model, $p<0.001$ uncorrected). Images are presented in radiological convention (De Meo *et al.*, 2019).
Figure 3.3.1	**Thalamic segmentation according to geodesic distance from CSF.** An example of thalamic segmentation obtained in a healthy subject is provided for a sagittal, coronal and axial slice, respectively (first row). A 3D representation of the same thalamic segmentation is also provided (second row). The red-

	yellow scale shows the different thalamic bands according to the geodesic distance from the CSF (De Meo *et al*, 2020b).
Figure 3.3.2	**Quantitative MRI metrics in the whole thalamus and thalamic white matter according to the distance from CSF.** (A) Fractional anisotropy (FA), (B) mean diffusivity (MD) and (C) T1/T2 ratio values in thalamic concentric bands obtained as a function of their geodesic distance from CSF are expressed as mean (solid lines) ± standard deviation (shaded area). (D) FA, (E) MD and (F) T1/T2 ratio values in thalamic white matter concentric bands obtained as a function of their geodesic distance from CSF are expressed as mean (solid lines) ± standard deviation (shaded area). Pediatric multiple sclerosis patients are represented in red and healthy controls in blue. Multivariate analysis adjusted for age, sex and thalamic volume was performed to compare thalamic quantitative MRI measures within each concentric band originating from CSF/thalamus-interface. For all analyses, statistically significant threshold was set at p-value <0.05, corrected for multiple comparisons (Bonferroni correction was applied). An asterisk (*) individuates the thalamic bands where metrics are significantly different between pediatric multiple sclerosis patients and healthy controls (De Meo *et al.*, 2020b).
Figure 3.3.3	**T2 hyperintense thalamic lesion volume distribution within the thalamus.** Boxplots show hyperintense focal thalamic lesions volume normalized for thalamic volume [ml] for each thalamic concentric band originating from the CSF/thalamus-interface. Each boxplot includes: the minimum (represented by the lowest data point excluding the outliers), the maximum (represented by the largest data point excluding the outliers), the sample median (the solid line within the box), and the first (the lower extremity of the box) and third quartiles (the upper extremity of the box). Outliers are represented as single dot (De Meo *et al.*, 2020b).
Figure 3.3.4	**Mechanisms of thalamic damage at CSF/thalamus interface and thalamus/WM interface in pediatric patients with multiple sclerosis.** (A) Mechanisms underlying thalamic damage at CSF/thalamus interface are represented as well as significant changes in quantitative MRI metrics observed at CSF/thalamus interface. In the picture, at the bottom is shown cortical thinning in pediatric multiple sclerosis patients that was associated with abnormalities in quantitative thalamic MRI metrics observed at CSF/thalamus interface (highlighted in

	blue). (B) Mechanisms of thalamic damage occurring at thalamus/WM interface are represented in green. In the MRI image at the top, WM lesions detected in a pediatric MS patient, which were associated with abnormalities of quantitative MRI metrics at thalamus/WM interface, are green filled for exemplificative purpose. At the bottom, pathological changes likely to underlay the MRI abnormalities detected are graphically represented (De Meo *et al.*, 2020b).
Figure 4.1.1	**Lesion distribution.** The pictures are representative of the seven brain regions considered in the study. Lesions located in the following compartments (highlighted by white circles and arrows) could be detected on FLAIR MRI sequences: (A) optic nerve; (B) periventricular region (one lesion); (C) periventricular region (three or more); (D) cortical/juxtacortical region; (E) cerebellum; (F) deep gray matter; (G) brainstem; (H) cervical cord (De Meo *et al*, 2021a).
Figure 4.1.2	**EDSS score at longest follow-up in pediatric multiple sclerosis patients.** Pediatric multiple sclerosis patients not worsened at last follow-up are represented in histograms with gray filling, while those worsened at follow-up are represented in histograms with black filling (De Meo *et al.*, 2021a).
Figure 4.1.3	**Risk of a first relapse in pediatric multiple sclerosis patients with and without optic nerve lesions.** (A) Survival curves of time from disease onset to first relapse in pediatric multiple sclerosis patients with and without optic nerve lesions. Pediatric multiple sclerosis patients with optic nerve lesions are represented in black while patients without optic nerve lesions are represented light gray. (B) Survival curves of time from disease onset to first relapse in pediatric multiple sclerosis patients on moderate and high efficacy disease modifying treatments (DMT). Pediatric multiple sclerosis patients on moderate efficacy DMT are represented in light gray, while patients on high efficacy DMT are represented in black (De Meo *et al.*, 2021a).
Figure 4.2.1	**Study flow-chart.** The diagram illustrates patients' selection to obtain the final dataset.
Figure 4.2.2	**Kaplan–Meier estimates of the time to reach disability milestones from birth or disease onset in early vs late onset pediatric MS patients.** Panels on the left represent Kaplan-Meier estimates of time to reach disability milestones (EDSS 3 in A, EDSS 4 in C and EDSS 6 in E) measured from birth. Panels on the right represent Kaplan- Meier estimates of time to reach

	disability milestones (EDSS 3 in B, EDSS 4 in D and EDSS 6 in F) measured from MS onset.
Figure 7.1.1	**Clinical and demographic features of clinical phenotypes.** Boxplots of age (A), disease duration (B), EDSS (C), age of onset (D), education (E), Montgomery-Asberg Depression Scale (F) and Fatigue Severity Scale scores are represented for each phenotype. In each graph, we reported statistically significant between-groups comparisons (black horizontal lines) and their significance level according to the following code: ***=p<.001; **=p<.01, *=p<.05. In (H) histograms show the relative frequencies as percentage of cognitive phenotype within clinical phenotypes from left to right: early relapsing-remitting multiple sclerosis (RRMS), RRMS, secondary progressive multiple sclerosis and primary progressive multiple sclerosis. "Preserved cognition" is represented in cyan blue, "mild- verbal memory/ semantic fluency" in purple, "mild-multi-domain" in green, "severe-attention/executive" in yellow and "severe-multi-domain" in red (De Meo *et al*, 2021c).
Figure 7.1.2	**MRI features of cognitive phenotypes.** Brain structures showing differences between each phenotype and healthy controls are yellow-colored, while those showing differences between each phenotype and both healthy controls and "preserved cognition" patients are red-colored (De Meo *et al.*, 2021c).
Figure e-7.1.1	**Latent Profile Analysis results.** The figure represents the cognitive performance of each phenotype: points indicate mean z-scores obtained at each neuropsychological test and error bars reflect the 95% confidence interval. "Preserved cognition" phenotype is represented in cyan blue, "mild-verbal memory/semantic fluency" in purple, "mild-multi-domain" in green, "severe-attention/executive" in yellow and "severe-multi-domain" in red (De Meo *et al.*, 2021c).
Figure 7.2.1	**Graphical representation of hippocampal subfields segmentation.** Axial, coronal and sagittal views of hippocampal subfields obtained in a healthy subject enrolled in the study. Hippocampal subfields are overlaid on the corresponding T1-weighted image by using FreeView visualization tool (https://surfer.nmr.mgh.harvard.edu/fswiki/FreeviewGuide/) (De Meo *et al*, 2021d).
	Tables
Table 3.1.1	Main demographic, clinical and structural MRI characteristics and Conner's Continuous Performance Test (CCPT)

	performance of healthy controls and pediatric patients with multiple sclerosis (MS), as a whole and according to the presence/absence of cognitive impairment.
Table 3.1.2	Neuropsychological tests from patients with pediatric MS.
Table 3.1.3	Brain regions showing significant correlations between fMRI activations/deactivations during the Conner's Continuous Performance Test (CCPT) load condition with clinical, neuropsychological and structural MRI variables in pediatric multiple sclerosis patients (multiple regression models adjusted for age and sex; $p < 0.001$ uncorrected).
Table e-3.1.1	Mean fractional anisotropy (FA) values of the tracts connecting brain regions identified by fMRI analysis as key regions involved in Conner's Continuous Performance test (CCPT) performance.
Table e-3.1.2	Brain regions significantly activated/deactivated during the Conner's Continuous Performance test (CCPT) load condition in pediatric healthy controls (HC) and pediatric patients with multiple sclerosis (MS) (one sample t-test, adjusted for age and sex, $p < 0.001$ uncorrected), and between group comparisons (two sample t-test, adjusted for age and sex, $p < 0.001$).
Table e-3.1.3	Brain regions significantly activated/deactivated during the CCPT load condition in cognitively preserved (CP) and cognitively impaired (CI) pediatric patients with multiple sclerosis (MS) (one-sample t-test, adjusted for age and sex, $p < 0.001$ uncorrected).
Table e-3.1.4	Brain regions showing significant differences of fMRI activations/deactivations during the CCPT load condition between cognitively preserved (CP), cognitively impaired (CI) pediatric multiple sclerosis (MS) patients and pediatric healthy controls (full factorial model adjusted for age and sex, $p < 0.001$ uncorrected).
Table 3.2.1	Main demographic, clinical and lesional MRI characteristics of pediatric multiple sclerosis (MS) patients and healthy controls enrolled at Hospital San Raffaele (HSR HC) and healthy controls from NIH-funded MRI Study of Normal Brain Development (NIH HC).
Table 3.2.2	Brain regions showing significant negative deviations from the sex- and age- expected gray matter volume developmental trajectories (z-scores<0) in pediatric multiple sclerosis patients ($p < 0.05$ FWE corrected for multiple comparisons).

Table 3.2.3	Brain regions showing significant correlations between z-scores (deviations from the sex- and age-expected gray matter volume trajectories) with clinical and lesional MRI variables in pediatric multiple sclerosis patients at baseline (multiple regression models. p<0.001 uncorrected).
Table 3.2.4	Brain regions showing significant increased and decreased z-scores (deviations from the sex- and age-expected gray matter volume developmental trajectories) during the follow-up in pediatric multiple sclerosis patients (p<0.001 uncorrected).
Table 3.2.5	Brain regions showing significant correlations between gray matter volume changes over time with baseline premorbid Intelligence Quotient (full scale and sub-scales) and T2 and T1 lesions volume changes in pediatric multiple sclerosis patients (multiple regression model adjusted for disease duration, follow-up duration and baseline Expanded Disability Status Scale score (p<0.001 uncorrected).
Table 3.3.1	Main demographic, clinical and conventional MRI characteristics of healthy controls and pediatric patients with multiple sclerosis.
Table 3.3.2	Analysis of correlation between thalamic quantitative MRI measures abnormalities and clinical, lesional and cortical thickness measures (multiple regression model adjusted for age, sex and thalamic volume (p<0.001).
Table 3.3.3	Summary of thalamic abnormalities in pediatric multiple sclerosis patients and their pathological correlates according to the tissue compartment explored.
Table 4.1.1	Main baseline clinical and MRI features of the study cohort grouped by clinical status at 9 years follow-up.
Table 4.1.2	Main clinical and brain MRI changes over the follow-up period grouped by clinical status at 9 years.
Table 4.1.3	Multivariable linear regression models investigating early clinical and MRI predictors of annualized relapse rate (ARR) in pediatric multiple sclerosis patients.
Table 4.1.4	Multivariable logistic regression models investigating early clinical and MRI predictors of EDSS worsening after 9 years.
Table 4.1.5	Multivariable linear regression models investigating early clinical and MRI predictors of EDSS score at 9 years.
Table e-4.1.1	Main clinical and MRI features of the study cohort grouped by exposure to moderate vs high efficacy disease modifying treatments.

Table 4.2.1	Main clinical and demographic features of the study cohort grouped by age at the disease onset.
Table 4.2.2	Cox models of time to EDSS 3, 4, and 6, and conversion to secondary progressive MS from birth or MS onset, comparing early vs late onset pediatric MS patients (the latter as reference group).
Table 4.2.3	Cox models of time to EDSS 3, 4, and 6, and conversion to secondary progressive MS from birth or MS onset, comparing early vs late onset pediatric MS patients (the latter as reference group).
Table 4.2.4	Multivariable Cox regression models of prognostic factors of time from disease onset to reach disability milestones (EDSS 3, 4 and 6) in early and late onset pediatric multiple sclerosis patients.
Table e-4.2.1	Cox models of time to EDSS 3, 4, and 6, and to conversion to secondary progressive MS from birth or MS onset, comparing early vs late onset pediatric MS patients (the latter as reference group).
Table e-4.2.2	Univariate Cox models of time from MS onset to EDSS 3, 4, and 6 early and late onset pediatric multiple sclerosis patients.
Table e-4.2.3	Multivariable Cox regression models of prognostic factors of time from disease onset to reach disability milestones (EDSS 3, 4 and 6) in early and late onset pediatric multiple sclerosis patients.
Table 7.1.1	Main demographic and clinical characteristics of healthy controls and patients with multiple sclerosis enrolled in the study.
Table 7.1.2	Mean z-scores and standard deviations (SD) of cognitive tests defining each cognitive phenotype.
Table 7.1.3	Estimated marginal means and standard error (SE) of MRI features of cognitive phenotypes from linear mixed effect models. P values were adjusted for multiple comparisons (Bonferroni method).
Table e-7.1.1	Fit indices of latent profile analysis models with 1 – 6 profiles.
Table e-7.1.2	Main clinical and demographic features of cognitive phenotypes.
Table 7.2.1	Main clinical, demographic and conventional MRI features of healthy controls and multiple sclerosis patients.
Table 7.2.2	Neuropsychological variables, reported as z-scores, in the whole group of multiple sclerosis (MS) patients and in MS patients grouped according to the presence of brain derived neurotrophic factor (BDNF) Val66Met polymorphism.

Table 7.2.3	Mean and standard deviations of left and right hippocampal subfield volumes are reported for multiple sclerosis (MS) patients and healthy controls as well as for MS patients grouped according to the presence of BDNF Val66Met polymorphism.
Table 7.2.4	Results of age-, sex-, phenotype- and disease duration-adjusted linear regression models for the effect of hippocampal subfields on neuropsychological variables.

Abstract

During this PhD research course, different advanced MRI techniques were applied in pediatric multiple sclerosis (MS) patients to characterize the neuroanatomical substrates of cognitive impairment, to explore the complex interplay between gray matter (GM) maturational processes and disease-related damage and to unravel *in vivo* potential pathogenetic mechanisms.

In details, inefficient regulation of the functional interaction between different areas of sustained attention system due to abnormal white matter (WM) integrity was identified as a potential substrate of cognitive impairment in pediatric MS patients.

In a longitudinal setting, we observed that pediatric MS patients experienced failures in GM development in several cortical and sub-cortical regions, as well as GM atrophy progression in most of these regions. These abnormalities were only partially related to focal MS lesions, thus suggesting the existence of early neurodegenerative processes independent from WM lesions. Furthermore, higher IQ, a proxy of cognitive reserve in pediatric patients, resulted as a protective factor against GM damage, being associated with reduced deviations from age-expected volumes of specific GM regions at baseline and during the follow-up.

Focusing on the thalamus, we observed a trend toward thalamic atrophy and we detected significant microstructural abnormalities as assessed by using different quantitative MRI measure (fractional anisotropy, mean diffusivity and T1/T2-weighted ratio). Segmenting the thalamus and thalamic WM into concentric bands originating from CSF/thalamus interface, we observed significant microstructural abnormalities in bands nearest to CSF and in those closest to WM. Moreover, the abnormalities detected at CSF/thalamus interface correlated with cortical thickness reduction, while those at thalamus/WM interface with WM lesion volume. These findings support the hypothesis of heterogeneous pathological processes, including retrograde degeneration from WM lesions and CSF-mediated damage, leading to thalamic microstructural abnormalities, likely preceding macroscopic tissue loss.

In a longitudinal setting, we identified several predictors of disease course and prognosis in pediatric MS patients. Shorter time to first relapse was predicted by optic nerve lesions, while longer time was predicted by high-efficacy treatment exposure.

Lesion location at baseline MRI scan together with disease activity during the first 2 years of disease significantly accounted for annualized relapse rate over 9-year of follow-up. The involvement of clinically eloquent sites (such as the optic nerve, brainstem, and spinal cord) at baseline, together with disability and MRI activity during the first 2 year of disease were found as significant predictors of 9-year disability.

Finally, analyzing data from the Italian MS Register, we showed that compared to post-pubertal, pre-pubertal onset pediatric MS patients took longer time from disease onset to convert to secondary progressive phenotype and to reach irreversible Expanded Disability Status Scale scores of 3, 4, and 6. These findings highlight a different natural history of pre- *vs* post-pubertal onset pediatric MS, pointing towards the existence of specific pathophysiological mechanisms, combined with a greater capacity of recovery to counteract damage, in younger pediatric MS patients.

Table of contents

ABSTRACT ---------- **17**

1. INTRODUCTION ---------- **2**

1.1 GENERAL CONSIDERATIONS 2
1.2 EPIDEMIOLOGY 3
1.3 GENETIC AND ENVIRONMENTAL RISK FACTORS 4
1.3.2 Low Vitamin D levels. *4*
1.3.3 Obesity *5*
1.3.4 Infections *5*
1.3.5 Gut microbiota *5*
1.3.6 Smoking *5*
1.4 IMMUNOPATHOPHYSIOLOGY IN PEDIATRIC MS 6
1.5 PATHOLOGY OF PEDIATRIC MS 7
1.6 CLINICAL MANIFESTATIONS 7
1.7 NATURAL HISTORY AND LONG TERM PROGNOSIS 9
1.8 COGNITIVE IMPAIRMENT 10
1.9 FATIGUE AND MOOD DISORDERS 11
1.10 DIAGNOSIS 13
1.10.1 Diagnostic procedures *13*
1.10.2 MRI. *13*
1.10.3 Evoked potentials *14*
1.10.4 Optical Coherence Tomography (OCT) *14*
1.10.5 Cerebrospinal fluid examination *16*
1.10.6 Autoantibodies *16*
1.10.7 Diagnostic criteria *16*
1.10.8 Differential diagnosis *18*
1.11 TREATMENT APPROACHES 21
1.12 THERAPIES FOR ACUTE EXACERBATIONS 21
1.12.1 Methylprednisolone *21*
1.12.2 Intravenous immunoglobulin (IVIG) *21*
1.12.3 Plasmapheresis (plasma exchange) *21*
1.13 DISEASE-MODIFYING THERAPIES 21
1.14 INJECTABLE THERAPIES 22
1.15 ORAL THERAPIES 23
1.15.1 Dimethyl fumarate (DMF) *23*
1.15.2 Fingolimod *23*
1.15.3 Teriflunomide *24*
1.15.4 Cladribin *24*

1.16 INFUSION THERAPHIES 24
1.16.1 Natalizumab *24*
1.16.2 Cyclophosphamide *25*
1.16.3 Rituximab *25*
1.16.4 Ocrelizumab *26*
1.16.5 Alemtuzumab *26*
1.17 SUPPORTIVE STRATEGIES 26
1.17.1 Vitamin D supplementation *26*
1.17.2 Symptomatic Treatment *26*
1.17.3 Counseling and support *27*
1.18 NEUROIMAGING FEATURES OF PEDIATRIC MS 28
1.19 GENERAL CONSIDERATIONS 28
1.20 WHITE MATTER LESIONS 28
1.20.1 Lesion appearance on conventional MRI sequences *28*
1.20.2 Lesion distribution and burden *29*
1.20.3 Myelin repair capability *30*
1.21 NORMAL APPEARING WHITE MATTER DAMAGE 31
1.21.1 ^{1}H-MR spectroscopy (^{1}H-MRS) *31*
1.21.2 Magnetization Transfer MRI (MT MRI) *32*
1.21.3 Diffusion Tensor Imaging (DTI) *32*
1.22 GRAY MATTER LESIONS 33
1.23 GRAY MATTER DAMAGE 34
1.24 ATROPHY AND FAILURE OF AGE-EXPECTED BRAIN GROWTH 34
1.25 FUNCTIONAL MRI 36
1.26 CORRELATION WITH PHYSICAL DISABILITY 37
1.27 CORRELATION WITH COGNITIVE IMPAIRMENT 39

2. AIMS OF THE WORK ---------- 43

3. CHARACTERIZATION OF PEDIATRIC MS BY USING ADVANCED MRI TECHNIQUE IN CROSS-SECTIONAL AND LONGITUDINAL SETTING ---------- 45

3.1 MRI SUBSTRATES OF SUSTAINED ATTENTION SYSTEM AND COGNITIVE IMPAIRMENT IN PEDIATRIC MS PATIENTS 45
3.2 DYNAMIC GRAY MATTER VOLUME CHANGES IN PEDIATRIC MULTIPLE SCLEROSIS: A 3.5 YEAR MRI STUDY 74
3.3 IN VIVO GRADIENTS OF THALAMIC DAMAGE IN PEDIATRIC MULTIPLE SCLEROSIS: A WINDOW INTO PATHOLOGY 102

4. ASSESSMENT OF CLINICAL AND MRI PREDICTORS OF LONG-TERM DISEASE COURSE IN PEDIATRIC MS ---------- 122

4.1 EARLY PREDICTORS OF 9-YEAR DISABILITY IN PEDIATRIC MULTIPLE SCLEROSIS 122
4.2 COMPARING NATURAL HISTORY OF PRE- AND POST-PUBERTAL ONSET MULTIPLE SCLEROSIS . 145

5. DISCUSSION ---------- 170

5.1 CHARACTERIZATION OF PEDIATRIC MS BY USING ADVANCED MRI TECHNIQUES IN CROSS-SECTIONAL AND LONGITUDINAL SETTING 170
5.2 ASSESSMENT OF CLINICAL AND MRI PREDICTORS OF LONG-TERM DISEASE COURSE IN PEDIATRIC MS 175

6. CONCLUSIONS AND FUTURE DIRECTIONS ---------- 178

7. OTHER STUDIES ---------- 180

7.1 IDENTIFYING THE DISTINCT COGNITIVE PHENOTYPES IN MULTIPLE SCLEROSIS 180
7.2 EFFECT OF BDNF VAL66MET POLYMORPHISM ON HIPPOCAMPAL SUBFIELDS IN MULTIPLE SCLEROSIS PATIENTS 207

8. REFERENCES ---------- 229

1. Introduction

1.1 General considerations

Multiple sclerosis (MS) is a chronic immune-mediated disease of the central nervous system (CNS) resulting in inflammation, demyelination and neurodegeneration. It represents one of the leading causes of disability in young adults. In about 2-5% of cases, MS presents with a first demyelinating event before age 18 years old, namely during childhood or adolescence (i.e., pediatric MS) (Boiko *et al*, 2002; Renoux *et al*, 2007).

MS always needs to be distinguished from other acquired demyelinating syndromes (ADS), especially in pediatric patients. The overall incidence of ADS in children and adolescents is estimated to be about 0.87 per 100'000 persons per year (Yan *et al*, 2020). Approximately 20% of children with ADS are diagnosed with MS (Fadda *et al*, 2018c). The clinical of the ADS varies across studies (Absoud *et al*, 2011; Banwell *et al*, 2011; Ketelslegers *et al*, 2012; Reinhardt *et al*, 2014): 22–36% of patients manifest an optic neuritis (ON), 19–24% acute disseminated encephalomyelitis (ADEM), 3–22% transverse myelitis (TM), 9–16% another monofocal ADS; and 2–4% neuromyelitis optica (NMO). Different parameters, including age at ADS onset, sex, clinical presentation, CSF profile, MRI features and environmental and genetic risk factors, contribute to the likelihood that an incident demyelinating attack represents the first episode of MS.

Pediatric MS initially follows a relapsing-remitting (RR) disease course in about 98% of cases, while primary progressive (PP) MS is rare (Waldman *et al*, 2014). Compared to adult, pediatric MS is characterized by more active inflammation (clinical relapses and MRI activity), but also better damage repair (complete recovery and MRI lesion volume reduction or even disappearance) (Banwell *et al*, 2016; Waldman *et al*, 2016). MS patients with onset during childhood or adolescence take longer time to reach irreversible disability and the secondary progressive (SP) stage compared to adult-onset ones (Harding *et al*, 2013; Renoux *et al.*, 2007). Nonetheless, due to the early onset, pediatric patients with MS become disabled at an earlier age compared to their adult counterparts (Waldman *et al.*, 2016). In addition, pediatric MS has a great impact on brain integrity, as evidenced by MRI metrics that quantify disruption of tissue microstructure. Finally, pediatric MS affects age-expected brain volume (Banwell *et al.*, 2016), cognitive

function and maturation (Amato *et al*, 2016), mood and behavior (Amato *et al.*, 2016; Krysko & O'Connor, 2016), and parental quality of life and family functioning (O'Mahony *et al*, 2018).

In this perspective, with an increase in diagnostic awareness of pediatric MS, the paradigm of early treatment has recently emerged as a consensus standard of care in order to prevent long-term sequelae, also leading to expand the therapeutic opportunity in this specific population as demonstrated by the increasing number of clinical trials in pediatric patients carried on in the last decade.

Finally, by virtue of their young age, children with MS have a limited time between the biologic onset of disease and clinical presentation, yielding the opportunity to study disease-related mechanisms operative at disease onset. The following chapters will discuss the current understanding of epidemiology, clinical presentation, diagnosis and differential diagnosis, therapeutic options and MRI features in pediatric MS.

1.2 Epidemiology

Epidemiological estimates of pediatric MS may vary depending on the geographical location (Wallin *et al*, 2019). A positive correlation between MS prevalence and distance from the Equator both in Southern and Northern hemispheres has been observed (Wallin *et al.*, 2019), suggesting that both geography and socioeconomic factors may contribute to the incidence and prevalence of pediatric MS. A recent metanalysis reported pooled global incidence and prevalence estimates as 0.87 per 100’000 individuals annually and 8.11 per 100’000 individuals, respectively (Yan *et al.*, 2020). Overall incidence rates ranged from 0.05 (95% confidence interval 0.03-0.08) per 100000 children (Tunisia) to 2.85 (95% confidence interval 2.83-2.86) per 100000 children (Sardinia). Overall prevalence rates ranged from 0.69 (95% confidence interval 0.58-0.80) per 100000 children (Japan) to 26.92 (95% confidence interval 26.61-27.23) per 100000 children (Sardinia) (Jeong *et al*, 2019).

In addition to latitude, different factors influence incidence and prevalence of MS in pediatric populations including: ancestry, sex and age (Yeh *et al*, 2009a). The proportion of Caucasian ethnicity in pediatric MS patients is lower than what is expected in an adult MS cohort (Boiko *et al.*, 2002; Chitnis *et al*, 2009; Kennedy *et al*, 2006). The female:male ratio of pediatric MS patients varies by age: form 0.8:1 below the age of 6

years, it increases to 1.6:1 between the ages of 6 and 10 years, and to 2.1:1 for children over the age of 10 years. Instead, the female:male ratio of adult MS patients is about 3:1 (Banwell *et al*, 2007a). Incidence of pediatric MS increases with age, most notably after age 12 years (only <1% of all MS cases present before age 12) (Waldman *et al.*, 2016). These sex- and age-related effects might be due to influences of sex hormones starting from puberty (Chitnis *et al.*, 2009), as well as to evolution in the myelination state of various areas of the CNS.

1.3 Genetic and environmental risk factors

Risk factors for MS include genetic haplotypes, specific single nucleotide polymorphisms, vitamin D insufficiency, smoking (including second-hand exposure), obesity (especially during childhood), and viral exposures (Otallah & Banwell, 2018).

1.3.1 Genetic risk factors. Human leukocyte antigen *(HLA)-DRB1**15:01 has been identified as a genetic risk factor for MS in children and adults (Waldman *et al.*, 2014). Furthermore, specific non-HLA single nucleotide polymorphisms (SNPs) were recently found to be associated with higher risk of developing MS in children, with synergistic roles if they occur in combination (Gianfrancesco *et al*, 2017). Furthermore, certain risk alleles, such as AHI1 and BDNF, may be associated with relapse rates, recovery from relapses and disability accumulation in children and adults with MS (Graves *et al*, 2017).

Epigenetic abnormalities, which alter gene transcription and cell function, are increasingly recognized to play a role in MS onset. They represent forms of gene-environment interactions. Among the many studies on the topic, we cite the increasingly recognized role of micro-RNA (miRNAs) in modulating MS risk, through an influence on the expression of genes involved in immune signalling and other cellular functions (Rhead *et al*, 2019).

1.3.2 Low Vitamin D levels. Similarly to adult MS patients (Rhead *et al*, 2016), low vitamin D levels are associated with an increased risk of developing pediatric MS (Jacobs *et al*, 2020). A causal and independent association of low levels of vitamin D and increased body mass index with the risk of pediatric MS was observed in a recent meta-analysis after adjusting for sex, ancestry, *HLA-DRB1**15:01, and over 100 non-HLA MS risk variants (Gianfrancesco *et al.*, 2017). Vitamin D levels have also been demonstrated

to affect disease course, with higher levels associated with lower risk of relapses (Mowry *et al*, 2010).

1.3.3 Obesity. Childhood obesity, especially before the age of 10 years old, is an independent risk factor for MS (Hedstrom *et al*, 2012; Jacobs *et al.*, 2020). Even if the precise biological explanation is still being investigated, several mechanisms have been proposed (Huitema & Schenk, 2018). Levels of leptin and other adipokines are known to modulate peripheral immune function (Guillemot-Legris & Muccioli, 2017; Keyhanian *et al*, 2019), and they may also influence CNS-resident microglia activation state in pediatric MS patients (Nyirenda *et al*, 2021). Obesity produces low-grade increased systemic inflammation, likely favoring autoimmune responses (Cook *et al*, 2000; Valle *et al*, 2005). Finally, obesity is associated with lower vitamin D levels, possibly due to decreased bioavailability (influencing response to vitamin D supplementation) and body surface-to-volume ratio (influencing vitamin D production from sun exposure) (Hypponen *et al*, 2001).

1.3.4 Infections. The role of viral infections acquired during childhood in determining MS has been widely explored, although only Epstein-Barr virus (EBV) infection has been consistently associated with increased risk for pediatric and adult-onset MS (Waubant *et al*, 2011; Waubant *et al*, 2016).

1.3.5 Gut microbiota. Alterations of gut microbiota are increasingly implicated in the etiopathogenesis of MS. In pediatric patients, higher abundance of Actinobacteria has been observed compared to healthy children, similar to other inflammatory conditions (Tremlett *et al*, 2016). In pediatric MS patients, depletion of Fusobacteria correlated with higher risk of relapses (Tremlett & Waubant, 2018a, b). Furthermore, not only individual gut microbial species, but also networks of interactions among them showed a significant association with decreased or increased hazard of clinical and MRI activity (Horton *et al*, 2021).

1.3.6 Smoking. Smoking and second hand smoke represent risk factors for pediatric MS (Mikaeloff *et al*, 2007). In a recent study, including 81 pediatric MS and 216 mono-ADS patients, the association of second hand smoke with the presence of HLA-DRB1*15:01 resulted as a risk factor for MS (Lavery *et al*, 2019).

1.4 Immunopathophysiology in pediatric MS

The peripheral activation of $CD4^+$ T cells in response to some stimulating antigen is likely to represent an early process in the immunopathophysiology of MS (Bar-Or, 2008). Indeed, activated T cells show an increased capability to interact with and transmigrate across the brain blood barrier, thus leading to CNS perivascular inflammatory damage (Bar-Or, 2008). This condition cause the exposition of additional CNS antigen, resulting in the so-called "epitope spreading," thus propagating a chronic immune response (Bar-Or, 2008; Chitnis, 2007). To date, the initial antigenic targets in MS are unknown. The only potential target identified for this early injury in pediatric MS is represented by the axoglial apparatus (Dhaunchak *et al*, 2012).

Several abnormalities in phenotype and function of both effector (Teff) and regulatory (Treg) T cells have recently been observed in pediatric MS patients (Mexhitaj *et al*, 2019). Furthermore, early immune senescence has been hypothesized in pediatric MS patients, as children with MS compared to their healthy counterpart showed an increased proportion of memory cells and fewer recent thymic emigrants (Balint *et al*, 2013). Indeed, in response to myelin peptides, pediatric MS patients compared to adults with MS and healthy children experienced a higher frequency of proliferating memory $CD4^+$ T cells and higher levels of interleukin-17 secretion, supporting the role of these T cells in disease-related pathogenetic mechanisms (Vargas-Lowy *et al*, 2013).

During the last decades, considering the new drugs available in adult MS patients targeting the CD20 surface molecule (rituximab, ocrelizumab, ofatumumab), the role of B cells in determining MS pathology has been widely explored. Compared to adult-onset, pediatric-onset MS patients showed a different B-cell patterns in CSF during an acute relapse (Balint *et al.*, 2013). In details, in pediatric MS patients a higher frequency of non-switched memory B cells and plasmablasts were found, while both pediatric and adult MS patients showed an expanded circulating $CD27^-IgD^+$ naive subset and a concomitantly contracted $CD27^+$ memory B-cell pool (Balint *et al.*, 2013). These results, indicative of age-independent variations in B-cell phenotype, confirmed the existence of an altered naive-to-memory cell ratio also in B cell compartment.

Finally, in pediatric MS, elevated plasmablasts in the periphery were observed, similarly to what occurs in prototypic autoantibody-driven autoimmune disorders, emphasizing a role for B cells in MS immune pathophysiology (Schwarz *et al*, 2017).

1.5 Pathology of pediatric MS

Some insight into the pathology of early disease stages is derived from studies of biopsy tissue from early RRMS cases. Demyelination of both white matter (WM) and gray matter (GM) is the pathologic hallmark of MS (Bar-Or *et al*, 2016). Multiple pathological mechanisms including the effect of cytotoxic cytokines, reactive oxygen or nitrogen species, the activation of macrophages, microglia and complement components or demyelinating antibodies are involved in MS-related demyelination (Bar-Or *et al.*, 2016). In other cases, signs of oligodendrocyte dystrophy were observed, reflected by impaired expression of certain myelin proteins, such as myelin-associated glycoprotein (MAG) or dystrophic changes in most distal oligodendrocyte processes (Lucchinetti *et al*, 2000). These different pathological features suggest a pathogenetic heterogeneity of demyelination in different MS lesions. In this scenario, heterogeneity of MS lesions also involves remyelination particularly evident in early disease stages and in the cortex compared to the WM.

A recent systematic analysis of pediatric MS WM lesions (Pfeifenbring *et al*, 2015) showed that compared to adults, pediatric MS patients experienced a 50% higher degree of acute damage to axons, with a negative correlation with patients' age at the time of either biopsy or autopsy. In this same study (Pfeifenbring *et al.*, 2015), prepubertal MS patients had the highest degree of damage to axons and of macrophage/microglia numbers in MS lesions, highlighting a clear age dependency for inflammation and innate immune reaction.

Considering the difficulty in obtaining pathological data, serum neurofilament level (sNfL) has recently emerged as a biomarker of neuro-axonal damage in MS. Although highest sNfL was observed in children presenting with ADEM, high sNfL were associated with a shorter time to clinically-definite MS diagnosis in ADS patients without ADEM (Wong *et al*, 2019).

1.6 Clinical manifestations

Optic neuritis (ON), acute transverse myelitis (TM), monofocal or polyfocal neurologic deficits extrinsic to the optic nerves or spinal cord, or ADEM are usually the first clinical manifestation of pediatric MS. Children often present with polyfocal

symptoms, whereas monofocal presentations are more common in adolescents and adults (Yeh *et al.*, 2009a). A polyfocal presentation of MS, characterized by neurologic symptoms referable to the involvement of multiple areas within the CNS, occurs in 50% to 70% of children (Mikaeloff *et al*, 2004c), whereas 30% to 50% of them present with monofocal symptoms (Banwell *et al*, 2007b). Approximately 10% to 23% of children with MS present with ON (Ghezzi *et al*, 2002; Verhey *et al*, 2013), and bilateral ON is associated with an increased MS risk compared with unilateral ON (Wilejto *et al*, 2006). Acute isolated TM occurs as a first attack of MS in only 2% to 14% children (Mikaeloff *et al.*, 2004c; Verhey *et al*, 2011), more frequently, acute TM represents a monophasic illness, or when co-occurring with ON, may represent the heralding features of NMO. Monofocal presentations of motor dysfunction occur in 30% of children with MS with different symptoms (Waldman *et al.*, 2016).

Another study has been conducted with the aim to recognize the typical presentation of MS in pre-pubertal patients (Huppke *et al*, 2014). Compared with post-pubertal, pre-pubertal children presented more commonly with a polysymptomatic onset (49% *vs*. 37%, $p = 0.24$) and a preponderance of motor (44.7% *vs*. 26.8%) and brainstem (42.5% *vs*. 26.8%) symptoms (comprising diplopia and facial weakness). Sensory symptoms (46.3% *vs*. 25.5%) and optic nerve lesions (31.7% *vs*. 14.9%) predominated in the post-pubertal group. Statistical significance was achieved for sensory symptoms ($p = 0.04$) and near significance for motor ($p = 0.08$) and optic lesions ($p = 0.06$). An encephalitic manifestation (12.8% *vs*. 2.5%, $p = 0.08$) and a severe first attack (26.8% *vs*. 10.5%, $p = 0.06$) were notably more common in the younger child with near significance for both. Seizures (6.4%) and sphincter dysfunction (6.4%) at onset were only seen in the pre-pubertal group.

Over the first 2 years of disease, the initial symptom pattern at onset was reinforced, reaching significance for all variables except cerebellar involvement. Motor (68.1% *vs*. 46.3%, $p = 0.039$), brainstem (59.6% *vs*. 39%, $p = 0.054$), sphincter (17% *vs*. 2.4%, $p = 0.024$) and cognitive disturbances (25.5% *vs*. 7.3%, $p = 0.023$) afflicted significantly more pre-pubertal patients while sensory (40.4% *vs*. 73.2%, $p = 0.002$) and optic nerve lesions (25.5% *vs*. 46.3%, $p = 0.04$) more post-pubertal patients. Cognitive impairment was documented for a quarter of pre-pubertal patients: 66% experienced

concentration problems, 42% a decline in school performance and 42% behavioral changes and mood swings (Huppke *et al.*, 2014).

1.7 Natural history and long term prognosis

More than 98% of children and adolescents diagnosed with MS follows a RR course (Waldman *et al.*, 2014), while primary progressive MS is extremely rare in children (less than 2%) (Renoux *et al.*, 2007). Children who have a progressive course from onset of a MS-like illness should undergo extensive assessment for alternative diagnoses, such as mitochondrial, neoplastic, and neurodegenerative disorders.

An MS relapse is characterized by neurologic symptoms that persist for at least 24 hours, separated from a previous attack by a minimum of 28 days (Poser *et al*, 1983). A complete recovery after the first demyelinating episode is reported in most of children (Duquette *et al*, 1987), who remain clinically stable between subsequent MS relapses. Annualized relapse rate (ARR), estimated between 0.38 and 0.87 (Ghezzi *et al.*, 2002; Simone *et al*, 2002), is higher in children compared with adults (Gorman *et al*, 2009). However, children recover significantly better from relapses than adults (Chitnis *et al*, 2020). Moreover recovery from relapses seems to be more rapid in children than in adult patients with MS (mean time of relapse-related symptoms: 4.3 weeks in pediatric MS *vs*. 6–8 weeks in adult MS) (Ruggieri *et al*, 2004).

High variability in the proportion of pediatric-onset MS patients reaching the secondary progressive (SP) phase has been observed because of differences in follow-up duration (Renoux *et al.*, 2007; Simone, 2002).

Although the rate of disability progression varies from individual to individual regardless of the age at onset, a consistent finding in most pediatric MS retrospective studies is lower disability scores compared with adult patients with MS while controlling for disease duration (McKay *et al*, 2019; Renoux *et al.*, 2007). Despite a slower development of irreversible disability in pediatric MS patients, the age when these patients are confronted with disease progression and neurologic deficits is 10 years younger than for the population with adult-onset MS, a time when one is expected to have a family and enter the workforce (Chitnis *et al*, 2011; McKay *et al.*, 2019; Renoux *et al.*, 2007).

1.8 Cognitive impairment

The onset of disease during the stage of acquisition of higher cognitive functions expose pediatric patients to a unique vulnerability to cognitive impairment (Amato *et al.*, 2016). The neuropsychosocial issues of pediatric MS encompass a variety of problems, including feelings of self-consciousness, worries related to the future, problems with family and friends, mood disorders, and cognitive impairment. Children experience a variety of academic difficulties secondary to school absences, severe fatigue, and cognitive complications (Amato *et al.*, 2016).

Across different test batteries and definitions of cognitive impairment, cognitive impairment is consistently reported in approximately one-third of patients with pediatric MS (Amato *et al.*, 2016). In a US cohort the complex attention (29.7%), poor naming (18.9%), receptive language problems (13.5%), immediate recall of visual information (8.1%), and delayed recall of visual (11%) and verbal (18.9%) information were found as the most common affected cognitive domains. In an Italian multicenter study (Amato *et al*, 2008) the most frequently affected cognitive domains were verbal ability (39%–53%), visuospatial memory (18%–56%), complex attention (28%–50%), and executive functions (41%).

Considering the impact of cognitive deficits during childhood and adolescence and moreover their consequences in the adulthood, it appears interesting to analyze the long-term outcome of cognitive functioning. Information about the long-term cognitive outcome in pediatric MS patients is scarce (Marin *et al*, 2013). Most but not all longitudinal studies to date (Abelev *et al*, 2014; Amato *et al*, 2014a; Amato *et al*, 2010; MacAllister *et al*, 2007b; Till *et al*, 2013) report cognitive worsening, with variable frequencies. During the short term, most younger individuals with MS appear to remain relatively stable (Charvet *et al*, 2014; Till *et al.*, 2013), but a decline within 5 years of follow-up has been found (Amato *et al.*, 2014a). Further, even during just 1 year of follow-up, younger individuals with pediatric MS can fail to acquire age-appropriate gains relative to their peers (Till *et al.*, 2013). At what exact point during childhood or adolescence the brain is most vulnerable to the cognitive involvement of MS remains unclear. Those with a younger age at onset could be expected to be at increased risk for cognitive problems (Hosseini *et al*, 2014), but older pediatric patients have been found to have higher rates of impairment in some reports (Wuerfel *et al*, 2018).

A recent study by McKay and colleagues reported that adults with pediatric onset MS compared to those with adult onset MS performed more slowly on Symbol Digit Modalities Test (SDMT), a widely used cognitive screening measure that tests information-processing speed. The Authors demonstrated that early in their course, patients with pediatric onset MS performed somewhat better than those with adult onset MS. However, the 2 groups diverged by the time pediatric onset MS patients reached 30 years of age, with slower performance in the pediatric onset MS group relative to the adult onset MS group, persisting over time. Although patients with pediatric onset MS had longer disease duration, the findings remained even adjusting the model for disease duration.

Against this background, it is mandatory the inclusion of neuropsychological testing and evaluation of school performance in the clinical monitoring of pediatric MS patients (Amato *et al.*, 2016; Lee & Chitnis, 2016).

1.9 Fatigue and mood disorders

Approximately the 30% of children with MS reports fatigue, described as a "pervasive sense of lack of energy limiting the child's participation in school, sport, and peer-related activities" (Amato *et al.*, 2016; Banwell, 2013). However, due to the difficulty in the assessment of fatigue in this specific population, discrepancies between self-reports and parent-reports of the presence and severity of fatigue have been described (MacAllister *et al*, 2009), with parents reporting fatigue more frequently than their children (Goretti *et al*, 2012; MacAllister *et al.*, 2009). Overall, fatigue is an extremely relevant symptom in pediatric MS as it affects both mood and cognitive performance (Goretti *et al.*, 2012).

Given that cognitive impairment affects quality of life and negatively affects school performance, special attention to school-related accommodations and emotional well-being is imperative to the multidisciplinary care of children with MS. The Schedule for Affective Disorders and Schizophrenia for School-Age Children-Present and Lifetime Version (KSADS) revealed that approximately 30% to 48% of children with MS or related conditions have affective disorders (Amato *et al.*, 2008; Weisbrot *et al*, 2010). The most common psychiatric conditions are major depression, anxiety disorder, a combination of anxiety and depressive disorders, panic disorder, bipolar disorder, and

adjustment disorder. As well as for fatigue also for mood disorders and behavioral problems, parents showed higher awareness of these symptoms than the children or adolescents (Amato *et al.*, 2014a; MacAllister *et al*, 2007a).

1.10 Diagnosis

1.10.1 Diagnostic procedures. The diagnosis of MS, in both children and adults, requires: (1) evidence of dissemination of disease activity within the CNS (dissemination in space – DIS) and over time (dissemination in time – DIT), (2) clinical symptoms typical of an MS attack, and (3) the exclusion of MS-mimicking disorders (Filippi *et al*, 2018; Lee & Chitnis, 2016). All three aspects must be confirmed.

In general, this is achieved with accurate clinical evaluation, imaging studies of the brain and/or spine, serologic and CSF analyses, with or without the aid of neurophysiological exams. Blind application of current diagnostic criteria to MRI findings may lead to a high number of wrong diagnoses, especially in pediatric patients.

1.10.2 MRI. In children and adolescents with a first demyelinating attack, the presence of 1 or more not-enhancing T_1-hypointense lesions or 2 or more periventricular lesions, has been associated with increased likelihood of MS diagnosis (Callen *et al*, 2009). Subsequently, the concomitant presence of 1 periventricular T_2-hyperintense lesion and at least 1 T_1-hypointense lesion resulted as a strong predictor of subsequent MS diagnosis (Verhey *et al.*, 2011). The presence of T_1-hypointense lesions is relevant for distinguishing MS form ADEM as they can be observed in fewer than 20% of children with ADEM (Deiva *et al*, 2012).

The International Pediatric Multiple Sclerosis Study Group (IPMSSG) consensus diagnostic criteria included the 2010 McDonald criteria (Krupp *et al*, 2013; Polman *et al*, 2011). Simplifying the requirements for DIS and DIT, these criteria improved early detection of MS while maintaining specificity and including a specific focus on pediatric MS.

While clinical and MRI features of adolescent MS patients resemble those of adult onset patients (Waubant *et al*, 2009; Yeh *et al*, 2009c), children younger than 11 years more frequently show large and ill-defined lesions (Banwell *et al*, 2007c; Chabas *et al*, 2008) that resolve over time early in the disease course (Chabas *et al.*, 2008). These features, being also likely to represent the initial presentation of myelin-oligodendrocyte glycoprotein antibody-associated disease (MOGAD), make the 2010 as well as the 2017 criteria less reliably predictive of confirmed relapsing MS in younger children (Fadda *et al*, 2018b; Hacohen *et al*, 2019; Verhey *et al.*, 2013; Wong *et al*, 2018).

Furthermore a higher likelihood of ADEM as first demyelinating event is reported in children younger than 11 years, delaying MS diagnosis in this population, as long as ADEM needs to be followed by further non-ADEM attacks and/or accrual of clinically silent new lesions before applying MS diagnostic criteria (Wong *et al.*, 2018).

Finally, also in pediatric population, it is possible to observe MRI features consistent with MS in children imaged for indications other than clinical demyelination. At present, children and adults with radiologically isolated syndrome (RIS), even those who show new lesions on serial imaging, do not meet criteria for MS unless a clinical attack occurs. It is important to perform paraclinical testing to evaluate for subclinical disease or for evidence of a prior attack that was not identified—a key issue in young children who may not have reported mild symptoms.

1.10.3 Evoked potentials. Multimodal evoked potentials (EP) may aid in the localization of lesions and confirm an organic basis of clinically ambiguous symptoms. Moreover, EP can identify clinically silent lesions and thereby could provide objective support for DIS in space in an individual with suspected MS (Gronseth & Ashman, 2000). In a retrospective study including 156 pediatric MS patients, 82% of children showed abnormal EP, thereby objectifying clinical findings as well as revealing clinically silent or unreported lesions. Altered visual EP (VEP) have been detected in 56% of children, although only 40% had prior abnormalities in vision, thus providing additional diagnostic support, particularly in situations in which few MRI abnormalities can be detected (McDonald *et al*, 2001; Pohl *et al*, 2006). In this same pediatric MS cohort (Pohl *et al.*, 2006), the combination of brainstem auditory (BAEP) and somatosensory (SEP) identified clinically silent lesions in 12% of patients. Although this is not a high percentage, it has to be considered that BAEP and SEP potentially reveal lesions in the brainstem and spinal cord, areas with limited MRI sensitivity (Comi *et al*, 1989). This is especially true for MRI of younger children, in whom movement artifacts are common, often impeding exact interpretation (Pohl *et al.*, 2006).

1.10.4 Optical Coherence Tomography (OCT). In order to obtain a more accurate assessment of the optic nerve integrity in MS the OCT has been introduced as a specialized method to trace and track exclusively the optic nerve also considered as potential localization for demyelinating lesions used for determination in space (Filippi *et al*, 2016). Indeed, VEP (Wilejto *et al.*, 2006) or optical coherence tomography (OCT)

features (Waldman *et al*, 2013; Yeh *et al*, 2009b) consistent with prior ON can be used to support a prior demyelinating event, which in combination with MRI evidence of DIT and DIS can confirm the diagnosis of MS.

The most frequently used OCT measure is represented by the retinal nerve fiber layer (RNFL) thickness, consisting of the axons of retinal ganglion cells forming the optic nerve. During an ON attack, RNFL thickness transiently increases (due to inflammation-mediated edema of the optic nerve) but decreases thereafter by approximately 20%.

The precise timing of OCT measurements within the clinical course is relevant, as false normal (or even increased) RNFL levels could be gauged during ongoing optic nerve demyelination also occurring without overt clinical signs of ON. In this perspective to overcome this issue the combined thickness of the ganglion cell and inner plexiform layer (GCIPL) has been considered. GCIPL thickness is less prone to fluctuations by an inflamed optic nerve and may also be useful to trace a past episode of ON or inflammatory optic nerve demyelination (Aktas & Hartung, 2019).

While there is an abundance of evidence supporting the role of OCT as a surrogate marker of neuroaxonal injury in adults, fewer studies with this technique have been performed in children with CNS demyelinating disorders.

The first study conducted in children by Yeh and colleagues (Yeh *et al.*, 2009b) demonstrated RFNL thinning in children with monophasic and recurrent demyelinating diseases even in the absence of overt ON, further supporting work that has shown abnormalities in VEP in children with MS, many of whom did not have a clinical history of ON (Pohl *et al.*, 2006). However, in pediatric population conflicting results have been reported. Indeed, Waldman and colleagues (Waldman *et al.*, 2013) demonstrated that unlike findings in adult-onset MS, children and adolescents with MS did not experience RNFL thinning.

In this perspective, a recent study aimed at describing the changes in RFNL and GCIPL thickness in the acute phase following pediatric ON (Wilbur *et al*, 2019) found that children with MS show less RNFL swelling in their ON-affected eyes at onset compared to children with monophasic demyelination. Lower GCIPL and temporal RNFL thickness in the clinically unaffected eyes of those children with unilateral ON suggested the presence of pre-existing neuroaxonal injury in children with MS presenting with a first episode of ON (Wilbur *et al.*, 2019).

1.10.5 Cerebrospinal fluid examination. Although not mandatory for MS diagnosis, CSF analysis plays a relevant role in diagnostic work-up of a first demyelinating event (Hintzen *et al*, 2016). CSF monocytic pleocytosis can be observed in the 50% of pediatric MS patients, while CSF neutrophils should suggest different aetiologies such as infection or NMO spectrum disorder (NMOSD) (Chabas *et al*, 2010; Huppke *et al.*, 2014; Pohl *et al*, 2004).

The presence of intrathecal OCBs is strongly supportive of an MS diagnosis and can be detected in up to 90% of patients (Chabas *et al.*, 2010; Huppke *et al.*, 2014; Pohl *et al.*, 2004). Two studies have investigated the presence of CSF OCBs in children with MS aged under and above 11 years; CSF OCBs were detected in about 55% of the younger group and 70% of the older group (Chabas *et al.*, 2010; Huppke *et al.*, 2014). Neutrophilic pleocytosis, a higher percentage of monocytes and the absence of intrathecal immunoglobulin-G synthesis was more frequently found in younger pediatric MS, suggesting a prominent involvement of the innate immune system; while lymphocytic pleocytosis and elevated CSF immunoglobulin-G were observed in late onset pediatric and adult onset MS, suggesting prominent activation of the adaptive immune system (Chabas *et al.*, 2010).

1.10.6 Autoantibodies. Autoantibodies (anti-aquaporin 4 [AQP4] or anti-MOG antibodies) should be tested in patients with atypical clinical and MRI features. Anti-MOG antibodies are detected in approximately 30% of children with ADS, of whom 50% are younger than 11 years at presentation, whereas a diagnosis of AQP4-NMOSD is made in less than 5% of children with ADS (Fadda *et al*, 2021). However, anti-MOG antibodies do not exclude MS diagnosis in patients with typical relapses and MRI features as they can be present also in children with typical RRMS (Hennes *et al*, 2017).

Anti-MOG antibody–positive children usually experience a monophasic disease, with clinical relapses occurring more commonly, although not exclusively, in children with persistent seropositivity. A favorable outcome was demonstrated in the most anti-MOG antibody–positive children so that presence of anti-MOG antibodies at the time of incident demyelination should not immediately prompt the initiation of long-term immunomodulatory therapy (Waters *et al*, 2020).

1.10.7 Diagnostic criteria. Diagnostic criteria for MS include clinical and paraclinical laboratory assessments (Poser *et al.*, 1983; Schumacher *et al*, 1965)

emphasizing the need to demonstrate DIS and DIT and to exclude alternative diagnoses. The diagnostic criteria recommended by the IPMSSG guidelines (2013 IPMSSG diagnostic criteria) enable a MS diagnosis at time of the first attack, if baseline MRI findings satisfy DIS and DIT, according to the 2010 McDonald criteria for MS from the International Panel on Diagnosis of MS (Krupp *et al.*, 2013; Polman *et al.*, 2011).

In 2017, the International Panel on Diagnosis of MS proposed modifications to the 2010 McDonald criteria with the aim to improve diagnostic accuracy, simplify application of the criteria, and enhance timeliness of MS diagnosis (Thompson *et al*, 2018). To date, three different studies (Fadda *et al.*, 2018b; Hacohen *et al.*, 2019; Wong *et al.*, 2018) validated 2017 McDonald criteria in pediatric population. The 2017 McDonald diagnostic criteria demonstrated higher accuracy and sensitivity, and slightly lower specificity, than the 2010 McDonald criteria. The specificity of criteria appeared to be mainly driven by DIT component as enhancing lesions or CSF oligoclonal bands are rare in children with monophasic demyelination, including ADEM (Fadda *et al.*, 2018b). As converse, the DIS component, including symptomatic lesions reduced specificity and increased sensitivity of 2017 McDonald, being met by 79% of children with ADEM, and by 20% of participants in the non-ADEM group without MS (Fadda *et al.*, 2018b; Hacohen *et al.*, 2019). The role of spinal cord lesions in contributing to DIS in the 2017 criteria not meaningfully changed their performance, however providing a more comprehensive assessment in cases in which there is diagnostic uncertainty (Banwell *et al.*, 2016). As no differences were observed in the performance of 2017 McDonald criteria in patients younger or older than 11 years, these diagnostic criteria could be routinely applied to children irrespective of age of onset, with special care needed in patients presenting with ADEM (Hacohen *et al.*, 2019; Wong *et al.*, 2018).

Fadda and colleagues (Fadda *et al.*, 2018b), also confirmed that one or more *T*1 hypointense lesions and *T2* periventricular lesions are strongly associated with a diagnosis of MS in children (Verhey criteria) (Verhey *et al.*, 2011). These latter criteria perform as well as the McDonald 2017 criteria and might be particularly useful given concerns regarding intracerebral accumulation of gadolinium (Kanda *et al*, 2015) and when CSF OCBs are not available, while testing for anti-MOG antibodies is likely to not improve performance of diagnostic criteria despite relevant in the assessment of children with relapsing disease atypical for MS.

1.10.8 Differential diagnosis. As in adults, the diagnosis of MS requires the exclusion of other diseases. Several "red flags" should be considered (Venkateswaran & Banwell, 2010):

- Given that primary progressive (PP)MS is exceptionally rare in children, progressive neurodegeneration without relapses should prompt consideration of inherited leukodystrophies (metachromatic leukodystrophy - diffuse WM involvement, adrenoleukodystrophy- posterior WM predominance, Alexander disease - frontal WM predominance, Krabbe disease - diffuse WM, vanishing WM disease - diffuse WM disease with areas of WM vacuolation), mitochondrial or other metabolic diseases;
- Although decline in cognitive performance may occur early in the disease, pre-existing developmental delay is not a typical feature of MS;
- A family history of neurodegenerative WM disease should lead to investigation of affected family members, and consideration of disorders such as cerebral autosomal dominant arteriopathy with subcortical infarcts and leukoencephalopathy (CADASIL - MRI involvement of external capsules and anterior temporal lobes), Pelizeaus Merzbacher, pigmentary orthochromatic leukodystrophy, as well as other inherited diseases;
- Persistent and prominent headache, joint pain, rashes, or systemic disease should lead to investigation for Systemic Lupus Erythematosus (SLE);
- Persistent headache alone warrants consideration of isolated small vessel vasculitis (angiogram negative, without systemic disease);
- Trigger by infection/trauma should prompt consideration of mitochondrial diseases and childhood ataxia with cerebral hypomyelination;
- Progressive lower limb spasticity, or family history of spastic diplegia, should lead to investigation of adrenoleukodystrophy, Pelizaeus-Merzbacher and familial spastic paraplegia, in addition to a new entity of MitCHAP-60 disease, a newly identified autosomal recessive Pelizaeus-Merzbacher-like disease.

Moreover, pediatric MS needs also to be distinguished from other demyelinating disorders including ADEM, NMOSD and MOGAD.

ADEM is a heterogeneous entity (see below) and is best viewed as a 'syndrome'

rather than a specific disorder. ADEM typically follows a monophasic disease course, although confirmation of monophasic ADEM is retrospective and requires prolonged observation. The clinical symptoms and radiologic findings of ADEM can fluctuate in severity and evolve in the first three months following disease onset. To diagnose pediatric ADEM, all the sequent criteria are required:

- A first polyfocal, clinical CNS event with presumed inflammatory demyelinating cause;
- Encephalopathy defined as an alteration in consciousness (e.g., stupor, lethargy) or behavioural change unexplained by fever, systemic illness or post-ictal symptoms;
- No new clinical and MRI findings three months or more after the onset;
- Abnormal brain MRI during the acute (three-month) phase.
- Typically on brain MRI:
    - Diffuse, poorly demarcated, large (>1–2 cm) lesions involving predominantly the cerebral WM;
    - Rare T_1 hypointense lesions in the WM;
    - Deep GM lesions (e.g. thalamus or basal ganglia).

In addition to monophasic ADEM a non-monophasic course has been described and two main entities have been identified in addition to NMO (Pohl *et al*, 2016):

- Multiphasic disseminated encephalomyelitis (MDEM): 2 episodes consistent with ADEM, separated by at least 3 months. A third demyelinating event is not more consistent with this definition, while suggesting a diagnosis of chronic demyelinating disease.
- ADEM ON: ADEM, MDEM, or multiple ADEM attacks followed by ON. This new entity has been recognized as a relapsing clinical phenotype associated with anti-MOG anti-bodies.(Huppke *et al*, 2013)
- NMO is an inflammatory CNS syndrome distinct from MS that is associated with serum AQP4 immunoglobulin G (AQP4-IgG).

Finally, pediatric MS also need to be distinguished from primary CNS vasculitis and secondary CNS vasculitis in patients with autoimmune diseases (Banwell *et al.*,

2007c). Other possible differential diagnosis also include neoplastic and paraneoplastic disease (Barraza *et al*, 2021).

1.11 Treatment approaches

The treatment of pediatric MS involves the management of acute attacks, the use of disease modifying treatments (DMT), vitamin D supplementation, symptomatic management, counselling and support.

1.12 Therapies for acute exacerbations

1.12.1 Methylprednisolone. The initial treatment of an acute demyelinating event is aimed to rapidly decrease inflammation and promote symptom recovery. Treatment typically consists of 30 mg/kg/day (up to 1 g/day) for 3–5 days. Clinical trials conducted in adult patients suggested that equivalent doses of oral corticosteroids might have similar efficacy to intravenous corticosteroids while improving accessibility to treatment and comfort for both patients and families (Le Page *et al*, 2015). Oral corticosteroid taper after completion of pulse corticosteroid therapy is controversial and not often required for children who have recovered markedly after intravenous corticosteroid dosing.

1.12.2 Intravenous immunoglobulin (IVIG). Only two trials evaluated the role of IVIG administration (as an adjunct to intravenous corticosteroids) in the management of acute relapses in adults MS patients (Soelberg Sorensen *et al*, 2004). Refractory cases of children with ON and ADEM showing improvement form treatment with IVIG (2g/kg given over 2–5 days) have been described (Shahar *et al*, 2002; Spalice *et al*, 2004; Straussberg *et al*, 2001). To date, the use of IVIG is limited to attacks that have responded poorly (poor recovery) to corticosteroids.

1.12.3 Plasmapheresis (plasma exchange). Plasma exchange has been recognized as well-tolerated second-line treatment option for pediatric patients with severe acute CNS demyelinating events with limited response to pulse steroids (Manguinao *et al*, 2019). Plasma exchange is preferred in the context of severe events, such as those in the brainstem or spinal cord (Bigi *et al*, 2014; Manguinao *et al.*, 2019).

1.13 Disease-Modifying Therapies

Treating children with disease-modifying therapies (DMT) has thus far largely relied on studies conducted on adult MS and case series, consensus, and international guidelines (Otallah & Banwell, 2018). To date, only one therapy (Fingolimod) has been

formally approved for pediatric MS on the basis of a phase 3 clinical trial evidence (Chitnis *et al*, 2018).

Based on recommendations by international expert panels (Chitnis *et al*, 2012; Ghezzi *et al*, 2010), pediatric MS patients should start DMT treatment soon after diagnosis, with regular follow-up:

1. To assess clinical response with regular clinical evaluations (every 3–6 months) and brain MRI (every 6–12 months);

2. To check the tolerability/safety profile (every 3–6 months) periodic assessment of blood cell count, and liver, thyroid and kidney function should be performed.

1.14 Injectable therapies

Injectable therapies commonly used as first line DMT in pediatric MS patients are Interferon-β (IFN-β) and Glatiramer Acetate (GA) (Chitnis *et al.*, 2012; Ghezzi *et al.*, 2010). Several phase 4 observational studies assessed safety and efficacy of IFN-β (Banwell *et al*, 2006; Ghezzi *et al*, 2009; Ghezzi *et al*, 2016; Mikaeloff *et al*, 2001; Pohl *et al*, 2005; Tenembaum & Segura, 2006; Waubant *et al*, 2001) and GA (Bergamaschi *et al*, 2009; Ghezzi *et al*, 2005; Kornek *et al*, 2003) in this population.

Some studies included children under the age of 10 years or 12 years, analyzing those subgroups separately: the clinical outcome was not different compared to patients with a higher age as well as the occurrence of adverse events; the only exception was increased rate of elevation of liver enzymes in the younger group of patients with MS in one study of IFN-β (Banwell *et al.*, 2006; Ghezzi *et al.*, 2016). Importantly, based on results from a recent study (Tenembaum *et al*, 2013), IFN-β-1a (22 or 44 mg) was approved by European Medicines Agency (EMA) in children between 2 and 11 years old. However, studies aimed at exploring pharmacodynamic or pharmacokinetic of IFN-β and GA in pediatric MS are not available to date (Ghezzi *et al.*, 2016). A retrospective analysis of 258 treated pediatric patients with MS revealed that 28% were considered by their health care practitioners to have refractory disease on their first therapy (mainly IFN and GA), and were therefore switched to a second therapy after a mean of 1.3 years (Chitnis *et al*, 2016). Another recent retrospective study including 741 children demonstrated that newer (oral and intravenous) DMT controlled disease activity better than IFN and GA, thus resulting in a larger reduction of ARR (rate ratio 0.45, 95% CI 0.29–0.70), new or

enlarging T2 lesions (hazard ratio 0.51, 95% CI 0.36–0.72), and gadolinium-enhanced lesions (0.38, 0.23–0.63) (Krysko *et al*, 2020).

Poor tolerance and low compliance after 1.1 years of treatment, accounted for the 16% of medication switches in this population (Yeh *et al*, 2011). Self-reported rate of nonadherence is as high as 41-47% (Schwartz *et al*, 2018; Thannhauser *et al*, 2009), and adherence was better in therapies with fewer weekly injections (Chitnis *et al.*, 2016).

1.15 Oral therapies

1.15.1 Dimethyl fumarate (DMF). The FOCUS trial of DMF was published in 2018 demonstrating safety data (Alroughani *et al*, 2018). This was an open-label 6-months phase 2 trial of DMF pharmacokinetics including 22 patients. The FOCUS trial consisted of an 8-week off-treatment baseline period and a 24-week treatment period. Form baseline to the final 8 weeks of DMF assumption a significantly reduced incidence of T_2-hyperintense lesions was observed. The most frequently reported adverse events were gastro-intestinal symptoms and flushing (Otallah & Banwell, 2018).

The CONNECTED study, the 96-week extension to FOCUS, assessed the long-term safety and efficacy of treatment with delayed-release DMF in pediatric MS patients. Twelve of the 17 patients completing the study had no new/newly enlarged T_2 lesions from weeks 16–24, two (12%) had one, and one each (6%) had two, three, or five or more lesions [median (range), 0 (0–6)]. Over the full 120-week treatment period, ARR was 0.2, an 84.5% relative reduction ($n = 20$; 95% confidence interval: 66.8–92.8; $p < 0.0001$) *vs* the year before DMF initiation. The most frequently reported adverse event was flushing while no serious adverse events were reported (Alroughani *et al*, 2021).

A phase III, double-blind, placebo-controlled, three-arm randomized controlled trial aiming on evaluating safety and efficacy of DMF compared with placebo and pegylated IFN β-1a is currently recruiting patients (ClinicalTrials.gov Identifier: NCT03870763).

1.15.2 Fingolimod. On the basis of PARADIGMS Fingolimod has been formally approved for pediatric MS (Chitnis *et al.*, 2018). This phase 3, 2-year randomized double-blind, double dummy study including 215 pediatric MS patients, showed significant reduction of ARR (82%), appearance of new or newly enlarged T_2 lesions (53%) and of gadolinium-enhancing lesions (66%) and reduced rate of brain atrophy at 2-year follow-

up. Adverse event reported included leukopenia, seizure, and hypersensitivity reactions. However, the overall incidence of infections was comparable between fingolimod and interferon, and no association was observed between nadir of absolute lymphocyte counts and infections (Chitnis *et al*, 2021).

Recently the Food and Drug Admninstration (FDA) and EMA extended fingolimod approval to pediatric patients younger than 10 years (Otallah & Banwell, 2018).

1.15.3 Teriflunomide was approved in adult onset MS based on the results of two placebo-controlled RCTs (Confavreux *et al*, 2014; O'Connor *et al*, 2011). There were no differences in treatment failure rate and ARR between teriflunomide and interferon-β-1a in adults, which indicated that although newer, teriflunomide has an efficacy similar to the injectable medications (Vermersch *et al*, 2014). A phase 3, double-blind, randomized, placebo-controlled trial evaluating the efficacy, safety, and pharmacokinetics of teriflunomide in children with relapsing-remitting MS aged 10 to 17 years reached completion on October 2019 (TERIKIDS, ClinicalTrials.gov identifier: NCT02201108). Preliminary results were presented at ECTRIMS 2020: teriflunomide reduced the risk of the time of clinical relapse or switch due to high MRI activity by 43% ($p = 0.041$) and the appearance of Gd-enhancing and new/enlarged T2 hyperintense lesions compared with placebo (1.9 vs. 7.5, $p < 0.0001$ and 4.7 vs. 10.5, $p = 0.0006$, respectively). Three SAEs were observed [pulmonary tuberculosis, acute pancreatitis, and alanine aminotransferase (ALT) increase].

1.15.4 Cladribine was approved for the treatment of RR and active SP adult onset MS in March 2019 following two RCTs (CLARITY and ORACLE-MS), and is recommended for patients who have had an inadequate response to or did not tolerate an alternate DMT (Giovannoni *et al*, 2010; Leist *et al*, 2014). It has not yet been studied in pediatric MS.

1.16 Infusion theraphies

1.16.1 Natalizumab has been utilized off label in highly active and refractory cases of pediatric MS. In a first observational study of pediatric MS patients treated with monthly infusion 15 relapses were observed in 9 of 101 patients included over a mean follow-up of 34 months. No cases of progressive multifocal leukoencephalitis (PML)

were reported, as expected considering the lower frequency of anti-John Cunningham virus (JCV) antibodies in pediatric patients compared to adults (Chitnis *et al.*, 2016).

In a retrospective single-center study in Germany, 40% of their 144 patients fulfilled their criteria for highly active MS. These patients demonstrated improved relapse rates and MRI markers of disease activity on both natalizumab and fingolimod with a trend toward greater response to natalizumab (Huppke *et al*, 2019). A recent study (Margoni *et al*, 2019) observed a significant reduction in the mean Expanded Disability Status Scale (EDSS) score after 2 years of treatment with natalizumab and a maintained no evidence of disease activity (NEDA-3) plus status (no relapse, no disease progression (EDSS score), no radiological activity and no cognitive decline) in the 80% of patients.

Discontinuation of natalizumab is often associated with rebound clinical and MRI activity.

1.16.2 Cyclophosphamide is not approved for the treatment of MS, although pulse cyclophosphamide has been shown to reduce disease activity in adult MS in class I studies (Weiner *et al*, 1993). Adults 40 years or under were better responders than those over 40 years (Weiner *et al.*, 1993). A retrospective study of cyclophosphamide treatment in 17 pediatric patients with severe MS revealed a reduction in the mean ARR while on therapy, although 75% of patients acquired new lesions on MRI over 12–24 months of treatment (Makhani, 2009). Adverse effects included nausea and vomiting (88%), anemia (59%) and reversible alopecia (59%). More-serious adverse effects included infection (three patients), osteoporosis (two patients), sterility (one male patient) and bladder carcinoma (one patient who was not prescribed mesna). The total cumulative treatment, which should be limited to 80g, is typically administered for no more than 24 months. Strategies for fertility preservation, as are offered to pediatric cancer patients, should be considered (Ginsberg, 2010).

1.16.3 Rituximab is not approved for the treatment of MS, but beneficial effects have been reported in a class I phase II study in adult RRMS, showing significant reduction of brain lesions and clinical relapses (Hauser *et al*, 2008). A recent study investigated the clinical experience of safety and efficacy with rituximab in children with demyelinating diseases of the CNS. Eight children with NMO, two with RRMS and one with SPMS received rituximab treatment. The median number of cycles was 3. Most patients (82%, n = 9) experienced reduction of relapses after initiating rituximab. There

were no serious infections. Rituximab was not discontinued in any child because of side effects. Two patients switched treatment therapy after 4.5 and 11 months because of relapses (Beres *et al*, 2014).

1.16.4 Ocrelizumab a fully humanized anti-CD20 monoclonal antibody is FDA approved to treat RRMS or PPMS in adults. To date, there are no published data about ocrelizumab administration in pediatric MS patients. However, there is an ongoing retrospective observational study involving both adult and pediatric onset MS on epidemiological data regarding ocrelizumab use in Latin America (NCT03784547).

1.16.5 Alemtuzumab was FDA approved to treat RRMS in adults in 2014 (Cohen *et al*, 2012; Coles *et al*, 2012). The only safety data of alemtuzumab in pediatric patients come from studies in transplant recipients, reporting mild to serious infections as adverse events (Das *et al*, 2017; Kaabak *et al*, 2013; Kim *et al*, 2017). There is an ongoing company-sponsored multicenter open-label trial aimed to study safety and efficacy of alemtuzumab in pediatric MS patients who have failed at least 2 DMT (NCT03368664).

1.17 Supportive strategies

1.17.1 Vitamin D supplementation. Vitamin D is a commonly available supplement, and lowered vitamin D (25-OH) levels are frequent (Wilejto *et al.*, 2006) and have been found to correlate with relapse rate in children with MS (Mowry *et al.*, 2010). Published recommendations suggest that children and adolescents with MS should begin vitamin D3 supplementation of 600–1000 IU daily, with the dose increased incrementally as necessary to obtain a target serum level of 75 nmol/L (30 ng/mL) (Lee & Chitnis, 2016).

1.17.2 Symptomatic Treatment. Even if MS relapses are under control, intermittent symptoms can be bother some of the child. Symptomatic therapies are likely underutilized in children with MS. Fatigue is a common complaint, and treatment should be considered if fatigue is of sufficient severity as to interfere with daily participation in activities or schoolwork. Lifestyle issues (such as poor sleep hygiene) and hypothyroidism must be excluded. Treatment with modafinil or amantadine can ameliorate fatigue, although medication should be taken in the morning or at noon, rather than in the evening to avoid sleep disruption. Spasticity is a common complaint of adult MS patients, and is particularly notable in individuals who have entered secondary

disease progression. Benzodiazepines, localized botulinum toxin injections, and tizanidine (an alpha-2 adrenergic agonist) may be effective. Tremor or ataxia caused by cerebellar involvement in MS is difficult to treat. Rehabilitative therapies, adaptive equipment, and even deep brain stimulation have been used to control functional impairment from tremors in adult patients with MS.

1.17.3 Counseling and support. The diagnosis of a lifelong, potentially disabling disease has a profound impact on the patient and family (Krupp *et al*, 2016). It is important that a strong therapeutic relationship be established, and that patients also have the opportunity to discuss their own concerns privately with the healthcare team. A multidisciplinary team composed of physicians and nurses familiar with demyelination in children, psychiatry, psychology, ophthalmology, physical and occupational therapy, and social work is required to address the full spectrum of pediatric MS care (Banwell, 2013).

1.18 Neuroimaging features of pediatric MS

1.19 General considerations

MRI represents the most relevant paraclinical tool for MS diagnosis, disease progression monitoring and treatment response assessment. The goals of MRI in MS include: confirmation of an MS diagnosis before a second clinical attack (Poser *et al.*, 1983) in individuals with an ADS (Polman *et al.*, 2011; Polman *et al*, 2005), exclusion of alternative diagnoses (Miller *et al*, 2008), and prediction of long-term prognosis. Furthermore, comparison of serial MRI scans is used to qualitatively evaluate the rate of new lesions accrual for diagnosis in patients not meeting diagnostic criteria at onset, to inform on treatment decisions, and to monitor disease evolution apparent by formation of confluent lesions and atrophy (Banwell *et al.*, 2016).

However, conventional MRI metrics only show weak association with clinical features of pediatric MS patients. Advanced MRI techniques, providing a better pathological characterization of disease-related damage, may play a major role in individuating the substrates of clinical and cognitive outcome in this population. However, these techniques are not routinely available for clinical use, because they require standardized acquisition, rigorous image analysis pipelines, MRI scanner quality-control monitoring, and control or reference data (Verhey & Sled, 2013). A summary of the main findings obtained by using each advanced MRI technique is reported in the next paragraphs.

1.20 White matter lesions

1.20.1 Lesion appearance on conventional MRI sequences. The MRI appearance of childhood MS is characterized by multiple WM lesions. The presentation of MS in adolescents appears similar to adults on MRI, with asymmetric lesions, typically located in the periventricular (involving the corpus callosum [CC]) and juxtacortical WM, and in infratentorial areas (often involving the pons and cerebellum). Their shape is usually oval or elliptical, distributed around a central vein (Ormerod IE, 1987). In children before age 11 years, MRI presentation of MS is characterized by WM T_2-hyperintese lesions involving the same regions as adolescents, but often also the deep GM. The lesions often show ill-defined borders or marked perilesional edema (McAdam *et al*, 2002), while contrast enhancement may be seen less often. Furthermore, WM (and GM) lesions tend

to reduce in volume or disappear altogether over time, suggesting a different pathological basis for these lesions in children compared to adolescents and adults. Possible explanations are nonspecific reactive oedema rather than demyelination, less axonal loss or an enhanced ability to remyelinate in children.

The appearance of giant or tumefactive demyelinating plaques has been reported in several children (McAdam *et al.*, 2002). In a study of 20 children with MS, a review of MRI scans found four children with tumefactive lesions (Hahn *et al*, 2004) with a dramatic resolution of the lesion following treatment with corticosteroids. Instead, lesion enhancement is less frequent in children compared to adults. In details, a French study including 61 pediatric patients detected enhancing lesions in 13% only of the children with monophasic illness and 24% of the children ultimately diagnosed with MS at their first demyelinating attack (Mikaeloff *et al*, 2004a), while 52% of adult MS patients at their first acute attack of demyelination have enhancing lesions (Korteweg *et al*, 2006). Nonetheless, the timing of MRI scan relative to treatment with corticosteroids was not described: different therapeutic approach might partly explain findings in pediatric compared to adult MS, since corticosteroid exposure reduces blood-brain barrier permeability and thus gadolinium enhancement.

1.20.2 Lesion distribution and burden. Studies performing a direct comparison of lesion distribution and volume between pediatric and adult MS cohorts are rare (Yeh *et al.*, 2009c). Compared to their adult counterpart, pediatric MS patients showed a prominent involvement of infratentorial regions (Ghassemi *et al*, 2014; Waubant *et al.*, 2009; Yeh *et al.*, 2009c), with pontine lesions being particularly frequent in male pediatric patients (Ghassemi *et al*, 2008; Ghassemi *et al.*, 2014). On the other hand, a similar supratentorial T_2 lesion distribution was observed in pediatric compared to adult MS patients (Ghassemi *et al.*, 2014). These findings imply that lesion accrual may not require a prolonged period of subclinical disease. Instead, the differences observed in lesion prevalence and location could reflect immunological differences or differences in the state of myelination in the pons relative to supratentorial WM between children and adults. Indeed, myelination proceeds along in a caudo-rostral gradient, completing in the pons earlier than in supratentorial brain regions (Paus, 2005). Moreover, the myelination of pons is actually earlier in males compared to females (De Bellis *et al*, 2001), which is

consistent with the observation of preferential MRI involvement of this structure in boys with MS.

Moreover, the longitudinal analysis of lesion volumes revealed that children with MS actually accrued greater volumes of T_2 and T_1-weighted lesions over time than their adult counterparts (Ghassemi *et al.*, 2014; Yeh *et al.*, 2009c). Together with a shorter disease duration (including the subclinical phase), this probably lead to similar lesion volumes – on average – compared to disease duration-matched adult patients. Interestingly, the increase in lesion volume differed by brain region. In details, in the supratentorial region, a smaller fraction of T_2–hyperintense lesion was T_1-hypointense in the children with MS than in the adults, whereas in the infratentorial region, the T_1:T_2 lesion volume ratio was similar. This finding raises the intriguing possibility that active primary myelination, as would be expected in the supratentorial regions during childhood and adolescence, might serve to more effectively remyelinate lesions in this region, limiting T_1-hypointense lesion formation (Ghassemi *et al.*, 2014).

1.20.3 Myelin repair capability. As above specified, overall lesion burden is similar in pediatric- and adult-onset MS (Ghassemi *et al.*, 2008; Yeh *et al.*, 2009c), so that the lower risk of physical disability cannot be attributed to a lower lesion burden in children and adolescents. In this perspective, Brown and colleagues investigated the remyelination capabilities in adult and pediatric MS patients by assessing sequential magnetization transfer ratio (MTR) within MS lesions. Young adolescents showed a heightened capacity for remyelination, lost as they enter adulthood, thus demonstrating the existence of an inverse relationship between age and capacity for remyelination.

These findings, were confirmed by Ghassemi and colleagues (Ghassemi *et al*, 2015c) that characterized the evolution of normalized T_1-weighted (N T_1) intensity of WM prior to, at the time of, and following recovery of new lesions in pediatric- and adult-onset MS patients. Reduced remyelination capacity in late adolescence could be caused by the loss of factors uniquely associated with brain development, which are lost at the end of adolescence, or by the same processes that produce slow decline in adults. Moreover, it is possible that patients who develop MS at a younger age may experience delayed development, retaining remyelination-enhancing developmental factors to an older age.

1.21 Normal appearing white matter damage

In MS, regions of normal appearing WM (NAWM) often contain abnormalities, including axonal spheroids and swellings, mild inflammation, microglial activation, gliosis, and increased expression of proteolytic enzymes (Moll *et al*, 2011). These abnormalities go undetected with conventional MRI, which represents the reason why only modest correlations between MRI-visible focal WM lesions and neurologic deficits are reported (Filippi, 2014).

1.21.1 ^{1}H-MR spectroscopy (^{1}H-MRS). ^{1}H-MRS acquires information from hydrogen nuclei of molecules or metabolites present in tissues, and this metabolic information has pathologic specificity not obtainable from water proton signals (Ross & Bluml, 2001). The presence of low *N*-acetylaspartate (NAA), measured both as an absolute concentration and as a ratio of NAA/creatin, has been confirmed within lesions, NAWM, and cortical GM of adult MS patients relative to HC (Caramanos *et al*, 2009). Decreases in NAA resonance intensity of up to 50% can be observed in the NAWM of adult patients (Fu *et al*, 1998) and of up to 80% in T_2 WM lesions (De Stefano *et al*, 1995). The loss in neuronal integrity measured by decreased NAA/creatin ratios follows a gradient around T_2 lesions, with greater injury proximal to the lesion relative to the more distal NAWM (Arnold *et al*, 1992).

The application of ^{1}H-MRS to children with MS has been limited to 3 studies. The first study including 8 pediatric MS patients, showed decreased resonances of NAA and creatin while increased resonances of choline and myoinositol within lesions, in pediatric MS patients compared to age-matched HC. Otherwise, no differences were observed in the NAWM ^{1}H-MR spectra of pediatric MS patients and HC (Bruhn *et al*, 1992b; Oguz *et al*, 2009). Considering the role of citrullination of MBP in stabilizing myelin structure (Pritzker *et al*, 2000a; Pritzker *et al*, 2000b), another study including 27 pediatric MS patients and 23 HC estimated the resonance of citrulline (Oguz *et al.*, 2009). The 44% of pediatric MS patients compared to the 13% of HC showed a citrulline peak both in the NAWM and T_2 hyperintense lesions (Oguz *et al.*, 2009), where increased citrullination results in myelin instability (Pritzker *et al.*, 2000a; Pritzker *et al.*, 2000b). Finally, ^{1}H-MRS has proven to contribute in differentiating monophasic ADEM from MS. Indeed, while pediatric MS patients had increased intralesional myoinositol/creatin

ratio, children with ADEM had a substantial reduction in the myoinositol/creatin ratio (Ben Sira *et al*, 2010).

1.21.2 Magnetization Transfer MRI (MT MRI). The application of MT MRI allows the calculation of MTR, an index of protons bound to brain tissue capability to exchange magnetization with the surrounding free water, thus providing an estimate of microstructural integrity.

Only few studies (Mezzapesa *et al*, 2004b; Tortorella *et al*, 2006; Yeh *et al.*, 2009c) evaluated microstructural tissue abnormalities in children with MS using MT MRI. These studies showed no significant differences in average MTR and histogram peak height measured in the normal-appearing brain tissue and cervical cord (Mezzapesa *et al.*, 2004b), in NAWM (Mezzapesa *et al*, 2004a), and GM (Tortorella *et al.*, 2006) between pediatric MS patients and age- and sex-matched HC. Lower MTR values were observed within T_2 lesions, NAWM, and GM in 33 adults with pediatric-onset MS compared to 381 adults with adult-onset disease. These last findings suggested a greater disruption of microstructural integrity in pediatric-onset MS patients, likely explained by longer disease duration.

1.21.3 Diffusion Tensor Imaging (DTI). DTI provides an *in vivo* measure of water diffusion within an image voxel, allowing to obtain information on brain and spinal cord microstructural integrity.

Several DTI studies showed structural abnormalities in the NAWM of pediatric RRMS patients (Rocca *et al*, 2010; Tortorella *et al.*, 2006; Vishwas *et al*, 2010). These findings were confirmed by a subsequent study (Absinta *et al*, 2011) reporting a similar extent of DTI abnormalities [reduced fractional anisotropy (FA) and increased mean diffusivity (MD)] in pediatric and adult patients with the RR phenotype of the disease. The NAWM DTI abnormalities observed, showed significant correlations with T_2 lesion burden, suggesting a role for Wallerian neurodegeneration from focal WM lesions, in determining NAWM damage.

Overall, these studies highlighted that a widespread NAWM microstructural integrity disruption occurs early in the disease course. Moreover, a more severe NAWM damage, independent form disease duration, has been observed in pediatric- compared to adult-onset MS patients by using Tract-Based Spatial Statistic (TBSS) . In the perspective of a different vulnerability to NAWM damage according to the age of onset, a recent

study (Rocca *et al*, 2016c) applied DTI to quantify abnormalities within a subset of brain WM tracts, considered to be representative of the major interhemispheric, intrahemispheric, and projection connections, in pediatric MS patients with disease onset prior to age 12 years. The Authors found that compared to HC, pediatric MS patients had reduced FA and increased MD in bilateral superior longitudinal fasciculus and CC. Only NAWM abnormalities in the CC appeared to be correlated with lesion volumes suggesting that Wallerian degeneration of tracts traversing lesions is only partially responsible for tissue integrity loss in non-lesional tissue in very young MS patients. These pathological changes not explained by MS-related macroscopic damage can be attributed to failure of maturational processes. To point in this same direction, is a recent study (Longoni *et al*, 2017) that demonstrated, by applying DTI, failure of WM maturational changes in pediatric onset MS patients and in patients with a single demyelinating attack and progressive WM integrity loss in pediatric MS patients.

1.22 Gray matter lesions

Double inversion recovery (DIR) sequence, increasing lesion contrast, has been optimized for the detection of cortical lesions (CLs) *in vivo* (Geurts *et al*, 2005). Although less sensitive than pathological assessment, DIR sequence allows to detect focal CLs in the majority of adult MS patients. Interestingly, CLs were found to be less frequent in pediatric patients (10%), compared to their adult counterparts (66%) (Absinta *et al.*, 2011). These results were substantially confirmed by other two studies: 12% (Rocca *et al*, 2015b) in a group of 41, and 34% (Calabrese *et al*, 2012) in a group of 35 pediatric MS patients. Same as for adults, by using more advanced MRI techniques, such as multi-contrast 3T (Maranzano *et al*, 2019) and 7T (Datta *et al*, 2017) MRI, a higher frequency of CLs was found in pediatric onset MS patients, compared to the above reported findings. The relationship of CLs count with age at onset and disease duration was also evaluated, finding that the number of CLs increases with the age at disease onset. Thus, older age at MS onset may be associated with a higher likelihood of having CLs. Possible explanation might be a lower propensity for CLs in very young MS patients, greater difficulty in distinguishing CLs from surrounding cortex in the less mature brain, a reduced vulnerability of GM where late myelination has not already occurred, or a heightened capacity to repair CLs in younger MS patients, a resiliency that is lost with increasing

age. Alternatively, adolescent and adult-onset MS patients might experience a longer period of lesion accrual during the "pre-clinical" MS phase, whose duration is still unknown.

1.23 Gray matter damage

Gray matter involvement in adult MS patients has been widely demonstrated by pathology (Bo *et al*, 2007) and MRI studies (Calabrese *et al*, 2009). However, only a few studies investigated extent and contribution to clinical disability and cognitive impairment of GM damage in pediatric MS patients, with conflicting findings. By using ^{1}H-MRS in pediatric MS patients, reduced NAA in cortical GM neighboring MS lesions was observed (Bruhn *et al*, 1992a). Subsequent DTI studies described sparing of cortical GM in pediatric MS patients (Absinta *et al*, 2010; Tortorella *et al.*, 2006). Finally, pediatric MS compared with age-matched HC showed T_2 hypointensity in the head of the left caudate nucleus (Ceccarelli *et al*, 2011), reflecting iron deposition in this structure (Stankiewicz *et al*, 2007).

1.24 Atrophy and failure of age-expected brain growth

Different MRI technique have been adopted to quantify GM and WM atrophy, including structure segmentation and voxel-based methods. Voxel-based morphometry (VBM), spatially normalizing individual GM tissue maps allows group analysis of specific tissue densities at the voxel level. By warping an individual brain to a common template space, and calculating Jacobian determinant for each voxel of the deformation field, tensor-based morphometry (TBM), provides a measure of tissue growth or shrinkage in each voxel.

One of the first CNS structures known to be affected by atrophy in MS is the thalamus (Eshaghi *et al*, 2018a). Lesions in the basal ganglia and thalami on the initial MRI have been reported in 25 to 46% of children with MS (Dale *et al*, 2000; Mikaeloff *et al.*, 2004a). Isolated thalamic atrophy, with sparing of cortical GM and of the remaining deep GM, was observed by applying VBM in a cohort of 28 pediatric MS patients (Mesaros *et al*, 2008a). Thalamic atrophy thus identified, correlated with T_2 lesion volume, suggesting that it might at least in part be due to retrograde degeneration after axonal transection within lesions (Mesaros *et al.*, 2008a). A subsequent TBM study

(Aubert-Broche *et al*, 2011) confirmed these findings, showing significant volume loss in the pulvinar and anterior nuclei of the left and right thalami and in the splenium of the CC in pediatric MS patients compared to HC (Aubert-Broche *et al.*, 2011).

Interestingly, a recent longitudinal study (Fadda *et al*, 2019) showed the presence of another mechanism of thalamic injury, characterized by an evolving, surface-in pattern of atrophy. This type of damage was observed since the time of initial clinical presentation in children with MS but not in children with monophasic demyelination. Given its distribution, this damaging mechanism might be due to diffusible CSF factors that exert a neurotoxic action on thalamic neurons, and it might be peculiar of MS, compared to other inflammatory conditions.

A ROI analysis represents an alternative approach for the quantification of atrophy. By adopting this techniques, Kerbrat et al. (Kerbrat *et al*, 2012) observed lower global brain volume, after correction for skull size, and lower thalamic volume, after correction for global brain volume, in pediatric MS patients compared to HC. These results indicate an even greater loss of thalamic tissue relative to more global brain measures in pediatric MS. Moreover, they found an inverse correlation between T_2 lesion volume and both brain and thalamic atrophy, confirming a role of lesion-induced damage in determining GM atrophy in pediatric MS.

Longitudinal studies added more conclusive information. In a study by Yeh et al. (Yeh *et al.*, 2009c), the Authors investigated two cohorts of disease duration-matched pediatric- and adult-onset MS patients. After 20 years of disease duration, they found similar degrees of brain atrophy in the two groups. It is known that age leads to significant yearly increases in atrophy. Thus, the finding of similar brain volumes in the two disease-matched cohorts, despite pediatric-onset patients being about 15 years younger than adult-onset ones, likely indicates a higher rate of MS-related damage in the first group (Yeh *et al.*, 2009c). These results were confirmed in a subsequent study (Donohue *et al*, 2014) showing no differences of regional GM atrophy between pediatric- and adult-onset MS patients matched for disease duration. Moreover, in the same study, pediatric-onset MS patients were also compared to a different cohort of age-matched adult-onset patients. The second group had a shorter disease duration than the first, again showing an accelerated GM atrophy in the pediatric-onset cohort during the course of MS.

A longitudinal study conducted by Calabrese et al. (Calabrese *et al.*, 2012) analyzed brain cortex atrophy, in terms of GM fraction, in pediatric and adult patients with MS within 1 year from clinical onset and thereafter for 3 years. The longitudinal evaluation of the GM fraction showed reduction over time at similar rates in both cohorts, independently of patient age, WM lesion load, or WM lesion accumulation. These results suggest that neuronal loss proceeds linearly over time in all groups, and that MS should be considered a "simultaneous 2-component" disease in which GM degeneration proceeds largely independent of WM inflammation.

More recent studies investigated the complex interplay between brain growth and the disease-related neurodegenerative processes. Aubert-Broche and colleagues (Aubert-Broche *et al*, 2014b) demonstrated that the onset of MS during childhood and adolescence leads to reduced brain volume for two different reasons. First, MS impairs the brain growth that is observed in age-matched HC (ie, age-expected brain growth). Furthermore, MS leads to a progressive brain volume loss, due to active disease-related atrophy. The Authors also demonstrated a disproportionate atrophy of the thalamus, compared to the whole brain, and that both mechanisms of brain atrophy are active for the thalamus, as well.

Moreover, a study by Weier et al. (Weier *et al*, 2016) focused on the cerebellum showed that the negative impact of inflammation on age-expected brain growth is not just typical of MS, but it also occurs in monophasic ADS. These results confirm a direct pathogenetic role of the acute inflammatory process in inciting a reduction or block of brain growth during childhood. Furthermore, this study confirmed the existence of a second parallel phenomenon of neurodegeneration determining cerebellum volume reduction over time, similar to what was previously demonstrated for the whole brain and the thalamus.

1.25 Functional MRI

The macroscopic and microscopic structural damage detected by applying the above-mentioned MRI techniques only partially explains the clinical manifestation of MS (Filippi & Rocca, 2004; Filippi *et al*, 2003; Hesselink, 2006). The lack of direct correlation between structural damage and clinical phenotype could be explained by the individual capability of response to brain damage in term of both recovery from tissue

damage (spontaneous remyelination) and cortical plasticity (Tomassini *et al*, 2012). Brain plasticity, and the derived *functional reorganization,* relies on molecular and cellular mechanisms, including increased axonal expression of sodium channels, synaptic changes, increased recruitment of parallel existing pathways or "latent" connections, and reorganization of distant sites (Waxman, 1998). These molecular and cellular alterations induce changes in systems-level functional responses, which are the proximal effectors of perception, action and cognition. The application of functional MRI (fMRI), based on changes in the blood-oxygenation level dependent (BOLD) signal, provides an indirect measure of neural activity, thus representing a powerful tool to measure brain plasticity *in vivo*. The application of functional MRI (fMRI) has shown that plastic cortical changes do occur after central nervous system (CNS) WM injury of different etiology, that such changes are related to the extent of WM damage, and that they can contribute in limiting the clinical consequences of widespread disease-related tissue damage (Rocca & Filippi, 2006, 2007). Conversely, the failure or the exhaustion of the adaptive properties of the cerebral cortex might be among the factors responsible for the accumulation of "fixed" neurological deficits in MS patients (Rocca & Filippi, 2006, 2007). Two different paradigms of fMRI exist: task-dependent fMRI, requiring stimulus presentation; and resting-state (RS) fMRI, allowing to explore brain networks without performing any specific tasks.

This technique, widely adopted in adult MS patients has frequently been adopted also in pediatric MS patients in order to provide a deeper insight in a developing brain functional strategy against structural damage (see below).

1.26 Correlation with physical disability

In adult patients with CIS, the volume of T_2 lesions at the time of the initial demyelinating event poorly correlates with physical disability. However, when longitudinally studied, the rate of accumulation of T_2 lesions in the first 5 years of disease shows a positive correlation with subsequent physical disability (as measured by EDSS scores) 20 years later (Brex *et al*, 2002).

Correlative and predictive studies in patients with pediatric MS are extremely rare and provided inconclusive results. Indeed, no significant correlations were found between physical disability and WM lesion number (Mikaeloff *et al*, 2004b), DT and MT MRI

measures of WM and GM damage (Absinta *et al.*, 2010; Tortorella *et al.*, 2006) or thalamic atrophy (Mesaros *et al.*, 2008a).

Considering that physical disability is mainly driven by motor functioning, by using fMRI during an active motor task, two studies evaluated cortical activation patterns and functional connectivity of the motor system in pediatric MS patients (Rocca *et al*, 2009; Rocca *et al.*, 2010). Compared to age- and sex-matched HC, children with MS experienced increased activation of contralateral sensorimotor cortex (Rocca *et al.*, 2009). This increased fMRI activity showed significant correlation with T_2 lesion volume, suggesting that the increased contralateral activation observed could represent an adaptive mechanism against tissue damage. Furthermore, compared to HC, pediatric MS patients also experienced reduced functional connectivity between several regions belonging to the motor network, suggesting that this connectivity downregulation is likely represent a compensatory mechanism as a functional reservoir to upregulate with the accrual of tissue loss (Rocca *et al.*, 2009).

By adopting a similar approach, the second study analyzed effective connectivity abnormalities within the motor network in pediatric MS compared with adult-onset patients (Rocca *et al.*, 2010). and considered the influence of structural damage of CC and corticospinal tracts on connectivity (Rocca *et al.*, 2010). A preserved effective connectivity was observed in children with MS, while increased effective intrahemispheric and interhemispheric motor network connectivity in adult with MS. Moreover, these connectivity changes showed significant associations with microstructural changes within the CC and corticospinal tracts as measured by MD and FA. Considered together, these findings suggest that the brain plasticity or the functional reservoir might deplete over time thus leading to accrual of clinical disability.

Finally, a recent study by adopting a multimodal MRI approach by modeling voxel-wise measures of microstructural integrity of WM tracts and GM volumes with those of intra- and internetwork functional connectivity (FC) investigated the potential substrates of short-medium term adaptive mechanisms occurring in pediatric onset MS patients. Three groups of subjects were enrolled: pediatric onset MS patients in their early adulthood with no or minimal disability, age- and disability-matched adult onset MS patients, and HC. Although pediatric and adult onset MS patients showed a similar macroscopic damage, the Authors observed that pediatric onset MS patients had: (i)

increased lesion frequency and reduced WM integrity, as assessed by DTI, along the posterior corona radiate fibers of the corticospinal tract (CST), and (ii) reduced long-range FC involving default mode network (DMN), a relevant hub for cognitive functioning.

1.27 Correlation with cognitive impairment

Substantial portions of the following section have been published (Portaccio et al, 2021)

MRI techniques have contributed to improve the understanding of the mechanisms responsible for the accumulation of cognitive impairment in pediatric patients with MS.

First, lesion-induced damage plays a role. Higher lesion volumes were associated with cognitive impairment in pediatric MS patients (Rocca *et al*, 2014a). Moreover, anatomo-functional correlations were demonstrated. For instance, the salient involvement of linguistic abilities in the pediatric population (Amato *et al.*, 2008) is consistent with a higher infratentorial lesion burden, affecting the afferent and efferent cerebellar pathways in children. The latter, in turn, was demonstrated to significantly affect performance in vocabulary tests . Only one study (Rocca *et al.*, 2015b) explored the role of cortical lesions in determining cognitive impairment in this population, without finding any association. In another study (Maranzano *et al.*, 2019), frontal lobe cortical lesion count was associated with reduced manual dexterity in pediatric-onset MS patients.

However, the correlations between lesion burden and cognitive performance were only modest in pediatric MS patients. Thus, more advanced MRI technique were applied, aiming to understand the neuroanatomical substrate of cognitive impairment in pediatric MS. Till et al. (Till *et al*, 2011a) explored the relationship between academic functioning and WM integrity among children with MS compared with age and sex-matched HC. These Authors specifically analyzed math performances, since they are strictly related to efficient (information processing speed) IPS, working memory (e.g., carrying and borrowing digits), and visual-spatial processing (e.g., alignment of columns), all of which are commonly affected by pediatric MS. Difficulties in written arithmetic ability were observed in 26% of patients' cohort and they were significantly associated with abnormalities in DTI metrics across all segments of the CC and in right frontal and parietal regions. A subsequent study (Rocca *et al.*, 2014a) extended these findings,

associating cognitive impairment in pediatric MS patients with DT MRI abnormalities in posterior CC and cingulum as well as in bilateral parieto-occipital regions. Importantly, it should be underscored that – same as for GM atrophy – the abnormalities in NAWM might be attributed to either direct disease-related damage or failure of WM maturational processes, or a combination of both. As matter of fact, the onset of MS during childhood has proven to lead to failure of age-expected WM maturational processes (Longoni *et al.*, 2017). So far, MRI studies have not been able to separate these aspects.

Moreover, Till et al. (Till *et al*, 2011b) evaluated the correlation between normalized brain volume and volumes of key brain areas relevant for efficient information processing (including the thalamus and CC), with cognitive impairment in 35 patients with pediatric MS. Thalamic volume was found to account for significant incremental variance in predicting global IQ, processing speed, and expressive vocabulary and was the most robust MRI predictor of cognitive impairment relative to other MRI metrics. Till and colleagues also explored the association of executive dysfunction with structural MRI abnormalities in pediatric MS patients, finding significant correlations with thalamic atrophy together with whole brain and frontal lobe atrophy. Fuentes et al. applied quantitative brain volumetric measures to better understand the neural correlates of learning and memory functioning in children and adolescents with MS. The Authors found significant associations of word-list learning with whole brain volume and hippocampal volume, whereas visual recognition memory correlated with thalamic volume. These findings were further confirmed in a subsequent study showing association between thalamic and hippocampal volume with aspect of episodic memory performance.

Another structure that has been found to be determinant for cognition in pediatric MS is the amygdala, whose total volume appeared to be associated with a lower level of competency in functional communication skills in pediatric MS patients (Green *et al*, 2018). The analysis of the lateralized amygdala volumes revealed that the left amygdala was associated with both *functional communication* and *social skills*, consistent with literature suggesting the left amygdala has strong connections with emotional and language domains (Markowitsch, 1998). The volume of the amygdala appeared to be also associated with visual memory, as shown by the lateralized role of the right amygdala in memory for visual information (Markowitsch, 1998).

The hippocampus is known to play a major role in cognitive processes. However, only one study (Rocca *et al*, 2016b) investigated the role of hippocampal damage in determining cognitive impairment in pediatric MS. In details, compared to cognitively preserved, cognitively impaired pediatric MS patients experienced atrophy of the right hippocampus at the level of the subiculum and the dentate gyrus. Moreover, significant correlations were found between performance at tests of language expression and comprehension with atrophy of subicular region of the right hippocampal head, cornu ammonis 1 of the right hippocampal tail and the dentate gyrus of the left hippocampal body. Furthermore, better performances at tests of attention and phrase comprehension were associated with an increased volume of the dentate gyrus, bilaterally, suggesting that hypertrophy of this region might confer protection against the onset of cognitive deficits.

Moving to the cortex, atrophy of the precuneus was related with reduced cognitive performance in pediatric MS patients (Rocca *et al.*, 2014a). Indeed, this region is involved in a wide spectrum of highly integrated tasks, including visuospatial imagery, episodic memory, and self-processing operations (Absinta *et al.*, 2010).

Finally, the cerebellum represents a strategic node in various segregated networks (motor, coordination, cognitive–behavioral loops), showing multiple connections to and from different cortical areas of the forebrain, the thalamus, and the spinal cord. Within this framework, it is not surprising that cerebellar posterior lobe volume reduction can adversely impact cognitive function and especially information processing speed and vocabulary abilities in pediatric MS patients (Weier *et al*, 2015), which is consistent with the role of the posterolateral hemispheres of the cerebellum in cognitive processing.

The poor correlation observed between structural MRI measures and cognitive performance in pediatric MS patients suggested a role for brain plasticity and derived functional reorganization in determining cognitive functioning in pediatric MS patients.

Considering the difficulty to perform task-dependent studies in the pediatric population, only few studies adopting active paradigms have been conducted. A study conducted in cognitively preserved pediatric-onset MS aimed to assess the patterns of fMRI activity during the Alphaspan task (Barlow-Krelina *et al*, 2019), a working memory paradigm with two levels of executive control demand. Cognitively preserved youth and young adults with pediatric-onset MS demonstrate greater activation than HC in regions

implicated in executive control during a working memory task. These results support the hypothesis of increased brain activity as compensatory mechanism to maintain an adequate cognitive performance.

More frequent is the application of RS fMRI paradigm in pediatric population. The analysis of RS FC within brain networks disclosed that functional abnormalities of the posterior regions of default mode network (in particular precuneus) paralleled abnormalities detected by structural MRI in pediatric patients with cognitive impairment (Rocca *et al.*, 2014a; Rocca *et al*, 2014b). Focusing on the DMN, increased RS FC in the anterior cingulate cortex was described in cognitively preserved pediatric MS patients, while cognitively impaired pediatric MS patients showed reduced RS FC in the precuneus (Rocca *et al.*, 2014a). Moreover, a distributed pattern of RS FC abnormalities within large-scale neuronal networks occurs in pediatric MS patients and contributes to their cognitive status (Rocca *et al.*, 2014b).

The pattern of fMRI abnormalities found in pediatric patients with MS with cognitive impairment differs from that described in adult patients, in whom a consistent reduced RS FC of the anterior regions of the DMN (Absinta *et al.*, 2010; Bonavita *et al*, 2011) and an enhanced RS FC of the posterior ones have been described (Bonavita *et al.*, 2011; Roosendaal *et al*, 2010). It could be speculated that the maturation effects might influence a different functional reorganization in adult *vs* pediatric patients with MS. Indeed, the long-range connections between the posterior cingulate cortex and the anterior prefrontal cortex have been shown to mature with age (being immature in 7-year-old children) (Fair *et al*, 2007; Supekar *et al*, 2010), and to be associated with the development of cognitive abilities (Paus, 2005).

Similar to structural imaging, the cerebellum is another region whose RS FC plays a major role in determining cognitive functioning in pediatric MS patients. Indeed, compared to both HC and cognitively preserved pediatric MS patients, cognitively impaired patients showed a widespread reduction of RS FC, not only between the dentate nucleus and the basal ganglia, but also between the dentate nucleus and bilateral regions located in the parietal, frontal and temporal lobes (Cirillo *et al*, 2015).

2. AIMS OF THE WORK

Conventional and advanced MRI techniques will be applied in pediatric MS patients in both cross-sectional and longitudinal settings, with the aim to unravel the pathogenetic mechanisms of disease, identify the neuroanatomical bases of cognitive impairment, understand the impact of disease onset during developmental age and describe long-term prognosis along with prognostic factors.

Specific aims of the present PhD project will be:

1) *Cross-sectional settings (or at baseline in longitudinal studies).* Comparisons will be performed in pediatric MS patients *vs* HC and in pediatric MS patients grouped by their cognitive performance, disability level or age at disease onset:
    i. to describe sustained attention system activity by using fMRI during the CCPT;
    ii. to assess the role of sustained attention system activity abnormalities in determining cognitive impairment;
    iii. to clarify the role of network structural abnormalities on fMRI findings by using DTI;
    iv. to identify GM regions whose volume showed significant deviations from normative data in pediatric MS patients;
    v. to test the outside-in CSF-mediated mechanism of damage investigating microstructural integrity disruption and demyelination in the whole thalamus and thalamic WM and in their segmented portions as a function of distance from CSF, using DTI measures and T1/T2 ratio;
    vi. to investigate the relationship between thalamic abnormalities with brain WM lesions and cortical thickness;
    vii. to identify distinguishing baseline features of pediatric MS patients experiencing long-term disability worsening;
    viii. to identify distinguishing baseline features of pediatric MS patients with disease onset before and after the pubertal age.

2) *Longitudinal settings.*

i. to assess the regional trajectories of GM volume modifications in pediatric patients with MS compared to those of normally developing children;

ii. to explore the correlation between GM volume changes observed in pediatric MS patients with clinical disability and IQ;

iii. to identify early (at disease onset and within the first 2 years of disease) clinical and MRI predictors of disease course in pediatric MS patients;

iv. to describe and compare the natural history of the disease and to determine prognostic factors for long-term disability in a large cohort of pediatric MS patients with pre- and post-pubertal onset.

3. Characterization of pediatric MS by using advanced MRI technique in cross-sectional and longitudinal setting

3.1 MRI substrates of sustained attention system and cognitive impairment in pediatric MS patients

The following data have been published (De Meo *et al.*, 2017).

MRI substrates of sustained attention system and cognitive impairment in pediatric MS patients

Ermelinda De Meo, MD
Lucia Moiola, MD
Angelo Ghezzi, MD
Pierangelo Veggiotti, MD
Ruggero Capra, MD
Maria Pia Amato, MD
Elisabetta Pagani, MSc
Agnese Fiorino, PhD
Lorena Pippolo, MD
Maria C. Pera, MD
Giancarlo Comi, MD
Andrea Falini, MD
Massimo Filippi, MD
Maria A. Rocca, MD

Correspondence to
Dr. Rocca:
rocca.mara@hsr.it

ABSTRACT

Objective: To explore the structural and functional integrity of the sustained attention system in patients with pediatric multiple sclerosis (MS) and its effect on cognitive impairment.

Methods: We enrolled 57 patients with pediatric MS and 14 age- and sex-matched healthy controls (HCs). Patients with >3 abnormal tests at neuropsychological evaluation were classified as cognitively impaired (CI). Sustained attention system activity was studied with fMRI during the Conners Continuous Performance Test (CCPT). Structural integrity of attention network connections was quantified with diffusion tensor (DT) MRI.

Results: Within-group analysis showed similar patterns of recruitment of the attention network in HCs and patients with pediatric MS. Diffuse network DT MRI structural abnormalities were found in patients with MS. During CCPT, with increasing task demand, patients with pediatric MS showed increased activation of the left thalamus, anterior insula, and anterior cingulate cortex (ACC) and decreased recruitment of the right precuneus compared to HCs. Thirteen patients (23%) were classified as CI. Compared to cognitively preserved patients, CI patients with pediatric MS had decreased recruitment of several areas located mainly in parietal and occipital lobes and cerebellum and increased deactivation of the ACC, combined with more severe structural damage of white matter tracts connecting these regions.

Conclusions: Our results suggest that the age-expected level of sustained attention system functional competence is achieved in patients with pediatric MS. Inefficient regulation of the functional interaction between different areas of this system, due to abnormal white matter integrity, may result in global cognitive impairment in these patients. *Neurology*® 2017;89:1265–1273

Introduction

Sustained attention represents a key executive function, underlying higher attentional processes (divided and selective attention) and global cognitive functioning (Sarter *et al*, 2001), whose functional maturation occurs during late childhood and adolescence, as demonstrated by fMRI (Rubia *et al*, 2010) and electroencephalography (EEG) (Segalowitz *et al*, 2010; Travis, 1998) investigations. In this perspective, the onset of MS in this critical age may have important and distinct consequences for cognitive abilities.

To evaluate sustained attention and cognitive control capabilities and their maturation during the developmental age, the CCPT has been frequently used (Fortenbaugh *et al*, 2017). Using fMRI during a sustained attention task (Smith *et al*, 2011), one previous study investigated brain functional changes between childhood and adulthood, describing an increased activation with development in fronto-temporo-parieto-cerebellar regions that mediate sustained attention, confirming a continued functional development of these regions throughout childhood to mid-adulthood.

Recent preliminary evidence in pediatric MS patients have resulted in the hypothesis that the disease may influence the maturation of brain structures. Using volumetric MRI, a longitudinal study showed a failure of age-expected brain growth in these patients (Aubert-Broche *et al.*, 2014b). A DT MRI study found impaired maturation of WM tracts in patients with very early onset disease (Rocca *et al.*, 2016c).

By applying an active fMRI paradigm aimed at testing sustained attention and executive functions, this study investigates the recruitment of the sustained attention system with increasing task demand in pediatric MS patients in comparison to age- and sex-matched HC to assess whether and how MS onset during childhood compromises this functional network. Starting from the consideration that abnormalities in sustained attention are frequently associated to behavioral, learning, emotional and cognitive difficulties in adolescence and that attention is one of the most frequent areas of impairment in pediatric MS patients (Amato *et al.*, 2016), we investigated the relationship between cognitive impairment and sustained attention system recruitment abnormalities in these patients. To clarify the role of network structural abnormalities on fMRI findings, we also quantified structural integrity of the connections between brain regions relevant to the task, using DT MRI.

Materials and Methods

Ethics committee approval. Approval was received from the local ethical standards committee on human experimentation, and written informed consent was obtained from all participants and their parents prior to study enrolment.

Participants. We enrolled 57 consecutive, right-handed, pediatric patients with RR MS referred to specialized centers for the diagnosis of pediatric MS. Inclusion and exclusion criteria are reported in Appendix e-1. Fourteen sex- and age-matched HC with no previous history of neurological dysfunction and a normal neurological examination served as the control group.

Clinical and neuropsychological assessment. All patients underwent a neurological examination with rating on the EDSS and a neuropsychological assessment using a Neuropsychological Battery for Children, standardized and validated for an Italian pediatric population with MS (see **Appendix e-3.1.1**) (Amato *et al.*, 2008; Portaccio *et al*, 2009). Global premorbid cognitive functioning with IQ was assessed through the Wechsler Intelligence Scale for children (WISC-R) (Wechsler, 1974). Patients with an abnormal performance in three or more tests were classified as cognitively impaired (CI) (Amato *et al.*, 2008). As previously described (Sepulcre *et al*, 2006), z-scores (based on a population of pediatric HC matched for age and education) (Fuentes *et al*, 2012) for each of the previous domains and a global z-score of cognitive function (obtained by averaging z-scores of all tests) were calculated.

fMRI experimental design. The computerized version of the CCPT was implemented with the Presentation software (www.neuro-bs.com, version 14.8), as described in details in **Appendix e-3.1.1**. All participants were trained to perform the task before MRI acquisition. Percentages of correct and incorrect responses as well as reaction times (RT) were recorded. All participants completed the fMRI acquisition without interruptions.

MRI acquisition and analysis. **Appendix e-3.1.1** provides a detailed description of the MRI acquisition and analysis protocol. From all participants, the following sequences were obtained: 1) T_2^*-weighted single-shot echo-planar imaging (EPI) scan during the CCPT task (SPM12); 2) DT MRI scan; 3) dual-echo (DE) turbo spin-echo (TSE) scan and 4) 3D T_1-weighted fast field echo (FFE) scan. T_2 hyperintense and T_1

hypointense lesion volumes (LV) were measured on the DE TSE and 3D T1-weighted scans using a local thresholding segmentation technique (Jim 6, Xinapse Systems). Normalized brain (NBV), white (WMV) and gray matter (GMV) volumes were measured on the 3D T_1-weighted scans using the SIENAx software, after T_1-hypointense lesion refilling (Chard *et al*, 2010).

Analysis of DTI data (FSL software) focused on tracts connecting brain regions identified by fMRI analysis as key regions involved in CCPT performance, using an approach similar that applied by previous authors (Aron *et al*, 2007; Bonnelle *et al*, 2012). Tracts were generated between 3-mm radius ROI based on the peak activation or deactivation during the CCPT from HC. Fourteen ROI were used and all possible combinations between them were explored. To overcome the problems associated with probabilistic tractography due to WM lesions, tract probability maps were obtained from the HC group and then back-projected in individual space in order to obtain a mean FA value per tract for all the study participants (Hua *et al*, 2008).

Statistical analysis. Between-group comparisons of clinical, demographic and structural MRI parameters were performed using the Pearson chi square test, Mann-Whitney U-test or Kruskal-Wallis test adjusted for age and sex and corrected for multiple comparisons, as appropriate. CCPT performance was compared between groups using an ANOVA, adjusted for age and sex.

A second-level analysis with SPM12 was performed to assess: 1) the average fMRI activation and deactivation during the CCPT (i.e., average activation of the ISI-1, ISI-2 and ISI-4 conditions) and the load effect in HC and pediatric MS patients (as a whole, and according to the presence/absence of cognitive impairment) (one-sample t-test); 2) the differences in fMRI activation between study groups (two-sample t-test and full factorial models, age and sex adjusted); and 3) the correlation between fMRI activity during the load condition and behavioral (accuracy, RT), clinical (EDSS, disease duration), neuropsychological (global z-score of cognitive performance and z-scores of single cognitive domains, including attention) and structural MRI variables (T_2 LV, atrophy and FA measures) (multiple regression models, adjusted for age and sex; one separate model for each variable).

To assess the fMRI abnormalities in a given patient group *vs* the others included in the full factorial models, we performed a conjunction analysis (Friston *et al*, 1995a),

which, by testing for the conjunction of different hypotheses (each described as a contrast), allows to identify where several fMRI clusters were jointly significant, by evaluating the significance of combined contrasts.

Results were tested both at $p < 0.001$ uncorrected, and at $p < 0.05$, family-wise error (FWE) corrected.

Results

Clinical, neuropsychological and structural MRI measures. **Table 3.1.1** summarizes the main demographic, clinical, and structural MRI measures of pediatric MS patients and HC. Compared to HC, pediatric MS patients had lower NBV (p=0.01), GMV (p=0.02) (**Table 3.1.1**) and FA values in all tracts analyzed (**Table e-3.1.1**). Thirteen (23%) pediatric MS patients were classified as CI. One MS patient scored <70 at IQ and 16 scored in the inferior range (<90). **Table 3.1.2** summarizes the results of the neuropsychological evaluation in MS patients. Thirty-six percent of CI and none of cognitively preserved (CP) patients had impairment at attention tests. Compared to CP, CI MS patients had longer disease duration (p=0.03), lower NBV (p=0.03), lower WMV (p=0.01) and lower FA values in the tracts connecting the left anterior insula to the anterior cingulate cortex (ACC) (p=0.01) and precuneus (p=0.04) (**Table e-3.1.1**).

CCPT fMRI task performance. During fMRI, CCPT performance (percentage of correct and incorrect responses, RT) did not differ between pediatric MS patients and HC. Compared to CP, CI MS patients had significantly worse performance (Figure e-3.1.1).

CCPT Task related activations/deactivations. **Table e-3.1.2** and **Figure 3.1.1** report brain regions significantly activated/deactivated during the CCPT task load condition in HC and pediatric MS patients. Similar fMRI patterns were detected during the ISI-1, ISI-2 and ISI-4 conditions, but with different t values (data not shown). Both groups showed task-related activations in bilateral precentral cortex, supplementary motor area (SMA), inferior parietal lobule (IPL), middle temporal gyrus (MTG), insula, basal ganglia and cerebellum as well as the right inferior frontal gyrus (IFG), middle frontal gyrus (MFG) and calcarine cortex. Both groups also showed deactivations in bilateral occipital cortex and in regions usually described as part of the DMN, bilaterally, including the precuneus, angular gyrus, superior temporal gyrus (STG), MFG (mesial part) and superior frontal gyrus (SFG).

Compared to HC, pediatric MS patients showed an increased activation of the left thalamus and left anterior insula and decreased deactivation of the left ACC. Compared to HC, MS patients also showed an increased deactivation of the right precuneus (Figure 1).

Effect of cognitive impairment. **Table e-3.1.3** reports brain regions significantly activated/deactivated during the CCPT task load condition in CP and CI MS patients, separately. **Table e-3.1.4** and **Figure 3.1.2** show the results of between-group comparisons.

During the CCPT load condition, compared to HC, CP MS had an increased activation of the left anterior insula and thalamus and a decreased deactivation of the ACC and right IFG. Compared to HC, CP MS patients also showed an increased deactivation of the right precuneus and superior parietal lobule (SPL).

Compared to HC, CI MS patients experienced decreased activation of the right PoCG and increased deactivation of bilateral precuneus. Compared to CI, CP pediatric MS patients had an increased recruitment of several areas mainly located in the parietal and occipital lobes and cerebellum (**Table e-3.1.4**). They also experienced a decreased deactivation of the ACC.

The conjunction analysis identified the left anterior insula and ACC as areas significantly more activated with increasing task difficulty in CP MS patients in comparison to the other study groups. Compared to HC and CP patients, CI MS patients had lower recruitment of the right PoCG, right lingual gyrus, right precuneus, left IPL and left SFG.

Analysis of correlations. In pediatric MS patients, significant correlations ($p<0.001$ uncorrected, **Table 3.1.3**) were found between:

increased activation of the left thalamus and lower GMV, higher global cognitive performance z-scores and higher z-scores in attentive-executive function domain;

increased deactivation of the right precuneus and higher number of incorrect responses at CCPT and lower FA value of the tract connecting the left anterior insula to ACC.

No correlations were found between fMRI findings and T_2 LV as well as performance at the remaining cognitive domains.

Discussion

Here, we applied an active fMRI paradigm to explore the functional competences of the sustained attention network in a relatively large cohort of pediatric MS patients, who underwent a standardized MRI protocol at high magnetic field, and a validated neuropsychological assessment. Since CI in these patients typically affects multiple domains, its definition is usually based on the number of failed tests at extended neuropsychological batteries (Amato *et al.*, 2016). In line with the literature (Amato *et al.*, 2016), more than 30% of our CI pediatric MS patients was impaired at attention tests. Despite this could represent a limitation for our study that was mainly focused on sustained attention, it has to be considered that sustained attention is needed for global cognitive functioning (Sarter *et al.*, 2001) and that only some of its subprocesses are explored by attention tests usually performed (Egeland & Kovalik-Gran, 2010). To explore the functional competence of the attention system in pediatric MS patients, we investigated the correlations between fMRI findings and CCPT performance during fMRI acquisition as well as z-score of the attentional domain. Regretfully, we could not obtain neuropsychological data from our sample of pediatric HC.

Despite we enrolled only a relatively small number of HC (thus resulting in limited pieces of information on normal variability of fMRI features of typically developing youth), the pattern of functional recruitment of the sustained attention network we found at within-group analysis in pediatric HC and MS patients resembled that described by previous studies in HC and patients with other neurological diseases using a similar fMRI paradigm (Strazzer *et al*, 2015; Tana *et al*, 2010), and was characterized by a distributed activation of regions located in the frontal, temporal, parietal and occipital lobes, and the cerebellum, all contributing to different aspects of sustained attention. The temporal lobes and parietal cortex mainly integrate polymodal pieces of information involved in exogenous stimuli processing, whereas frontal regions and the cerebellum play a role in reorientering attention to an exogenous stimulus. We also detected a consistent deactivation of regions usually described as part of the DMN (Raichle *et al*, 2001), a network of regions characterized by high activity at rest and low activity during cognitive tasks with focused attention on the external environment. Even if a longitudinal design is needed to confirm our hypothesis, these results suggest the achievement of the age-expected level of functional maturation of the network in pediatric

MS patients, in terms of ability to activate and deactivate the main regions of the network and topographical representation of these regions.

With increasing CCPT demand, compared to HC, pediatric MS patients showed an increased activation of the left thalamus, anterior insula and ACC. They also experienced an increased deactivation of the precuneus. Several studies have demonstrated that the basal ganglia, in particular the thalamus, play a crucial role in executive or supervisory mechanisms of attention, including regulation, error monitoring or processing and sustained vigilance (Fan *et al*, 2008; Posner *et al*, 2007). In adult patients (mean age at evaluation around 19 years) with disease onset during childhood, a recent study (Akbar *et al*, 2016a) found that a greater activation of the thalamus in patients in comparison to HC during an information processing speed task correlated with better task performance, whereas a RS functional connectivity (FC) study of the DMN found a reduced FC of the thalamus, which was associated with thalamic atrophy (Akbar *et al*, 2016c). In our pediatric MS patients, increased thalamic recruitment during the CCPT task correlated with preserved cognitive performance (particularly with preserved performance in attentive-executive functions) and with more pronounced GM atrophy. Combined with the results of the previous studies (Akbar *et al.*, 2016a; Akbar *et al.*, 2016c), these data suggest that thalamic functional abnormalities tend to occur relatively early in the course of the disease as a possible response to disease-related structural damage, in the attempt to preserve cognitive abilities.

Compared to HC, pediatric MS patients had also higher recruitment of the anterior insula and ACC. Also in this case, such activation helped to distinguish CP MS patients from the other two study groups. The anterior insula and ACC are among the key regions of the 'salience' network, which functions to identify the most relevant among several internal and extra-personal stimuli to guide behavior (Seeley *et al*, 2007). Network-analysis studies have consistently demonstrated that these two regions are involved in switching between brain networks (particularly the executive control and DMN) across task paradigms (Chen *et al*, 2016; Menon & Uddin, 2010). Based on this, a model has been proposed that posits that the core function of the anterior insula is to first identify stimuli from the vast and continuous stream of sensory stimuli that impact the senses, and then facilitate task-related information processing by initiating appropriate transient control signals to engage brain areas mediating attention, working memory, and higher

order cognitive processes, while disengaging the DMN. The ACC is involved in a variety of monitoring, decision-making, and cognitive control processes (Dosenbach *et al*, 2007). Starting from these considerations, the increased recruitment of the insula and ACC detected in CP pediatric MS patients may represent a key compensatory mechanism for efficient detection of important environmental stimuli and attention shift towards or away from internal cues, to maintain adequate performance during a sustained attention task. Supporting this hypothesis, we found higher integrity of the WM tracts connecting the left anterior insula to the ACC and precuneus in CP compared to CI MS patients.

Concomitantly with the presence of areas with increased activation in pediatric MS patients, we also detected a decreased activation of nodal regions of the DMN, such as the precuneus and SPL, which was due to a higher deactivation in patients in comparison to controls. This is likely to reflect a maladaptive mechanism in pediatric MS patients, since it was more pronounced in patients with cognitive impairment and correlated with a poorer performance (higher number of errors) during the CCPT execution. Interestingly, while CP MS patients experienced an increased deactivation of the right precuneus only, CI MS patients had a bilateral deactivation of this region. Combined with the previous findings (increased recruitment of the ACC in CP MS patients), these results suggest that an initial increased deactivation of the precuneus together with a reduced deactivation of the ACC, as experienced in CP MS patients, may represent a compensatory mechanism allowing the patients to maintain an adequate cognitive profile. With disease progression (as reflected by the longer disease duration of CI MS patients) and accumulation of WM damage (as reflected by decreased FA values in connecting WM tracts in CI MS patients), a more extended pattern of deactivation (involving the precuneus and SFG), was detected, which represents a maladaptive mechanism of cortical reorganization, characterized by an alteration of the shift from RS condition to sustained attention task performance.

Our results confirm the role of abnormalities of the DMN, in particular of its posterior node centered in the precuneus, in determining cognitive dysfunction in pediatric MS patients. That the precuneus might be among the first regions affected by the disease in these patients is in line with previous studies (Akbar *et al*, 2016b; Rocca *et al.*, 2014a) which, by integrating measures derived from structural and functional MRI techniques, have demonstrated functional abnormalities at this level, which tended to co-

localize with altered structural integrity. Similar to the current findings, a previous RS fMRI study found structural and functional MRI abnormalities of the posterior node of the DMN in CI pediatric MS patients and increased RS FC of the ACC in CP patients (Rocca *et al.*, 2014a). A reduced capability to modulate DMN deactivation with increasing task complexity has been also demonstrated by studies in adult patients with MS (Morgen *et al*, 2007; Rocca *et al*, 2014c).

Recent theories, which tend to view the brain as a complex dynamic network, have postulated that abnormalities of interaction over time between the posterior core of the DMN and fronto-parietal and subcortical networks, in particular the salience network, might help to explain deficits of cognitive processes after brain damage (Bonnelle *et al.*, 2012; Chen *et al.*, 2016; Leech & Sharp, 2014; Menon & Uddin, 2010). The correlation we found between functional abnormalities of these networks and disruption of structural integrity of critical WM tracts within the networks (in particular the tract connecting the left anterior insula to the ACC) suggests that in patients with pediatric MS, the accumulation of disease-related structural damage might cause a disconnection syndrome resulting in functional and clinical abnormalities. Clearly, longitudinal studies, possibly enrolling very young participants, are now needed to prove such a hypothesis.

Table 3.1.1. *Main demographic, clinical and structural MRI characteristics and Conner's Continuous Performance Test (CCPT) performance of healthy controls and pediatric patients with multiple sclerosis (MS), as a whole and according to the presence/absence of cognitive impairment.*

	Healthy Controls	**Pediatric MS patients**	***p* values**	**CP MS patients**	**CI MS Patients**	***p* values**
Number of participants	14	57	-	44	13	-
Girls/Boys	8/6	36/21	**0.17	30/14	6/7	**0.40
Mean age (range) [years]	13.6 (8.8-17.9)	15.0 (7.6-18.0)	0.12	15.2 (11.1-18.0)	15.1 (7.6-17.7)	0.58
Median EDSS (range)	-	1.0 (0.0-4.0)	-	1.0 (0.0-4.0)	1.5 (0.0-4.0)	0.37
Median disease duration (range) [years]	-	1.7 (0.1-8.1)	-	1.4 (0.1-6.8)	3.5 (0.2-8.1)	0.03
Mean T_2 LV (SD) [ml]	-	6.0 (7.8)	-	4.2 (5.2)	9.6 (11.6)	0.26
Mean T_1 LV (SD) [ml]	-	3.7 (5.0)	-	2.6 (3.0)	6.5 (8.6)	0.31
Mean NBV (SD) [ml]	1728 (74)	1660 (79)	0.01	1674 (68)	1612 (88)	0.03
Mean GMV (SD) [ml]	882 (67)	830 (55)	0.02	835 (55)	808 (59)	0.12
Mean WMV (SD) [ml]	846 (37)	830 (48)	0.43	839 (38)	803 (46)	0.01
Mean L Anterior Insula/ACC FA (SD)	0.54 (0.02)	0.51 (0.04)	0.02	0.52 (0.03)	0.47 (0.04)	0.01
Mean L Anterior Insula/Precuneus FA (SD)	0.48 (0.05)	0.42 (0.14)	0.04	0.47 (0.10)	0.29 (0.22)	0.04
Mean CCPT correct responses (range) [%]	95 (82-100)	93 (84-100)	0.21	94 (88-100)	93 (87-98)	0.04
Mean CCPT Reaction Time (SD) [ms]	0.4 (0.1)	0.4 (0.1)	0.55	0.4 (0.6)	0.4 (0.7)	0.41

**Mann Whitney U test; **Chi square test.*
Abbreviations: MS=multiple sclerosis; CI=cognitively impaired; CP=cognitively preserved; EDSS=Expanded Disability Status Scale; LV=lesion volume; SD=standard deviation; NBV=normalized brain volume; GMV=gray matter volume; WMV=white matter volume; L=left; ACC=anterior cingulate cortex; FA=fractional anisotropy.

Table 3.1.2. *Neuropsychological tests from patients with pediatric MS.*

	All pediatric MS patients	**Pediatric CP MS patients**	**Pediatric CI MS patients**
[a]Education (years)	8.7 (2.0)	8.6 (1.9)	8.8 (2.4)
[a]Global IQ	97.8 (18.5)	99.2 (18.4)	92.6 (19.1)
[a]CDI	7.9 (5.8)	7.6 (5.7)	8.6 (6.4)
[a]FSS	27.1 (12.1)	27.4 (11.6)	26.0 (14.2)
Memory			
[b]SRT-LTS	0.08 (1.33)	0.38 (1.03)	-1.01 (1.73)
[b]SRT-CLTR	0.07 (1.17)	0.39 (0.95)	-1.08 (1.18)
[b]SRT-D	0.02 (1.26)	0.30 (0.89)	-0.96 (1.84)
[b]SPART	-0.30 (1.88)	0.15 (1.59)	-1.87 (2.05)
[b]SPART-D	-0.23 (1.44)	0.05 (1.19)	-1.19 (1.84)
Abstract/conceptual reasoning			
[b]MCST	-0.31 (1.39)	-0.16 (1.37)	-0.89 (1.44)
Attention/concentration			
[b]SDMT	-0.20 (0.99)	-0.07 (0.99)	-0.66 (0.87)
[b]TMT-A	-0.27 (1.18)	0.01 (0.94)	-1.26 (1.47)
[b]TMT-B	-0.40 (1.46)	0.00 (0.96)	-1.82 (2.05)
Language			
[b]Semantic verbal fluency test	-0.25 (0.84)	-0.13 (0.81)	-0.65 (0.86)
[b]Phonemic verbal fluency test	-0.24 (0.85)	-0.13 (0.89)	-0.65 (0.58)
IPT	NA	NA	NA
[b]PCT	-0.58 (5.74)	-0.38 (6.24)	-1.30 (3.61)
[b]Token test	-0.88 (1.46)	-0.86 (1.35)	-0.97 (1.88)
[b]ODT	-0.48 (1.31)	-0.27 (1.05)	-1.24 (1.84)

[a]Mean values and standard deviations (SD).
[b]z-scores and SD based on a population of pediatric healthy controls matched for age and education (Amato et al., 2008)
MS=multiple sclerosis; IQ=intelligence quotient; CDI=children depression inventory; FSS=fatigue severity scale; SRT-LTS=selective reminding test long-term storage; SRT-

CLTR=selective reminding test consistent long-term retrieval; SPART=10/36 spatial recall test; SDMT=symbol digit modalities test; TMT-A/B=trail making test A/B; SRT-D=selective reminding test delayed; SPART-D=10/36 spatial recall test delayed; MCST=modified card sorting test; IPT=indication of pictures test; PCT=phrase comprehension test; ODT=oral denomination test; NA: not applicable.

Table 3.1.3. *Brain regions showing significant correlations between fMRI activations/deactivations during the Conner's Continuous Performance Test (CCPT) load condition with clinical, neuropsychological and structural MRI variables in pediatric multiple sclerosis patients (multiple regression models adjusted for age and sex; $p < 0.001$ uncorrected).*

Variables	**CCPT load activations**		**CCPT load deactivations**	
	Brain regions	**R**	**Brain regions**	**R**
GMV	L Thalamus	-0.57	-	-
L Anterior insula/L ACC FA			R Precuneus	-0.55
CCPT incorrect responses	-	-	R Precuneus	-0.53
Global cognitive z-score	L Thalamus	0.63	-	-
z-score of attentive-executive functions	L Thalamus	0.49	-	-

Abbreviations: L=left; R=right; WMV=white matter volume; GMV=gray matter volume; FA=fractional anisotropy; ACC=anterior cingulate cortex.

Figure 3.1.1. *fMRI patterns of activation and deactivation during CCPT in HC and pediatric MS patients.*

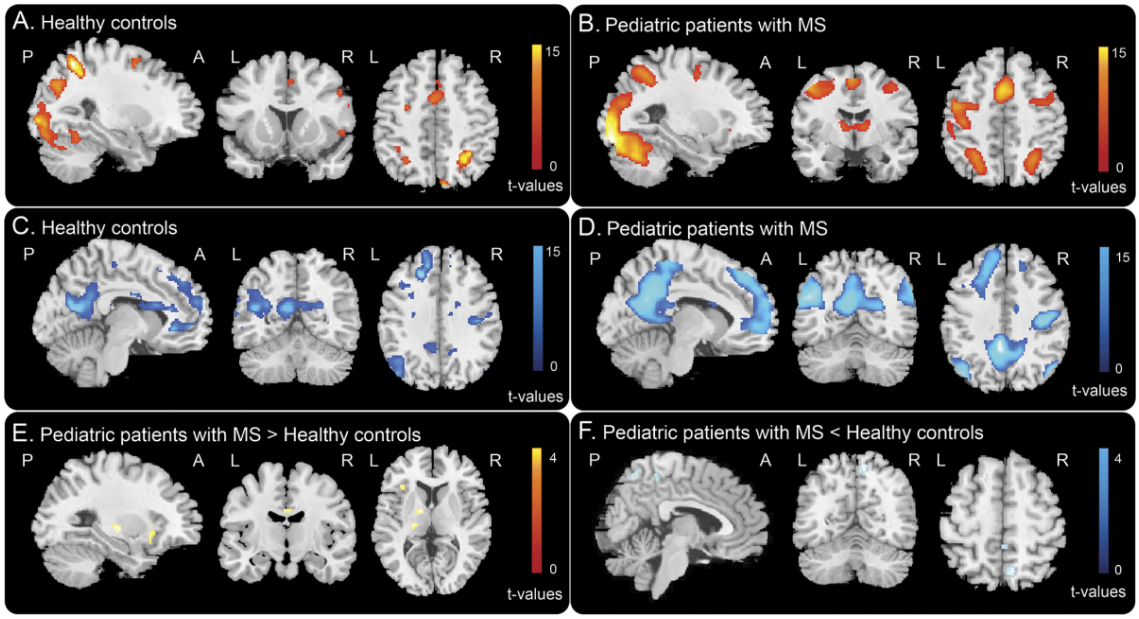

Brain regions showing linearly increasing functional magnetic resonance imaging (fMRI) activations (A, B) and deactivations (C, D) with increasing Conner's Continuous Performance Test (CCPT) difficulty in healthy controls (HC) (A, C) and pediatric patients with multiple sclerosis (MS) (B, D) (one-sample t-tests, $p < 0.001$ uncorrected). Areas showing increased activation with increasing CCPT load in pediatric MS patients versus healthy controls are shown in E, while brain areas showing reduced activation are shown in F. Images are displayed with the neurological convention (De Meo et al., 2017).
Abbreviations: A=Anterior; P=posterior; L=left; R=right.

Figure 3.1.2. *fMRI patterns of activation and deactivation during CCPT in CP and CI pediatric MS patients.*

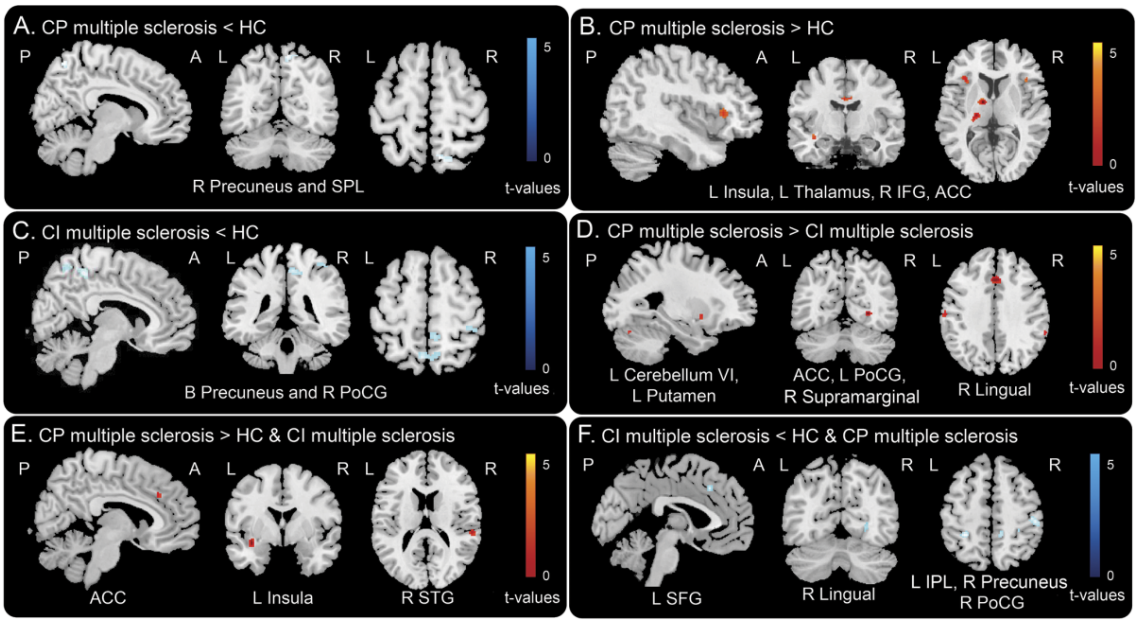

Brain regions showing significantly different fMRI activations and deactivations with increasing Conner's Continuous Performance Test (CCPT) difficulty in cognitively preserved (CP) and cognitively impaired (CI) patients with multiple sclerosis (MS). Results are shown at $p < 0.001$, uncorrected. Images are displayed with the neurological convention (De Meo et al., 2017).
Abbreviations: A=Anterior; P=posterior; L=left; B=bilateral; R=right; MS=multiple sclerosis; CP=cognitively preserved; CI=cognitively impaired; HC=healthy controls PoCG=postcentral gyrus; SPL=superior parietal lobule; IPL=inferior parietal lobule; MCC=middle cingulate cortex; SFG=superior frontal gyrus; IFG=inferior frontal gyrus.

Appendix e-3.1.1

Inclusion and exclusion criteria. Patients with acute disseminated encephalomyelitis were excluded according to published operational criteria (Krupp *et al.*, 2013). None of the patients had a diagnosis of clinically isolated syndrome at the time of study inclusion and all of them had at least two clinical attacks and the formation of new CNS lesions seen on serial MRI, according to revised McDonald's diagnostic criteria (Polman *et al.*, 2011). Whenever needed, appropriate genetic testing was performed to exclude leukodystrophies. MS patients had to be relapse- and steroid-free for at least three months prior to the study. Exclusion criteria were concomitant therapy with antidepressants, psychoactive drugs, or a history of other primary neurological or medical disorders in addition to MS. Participants judged by their neurologist to have primary psychiatric impairment in addition to their MS were also excluded.

Neuropsychological assessment. All patients underwent a neuropsychological assessment using a Neuropsychological Battery for Children, standardized and validated for an Italian pediatric population (Amato *et al.*, 2008), which included: a) global cognitive functioning with IQ assessed through the Wechsler Intelligence Scale for children (WISC-R) (Wechsler, 1974); b) verbal learning and delayed recall with the Selective Reminding Test (SRT, SRT-Delayed); c) visuospatial learning and delayed recall with the Spatial Recall Test (SPART, SPART-Delayed); d) attention and concentration with the SDMT and the Trail Making Test (TMT-A and TMT-B); e) abstract reasoning through the Modified Card Sorting Test; f) expressive language through a Semantic and Phonemic verbal fluency test and an Oral Denomination test; and g) receptive language using the Token test, the Indication of Pictures from the Neuropsychological Examination for Aphasia, and the Phrase Comprehension test from the Battery for the Analysis of Aphasic Deficits. The 5th or 95th percentile of the corrected scores of a population of pediatric HC matched for age and education was used as the cut-off values for determining failure in a given test (Amato *et al.*, 2008).

Depression and fatigue were self-assessed by patients and controls using the Children Depression Inventory (Kovacs *et al*, 1988) and the Fatigue Severity Scale (Krupp *et al*, 1989). Both neurological and neuropsychological assessments were performed within three days of the MRI study by an experienced observer blinded to the MRI results.

fMRI experimental design. The computerized version of the Conners' Continuous Performance Test (CCPT) (Homack & Riccio, 2006) was implemented with the Presentation software (www.neuro-bs.com, version 14.8). Stimuli consisted of alphabetical letters, presented in a pseudo-randomized sequence, one at a time, at the centre of the MRI screen. Letters were black on a white background. Stimuli were back-projected in the scanner room onto a screen, which the subjects viewed through a standard mirror system located on the scanner's head coil. A four-button response-box, held with the right-hand, was used to record responses. Subjects were given standardized instructions to respond as fast as possible whenever a letter other than X appeared and to withhold the response when the letter X was shown. The total number of presented stimuli was 252, and every stimulus remained on the screen for 500 ms (stimulus duration). The probability of the infrequent stimulus (X) was set at 14.3% (n=36). The test was administered in 6 stimulation blocks, each lasting 98 seconds. Each block consisted of three sub-blocks, in which stimuli were presented in random order with different inter-stimulus intervals (ISI) (fixed at 1, 2 and 4 seconds, respectively). Blocks were interleaved by rest periods, during which a meaningless image (randomly oriented geometrical lines) was shown to the subjects for 20 seconds. The total experiment duration was 11.8 minutes.

MRI acquisition. Using a 3.0 Tesla (Philips Intera) scanner, the following sequences of the brain were acquired from all subjects during a single session: a) T2*-weighted single-shot EPI sequence during the CCPT task (repetition time [TR]/echo time [TE]=2000/30 ms; flip angle=85°; field of view=240 mm2; matrix=128×128; slice thickness=4 mm; 354 sets of 30 contiguous axial sections); b) pulsed-gradient SE EPI (TR/TE=8775/58 ms, matrix size=112x88, FOV=240x231 mm2, 55 contiguous, 2.3 mm thick axial slices) with SENSE (acceleration factor=2) and diffusion gradients applied in 35 non-collinear directions. Two optimized b factors were used for acquiring diffusion weighted images (b1=0, b2=900 s/mm2); c) dual-echo (DE) turbo SE (TR/TE=2599/16,80 ms, echo train length [ETL]=6; flip angle=90º, matrix size=256x256, FOV=240x240 mm2, 44 axial 3mm-thick slices); and d) 3D T1-weighted fast field echo (FFE) (TR/TE=25/4.6 ms; flip angle=30°; matrix size=256x256; FOV=230x230 mm2; 220 contiguous, axial slices with voxel size=0.89x0.89x0.8 mm).

For all scans, the slices were positioned to run parallel to a line that joined the most infero-anterior and infero-posterior margins of the corpus callosum.

fMRI analysis. fMRI data were analyzed using SPM12 software. Prior to statistical analysis, all images were realigned to the mean image, coregistered with the 3D T1-weighted scan, normalized to the standard template in the MNI space, and smoothed with a 10-mm, three dimensional Gaussian kernel. Subjects included in the subsequent statistical analysis had a maximum cumulative translation less than 3.0 mm (less than 1.0 mm for each of the x, y or z directions separately) or a maximum cumulative rotation of 0.5° (none of the subjects was excluded). Changes in blood oxygenation level dependent contrast associated with the performance of the CCPT task were assessed on a voxel-by-voxel basis, using the general linear model and the theory of Gaussian fields (Friston *et al*, 1995b). A first-level design matrix, including motion parameters as regressors, was built and specific effects were tested by applying appropriate linear contrasts (activations and deactivations). For each subject, the three task conditions (ISI-1, ISI-2, and ISI- 4) were contrasted with the rest condition. Areas showing increasing activation (or deactivation) with increasing task difficulty were identified by creating a linear contrast (CCPT load) from ISI-4 to ISI-1. Peaks of fMRI activity were localized using the Automatic Anatomical Labelling toolbox (Tzourio-Mazoyer *et al*, 2002) in the MNI standard space.

Table e-3.1.1. *Mean fractional anisotropy (FA) values of the tracts connecting brain regions identified by fMRI analysis as key regions involved in Conner's Continuous Performance test (CCPT) performance.*

Mean FA values (SD)	**Healthy Controls**	**Pediatric MS patients**	***p* values**	**CP MS patients**	**CI MS patients**	***p* values**
L Anterior Insula/ACC	0.54 (0.02)	0.51 (0.04)	0.02	0.52 (0.03)	0.47 (0.04)	0.01
L ACC/Precuneus	0.60 (0.02)	0.57 (0.04)	0.01	0.60 (0.02)	0.56 (0.03)	0.1
R ACC/Precuneus	0.59 (0.03)	0.56 (0.04)	0.006	0.56 (0.04)	0.56 (0.04)	0.07
L ACC/Thalamus	0.55 (0.02)	0.52 (0.03)	0.005	0.52 (0.03)	0.51 (0.04)	0.49
R ACC/Thalamus	0.55 (0.02)	0.52 (0.03)	0.01	0.52 (0.03)	0.51 (0.04)	1.0
L Anterior Insula/Precuneus	0.48 (0.05)	0.42 (0.14)	0.04	0.47 (0.10)	0.29 (0.22)	0.04
L Anterior Insula/Thalamus	0.47 (0.02)	0.45 (0.03)	0.004	0.45 (0.02)	0.44 (0.04)	1.000
R Anterior Insula/Thalamus	0.47 (0.02)	0.45 (0.03)	0.008	0.45 (0.02)	0.45 (0.03)	1.0
L MCC/Precuneus	0.57 (0.02)	0.54 (0.03)	0.01	0.53 (0.03)	0.54 (0.05)	1.0
R MCC/Precuneus	0.57 (0.02)	0.53 (0.03)	<0.001	0.53 (0.03)	0.53 (0.04)	0.39
L MCC/Thalamus	0.58 (0.02)	0.55 (0.03)	0.01	0.56 (0.04)	0.55 (0.04)	1.0
R MCC/Thalamus	0.60 (0.03)	0.56 (0.04)	0.006	0.56 (0.04)	0.56 (0.05)	1.0
L Precuneus/Thalamus	0.61 (0.02)	0.57 (0.03)	0.007	0.57 (0.03)	0.57 (0.04)	0.92
R Precuneus/Thalamus	0.64 (0.02)	0.59 (0.03)	<0.001	0.59 (0.03)	0.59 (0.04)	1.0

**Adjusted for multiple comparisons (Bonferroni corrected).*
Abbreviations: SD=standard deviation; L=left; R=right; ACC=anterior cingulate cortex; MCC=middle cingulate cortex.

Table e-3.1.2. *Brain regions significantly activated/deactivated during the Conner's Continuous Performance test (CCPT) load condition in pediatric healthy controls (HC) and pediatric patients with multiple sclerosis (MS) (one sample t-test, adjusted for age and sex, p < 0.001 uncorrected), and between group comparisons (two sample t-test, adjusted for age and sex, p < 0.001).*

Group	Contrast	Brain regions	Side	BA	MNI space Coordinates x, y z	Cluster extent k	t values
Healthy controls	**CCPT load activations**	IPL	R	40	34 -48 50	448	*13.20
		SMA	L	6	-4 -2 58	436	9.54
			R	6	6 6 52		5.54
		ACC	R	32	6 20 44		5.48
		Cuneus	R	7	10 -80 46	183	8.83
		MFG	R	6	34 2 56	136	7.69
		MOG	R	19	30 -74 34	224	7.07
		PCG	L	6	-42 0 32	75	6.28
		PCG	R	44	48 12 36	22	5.16
		SPL	L	7	-26 -56 50	88	5.80
		Cerebellum (crus I)	L	19	-34 -74 -24	6896	*12.88
		ITG	L	37	-42 -62 -8		*11.99
Healthy controls	**CCPT load deactivations**	SFG	L	9	-20 32 38	2665	*15.03
		SFG	R	9	18 32 46	58	*6.88
		STG	R	48	44 -16 4	11132	*13.80
		STG	L	22	-66 -38 16	27	*5.42
		Hippocampus	R	37	28 -36 4		*13.51
		MTG	L	39	-52 -70 20		12.35
		Angular gyrus	R	39	46 -72 32	25	4.99
		ACC	L	11	-6 32 2	463	9.72
		ACC	R	25	4 34 6		6.93
		IFG	R	32	18 50 18	528	8.58
		PoCG	L	48	-56 -8 20	55	7.45
		Precuneus	R	23	16 -46 40	21	4.84

Pediatric MS patients	**CCPT load activations**	SMA	R	6	2 2 54	1270	*12.28
		SMA	L	32	-2 12 46		*12.11
		ACC	R	24	4 20 38		*9.76
		Lingual gyrus	L	18	-26 -88 -12	14082	*19.25
		ITG	R	19	44 -72 -6		*18.14
		IOG	R	19	38 -82 -8		*18.14
		Insula	R	48	34 22 4	1951	*11.40
		PCG	R	44	48 8 32		*11.21
		PCG	L	6	-44 -12 54	1166	*10.40
		PoCG	L	6	-50 2 46		*7.59
		Insula	L	47	-32 22 4	219	*9.25
		Thalamus	R	10	8 -18 10	740	*8.76
		Thalamus	L	8	-12 -18 8		*7.64
		MFG	R	46	36 42 36	452	*8.48
		MFG	L	46	-36 48 30	21	*5.64
		STG	L		-48 12 -4	103	*6.99
Pediatric MS patients	**CCPT load deactivations**	ACC	L	23	-4 -46 36	22189	*16.10
		Precuneus	L	7	-2 -64 48		*15.03
		Precuneus	R	7	8 -62 62		*14.80
		Angular gyrus	L	39	-50 -64 26		*14.60
		SFG	L	9	-20 30 46	5798	*14.23
		SFG	R	9	18 38 46	223	*8.31
		IFG	L	47	-30 34 -12		*11.11
		IFG	R	47	40 34 -12	247	*9.04
		Cerebellum (crus II)	R		38 -76 -38	73	*7.90
		Insula	R	48	34 6 14	26	*6.02
		Insula	L	48	-34 4 12	14	*5.91
Pediatric MS patients > healthy controls	**CCPT load activations**	Thalamus	L	10	-20 -20 8	136	4.14
		Thalamus	L	8	-12 -4 8	38	4.11

		Insula	L	47	-34 24 6	77	3.70
		ACC	L	23	-2 -10 32	15	3.59
Pediatric MS patients < healthy controls		Precuneus	R	7	8 -62 62	77	3.97
		Precuneus	R	7	2 -40 56	24	3.50

**p<0.05, family-wise error corrected for multiple comparisons.*
L=left; R=right; BA=Brodmann area; IPL=inferior parietal lobule; SMA=supplementary motor area; MFG=middle frontal gyrus; MOG=middle occipital gyrus; PCG=precentral gyrus; PoCG=postcentral gyrus; SPL=superior parietal lobule; ITG=inferior temporal gyrus; SFG=superior frontal gyrus; STG=superior temporal gyrus; MTG=middle temporal gyrus; ACC=anterior cingulate cortex; IFG=inferior frontal gyrus; IOG=inferior occipital gyrus.

Table e-3.1.3. *Brain regions significantly activated/deactivated during the CCPT load condition in cognitively preserved (CP) and cognitively impaired (CI) pediatric patients with multiple sclerosis (MS) (one-sample t-test, adjusted for age and sex, p < 0.001 uncorrected).*

Group	Contrast	Brain regions	Side	BA	MNI space coordinates x, y, z	Cluster extent k	t values
Pediatric CP MS patients	**CCPT load activations**	ITG	R	19	44 -72 -4	12783	*16.79
		IOG	R	19	32 -84 -10		*16.52
		Cerebellum (crus I)	L		-34 -58 -30		*16.03
		SMA	R	6	4 2 556	1043	*11.75
		SMA	L	32	-2 12 46		*10.29
		MCC	R	24	2 22 40		*10.63
		Insula	R	48	36 22 4	665	*7.53
		IFG	R	48	54 12 28		*5.19
		PCG	R	44	48 8 32	553	*9.49
		MFG	R	6	38 0 54		*6.82
		MFG	R	46	34 58 18	179	*7.23
		Insula	L	47	-32 22 4	169	*9.24
		PCG	L	6	-46 -6 50	570	*9.21
		Thalamus	R		10 -16 12	415	*8.24
		Thalamus	L		-12 -18 8	63	*7.26
		IPL	L	3	-54 -26 44	80	*5.32
Pediatric CP MS patients	**CCPT load deactivations**	ACC	L	23	-4 -44 44	9238	*13.63
		PCC	L	23	-4 -46 34		*13.49
		Precuneus	R	7	2 -52 34		*9.39
		Precuneus	L	7	-4 -56 34		*9.37
		Insula	R	48	40 -14 16	461	*8.5
		SFG	R	9	18 36 44	85	*7.57
		SFG	L	9	-22 30 48	3454	*13.06
		ACC	L	10	-8 48 2		*10.43
		Angular gyrus	L	39	-50 -64 26	1258	*12.59
		MOG	L	39	-42 -76 32		*12.05

		IPL	L	40	-50 -54 48		*7.21
		IFG	L	47	-30 34 12	886	*10.82
		IFG	R	47	38 36 -10	126	*9.11
		Angular gyrus	R	39	48 -68 38	440	*9.88
		MOG	R	39	52 -68 28		*9.15
		Parahippocampal gyrus	R	35	22 -16 -22	370	*9.67
		MTG	R	20	48 8 -30	211	*7.18
		MTG	L	20	-48 2 -28	2013	*9.81
		PoCG	L	4	-48 -12 30		*6.79
		Cerebellum (crus II)	R		36 -78 40	63	*8.16
Pediatric CI MS patients	**CCPT load activations**	Cerebellum (crus I)	R	37	38 -56 -28	4182	*18.23
		Cerebellum (lobule VI)	L	37	-34 -54 -24		*12.91
		IFG	R	48	58 14 2	28	6.95
		MOG	R	18	28 -92 4	45	6.13
		SMA	R	6	2 -2 60	108	5.60
		SMA	L	6	0 2 52		5.56
		Insula	R	47	36 30 0	9	5.28
		PoCG	L	6	-46 -14 56	16	5.26
		MFG	R	6	30 2 60	8	5.24
		Thalamus	R		6 -18 12	7	4.93
		PCG	R	44	46 6 30	16	4.86
Pediatric CI MS patients	**CCPT load deactivations**	Insula	R	48	38 -12 14	12233	*29.45
		PoCG	R	5	12 -40 62		*19.56
		ACC	L	23	-2 -44 54		*8.54
		Precuneus	R	7	12 -50 34		*7.24
		Precuneus	L	7	-12 -52 34		*6.23
		MTG	R	20	40 8 -32	138	13.7
		Hippocampus	R	37	32 -36 -4	68	4.82
		SFG	L	9	-14 56 20	448	11.57
		SFG	R	32	18 38 38	59	10.03

		SFG	L	32	-16 36 36	951	11.06
		ACC	L	25	-2 28 8		10.25
		MOG	L	39	42 -68 26	858	10.89
		Angular gyrus	L	39	-52 -66 26		9.69
		Hippocampus	R	20	38 -20 -18	206	8.01
		MFG	R	10	4 68 -4	36	7.42
		Cerebellum (crus II)	R		30 -80 -42	23	5.54

**p<0.05, family-wise error corrected for multiple comparisons.*
L=left; R=right; BA=Brodmann area; IPL=inferior parietal lobule; SMA=supplementary motor area; MCC=middle cingulate cortex; MFG=middle frontal gyrus; MOG=middle occipital gyrus; PCG=precentral gyrus; PoCG=postcentral gyrus; SPL=superior parietal lobule; ITG=inferior temporal gyrus; SFG=superior frontal gyrus; STG=superior temporal gyrus; MTG=middle temporal gyrus; ACC=anterior cingulate cortex; IFG=inferior frontal gyrus; IOG=inferior occipital gyrus.

Table e-3.1.4. *Brain regions showing significant differences of fMRI activations/deactivations during the CCPT load condition between cognitively preserved (CP), cognitively impaired (CI) pediatric multiple sclerosis (MS) patients and pediatric healthy controls (full factorial model adjusted for age and sex, p < 0.001 uncorrected).*

Contrast	Mechanism	Brain regions	Side	BA	MNI space coordinates x, y, z	Cluster extent k	T values
CP MS patients < HC	**Increased deactivation**	Precuneus	R	7	8 -62 62	35	3.73
		SPL	R	7	16 -64 62		3.48
CP MS patients > HC	**Increased activation**	Thalamus	L		-12 -4 8	46	4.41
		Insula	L	48	-34 24 6	48	3.83
	Reduced deactivation	IFG	R	46	36 32 28	20	3.46
		ACC	L	23	-2 -8 32	29	3.64
CI MS patients < HC	**Decreased activation**	PoCG	R	3	36 -36 60	30	3.53
	Increased deactivation	Precuneus	R	7	12 -42 52	131	4.03
		Precuneus	L	7	-6 -62 58	67	3.76
CI MS > HC	**-**	-	-	-	-	-	-
CP MS > CI MS patients	**Increased activation**	Lingual gyrus	R	19	26 -64 0	64	4.05
		PoCG	L	43	-60 -18 34	24	3.71
		Putamen	L	48	-24 8 -4	22	3.67
		Cuneus	L	18	0 -88 22	17	3.65
		Supramarginal gyrus	R	40	62 -40 36	12	3.61
		Cerebellum (lobule VI)	L	19	-30 -70 -22	14	3.57
	Reduced deactivation	ACC	L	23	0 24 38	66	4.12
CI MS > CP MS patients	**-**	-	-	-	-	-	-

CP MS > HC & CI MS patients	**Increased activation**	Insula	L	48	-36 0 -12	63	3.09
		STG	R	42	56 -30 16	25	2.83
	Reduced deactivation	ACC	R	32	6 30 34	10	2.68
CI MS < HC & CP MS	**Reduced activation**	IPL	L	40	-30 -42 54	11	2.99
		Lingual gyrus	R	19	24 -66 0	21	2.71
		PoCG	R	3	46 -26 52	24	2.81
	Increased deactivation	SFG	L	40	-2 24 40	10	3.06
		Precuneus	R	7	12 -40 52	21	2.70

Abbreviations: L=left; R=right; BA=Brodmann area; IPL=inferior parietal lobule; IFG=inferior frontal gyrus; PoCG=postcentral gyrus; ACC=anterior cingulate cortex; SPL=superior parietal lobule; SFG=superior frontal gyrus.

Figure e-3.1.1. *Box plots of correct responses in pediatric MS patients.*

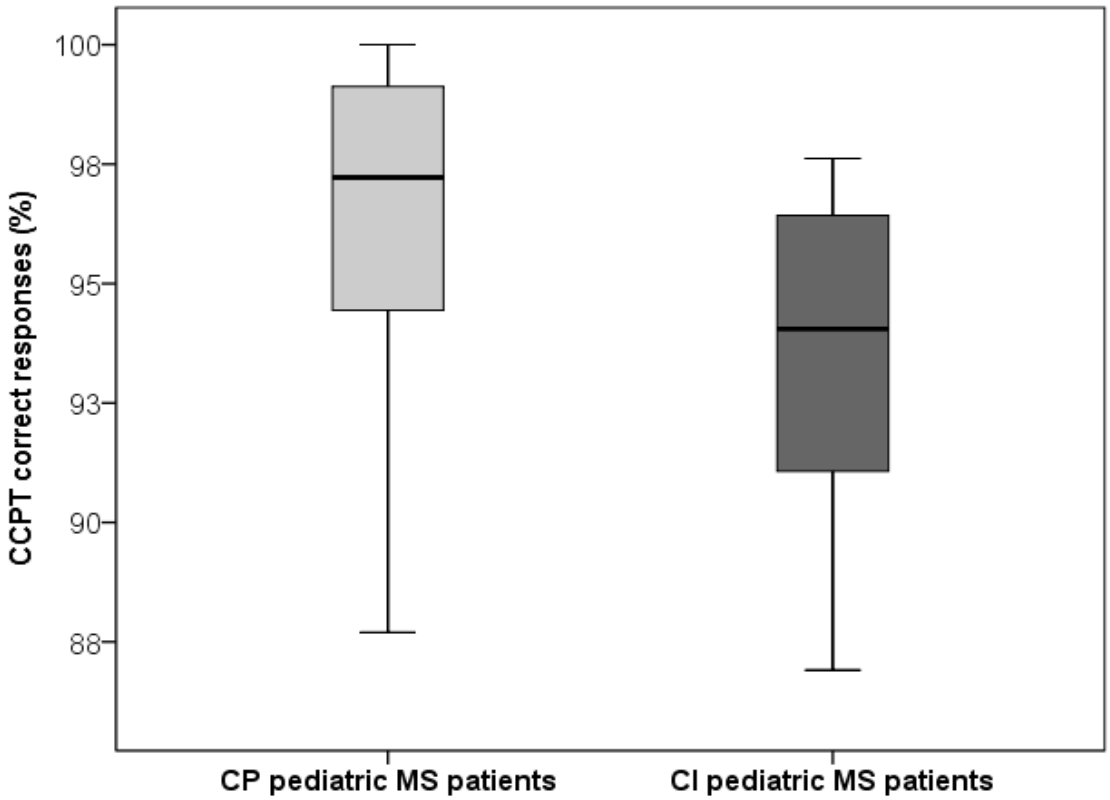

Correct responses at Conner's Continuous Performance Test (CCPT) were reported as percentages. The light gray box plot represents cognitively preserved (CP) pediatric multiple sclerosis (MS) patients' percentage of correct responses; the dark gray box plot represents the percentage of correct responses in cognitively impaired (CI) pediatric MS patients (De Meo et al., 2017).

3.2 Dynamic gray matter volume changes in pediatric multiple sclerosis: a 3.5 year MRI study

The following data have been published (De Meo *et al.*, 2019).

ARTICLE

Dynamic gray matter volume changes in pediatric multiple sclerosis

A 3.5 year MRI study

Ermelinda De Meo, MD, Alessandro Meani, MSc, Lucia Moiola, MD, Angelo Ghezzi, MD, Pierangelo Veggiotti, MD, Massimo Filippi, MD, and Maria A. Rocca, MD

Neurology® 2019;92:e1709-e1723. doi:10.1212/WNL.0000000000007267

Correspondence
Dr. Rocca
rocca.mara@hsr.it

RELATED ARTICLE

Editorial
Evolution of regional brain atrophy in children with multiple sclerosis: Gray matters

Page 694

Abstract

Objectives

To assess, using MRI, the spatial patterns of gray matter (GM) atrophy in pediatric patients with multiple sclerosis (MS), their dynamic changes over time, and their clinical relevance.

Methods

Sixty-eight pediatric patients with MS (30 with a clinical and MRI follow-up after 3.5 years) and 26 healthy controls (HC) underwent clinical and MRI evaluation. To overcome difficulties in obtaining longitudinal scans in pediatric HC, a group of 317 pediatric HC from an NIH-funded MRI Study of Normal Brain Development was used to estimate GM developmental trajectories. In pediatric patients with MS, deviations from normative GM volume values at the voxel level were assessed at baseline and during the follow-up, using linear mixed-effects models. Correlations between GM volume deviations and disability, IQ, and white matter (WM) lesion volumes (LV) were estimated.

Results

Pediatric patients with MS showed failures in GM development in several cortical and subcortical regions, as well as GM atrophy progression in most of these regions, which were only partially related to focal WM LV. Significant correlations were found between regional GM atrophy (particularly of deep GM regions) and disability, whereas higher IQ was associated with reduced deviations from age-expected GM volumes of specific GM regions at baseline and during the follow-up.

Conclusions

Impaired GM maturation occurs in pediatric patients with MS, which is only partially driven by WM inflammation, suggesting that early neurodegenerative phenomena contribute to disability. High IQ, a measure of reserve, may offer protection by promoting remodeling of GM pruning in this young age.

Introduction

Widespread focal demyelinating lesions in the myelin-rich WM are one of the pathological hallmarks of MS However, it is now well-established that the GM is not spared by the disease, even during the earliest phases (Reich *et al*, 2018). Early GM tissue loss (i.e., atrophy), measured using MRI, has been associated with long-term accumulation of disability and cognitive impairment in MS patients (Filippi *et al*, 2013). Studying the dynamics of GM atrophy development during the first stages of the disease may therefore provide important clues about the factors responsible for long-term clinical outcomes. The most suitable patient groups for such studies are those who present with clinically isolated syndromes and pediatric patients.

Given the rarity of pediatric MS, MRI studies of this population are relatively scarce. Cross-sectional investigations have demonstrated reduced volumes of the thalamus (Aubert-Broche *et al.*, 2011; Mesaros *et al.*, 2008a) and whole brain (Kerbrat *et al.*, 2012) in pediatric MS patients compared to age- and sex-matched HC. During childhood and adolescence, subtle modifications of brain structures related to maturational phenomena occurring in the brain WM and GM (myelination and synaptic pruning) have been demonstrated using volumetric MRI measurements in healthy youths (Giorgio *et al*, 2010). Thus it is possible that disease onset during such a critical period of life might affect the physiological trajectories of maturation. In line with this hypothesis, a two-year longitudinal study (Aubert-Broche *et al.*, 2014b) showed that disease onset during childhood leads to a failure of age-expected primary brain growth and subsequent brain atrophy.

Several studies in both adult and pediatric MS patients have consistently shown regional variations in atrophy development, with the early involvement of deep GM nuclei, followed by several cortical regions located in the frontal, parietal and temporal lobes (Ceccarelli *et al*, 2008; Eshaghi *et al*, 2018b; Rocca *et al.*, 2016b). Whether this regional pattern is partially due to a failure of region-specific age-related brain growth in pediatric patients has not yet been investigated.

Starting from these considerations, this longitudinal study investigates the complex interplay between brain growth and disease-related pathology on the regional trajectories of GM volume modifications in pediatric patients with MS. To explore the influence of WM inflammation on our findings, the relationship between GM volume and

focal T2-hyperintense WM lesions was assessed. To determine the clinical relevance of GM volume changes, their correlation with clinical disability and IQ (Deary *et al*, 2010) was studied.

Materials and Methods

Ethics committee approval. Approval was received from the local ethical standards committee on human experimentation, and written informed consent was obtained from all participants and their parents prior to study enrollment.

Participants. Sixty-eight right-handed pediatric patients with RRMS were enrolled and underwent baseline clinical and MRI evaluation. Thirty of them were re-assessed with clinical and MRI evaluation after a median follow-up of 3.5 years (range=1.2-6.3 years). Twenty-eight patients refused the follow-up evaluation, and the remaining 10 had the baseline evaluation performed only recently (less than one year of follow-up).

For all evaluations, MS patients had to be relapse- and steroid-free for at least one month prior to clinical and MRI assessment. In addition, they had to be in stable treatment for MS from at least six months.

Patients with acute disseminated encephalomyelitis were excluded according to published operational criteria (Krupp *et al.*, 2013). None of the patients had a diagnosis of a clinically isolated syndrome at the time of study inclusion and all of them had at least two clinical attacks and the formation of new CNS lesions on serial MRI. Whenever needed, appropriate genetic testing was performed to exclude leukodystrophies. Exclusion criteria were concomitant therapy with antidepressants, psychoactive drugs, or a history of other primary neurological or medical disorders in addition to MS. Participants judged by their neurologist to have primary psychiatric impairment in addition to MS were also excluded.

To overcome the difficulty of obtaining longitudinal MRI scans from pediatric HC, two groups of pediatric HC were selected for comparison of MRI volumes: 1) a group of 26 sex- and age-matched HC recruited at Hospital San Raffaele (HSR) with no previous history of neurological dysfunction and a normal neurological exam, studied on the same MRI scanner of MS patients at baseline; and 2) a group of 317 pediatric HC from an NIH-funded MRI Study of Normal Brain Development (NIH HC) with longitudinal MRI assessments for brain volume quantification (median follow-up: 3.6,

range=0.9-5.4 years) (Evans & Brain Development Cooperative, 2006). The data from the NIH-funded MRI Study of Normal Brain Development were downloaded in June 2016. MRI data from all available healthy participants were initially downloaded, then an images quality check for motion and other artifacts was performed. From the 317 NIH HC considered suitable for the analysis, a subset was followed-up once (N=163; median follow-up: 2.0, range=0.9-4.3 years) and another twice (N=154; median follow-up: 3.9, range=2.0-5.4 years) aged from 4.2 years at the first MRI scan up to 22.3 years at the last MRI scan. All the study participants enrolled were Caucasian.

Clinical assessment. All patients underwent a neurological examination with rating on the EDSS at baseline and follow-up. At baseline, patients also underwent an assessment of premorbid IQ through the Wechsler Intelligence Scale for children (WISC-R) (Wechsler, 1974).

MRI acquisition. Scans from pediatric MS patients and pediatric HC acquired at HSR were obtained using a 3.0 Tesla scanner (Intera, Philips Medical Systems, Best, The Netherlands) under a program of regular maintenance (no major scanner hardware or software upgrades occurred during the study) at baseline and follow-up. The following brain MRI images were acquired: a) dual-echo (DE) turbo spin-echo (TSE) (TR/TE=2599/16,80 ms, ETL=6; flip angle=90º, matrix size=256×256, FOV=240×240 mm2, 44 axial 3mm-thick slices), and b) 3D T1-weighted fast field echo (FFE) (TR/TE=25/4.6 ms; flip angle=30°; matrix size=256×256; FOV=230×230 mm2; 220 contiguous, axial slices with voxel size=0.89×0.89×0.8 mm3). For all scans, the slices were positioned to run parallel to a line that joins the most infero-anterior and infero-posterior parts of the corpus callosum (CC), with careful repositioning at follow-up.

Scans of the NIH HC were obtained at six pediatric centers on GE and Siemens 1.5 Tesla scanners. The standardized MRI protocol included: a) DE TSE (TR/TE=3500/5-119 ms; ETL=8; flip angle=90°; matrix size=256×256; FOV=256×224 mm2; 2-mm-thick axial slices); b) whole brain 3D T1W RF-spoiled gradient echo sequence (TR=22-25 ms, TE=10-11 ms, flip angle=30°, FOV=256× (160-180) mm2, matrix=256×256, slice thickness=1.0 mm). Additional details on acquisition parameters and participants are described in Evans et al. (Evans & Brain Development Cooperative, 2006).

Lesional analysis. MRI analysis was performed by a single experienced observer, unaware of to whom the scans belonged. T2-hyperintense and T1-hypointense lesion

volumes (LV) were measured on the DE and 3D T1-weighted scans respectively, using a local thresholding segmentation technique (Jim 6, Xinapse Systems, Colchester, United Kingdom). The 3D T1-weighted images were coregistered and resliced to match the T2-weighted scans before identification and segmention of the T1-hypointense lesions and underwent lesion refilling before GM volumetric analysis (Chard *et al.*, 2010).

GM volume analysis. Regional GM growth modeling in HC and the evaluation of deviations from normative data in MS patients required the alignment of participant's images to MNI standard space. Taking into account the longitudinal consistency of MRI scans belonging to the same participant, within-subject serial longitudinal registration as implemented in SPM12 was used to align the available 3D T1-weighted images (either 2 or 3) (Ashburner & Ridgway, 2012). For each participant, this step creates an image of the Jacobian determinants of the transformation between each timepoint and the mid-point average template. Then, mid-point average templates and baseline scans (for participants who had only a single scan available) were used for groupwise alignment: first, they were segmented into different tissue types via the Segmentation routine (Ashburner & Friston, 2005). Then, GM and WM segmented images of all participants, in the closest possible rigid-body alignment with each other, were used to produce initial GM and WM templates and to drive the deformation to the templates. At each iteration, the deformations, calculated using the Diffeomorphic Anatomical Registration using Exponentiated Lie algebra (DARTEL) registration method (Ashburner, 2007), were applied to GM and WM, with an increasingly good alignment of participant morphology, to produce templates. Finally, an affine transformation that maps from the population average template to MNI space was calculated. With the aim of transforming each timepoint of each participant into standard space, the mid-point average templates were intensity modulated using the Jacobian determinant (obtained by applying serial longitudinal registration), and then each group of timepoints, including baseline scans, was spatially normalized (DARTEL registration), modulated and smoothed with a 4 mm Gaussian kernel using the DARTEL tool "Normalize to MNI Space". The result of this pre-processing procedure was a modulated, smoothed and normalized GM image for each participant at each timepoint; these were subsequently used to estimate regional GM volume developmental trajectories in HC and evaluate potential deviations in MS patients.

Statistical analysis. Between-group comparisons of demographic, clinical and structural MRI parameters at baseline and their changes over time were performed using the Pearson's chi-square test, Mann-Whitney U-test, two-sample t-test and linear mixed effects models (for longitudinal data) as appropriate. T2 and T1 lesion volumes underwent logarithmic transformation, to reduce skewness.

To estimate normative sex- and age-expected GM growth curves, using Matlab's "fitlme" function (Statistics and Machine Learning Toolbox), the following(Aubert-Broche *et al.*, 2014b) linear mixed-effects model (LMEM) was fitted voxel-wise to HC preprocessed GM maps:

$$Y_{\mathrm{ij}} = \beta_0 + \mathrm{b}_{\mathrm{i0}} + (\beta_1 + \mathrm{b}_{\mathrm{i1}})Age_{\mathrm{ij}} + \beta_2 Sex_{\mathrm{i}} + \beta_3 Age_{\mathrm{ij}} Sex_i + \beta_4 Age_{\mathrm{ij}}^2 + \beta_5 MFS_{\mathrm{i}} + \varepsilon_{\mathrm{ij}}$$

where Yij represents the GM amount at voxel level, Ageij the mean-centered age, Sexi the sex (binary variable) of participant i at time point j. Another binary variable to account for differences in magnetic field strength (MFSi) and acquisition protocol was also added to overcome potential biases. A bivariate normal distribution was assumed for the vector of random effects (bi0, bi1), independent of the homoscedastic normal error term. To explore the influence of MFS on HC developmental trajectories estimate, in comparison to the effect of interests, we derived partial correlation r maps for each regressor and compared the overall distributions of their absolute values by a Wilcoxon signed-rank test.

At each HC age decile, the first-order derivative of the model was evaluated to test for nullity of the growth rate in healthy males and females. As previously suggested (Aubert-Broche *et al*, 2017), to provide a standardized measure of the deviation from the normative expected value of each participant's GM volume at each time point, a z-score map was computed from each GM map using the estimated sex- and age-specific, population-averaged, marginal mean and standard deviation. The procedure is illustrated in **Figure 3.2.1A** for the left thalamus (as an example).

At baseline, linear models (SPM12) were applied to estimate for the whole group of pediatric MS patients (n=68) mean z-scores and their correlation (considering those regions significantly divergent from sex- and age-specific expected values in pediatric MS patients) with disease duration, EDSS, premorbid IQ full-scale and subscales, as well as T2 LV and T1 LV (Menary *et al*, 2013). Mean z-scores between patients with (n=30) and without (n=38) follow-up evaluation were also compared. In patients with a follow-

up evaluation (n=30), linear models, adjusted for follow-up duration, baseline EDSS and disease duration, were applied to estimate changes over time of z-scores and their correlation (for those regions showing significant decreased or increased deviations from normative values) with baseline premorbid IQ full-scale and subscales as well as changes in T2 LV and T1 LV. Intracranial volume was not included in these models because previous studies showed that the growth of brain and skull dissociates to a small but significant extent in children with MS, making skull-based normalization unreliable (Aubert-Broche *et al*, 2014a).

Results were tested at $p < 0.05$, family-wise error (FWE) corrected for multiple comparisons. However, in consideration of the small number of pediatric MS patients enrolled, and in particular of those provided with a longitudinal assessment, in order to increase the power of detection, as explorative analysis the results were also tested at $p<0.001$ uncorrected.

Data availability. The dataset used and analyzed during the current study are available from the corresponding author on reasonable request.

Results

Clinical and lesional MRI data. Demographic, clinical and lesional MRI data from the three study groups at baseline and their longitudinal changes are summarized in **Table 3.2.1**. At baseline, all pediatric MS patients were receiving disease modifying treatments (Interferon Beta=41 (60%), Glatiramer Acetate=16 (24%); natalizumab=11(16%)). Except for IQ sub-scale score, at baseline no differences were found for all variables explored when comparing pediatric MS patients with and those without follow-up. Sixteen (23%) pediatric MS patients showed a low IQ(Wechsler, 1974) (range 70-90), including 5 patients with and 11 without follow-up. In the group of pediatric MS patients with follow-up, median EDSS scores remained stable over time (p=0.28). None of the patients changed treatment during the follow-up. During the follow-up, pediatric MS patients had a median annualized relapse rate of 0 (range: 0-1.23). T2 LV did not change significantly over time (p=0.06), whereas a significant increase in T1 LV was found (p=0.03).

Effect of MFS on HC developmental trajectories. MFS showed the lowest absolute r-values (median (IQR) absolute r-values: Age= 0.16 (0.09-0.25), Sex= 0.17

(0.13-0.21), Age×Sex= 0.11 (0.09-0.14), Age2= 0.32 (0.20-0.39), MFS= 0.07(0.03-0.11); p<0.0001).

HC developmental trajectories. GM volume developmental trajectories as estimated in all HC are shown separately for males and females in Figure 3.2.2. In line with previous studies, different GM developmental trajectories were found in males and females (Lenroot *et al*, 2007). Developmental trajectories were also different in the main brain regions (Giedd, 2004), confirming the existence of a heterocronic maturational process. Brain regions showing negative GM volume change per year (growth rate) reached their maturational peak first, while brain regions showing a positive growth rate continued their maturation across the whole age range explored, in line with the inverted-U shape developmental trajectory previously described (Gogtay *et al*, 2004). At 7.3 years (first decile of HC age distribution) both males and females experienced positive GM volume growth rate in cortical and subcortical regions and cerebellum, only excluding small areas of the occipital and parietal lobes. At 12.1 years, under hormonal pubertal influence (Herting & Sowell, 2017), male and female developmental trajectories started to diverge: males showed positive GM volume growth rate in frontal and temporal regions, basal ganglia and cerebellum, while females showed smaller regions of positive GM volume growth rate in the same brain regions and negative growth rate in the parietal lobe. At 14.9 years, males showed positive GM volume growth rate in temporal regions, basal ganglia and cerebellum and negative growth rate in parietal lobe, while females showed positive GM volume growth rate in the thalamus, hippocampus and small cerebellar regions and negative growth rate in brain regions belonging to the frontal, parietal, temporal and occipital lobes. Such a pattern was evident in males at 18.1 years, when females experienced a negative GM growth rate in frontal, temporal, parietal and occipital lobes and in the cerebellum.

Pediatric MS patients: baseline. Compared to sex- and age-expected GM volume developmental trajectories as estimated in the HC cohort, pediatric MS patients showed significant GM volume deviations (reduction from the expected values) in several cortical and subcortical regions, including the basal ganglia, and several regions located in the frontal, parietal, temporal and occipital lobes and cerebellum (**Table 3.2.2** and Figure **3.2.1B**). No GM regions with positive deviations from normative values were detected.

No differences were found when comparing pediatric MS patients with and without follow-up (data not shown).

Table 3.2.3 summarizes the correlations between GM volume z-scores and clinical and lesional MRI variables in pediatric MS patients. Significant correlations ($p<0.001$) were found between:

- higher EDSS and more severe GM damage in the bilateral thalamus, left caudate nucleus, left IFG and right precuneus;
- longer disease duration and more severe GM damage in the cingulate cortex, frontal and temporal regions;
- higher IQ scores (in terms of both full-scale and subscales) and less severe GM damage in the cingulate cortex, thalamus, and several regions located in the frontal, temporal, parietal and occipital lobes and cerebellum;
- higher T2 and T1 LV and more severe GM damage in the thalamus, caudate nucleus and several regions located in the frontal and temporal lobes, bilaterally.

Pediatric MS patients: longitudinal GM volume changes. During the follow-up, pediatric MS patients showed both increases and decreases of their deviations from the sex- and age-expected GM volume values (estimated on normally developing participants as explained above). In detail, pediatric MS patients showed progression of GM atrophy in the bilateral thalamus and putamen, SMA, precuneus, superior, middle and inferior frontal gyri, cingulate cortex, precentral gyrus (PCG) and PoCG, insula, hippocampus, parahippocampal gyrus, paracentral lobule, IPL, rolandic operculum, calcarine cortex and cuneus, in left Heschl gyrus, amygdala, superior and middle occipital gyrus, fusiform gyrus and cerebellum, and in the right supramarginal gyrus and superior parietal lobule (**Table 3.2.4** and **Figure 3.2.1C**). Pediatric MS patients, over time, also showed reduced deviation from the sex- and age-expected GM volume values in the left IPL, SPL, supramarginal gyrus, angular gyrus, PoCG, middle temporal gyrus (MTG) and cerebellar crus I and in right inferior temporal gyrus (ITG), superior, middle and inferior occipital gyrus (**Table 3.2.4** and Figure **3.2.1C**).

Table 3.2.5 summarizes significant correlations between GM volume changes and premorbid IQ as well as changes in lesional MRI variables ($p<0.001$):

- higher baseline premorbid IQ (full scale and sub-scales) scores were significantly correlated with lower progression rate of GM volume loss in the cingulate cortex and in brain regions located in frontal, parietal, occipital and temporal regions;
- T2 LV and T1 LV changes were significantly correlated with progression of GM atrophy in the bilateral thalamus, PoCG and left PCG.

Discussion

The determination of the patterns of GM volume modifications in pediatric patients with MS is challenging due to the complex interplay between brain development processes, brain plasticity and disease-related damaging phenomena.

Previous studies (Aubert-Broche *et al.*, 2014a; Aubert-Broche *et al.*, 2017) that aimed to compare the developmental trajectories of children affected by demyelinating syndromes (including both monophasic acute demyelinating diseases and MS) to those of healthy children have analyzed brain and GM volumes as a whole. However, studies in growing healthy children have shown that brain development is structurally and functionally a non-linear process (Gogtay *et al.*, 2004), and that individual GM regions follow temporally distinct maturational trajectories (Wierenga *et al*, 2014). To determine whether the physiological processes involved in maturation are affected in MS and whether susceptibility to disease-related processes differs between the main GM regions, we used a voxel-wise technique to analyze high-resolution images of the brain and trace the spatial patterns of GM volume modifications in a relatively large group of pediatric MS patients.

Previous MRI studies in healthy children have applied different measures to identify, in vivo, processes involved in GM modification during development, and how these processes are influenced by evolutionary (Geschwind & Rakic, 2013; Rakic, 1995), genetic (Chen *et al*, 2013) and cellular factors (Chenn & Walsh, 2002), resulting in unique trajectories across the lifespan. GM volume modifications assessed at the voxel level during development have been attributed to dynamic synaptic reorganization, characterized by synapse number reduction and reduced complexity of axons ramifications (so-called synaptic pruning) as well as continued intracortical myelination

and the expansion of subcortical WM (Gennatas *et al*, 2017; Sowell *et al*, 2004; Stiles & Jernigan, 2010).

To determine whether GM changes detected in pediatric MS patients were due to failure of normal age-related brain growth or to abnormal volume loss, we first estimated physiological variations of GM volume trajectories during development from a large cohort of pediatric HC, including participants studied on the same scanner as the MS patients as well as those from the Pediatric MRI Data Repository created by the NIH MRI Study of Normal Brain Development. In line with previous imaging studies (Wierenga *et al.*, 2014), we detected a heterochronic process of maturation (Gogtay *et al.*, 2004; Sowell *et al*, 2001), comprising an initial increase, followed by GM volume reduction (Lenroot *et al.*, 2007), resulting in different ages for peak GM volume. As previously shown in a two-year longitudinal study (Tiemeier *et al*, 2010), this inverted U-shape GM maturational trend was also seen in the cerebellum. Additionally, different GM maturation trajectories were detected for males and females (Aubert-Broche *et al.*, 2014a; Lenroot *et al.*, 2007), underpinning the importance of considering sex in the analysis of pediatric patients. Also in line with previous studies (Gogtay *et al.*, 2004), we confirmed the dynamic progression of GM region development, in which higher-order association areas mature after lower-order sensorimotor regions, following a functional order and a phylogenetically based principle according to which evolutionarily older cortical areas mature first. Specifically, brain regions showing a negative growth rate first, such as those in the parietal cortex, are thought to mature earlier than frontal regions, reflecting the temporal achievement of the main milestones in cognitive and functional development.

Once the GM volume developmental trajectories of the HC cohort were established, we estimated the deviations of pediatric MS patients from the expected values at the voxel level, as well as their change over the follow-up period. In line with previous studies demonstrating a failure of whole-brain age-expected brain growth (Aubert-Broche *et al.*, 2014a; Aubert-Broche *et al.*, 2017), we found a failure from the sex- and age-expected GM developmental trajectories in pediatric MS patients in several cortical regions belonging to the frontal, temporal, parietal, occipital lobes and cerebellum, as well as subcortical regions comprising the thalamus and caudate nucleus. The analysis of correlations showed that highly interconnected brain regions, such as the basal ganglia (Cavanna & Trimble, 2006), and late developing areas, such as anterior

fronto-temporal regions (Ziegler *et al*, 2017), were more influenced by the presence of focal WM lesions and by the prolonged exposure to disease-related processes (as reflected by the correlation with disease duration). Based on this, it is tempting to speculate that MS-related damage may lead to a failure of brain development by depriving late-developing regions of the afferent input needed for their proper maturation, possibly as a consequence of Wallerian degeneration phenomena due to focal lesions along WM tracts. The possibility of impaired maturation of WM tracts connecting these regions should also be considered, as suggested by a recent diffusion tensor MRI investigation in very young pediatric MS patients (below the age of 12 years), which detected an age-dependent regional vulnerability to MS pathology in the WM (Rocca *et al.*, 2016c).

Of note, we also identified several regions with significant deviations from sex- and age-expected GM volume values where differences were not associated with focal WM lesions. This suggests that other processes, not strictly related to the presence of focal inflammatory-demyelinating lesions in the WM, lead to GM alterations in the early stages of the disease. Early GM involvement in MS patients has also been seen in previous studies of adult patients with early RRMS and radiologically isolated syndromes (Giorgio *et al*, 2011).

To better characterize abnormalities of GM volume, we also explored the trajectories of their evolution over a 3.5 year follow-up in a subgroup of MS patients who had a longitudinal MRI assessment. This analysis showed that in pediatric MS patients there were continued deviations from the expected maturation trajectories in the majority of GM areas, including several cortical and subcortical regions. The correlations with the increase in T2 LV confirmed, once again, that only for some of these regions (the thalamus and a few regions located in the precentral and postcentral gyri) maturational trajectory deviation was influenced by the accumulation of focal WM lesions. Combined with the results of baseline assessment, these findings suggest the existence of at least two mechanisms explaining GM damage: the first, more related to the inflammatory WM lesion-dependent component of the disease, mainly occurs at the earliest stages of the disease and involves highly-connected regions, while the second is characterized by a primary involvement of the GM. Even though this aspect was not investigated in the current study, focal lesions within the GM are unlikely to explain these volumetric

abnormalities, since they have been found to be relatively rare in pediatric MS patients (Absinta *et al.*, 2011; Rocca *et al.*, 2015b).

The longitudinal analysis also allowed the identification of a few areas in which deviations from normal maturational trajectories tended to reduce over time. In the absence of a pathological assessment, we can only speculate on the possible reasons for this. Clearly, it may simply reflect reaching of a plateauing limit of tissue loss, which might occur with different timing in different GM structures. Alternatively, it is tempting to hypothesize that by virtue of their young age, high brain plasticity potential (Rocca *et al.*, 2010) and remyelination capabilities (Ghassemi *et al*, 2015a), pediatric patients may benefit from some reparative mechanisms that help to preserve the GM. In line with this, a previous two-year study which has analyzed T1-weighted signal intensity recovery in newly-formed WM lesions in pediatric and adult MS patients showed greater lesional recovery in pediatric patients, which was suggestive of a greater reparative capacity.

To determine the clinical relevance of the GM changes, we explored their correlations with disability and premorbid IQ. In contrast to a previous cross-sectional study by our group (Mesaros *et al.*, 2008a) that found no correlation between GM atrophy and clinical disability (likely due to the smaller number of patients and different method of analysis), in the current investigation failure of GM development in key brain regions, such as the thalamus, caudate nucleus, precuneus and frontal regions, was associated with the severity of clinical disability. This is in agreement with many studies performed in adult patients with MS, including a recent one (Azevedo *et al*, 2018; Eshaghi *et al.*, 2018b) that demonstrated such an association in all clinical phenotypes of the disease, including clinically isolated syndrome patients.

General intelligence is influenced by genetic factors, with an effect of heritability that increases with age (about 30% in early childhood to 80% in adulthood) (Deary *et al.*, 2010). Higher IQ has been linked to higher brain volume, higher GM volume, greater cortical thickness, neural efficiency and WM integrity (Deary *et al.*, 2010). Using regional methods of analysis, a network of brain regions mostly located in the frontal and parietal lobes as well as specific regions in the temporal and occipital lobes, have been related to individual intelligence (Jung & Haier, 2007). In line with this, at baseline we found a relationship between higher premorbid IQ and GM volume preservation in the cingulate cortex, thalamus and other strategic brain regions belonging to the frontal,

parietal, temporal lobes and cerebellum. Consistent with our results, the volume of these regions has been related not only to general intelligence, but also to verbal and non-verbal intelligence (Ramsden *et al*, 2011). Higher IQ was also found to be protective against tissue loss during the follow-up in the cingulate cortex, precuneus, and several regions located in the frontal and temporal lobes and the cerebellum, which might be due to GM pruning which selectively eliminates GM that does not effectively contribute to cognition, as suggested by a study in healthy children (Wilke *et al*, 2003).

This study is not without limitations. First, only part of our patients underwent a clinical and MRI follow-up assessment. Although the number of patients assessed at follow-up may seem small (n=30), it should be considered that the prevalence of pediatric MS is relatively low. Second, due to the lacking of this information for all the study participants we did not consider the socio-economical features of our cohort despite their importance in cognitive reserve. Finally, the stability of disability during the study period did not allow any analysis of prediction of disability worsening. As a consequence, a longer follow-up is needed to ascertain the clinical relevance of GM volumetric abnormalities in pediatric MS patients.

Our results demonstrate that in pediatric MS patients, the expected resilience to CNS injury and greater repair potential (Ghassemi *et al.*, 2015a) are not sufficient to prevent GM atrophy. Since at least part of GM damage in these patients is related to focal WM inflammation, our findings emphasize the importance of therapeutic strategies focused on neuroprotection and neurorepair, to prevent disability accrual over the long term.

Table 3.2.1. *Main demographic, clinical and lesional MRI characteristics of pediatric multiple sclerosis (MS) patients and healthy controls enrolled at Hospital San Raffaele (HSR HC) and healthy controls from NIH-funded MRI Study of Normal Brain Development (NIH HC).*

	HSR HC	**NIH HC**	**Pediatric MS patients (whole group)**	***p* values**	**Pediatric MS patients with FU**	**Pediatric MS patients without FU**	***p* values**
Number of participants	26	317	68	-	30	38	-
Female/male	15/11	166/151	40/28	*0.57 *§0.92	18/12	22/16	*0.86
Median follow-up duration (range) [years]	-	3.6 (0.9-5.4)	-	-	3.5 (1.2-6.3)	-	-
Mean age (SD) [years]	15.4 (3.8)	10.8 (3.7)	15.1 (2.2)	^§0.58	15.5 (1.7)	14.7 (2.5)	^0.15
Median disease duration (IQR) [years]	-	-	1.2 (0.4-2.3)	-	1.1 (0.3-2.3)	1.2 (0.6-2.3)	^°0.68
Mean total IQ score (SD)	-	-	98.59 (16.41)	-	102.82 (17.24)	94.63 (14.81)	^0.06
Mean verbal IQ score (SD)	-	-	97.93 (17.43)	-	101.64 (17.67)	94.47 (16.75)	^0.12
Mean performance IQ score (SD)	-	-	99.10 (17.58)	-	104.61 (17.17)	93.97 (16.63)	^0.02
Median EDSS at baseline [IQR]	-	-	1.5 (1.0-1.5)	-	1.0 (1.0-1.5)	1.5 (1.0-2.0)	#0.09
Median EDSS at follow-up [IQR]	-	-	-	-	1.0 (1.0-1.5)	-	**0.28
Mean T2 LV at baseline (SD) [ml]	-	-	5.9 (7.3)	-	5.1 (6.7)	6.5 (7.7)	°0.21
Mean T2 LV at follow-up (SD) [ml]	-	-	-	-	6.7 (8.9)	-	**°0.06
Mean T1 LV at baseline (SD) [ml]	-	-	3.3 (4.4)	-	2.7 (3.6)	3.7 (5.0)	°0.16
Mean T1 LV at follow-up (SD) [ml]	-	-	-	-	4.2 (5.6)	-	**°0.03

*§p values for between-groups comparison HSR HC vs pediatric MS patients; ^two-sample t-test; *Chi square test; °comparison performed on log-transformed data; #Mann Whitney U test; **time-effect in linear mixed effect models for longitudinal data.*
Abbreviations: MS=multiple sclerosis; SD=standard deviation; IQR=interquartile range; FU=follow-up; IQ=intelligence quotient; EDSS=Expanded Disability Status Scale; LV=lesion volume.

Table 3.2.2. *Brain regions showing significant negative deviations from the sex- and age-expected gray matter volume developmental trajectories (z-scores<0) in pediatric multiple sclerosis patients (p < 0.05 FWE corrected for multiple comparisons).*

Brain Regions	Side	BA	MNI coordinates (x, y, z)			Cluster extent k	t values	Mean z-scores (SE)
Hippocampus	L	28	-20	-33	2	154	10.97	-1.41 (0.13)
Hippocampus	R	28	12	-32	10	83	10.06	-1.14 (0.11)
Calcarine cortex	L	17	-9	-86	-3	844	10.28	-0.93 (0.09)
Calcarine cortex	R	17	15	-66	14	130	7	-0.76 (0.11)
Superior occipital gyrus	L	17	-12	-93	4	127	9.81	-0.82 (0.08)
Cerebellum lobule VIII	L	-	-8	-66	-33	179	9.72	-0.95 (0.10)
Cerebellum lobule VIII	R	-	10	-70	-36	111	8.17	-0.90 (0.11)
Thalamus	L	-	-18	-32	2	546	9.6	-1.33 (0.14)
Thalamus	R	-	9	-30	9	559	9.67	-1.01 (0.10)
Lingual gyrus	L	27	-12	-36	0	424	9.46	-1.12 (0.12)
Middle temporal gyrus	L	37	-66	-50	-6	498	8.23	-0.81 (0.10)
Middle temporal gyrus	R	21	64	-39	-4	693	9.39	-0.92 (0.10)
Precuneus	L	27	-12	-36	2	296	9.39	-1.10 (0.12)
Precuneus	R	27	14	-36	6	117	7.68	-0.85 (0.11)
Superior temporal pole	R	38	57	10	-2	113	9.38	-0.87 (0.09)
Heschl gyrus	L	48	-36	-21	6	44	9.37	-0.96 (0.10)
Insula	L	48	-36	-20	6	119	8.58	-0.90 (0.11)
Insula	R	-	50	10	-6	78	9.25	-0.91 (0.10)
Fusiform gyrus	L	19	-30	-60	-15	469	9.23	-0.85 (0.09)
Superior frontal gyrus	L	8	0	28	52	137	9.18	-0.88 (0.10)
Superior frontal gyrus	R	9	14	46	42	195	7.23	-0.82 (0.11)

Superior parietal lobule	L	7	-30	-64	52	185	9.08	-0.96 (0.11)
Caudate nucleus	L	-	-10	3	20	459	7.2	-0.95 (0.13)
Caudate nucleus	R	-	12	18	-9	733	9.06	-1.03 (0.11)
Amygdala	R	34	16	2	-16	42	9.02	-0.77 (0.08)
Parahippocampal gyrus	L	27	-16	-32	-4	179	8.96	-1.15 (0.13)
Parahippocampal gyrus	R	34	16	3	-18	84	8.09	-0.78 (0.10)
Inferior temporal gyrus	L	20	-40	-27	-21	623	8.94	-0.78 (0.09)
Inferior temporal gyrus	R	20	64	-44	-8	328	7.21	-0.68 (0.09)
Inferior parietal lobule	L	40	-30	-45	39	480	8.76	-0.71 (0.08)
Superior parietal lobule	R	39	48	-56	44	119	8.24	-0.78 (0.09)
Precentral gyrus	L	6	-36	-26	66	131	8.57	-0.70 (0.08)
Precentral gyrus	R	6	27	-24	69	310	8.75	-0.78 (0.09)
Angular gyrus	R	7	33	-58	51	264	8.67	-0.81 (0.09)
Cuneus	L	19	-9	-87	24	211	8.27	-0.79 (0.10)
Cuneus	R	18	9	-72	21	154	8.65	-0.69 (0.08)
Postcentral gyrus	L	6	-30	-27	69	80	8.21	-0.73 (0.09)
Middle occipital gyrus	L	17	-12	-93	2	175	8.47	-0.75 (0.09)
Middle occipital gyrus	R	19	36	-82	21	158	7.38	-0.77 (0.10)
Cerebellum Crus II	L	-	-34	-63	-38	24	7.68	-0.86 (0.11)
Cerebellum Crus II	R	-	10	-72	-36	82	8.45	-0.86 (0.10)
Rolandic operculum	R	48	56	9	2	200	8.42	-0.86 (0.10)
Middle frontal gyrus	L	46	-32	45	10	129	6.79	-0.61 (0.09)
Middle frontal gyrus	R	46	45	50	10	653	8.36	-0.94 (0.11)
Anterior cingulate cortex	R	32	9	45	6	496	8.26	-0.83 (0.10)
Middle cingulate cortex	L	23	-9	-16	38	126	6.92	-0.55 (0.08)
Inferior frontal gyrus	L	-	-48	18	0	222	8.2	-0.77 (0.09)

Inferior frontal gyrus	R	-	54	30	-6	241	7.45	-0.80 (0.11)
Cerebellum lobule VI	L	37	-30	-58	-16	197	8.15	-0.75 (0.09)
Gyrus rectus	L	11	2	33	-14	75	7.99	-0.70 (0.09)
Gyrus rectus	R	11	14	16	-10	186	7.85	-0.86 (0.11)
Cerebellum lobule VII	L	-	-15	-70	-40	43	7.93	-0.76 (0.10)
Superior temporal gyrus	L	41	-44	-32	15	304	7.61	-0.92 (0.12)
Superior temporal gyrus	R	22	63	-16	14	305	7.39	-0.94 (0.13)
Supramarginal gyrus	L	48	-63	-45	27	135	7.59	-0.83 (0.11)
Supramarginal gyrus	R	40	34	-38	45	212	7.4	-0.73 (0.10)
Cerebellum crus I	L	-	-36	-62	-36	238	7.5	-0.97 (0.13)
Inferior occipital gyrus	L	19	-36	-75	-10	94	7.03	-0.62 (0.09)
Inferior occipital gyrus	R	19	44	-80	-2	50	7.02	-0.73 (0.10)

Abbreviations: R=right; L=left; MNI=Montreal Neurological Institute; BA=Brodmann area; SE=standard error.

Table 3.2.3. *Brain regions showing significant correlations between z-scores (deviations from the sex- and age-expected gray matter volume trajectories) with clinical and lesional MRI variables in pediatric multiple sclerosis patients at baseline (multiple regression models. p<0.001 uncorrected).*

Variables	**Brain Regions**	**Side**	**r**
EDSS	Inferior frontal gyrus	L	-0.46
	Caudate	L	-0.45
	Thalamus	L	-0.42
	Thalamus	R	-0.38
	Precuneus	R	-0.42
Disesase duration	Anterior cingulate cortex	L	-0.47
	Anterior cingulate cortex	R	-0.53
	Middle cingulate cortex	L	*-0.48
	Middle cingulate cortex	R	*-0.49
	Supramarginal gyrus	R	-0.49
	Precentral gyrus	L	-0.48
	Inferior frontal gyrus	R	-0.44
	Insula	R	-0.38
	Heschl gyrus	R	-0.44
	Superior temporal gyrus	L	-0.44
	Superior frontal gyrus	L	-0.42
	Postcentral gyrus	R	-0.42
	Fusiform gyrus	L	-0.41
IQ total score	Rectus gyrus	L	*0.60
	Middle frontal gyrus	R	0.51
	Middle frontal gyrus	L	0.52
	Superior frontal gyrus	L	*0.58
	Superior frontal gyrus	R	*0.59
	Cerebellum Crus I	L	0.55
	Fusiform gyrus	L	0.55
	Precuneus	L	0.55
	Postcentral gyrus	L	0.55
	Lingual gyrus	R	0.54
	Inferior frontal gyrus	R	0.54
	Middle cingulate cortex	L	0.51
	Middle cingulate cortex	R	0.53
	Anterior cingulate cortex	L	0.52
	Anterior cingulate cortex	R	0.53

	Supplementary motor area	L	0.49
	Fusiform gyrus	R	0.48
	Inferior temporal gyrus	L	0.44
	Inferior temporal gyrus	R	0.47
	Cerebellum lobule IV-V	R	0.46
	Thalamus	R	0.45
	Middle temporal gyrus	L	0.45
	Amygdala	R	0.44
	Hippocampus	R	0.43
IQ verbal score	Middle frontal gyrus	L	0.54
	Middle frontal gyrus	R	*0.62
	Rectus gyrus	L	*0.57
	Rectus gyrus	R	0.49
	Anterior cingulate cortex	L	0.44
	Anterior cingulate cortex	R	*0.57
	Middle cingulate cortex	L	0.50
	Middle cingulate cortex	R	*0.57
	Precuneus	L	*0.57
	Precuneus	R	0.46
	Superior frontal gyrus	L	0.55
	Superior frontal gyrus	R	0.54
	Middle frontal gyrus	R	0.51
	Cerebellum Lobule VI	L	0.50
	Fusiform gyrus	L	0.50
	Postcentral gyrus	L	0.49
	Middle temporal gyrus	R	0.49
	Inferior frontal gyrus	L	0.47
	Inferior frontal gyrus	R	0.49
	Cerebellum Crus I	L	0.47
	Posterior cingulate cortex	L	0.46
	Supplementary motor area	L	0.46
	Inferior temporal gyrus	L	0.46
IQ performance score	Superior frontal gyrus	L	*0.59
	Superior frontal gyrus	R	0.45
	Precentral gyrus	R	0.57
	Middle frontal gyrus	R	0.55
	Lingual gyrus	R	0.55
	Fusiform gyrus	L	0.53
	Rolandic operculum	R	0.51

	Rectus gyrus	L	0.49
	Thalamus	R	0.49
	Middle cingulate cortex	L	0.47
	Middle cingulate cortex	R	0.48
	Precuneus	R	0.48
	Calcarine cortex	R	0.48
	Cerebellum Crus II	L	0.48
	Cerebellum Crus II	R	0.47
	Cerebellum Lobule VI	L	0.48
	Inferior frontal gyrus	L	0.47
	Inferior frontal gyrus	R	0.46
	Inferior temporal gyrus	L	0.47
	Inferior temporal gyrus	R	0.47
	Cerebellum Crus I	L	0.47
	Cerebellum Crus I	R	0.46
	Supplementary motor area	L	0.47
	Postcentral gyrus	L	0.47
	Anterior cingulate cortex	L	0.46
T2 lesion volume	Thalamus	R	*-0.55
	Thalamus	L	*-0.54
	Heschl gyrus	R	-0.48
	Caudate nucleus	L	-0.42
	Inferior frontal gyrus	L	-0.40
T1 lesion volume	Thalamus	R	*-0.59
	Thalamus	L	*-0.58
	Heschl gyrus	R	-0.49
	Caudate nucleus	L	-0.48
	Calcarine cortex	L	-0.48
	Inferior frontal gyrus	L	-0.45
	Superior temporal gyrus	R	-0.44

**p<0.05 FWE corrected.*
Abbreviations: EDSS: Expanded Disability Status Scale; IQ=intelligence quotient; R=right; L=left.

Table 3.2.4. *Brain regions showing significant increased and decreased z-scores (deviations from the sex- and age-expected gray matter volume developmental trajectories) during the follow-up in pediatric multiple sclerosis patients (p<0.001 uncorrected).*

Contrast	Brain Regions	Side	BA	MNI coordinates (x. y, z)			Cluster extent k	t values	Mean estimated z-score changes (SE)
Pediatric MS: progression of deviation from the expected GM values	Thalamus	L	-	-12	-33	4	912	*7.29	-0.34 (0.05)
	Thalamus	R	-	10	-30	6	1081	*9.26	-0.35 (0.04)
	Supplementary motor area	L	6	-3	-3	51	657	*7.92	-0.13 (0.02)
	Supplementary motor area	R	6	9	-9	57	927	*8.99	-0.09 (0.01)
	Precuneus	L	-	-10	-36	4	290	*8.8	-0.33 (0.04)
	Precuneus	R	23	16	-56	22	350	7.2	-0.14 (0.02)
	Lingual gyrus	L	-	-9	-36	3	186	*8.7	-0.27 (0.03)
	Lingual gyrus	R	-	10	-30	-3	92	7.36	-0.19 (0.03)
	Postcentral gyrus	L	48	-66	-14	20	377	6.4	-0.23 (0.04)
	Postcentral gyrus	R	3	38	-16	38	694	*8.63	-0.13 (0.01)
	Precentral gyrus	L	6	-26	-14	52	324	*7.65	-0.13 (0.02)
	Precentral gyrus	R	-	38	-15	39	677	*8.6	-0.12 (0.01)
	Hippocampus	L	-	-12	-36	6	402	*7.42	-0.31 (0.04)
	Hippocampus	R	27	12	-33	8	253	*8.04	-0.24 (0.03)
	Anterior cingulate cortex	L	24	2	30	20	249	5.11	-0.12 (0.02)
	Anterior cingulate cortex	R	24	6	30	21	788	*7.75	-0.15 (0.02)
	Middle cingulate cortex	L	-	-12	-12	44	1001	6.83	-0.15 (0.02)
	Middle cingulate cortex	R	-	8	-10	51	902	6.79	-0.14 (0.02)
	Posterior cingulate cortex	L	26	-6	-39	22	337	6.66	-0.20 (0.03)
	Posterior cingulate cortex	R	26	8	-38	22	86	6.23	-0.17 (0.03)
	Insula	L	48	-32	-20	16	452	*7.5	-0.16 (0.02)
	Insula	R	48	40	-6	15	251	5.65	-0.16 (0.03)
	Caudate nucleus	L	-	-16	-6	24	376	6.4	-0.21 (0.03)
	Caudate nucleus	R	-	18	16	15	766	*7.49	-0.25 (0.03)
	Putamen	L	-	-28	-9	-4	491	7.1	-0.18 (0.03)
	Putamen	R	48	32	-14	-2	585	6.15	-0.15 (0.02)
	Nucleus Pallidus	L	48	-24	0	-3	110	6.95	-0.14 (0.02)
	Nucleus Pallidus	R	-	30	-10	-3	57	5.22	-0.16 (0.03)
	Supramarginal gyrus	R	40	30	-36	45	97	6.89	-0.09 (0.01)
	Superior frontal gyrus	L	6	-14	8	60	289	5.4	-0.07 (0.01)
	Superior frontal gyrus	R	6	20	6	68	372	6.79	-0.20 (0.03)
	Middle frontal gyrus	L	6	-24	-12	51	317	6.61	-0.15 (0.02)
	Middle frontal gyrus	R	9	39	10	58	744	5.49	-0.19 (0.04)
	Paracentral lobule	L	6	-4	-15	64	143	6.6	-0.13 (0.02)
	Paracentral lobule	R	4	8	-30	54	137	5.77	-0.10 (0.02)
	Rolandic operculum	L	48	-32	-30	18	158	6.55	-0.15 (0.02)

	Rolandic operculum	R	48	42	-4	15	193	6.36	-0.17 (0.03)
	Heschl gyrus	L	48	-32	-26	8	56	6.34	-0.18 (0.03)
	Amygdala	L	-	-30	-2	-21	129	6.33	-0.21 (0.03)
	Calcarine cortex	L	17	-21	-63	10	444	6.09	-0.09 (0.01)
	Calcarine cortex	R	17	20	-52	10	466	6.23	-0.14 (0.02)
	Cuneus	L	18	-8	-80	16	142	4.93	-0.05 (0.01)
	Cuneus	R	-	15	-56	21	211	6.11	-0.13 (0.02)
	Fusiform gyrus	L	35	-22	-3	-38	206	6.05	-0.20 (0.03)
	Inferior frontal gyrus	L	48	-44	14	4	94	4.75	-0.16 (0.03)
	Inferior frontal gyrus	R	48	36	20	30	158	5.97	-0.07 (0.01)
	Inferior parietal lobule	L	40	-27	-51	39	101	5.97	-0.10 (0.02)
	Inferior parietal lobule	R	3	28	-38	51	51	5.15	-0.08 (0.01)
	Middle occipital gyrus	L	19	-27	-80	16	464	5.8	-0.07 (0.01)
	Cerebellum lobule VIII	L	-	-36	-52	-44	146	5.52	-0.14 (0.03)
	Superior occipital gyrus	L	19	-26	-68	27	91	5.39	-0.11 (0.02)
	Parahippocampal gyrus	L	27	-20	-32	-8	170	5.17	-0.18 (0.04)
	Parahippocampal gyrus	R	27	21	-32	-8	70	5.01	-0.19 (0.04)
	Superior temporal pole	L	38	-40	18	-18	55	4.94	-0.12 (0.02)
	Cerebellum lobule IV-V	L	18	-9	-54	-20	87	4.94	-0.17 (0.03)
	Cerebellum lobule IX	L	-	-4	-51	-46	163	4.92	-0.12 (0.02)
	Superior parietal lobule	R	7	28	-50	66	65	4.68	-0.12 (0.03)
Pediatric MS: reduction of deviation from expected GM values	Inferior temporal gyrus	R	37	56	-54	-18	332	*7.35	0.18 (0.02)
	Inferior parietal lobule	L	40	-50	-46	50	257	6.67	0.15 (0.02)
	Supramarginal gyrus	L	40	-58	-38	38		4.11	0.10 (0.02)
	Postcentral gyrus	L	2	-39	-38	60	109	6.34	0.11 (0.02)
	Superior occipital gyrus	R	19	30	-80	39	272	6.31	0.14 (0.02)
	Middle occipital gyrus	R	-	30	-87	33		4.68	0.11 (0.02)
	Superior parietal lobule	L	7	-30	-64	52	127	5.66	0.13 (0.02)
	Angular gyrus	L	39	-48	-58	40	81	5.43	0.11 (0.02)
	Inferior occipital gyrus	R	-	50	-72	-12	65	5.33	0.16 (0.03)
	Middle temporal gyrus	L	21	-58	-51	6	63	5.07	0.11 (0.02)
	Cerebellum Crus I	L	19	-39	-68	-20	124	5.04	0.10 (0.02)
	Lingual gyrus	R	18	20	-99	9	37	4.64	0.06 (0.01)

**p<0.05 FWE corrected.*
Abbreviations: R=right; L=left; MNI= Montreal Neurological Institute; BA=Brodmann area; GM=gray matter: MS=multiple sclerosis; SE=standard error.

Table 3.2.5. *Brain regions showing significant correlations between gray matter volume changes over time with baseline premorbid Intelligence Quotient (full scale and sub-scales) and T2 and T1 lesions volume changes in pediatric multiple sclerosis patients (multiple regression model adjusted for disease duration, follow-up duration and baseline Expanded Disability Status Scale score (p<0.001 uncorrected).*

Variables	**Brain region**	**Side**	**r**
IQ total score	Precentral gyrus	L	0.49
	Anterior cingulate cortex	L	0.51
	Middle frontal gyrus	L	0.62
	Superior frontal gyrus	L	0.57
	Superior frontal gyrus	R	0.63
	Inferior frontal gyrus	L	0.45
	Inferior frontal gyrus	R	0.54
	Precuneus	L	0.61
	Precuneus	R	0.53
	Cerebellum Crus I	L	0.56
	Postcentral gyrus	L	0.38
	Insula	L	0.50
	Postcentral gyrus	R	0.59
	Inferior temporal gyrus	L	0.57
	Inferior temporal gyrus	R	0.63
IQ verbal score	Middle frontal gyrus	L	0.56
	Inferior frontal gyrus	L	0.63
	Precuneus	L	0.53
	Precuneus	R	0.53
	Postcentral gyrus	L	0.57
	Anterior cingulate cortex	L	0.53
	Anterior cingulate cortex	R	0.52
	Middle cingulate cortex	L	0.59
	Precentral gyrus	L	0.54
	Precentral gyrus	R	0.44
	Superior frontal gyrus	L	0.65
	Superior frontal gyrus	R	0.66
	Middle temporal gyrus	L	0.60
	Insula	L	0.51
	Cerebellum Crus I	L	0.59
IQ performance score	Superior frontal gyrus	L	0.59
	Superior frontal gyrus	R	0.43
	Middle frontal gyrus	R	0.45

	Inferior frontal gyrus	R	0.59
	Anterior cingulate cortex	L	0.52
	Fusiform gyrus	L	0.57
	Lingual gyrus	R	0.58
	Calcarine cortex	R	0.50
	Middle cingulate cortex	L	0.41
	Middle cingulate cortex	R	0.45
	Inferior temporal gyrus	R	0.46
T2 lesion volume changes	Precentral gyrus	L	-0.63
	Postcentral gyrus	R	-0.61
	Thalamus	L	-0.54
T1 lesion volume changes	Postcentral gyrus	L	-0.71
	Thalamus	R	-0.70

Abbreviations: IQ=intelligence quotient; R=right; L=left.

Figure 3.2.1. *Gray matter developmental trajectories estimation and assessment of deviations from them in pediatric multiple sclerosis patients.*

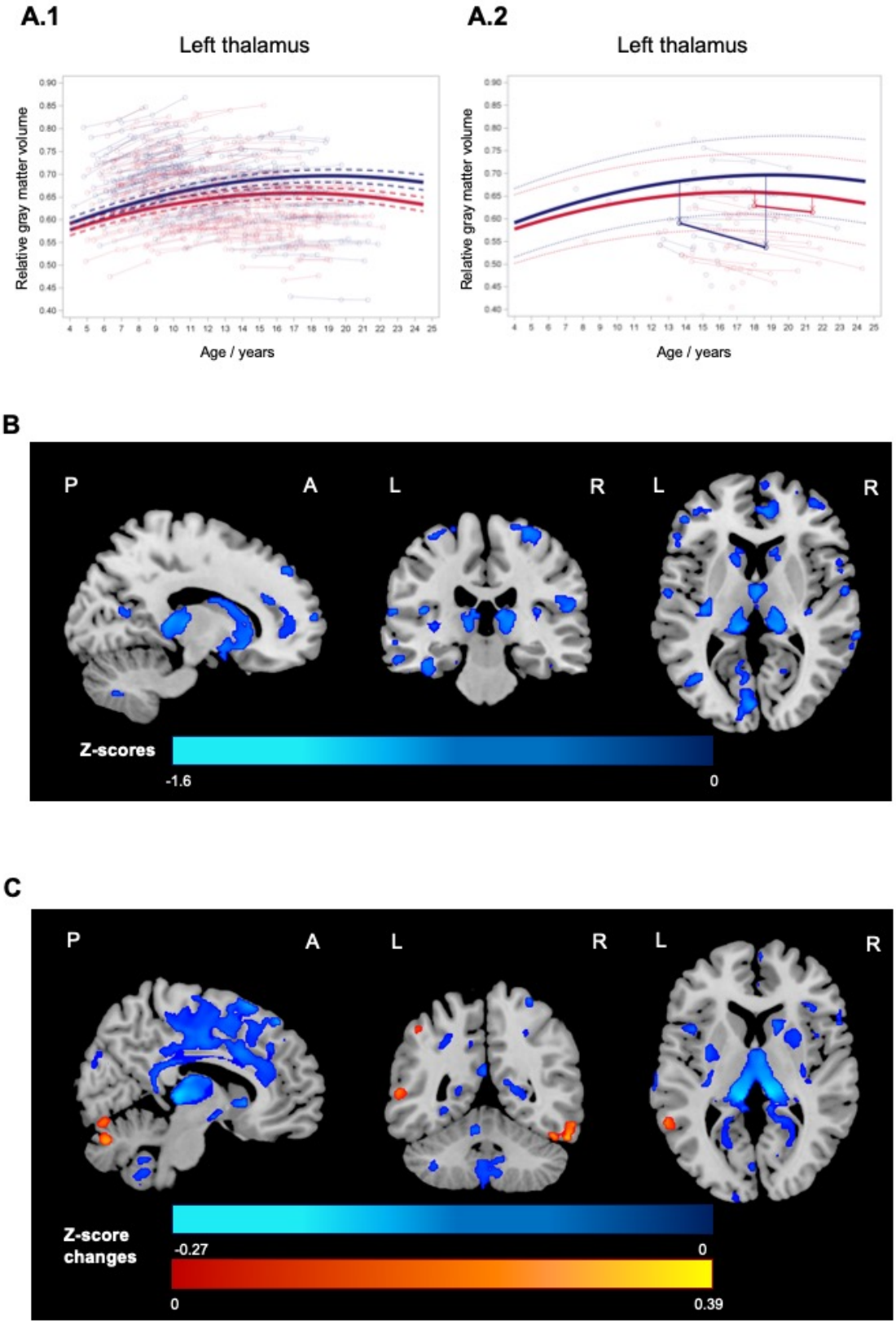

(A.1) Left thalamus gray matter (GM) developmental trajectories are represented as estimated in the whole group of HC (means are represented by solid lines and 95% confidence interval by dashed lines). The model was estimated, for illustrative purpose, from average relative GM volumes (representing the amount of GM relative to the voxel size) within the left thalamus mask from Automatic Anatomical Labelling (AAL) atlas (Tzourio-Mazoyer et al., 2002). Spaghetti lines for each participant's measurements over time are also shown. (A.2) Graphical representation for the pediatric multiple sclerosis (MS) patients of deviations from the sex- and age-specific GM developmental trajectories. One male and one female MS patient whose longitudinal scans were available, were taken as examples to show their deviation from the expected values (vertical solid arrows) as assessed at baseline and at follow-up. From magnetic-field-strength-adjusted measurements obtained for each MS patient at each time point, z-scores were computed by subtracting and dividing by the normative sex- and age-specific estimated mean (solid line) and standard deviation (SD) respectively. Mean ± 1 SD reference lines are also represented (dotted lines) for comparison. (B) GM volume deviations from the expected values in pediatric MS patients (represented in terms of mean z-scores) at baseline (one sample t-test, $p<0.05$ FWE corrected). Brain regions experiencing significantly greater loss of GM are highlighted on the blue-light blue scale. (C) Longitudinal changes (expressed as mean estimated z-score changes) in GM volume deviations from the expected values in pediatric MS patients (one-sample t-test, adjusted for follow-up duration, baseline EDSS and disease duration, $p<0.001$ uncorrected). Brain regions experiencing GM damage progression are highlighted using the blue/light blue scale, while those experiencing reduced deviation from the expected values are highlighted using the red/yellow scale. Images are presented in neurological convention (De Meo et al., 2019).
Abbreviations: MS=multiple sclerosis; GM=gray matter, A=Anterior; P=posterior; L=left; R=right.

Figure 3.2.2. *Gray matter growth rate in the whole group of healthy controls.*

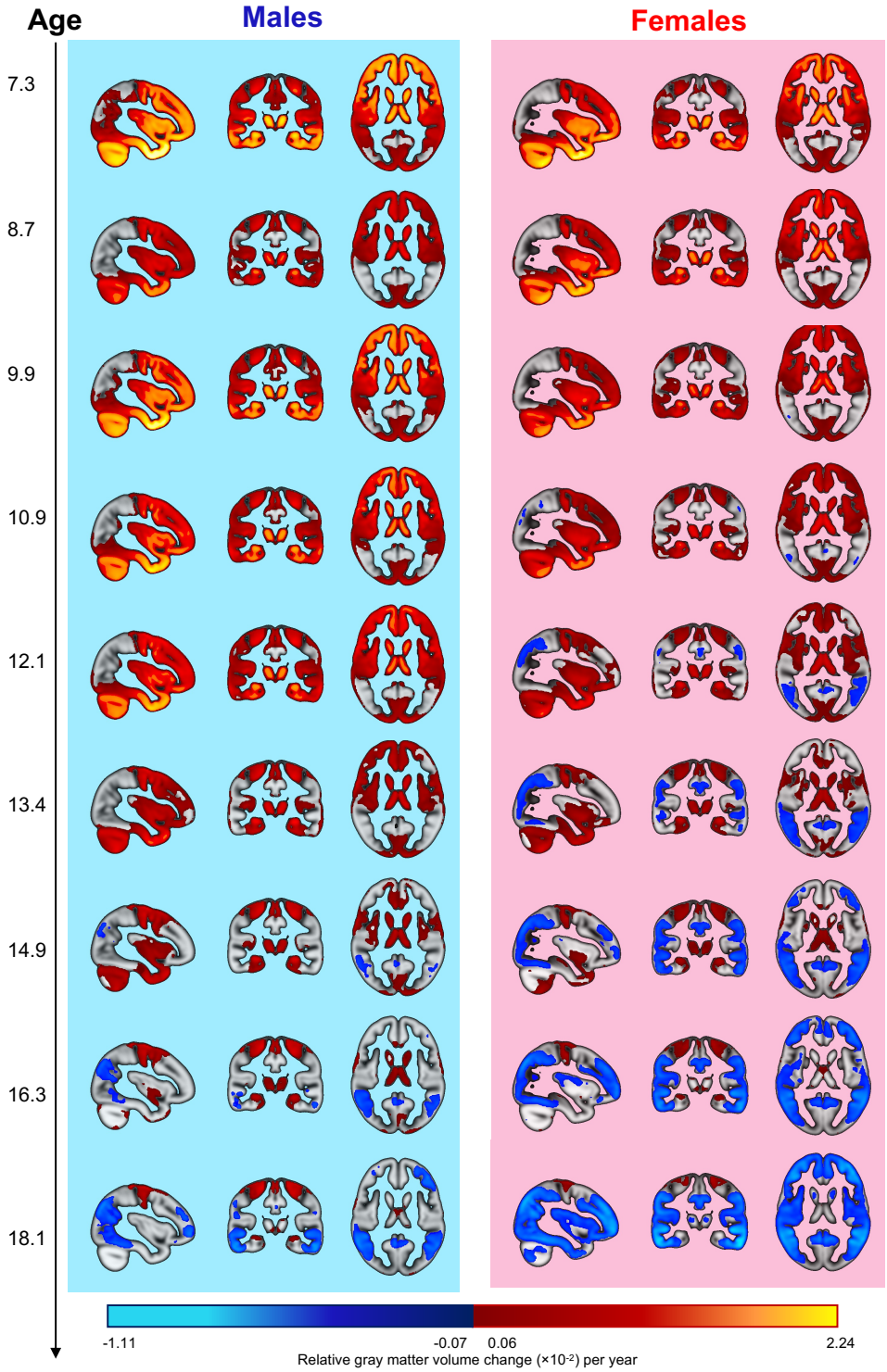

Relative gray matter (GM) volume change per year in healthy controls at each age decile, shown separately for males and females. Brain regions showing a significant increase of relative GM volume per year are red-yellow, while brain regions showing a significant negative GM volume change per year are represented in blue-light blue (linear mixed-effects model, $p<0.001$ uncorrected). Images are presented in radiological convention (De Meo et al., 2019).

3.3 In vivo gradients of thalamic damage in pediatric multiple sclerosis: a window into pathology

The following data have been published (De Meo *et al.*, 2020b).

doi:10.1093/brain/awaa379 BRAIN 2021: 144; 186–197 | 186

BRAIN
A JOURNAL OF NEUROLOGY

In vivo gradients of thalamic damage in paediatric multiple sclerosis: a window into pathology

Ermelinda De Meo,[1,2] Loredana Storelli,[1] Lucia Moiola,[3] Angelo Ghezzi,[4] Pierangelo Veggiotti,[5,6] Massimo Filippi[1,2,3,7] and Maria A. Rocca[1,2,3]

The thalamus represents one of the first structures affected by neurodegenerative processes in multiple sclerosis. A greater thalamic volume reduction over time, on its CSF side, has been described in paediatric multiple sclerosis patients. However, its determinants and the underlying pathological changes, likely occurring before this phenomenon becomes measurable, have never been explored. Using a multiparametric magnetic resonance approach, we quantified, *in vivo*, the different processes that can involve the thalamus in terms of focal lesions, microstructural damage and atrophy in paediatric multiple sclerosis patients and their distribution according to the distance from CSF/thalamus interface and thalamus/white matter interface. In 70 paediatric multiple sclerosis patients and 26 age- and sex-matched healthy controls, we tested for differences in thalamic volume and quantitative MRI metrics—including fractional anisotropy, mean diffusivity and T_1/T_2-weighted ratio—in the whole thalamus and in thalamic white matter, globally and within concentric bands originating from CSF/thalamus interface. In paediatric multiple sclerosis patients, the relationship of thalamic abnormalities with cortical thickness and white matter lesions was also investigated. Compared to healthy controls, patients had significantly increased fractional anisotropy in whole thalamus (f^2 = 0.145; P = 0.03), reduced fractional anisotropy (f^2 = 0.219; P = 0.006) and increased mean diffusivity (f^2 = 0.178; P = 0.009) in thalamic white matter and a trend towards a reduced thalamic volume (f^2 = 0.027; P = 0.058). By segmenting the whole thalamus and thalamic white matter into concentric bands, in paediatric multiple sclerosis we detected significant fractional anisotropy abnormalities in bands nearest to CSF (f^2 = 0.208; P = 0.002) and in those closest to white matter (f^2 range = 0.183–0.369; P range = 0.010–0.046), while we found significant mean diffusivity (f^2 range = 0.101–0.369; P range = 0.018–0.042) and T_1/T_2-weighted ratio (f^2 = 0.773; P = 0.001) abnormalities in thalamic bands closest to CSF. The increase in fractional anisotropy and decrease in mean diffusivity detected at the CSF/thalamus interface correlated with cortical thickness reduction (r range = –0.27–0.34; P range = 0.004–0.028), whereas the increase in fractional anisotropy detected at the thalamus/white matter interface correlated with white matter lesion volumes (r range = 0.24–0.27; P range = 0.006–0.050). Globally, our results support the hypothesis of heterogeneous pathological processes, including retrograde degeneration from white matter lesions and CSF-mediated damage, leading to thalamic microstructural abnormalities, likely preceding macroscopic tissue loss. Assessing thalamic microstructural changes using a multiparametric magnetic resonance approach may represent a target to monitor the efficacy of neuroprotective strategies early in the disease course.

1 Neuroimaging Research Unit, Institute of Experimental Neurology, Division of Neuroscience, IRCCS San Raffaele Scientific Institute, Milan, Italy
2 Vita-Salute San Raffaele University, Milan, Italy
3 Neurology Unit, IRCCS San Raffaele Scientific Institute, Milan, Italy
4 Multiple Sclerosis Center, Ospedale di Gallarate, Gallarate, Italy
5 Paediatric Neurology Unit, V. Buzzi Children's Hospital, Milan, Italy
6 Biomedical and Clinical Science Department, University of Milan, Milan, Italy
7 Neurophysiology Unit, IRCCS San Raffaele Scientific Institute, Milan, Italy

Received March 19, 2020. Revised August 12, 2020. Accepted August 21, 2020. Advance access publication November 21, 2020

Introduction

Neurodegeneration is one of the pathological hallmarks of MS (Filippi *et al*, 2019b). Quantification of atrophy using MRI-based techniques is accepted as an in-vivo measure of neurodegeneration (Rocca *et al*, 2017), as it has shown a good correlation with pathological findings (Filippi *et al*, 2012) and contributes to explain disease clinical severity (Eshaghi *et al*, 2018c). Several combined clinical-MRI studies have consistently demonstrated that GM atrophy is more clinically relevant than WM atrophy in MS, contributing to differentiate the main disease clinical phenotypes (Eshaghi *et al.*, 2018c) and to predict long-term clinical outcomes (Filippi *et al.*, 2013).

Multiple sclerosis-related GM atrophy develops following a trajectory that starts from the deep GM nuclei and spreads, over time, to many cortical GM regions (De Meo *et al.*, 2019; Eshaghi *et al.*, 2018c). In this scenario, the thalamus is one of the first GM structures affected from the beginning of the disease, including patients with clinically isolated syndromes (CIS) (Azevedo *et al.*, 2018; Eshaghi *et al.*, 2018c) and pediatric MS (Aubert-Broche *et al.*, 2014b; Mesaros *et al*, 2008b; Till *et al.*, 2011b). Although thalamic atrophy represents an early phenomenon in the disease course, before it could be detectable several subtle microstructural changes are likely to occur.

Due to its central location between the WM and the CSF interface, as demonstrated in pathological studies (Minagar *et al*, 2013), the thalamus may be susceptible to both retrograde Wallerian degeneration from WM lesions (Vercellino *et al*, 2009) and CSF immune cytotoxic factor-mediated damage (Gilmore *et al*, 2009). In addition, intrinsic thalamic pathology may disrupt its complex organization and dense pattern of connections.

As support of the hypothesis of thalamic neuronal loss not related to direct demyelination within this structure (Evangelou *et al*, 2001), a DT MRI study has shown a tract-specific pattern of cortico-thalamic neurodegeneration in adult patients with MS (Bisecco *et al*, 2015), which was attributed to Wallerian or transsynaptic degeneration. On the other side, recent quantitative MR-based studies have demonstrated a gradient of microstructural integrity disruption in the periventricular WM and deep GM (Brown *et al*, 2017; Liu *et al*, 2015; Pardini *et al*, 2016) as well as of volume loss within the thalamus (Fadda *et al.*, 2019), supporting the existence of an outside-in CSF-mediated pathophysiological mechanism of damage. Another study, performed using ultra-high

field quantitative imaging in adult MS patients suggested that heterogeneous processes contribute to thalamic microstructural changes reflecting alterations in myelin and iron content, with focal lesions being mainly driven by CSF-mediated factors and thalamic atrophy being associated with WM lesions.

The assessment of the mechanisms contributing to thalamic microstructural integrity abnormalities in patients with pediatric MS offers the unique opportunity to unravel the earliest pathogenetic mechanisms in this condition. With this goal, we applied a multiparametric MR approach to quantify, in-vivo, the different processes that can involve this structure in terms of focal lesions, microstructural damage and atrophy.

To test the outside-in CSF-mediated mechanism of damage, microstructural integrity disruption and demyelination were investigated both in the whole thalamus and thalamic WM and in their segmented portions as a function of distance from CSF, using DTI measures and T_1/T_2 ratio. This latter method, which is based on the calculation of the ratio of T_1- and T_2-weighted image signal intensities obtained using conventionally acquired MRI sequences, is thought to provide an indirect evidence of myelin content (Glasser *et al*, 2016; Nieuwenhuys & Broere, 2017; Righart *et al*, 2017), being particularly attractive for pediatric patients (Soun *et al*, 2017), as it does not increase the duration of MRI acquisition. In order to provide possible causal inferences of thalamic microstructural damage and processes occurring in WM (i.e., accumulation of focal lesions) or at the interface with the CSF (i.e., cortical atrophy), we also investigated the relationship between thalamic abnormalities and brain WM lesions and cortical thickness. We hypothesized that both these processes may contribute to explain thalamic microstructural abnormalities in such an early stage of the disease.

Materials and Methods

Ethics committee approval. Approval was received from the local ethical standards committee on human experimentation, and written informed consent was obtained from all participants and their parents prior to study enrollment.

Participants. We enrolled 70 consecutive, right-handed, pediatric patients with relapsing-remitting MS (Polman *et al.*, 2011) referred to specialized centers for the diagnosis of pediatric MS. Patients with ADEM or ADEM-like presentation were excluded according to published operational criteria (Krupp *et al.*, 2013). None of the patients had a diagnosis

of a CIS or anti-myelin oligodendrocyte glycoprotein disease at the time of study inclusion and all of them had at least two clinical attacks and the formation of new CNS lesions on serial MRI.

Patients had to be relapse- and steroid-free for at least one month prior to clinical and MRI assessment. Whenever needed, appropriate genetic testing was performed to exclude leukodystrophies. Exclusion criteria were concomitant therapy with antidepressants, psychoactive drugs, or a history of other primary neurological or medical disorders in addition to MS. Participants judged by their neurologist to have primary psychiatric impairment in addition to MS were also excluded. On the day of MRI acquisition, all patients underwent a neurological examination with rating on the Expanded Disability Status Scale (EDSS) (Kurtzke, 1983).

Twenty-six sex- and age-matched HC with no previous history of neurological dysfunction and a normal neurological examination served as the control group.

MRI acquisition. Using a 3.0 Tesla Philips Intera MR scanner with 8-channel head coil (Philips Medical System, Best, The Netherlands), the following sequences of the brain were acquired from all subjects during a single session: a) 3D T1-weighted turbo field echo (TFE) (TR/TE=25/4.6 ms; echo train length [ETL]=1; flip angle=30°; matrix size=256x256; field of view [FOV]=230x230 mm2; 220 contiguous, axial slices with voxel size=1x1x1 mm); b) dual-echo (DE) turbo spin echo (SE) (TR/TE=2599/16.80 ms, ETL=6; flip angle=90º, matrix size=256x256, FOV=240x240 mm2, 44 axial 3mm-thick slices); c) pulsed-gradient SE EPI (TR/TE=8775/58 ms, matrix size=112x88, FOV=240x231 mm2, 55 contiguous, 2.3 mm thick axial slices) with SENSE (acceleration factor=2) and diffusion gradients applied in 35 non-collinear directions. Two optimized b factors were used for acquiring diffusion weighted images (b1=0, b2=900 s/mm2). For all scans, the slices were positioned to run parallel to a line that joined the most infero-anterior and infero-posterior margins of the corpus callosum.

Conventional MRI analysis. In MS patients, T2-hyperintense and T_1-hypointense lesion volumes (LV) were measured on the DE and 3D T1-weighted scans respectively, using a local thresholding segmentation technique (Jim 8, Xinapse Systems, Colchester, United Kingdom). Normalized brain (NBV), WM (NWMV) and GM (NGMV) volumes were measured on the 3D T_1-weighted scans using the SIENAx software, after T1-hypointense lesion refilling (Chard *et al.*, 2010).

Cortical surface reconstruction. Cortical surface reconstruction and mean cortical thickness measurement were performed using the FreeSurfer software, version 6.0.0 (http://surfer.nmr.mgh.harvard.edu/) on 3D T_1-weighted scans. Topological defects in cortical surface reconstruction caused by WM and/or leukocortical lesions were corrected by adding control points or modifying the WM mask, as needed.

T_1/T_2 ratio image reconstruction. To obtain T_1/T_2 ratio maps, 3D T_1-weighted and T_2-weighted images were pre-processed and combined using an in-house dedicated pipeline adapted from Ganzetti et al.(Ganzetti *et al*, 2014). This includes bias correction and intensity calibration on each of the two MRI sequences and the subsequent calculation of their ratio. In details, 3D T_1-weighted and T_2-weighted image intensities were first scaled according to the vendor-specific image scaling factor detected in Philips images to obtain the original pixel floating-point values. These parameters were available in public tags of the Philips MR DICOM for each sequence (Chenevert *et al*, 2014). T_2-weighted image was then co-registered to the 3D T1-weighted image space through a rigid-body transformation using FLIRT tool (FSL Library) and both sequences underwent the intensity N4 bias field correction from the ANTs toolbox (http://stnava.github.io/ANTs/) (Glasser *et al*, 2014; Glasser & Van Essen, 2011; Tustison *et al*, 2010). After correcting for intensity non-uniformity, 3D T_1-weighted and co-registered T_2-weighted images were further processed to normalize their histograms using a linear scaling procedure described in Ganzetti et al. (Ganzetti *et al.*, 2014): the intensity histograms were adjusted using the lowest and the highest intensity peaks derived from the ocular and temporal muscles masks extracted on both T_1- and T_2-weighted images (calibrated images). After intensity calibration, the ratio between these images was calculated, thus T_1/T_2 ratio maps were obtained. The entire pipeline was implemented in Matlab® environment.

DTI analysis. Diffusion weighted images were first corrected for distortions caused by the eddy currents and for head movements (http://white.stanford.edu/newlm/index.php/DTI_Preprocessing). Then, using the FSL - FMRIB's Diffusion Toolbox (FDT tool), DT measures were estimated for each voxel by linear regression (Basser *et al*, 1994), and FA and mean diffusivity (MD) maps were derived. The tract-based spatial statistics (TBSS) pipeline (Smith *et al*, 2006) was then used to generate skeletonized WM maps. All subjects' FA data were aligned into a

common space using nonlinear registration. The mean FA image was then thinned to create a mean FA skeleton which represents the center of all tracts common to the group. Each subject's aligned FA and MD data were then projected onto this skeleton. Finally, WM skeleton was back-projected in the subject space for thalamic analysis.

Thalamic analysis. Thalamic segmentation was performed using FIRST toolbox on 3D T_1-weighted images. Global thalamic volume was computed as the mean of the right and left thalamic volumes obtained from the FIRST segmentation, corrected for boundary voxels and normalized by the head-scaling factor derived from SIENAx.

The thalami masks were co-registered to T_1/T_2 ratio, DTI maps and TBSS skeleton. For DT MRI metrics, the WM skeleton obtained with the TBSS procedure was superimposed on the thalamus mask of each patient previously co-registered on DTI maps, in order to obtain thalamic WM segmentation in DTI space. To test the hypothesis of a damaging process within the thalamus driven by CSF-mediated factors, the binary mask of the CSF obtained from FreeSurfer segmentation was also resampled onto T_1/T_2 ratio, DTI maps and TBSS skeleton. We applied a dilation of 1 voxel on the CSF mask using DilM (part of the FSL Software Library) to obtain the intersection between the thalamus and the dilated CSF masks. This intersection was the seed region to calculate the geodesic distance of each thalamic voxel and thalamic WM voxel from CSF, in the three dimensions. According to this procedure, the thalamus was divided in 15 concentric bands each including all voxels at the same geodesic distance from CSF (**Figure 3.3.1**). To minimize partial volume effects, the first and the last bands were excluded from the analysis (Liu *et al.*, 2015). For each participant, FA, MD and T_1/T_2 ratio measures were estimated within each band. In pediatric MS patients, T_2 hyperintense thalamic LV was also estimated. All the co-registration and segmentation procedures were visually checked to avoid any potential errors.

Thalamic atrophy. To assess thalamic atrophy at individual level, we calculated age- and sex-adjusted z-scores of thalamic volume, based on pediatric HC. To define thalamic atrophy, we set a cut-off at z-score < -1.96 (Hanninen *et al*, 2019).

Statistical analysis. Between-group comparisons of demographic, clinical and MRI parameters were performed using Pearson's chi square tests, Mann-Whitney and linear models, as appropriate, according to normality distribution assessment performed by using Shapiro-Wilk test.

Age- and sex-adjusted multivariate analysis was performed to compare cortical thickness, thalamic volume and thalamic quantitative MRI measures (including thalamic volume as covariate) between pediatric MS patients and HC. Linear mixed effects models were used to assess the relationship between T_2 thalamic LV within each band and its distance from CSF. To assess the influence of thalamic atrophy on quantitative MRI metrics, we re-run the analysis excluding pediatric MS patients with thalamic atrophy at individual level. To provide a measure of effect size for multiple regression models, we also estimated Cohen's f^2.

Multiple linear regression models adjusted for age, sex and thalamic volume were performed to assess the relationship between thalamic abnormalities with clinical features, brain WM lesions and cortical thickness. To identify the most relevant associations, multivariate analysis with stepwise variable selection was performed ($p = 0.10$ for entry and $p = 0.05$ to remain in the multivariate model).

Bonferroni correction was applied to control for type I error in the comparison of quantitative MRI variables, accounting for the overall number of pairwise contrasts performed. The same correction procedure was separately used for the association of quantitative MRI variables with cortical thickness and WM LV. For all analyses, statistically significant threshold was set at p-value<0.05.

Data availability. The dataset used and analyzed during the current study are available from the corresponding author on reasonable request.

Results

Clinical and conventional MRI measures. **Table 3.3.1** summarizes the main demographic, clinical and conventional MRI features of pediatric MS patients and HC. Compared to HC, pediatric MS patients had lower NBV, NWMV and cortical thickness, as well as a trend towards a reduced normalized thalamic volume (f^2=0.027; p=0.058).

Thalamic global quantitative MRI analysis. Considering the whole thalamus, compared to HC, pediatric MS patients showed increased mean FA (0.35 ± 0.03 *vs* 0.33 ± 0.02; f^2=0.145; p=0.030) and no significant differences for MD (0.76 ± 0.04 *vs* 0.78 ± 0.08; f^2=0.008; p=0.470) and T1/T2 ratio (1.03 ± 0.12 *vs* 1.03 ± 0.15; f^2=0.000; p=0.910). Considering thalamic WM, compared to HC, pediatric MS patients showed reduced FA (0.32 ± 0.02 *vs* 0.34 ± 0.02; f^2=0.219; p=0.006), increased MD (0.70 ± 0.04 *vs* 0.67 ±

0.03; f^2=0.178; p=0.009) and no significant differences for T1/T2 ratio values (1.03 ± 0.14 *vs* 1.03 ± 0.12; f^2=0.000; p=0.819).

Thalamic laminar quantitative MRI analysis. **Figure 3.3.2** shows the results of the laminar analysis of quantitative MRI measures within the thalamus as a function of geodesic distance from CSF. Both pediatric MS patients and HC had a progressive increase of FA and T_1/T_2 ratio and decrease of MD from the regions closest to CSF/thalamus-interface to those closest to thalamus/WM-interface. An analogous trend of these quantitative measures was observed in the thalamic WM, except for MD, which increased from the inner to the outer bands. Quantitative MRI abnormalities were observed at both thalamic interfaces, as detailed below.

Laminar quantitative MRI analysis of whole thalamus. Compared to HC, pediatric MS patients showed higher FA values in the band closest to CSF/thalamus-interface and in those closest to thalamus/WM-interface. They also had lower MD and T_1/T_2 ratio values in the band closest to CSF/thalamus-interface. These findings support microstructural abnormalities at both CSF/thalamus-interface and thalamus/WM-interface and demyelination/iron deposition at CSF/thalamus-interface.

Laminar quantitative MRI analysis of thalamic WM. Compared to HC, pediatric MS patients showed reduced FA in the three bands closest to thalamus/WM-interface and increased MD in the three bands closest to CSF/thalamus-interface. No significant differences were found in T_1/T_2 ratio values. These findings support demyelination, neuronal loss and reduction of fiber density at both CSF/thalamus-interface and thalamus/WM-interface.

Thalamic focal lesion distribution. T_2-hyperintense focal thalamic LV decreased in function of geodesic distance from the CSF (p<0.001) (**Figure 3.3.3**).

Thalamic atrophy effect. Twelve pediatric MS patients had thalamic atrophy at individual level. By re-running the previous analyses excluding these patients with thalamic atrophy, results of between-group comparisons did not change (data not shown).

Correlation analysis. **Table 3.3.2** summarizes significant correlations between thalamic quantitative MRI measures and clinical and conventional MRI measures in pediatric MS patients.

At multivariate analysis, the following correlations were found:

- FA and MD abnormalities detected in thalamic WM vs a younger age at disease onset and longer disease duration;
- FA increase in the bands closest to thalamus/WM-interface vs higher global T_2- and T_1-LV;
- FA and MD abnormalities in the bands closest to CSF/thalamus-interface vs lower cortical thickness.

In Figure **3.3.4**, a graphical and integrated model of thalamic damage is proposed. Table **3.3.3** summarizes the main abnormalities of quantitative MRI metrics and their possible underlying pathological substrates.

Discussion

In this study, we combined several quantitative MR techniques, sensitive towards different pathological substrates of MS, to obtain in vivo information on the possible pathological mechanisms of thalamic damage in pediatric patients with MS.

The analysis of the thalamus as a whole showed that pediatric MS patients had a trend towards a reduction of thalamic volume and significantly higher thalamic FA values compared to HC. Both increased (Bisecco *et al.*, 2015; Ciccarelli *et al*, 2001; Tovar-Moll *et al*, 2009) and decreased (Cappellani *et al*, 2014; Deppe *et al*, 2016; Mesaros *et al*, 2011) thalamic FA values have been observed in previous studies in MS patients compared to healthy subjects. The architectural complexity of the thalamus, which comprises both nuclear complexes and WM fibers, contributes to explain these conflicting results (Minagar *et al.*, 2013).

To better understand thalamic microstructural abnormalities, we repeated the assessment of quantitative MRI metrics considering thalamic WM only. In line with previous studies conducted in adult MS patients (Benedict *et al*, 2013; Bergsland *et al*, 2018; Schoonheim *et al*, 2015), such an approach showed reduced FA and increased MD in the thalamic WM in pediatric MS patients compared to HC.

These results, which were not due to the presence of thalamic atrophy, support the notion that microstructural damage is likely to precede atrophy in MS (Deppe *et al.*, 2016). Despite microstructural abnormalities within the thalamus are likely to represent the first MR detectable sign of an ongoing damaging process, its determinants remain largely unknown. To provide additional insights into the mechanisms associated with

thalamic damage, we integrated the whole thalamic with a laminar analysis, by studying thalamic quantitative MRI metrics according to their geodesic distance from the CSF/thalamus-interface. In this way, we were able to investigate both the effect of CSF immune cytotoxic factors and of WM lesion-related Wallerian degeneration on thalamic damage.

In support of the hypothesis of a CSF immune-cytotoxic factor-mediated mechanism (Liu *et al.*, 2015; Louapre *et al*, 2017), we found a dependency of thalamic T_2 LV from the distance from CSF and a disruption of microstructural integrity together with evidence of demyelination in the same regions, as reflected by increased FA, reduced MD and reduced T_1/T_2 ratio values. The preferential location of T_2 lesions in thalamic regions nearest the CSF/thalamus interface agrees with pathological evidences describing subependymal GM lesions extending over a relatively large area in MS (Gilmore *et al.*, 2009; Vercellino *et al.*, 2009). Inflammatory processes have been found not only in lesions but also in the normal appearing deep GM (Vercellino *et al.*, 2009), leading to diffuse oxidative injury and neurodegeneration (Haider *et al*, 2014).

These inflammatory processes originating from the CSF are likely to mediate changes of thalamic FA through different mechanisms, including microglial activation (Davalos *et al*, 2005; Nimmerjahn *et al*, 2005), an altered metabolism, as described in previous studies using MRI and Positron Emission Tomography (Ciccarelli *et al.*, 2001; Herranz *et al*, 2016), and mitochondrial dysfunction, induced by the increased CSF levels of C16:0 and C24:0 ceramides detected in MS patients (Vidaurre *et al*, 2014).

We also found reduced T_1/T_2 ratio values, likely reflecting reduced intrathalamic myelin content, iron deposition (Grydeland *et al*, 2013) and altered dendrite density (Righart *et al.*, 2017).

Thalamic abnormalities in the bands nearest to CSF/thalamus interface significantly correlated with cortical thinning, suggesting a shared mechanism of damage for subpial and subependimal pathology, likely coming from the CSF. Indeed, as cortical pathology appears mainly represented by an extensive subpial demyelination (Junker *et al*, 2020), also thalamic demyelination has been demonstrated to occur more frequently in the paraventricular nuclei of the thalamus (Gilmore *et al.*, 2009). Both subpial and subependimal demyelination have been associated with the presence of B lymphocyte follicles (Minagar *et al.*, 2013). The latter may release soluble factors in the CSF (Lisak

et al, 2012), damaging GM tissue directly or indirectly by microglia activation (Howell *et al*, 2011).

From the MRI point of view, significant association between cortical thinning and periventricular damage has been demonstrated both in CIS and in relapsing-remitting MS patients (Jehna *et al*, 2015). Furthermore, the notion of a common CSF-mediated mechanism of damage in the thalamus and cortex is in line with the results of a recent 7T quantitative MRI study which found a gradient of demyelination and iron deposition across the cortex with a prominent involvement of the outer layers, extending to deeper cortical laminae with disease progression and affecting the whole cortical width in secondary progressive MS (Mainero *et al*, 2015). In summary, the preferential location of lesions at the CSF/GM interface, together with the gradient of thalamic and cortical damage diminishing from the CSF/GM interface inwards, suggest a shared mechanism of damage originating from the CSF.

In support of the hypothesis of thalamic WM lesion-related Wallerian degeneration, we found increased FA in thalamic bands nearest to thalamus/WM interface that correlated with brain T_2 LV. Neuronal loss outside demyelinated regions has been attributed to anterograde and retrograde neuronal degeneration due to lesions in connected fiber tracts (Kolasinski *et al*, 2012). The loss of afferent and efferent pathways results not only in neuronal loss but also in dendritic attenuation (Mukherjee *et al*, 2002). These microstructural changes can lead to increased anisotropy of thalamic microstructure, as demonstrated in vivo by FA increase we observed in thalamic bands nearest to thalamus/WM interface. Additionally, the intrinsic connections of the thalamus might show an increase of their coherence following damage to the WM fibers connecting the thalamus to the cortex, resulting in the increased FA (Ciccarelli *et al.*, 2001). In line with this, previous studies found correlations between WM lesions and thalamic atrophy (Mesaros *et al.*, 2008b) or microstructural damage (Bisecco *et al.*, 2015).

The dual-mechanism of thalamic damage evidenced by the laminar analysis was confirmed when the analysis was repeated considering the thalamic WM only. Pathological studies aimed at specifically exploring thalamic WM are still lacking, but WM damage is a hallmark of MS. Changes in WM fiber density and integrity have frequently been associated with FA decrease and MD increase (Kolasinski *et al.*, 2012; Moll *et al.*, 2011). These abnormalities in DT metrics have been detected by previous

MRI studies analyzing thalamic WM in adult MS patients and have been associated with cognitive deficits (Benedict *et al.*, 2013; Bergsland *et al.*, 2018; Schoonheim *et al.*, 2015).

In this study, we detected decreased FA in bands nearest to thalamus/WM-interface and increased MD in those nearest to CSF/thalamus-interface. Considering the sub-nuclei distribution within the thalamus and the differential susceptibility to MS-related injury according to axonal diameter (Minagar *et al.*, 2013), it is tempting to make a few speculations. The increased MD in the bands nearest the CSF/thalamus-interface might be attributed to an anterograde trans-neuronal damage, reflecting the presence of more space between axons, as potentially derived from the death of neuronal cells located at the CSF/thalamus-interface. Reduced FA in the bands closest to thalamus/WM-interface might be attributed to retrograde degeneration, being FA more representative of WM fiber-density and, above all, of the integrity of connections. Thus, decreased FA might be the expression of Wallerian degeneration, as described in pathological studies for fiber tracts connecting the lateral thalamic nuclei with the cortex (Kipp *et al*, 2015).

This study is not without limitations. First, it is cross-sectional. As a consequence, we cannot speculate any causal relation between the different measures analyzed. Second, due to the difficulty in the enrollment of pediatric healthy subjects in MRI studies, we only have 26 HC, potentially limiting the extent of normal variability in quantitative MRI metrics, especially in developing subjects. Third, we did not have CSF biomarkers to correlate with the MRI abnormalities detected. However, it is difficult to obtain this kind of data because, if lumbar puncture is not strictly necessary for the diagnosis, it is not routinely performed in pediatric MS patients. From a technical point of view, the lower resolution of T_2-weighted images with respect to the 3D T_1-weighted MRI could increase partial volume effects on T_1/T_2 ratio maps. The use of isotropic acquisitions for both T_2- and T_1-weighted MRI is preferable for future studies. Finally, we did not explore the correlations between thalamic damage and cognitive performance, despite the well-known key role of the thalamus for cognitive functioning. This was done on purpose, considering thalamic segmentation according to geodesic distance from the CSF/thalamus-interface not appropriate to investigate this aspect. As a matter of fact, a segmentation method aimed at isolating function-specific compartments is needed to explore this topic. However, this was beyond the scope of the current investigation.

In conclusion, our findings underscore the existence of heterogeneous pathogenetic mechanisms involving the thalamus in pediatric MS. In line with the finding in a longitudinal study (Fadda *et al.*, 2019) of volume loss at both CSF/thalamus interface and thalamus/WM interface, we demonstrated the existence of microstructural alterations in the same regions. The abnormalities we detected – also present in patients without thalamic atrophy – are likely to represent subtle and early changes preceding tissue loss. Our data suggested that microstructural changes at CSF/thalamus interface could be due to CSF immune cytotoxic factors, while those at thalamus/WM interface to WM lesions. Monitoring thalamic abnormalities could represent an early biomarker for diffuse damage and an ideal MRI outcome in clinical trials aimed at testing neuroprotective strategies especially in pediatric MS in whom more subtle changes need to be analyzed.

Table 3.3.1. *Main demographic, clinical and conventional MRI characteristics of healthy controls and pediatric patients with multiple sclerosis.*

	Healthy Controls	**Pediatric multiple sclerosis patients**	***p* values**
Number of participants	26	70	-
Girls/Boys	16/10	44/26	0.94**
Median age (IQR) [years]	15.7 (13.6-17.5)	15.6 (14.0-16.7)	0.20*
Median EDSS (range)	-	1.5 (0.0-4.0)	-
Median disease duration (range) [years]	-	1.7 (0.1-8.1)	-
Median T_2 LV (IQR) [ml]	-	2.9 (1.3-6.3)	-
Median T_1 LV (IQR) [ml]	-	1.7 (0.7-3.8)	-
Mean NBV (SD) [ml]	1704 (90)	1665 (81)	0.02§
Mean NGMV (SD) [ml]	849 (42)	831 (49)	0.15§
Mean NWMV (SD) [ml]	855 (68)	834 (55)	0.01§
Mean normalized thalamic volume (SD) [ml]	11.1 (1.0)	10.4 (2.0)	0.06§
Median T2 thalamic LV (normalized for thalamic volume) (IQR) ml	-	0.0 (0.0-0.8)	-
Mean cortical thickness (SD) [mm]	2.4 (0.1)	2.3 (0.1)	0.04§

**Mann Whitney U test; **Chi square test; §linear regression models, age- and sex-adjusted. Abbreviations: EDSS = Expanded Disability Status Scale; IQR = interquartile range; LV = lesion volume; SD = standard deviation; NBV = normalized brain volume; NGMV = normalized gray matter volume; NWMV = normalized white matter volume.*

Table 3.3.2. *Analysis of correlation between thalamic quantitative MRI measures abnormalities and clinical, lesional and cortical thickness measures (multiple regression model adjusted for age, sex and thalamic volume (p<0.001).*

Variables	**Thalamic regions**	**FA**		**MD**		**T1/T2 ratio**		**WM FA**		**WM MD**	
		r	***p* values**	**r**	***p* values**	**r**	***p* values**	**r**	***p* values**	**r**	***p* values**
Disease duration	Whole thalamus	-	-	-	-	-	-	-	-	0.32	0.009*
Age at onset	Whole thalamus	-	-	-	-	-	-	0.28	0.026*	-0.26	0.035*
	Thalamic band 2	-	-	-	-	0.34	0.003	-	-	-	-
***T_2* LV**	Thalamic band 10	0.27	0.027	-	-	-	-	-	-	0.25	0.050
	Thalamic band 14	0.24	0.050*	-	-	-	-	-	-	-	-
***T_1* LV**	Thalamic band 10	0.35	0.006	-	-	-	-	-	-	-	-
	Thalamic band 12	0.26	0.047	-	-	-	-	-	-	-	-
	Thalamic band 13	0.26	0.040	-	-	-	-	-	-	-	-
	Thalamic band 14	0.27	0.036*	-	-	-	-	-	-	-	-
Mean cortical thickness	Thalamic band 2	-0.27	0.028*	0.034	0.004*	-	-	-	-	-	-

**associations statistically significant at the multivariate analysis.*
Abbreviations: FA = fractional anisotropy; MD = mean diffusivity; LV = lesion volume; WM = white matter.

Table 3.3.3. *Summary of thalamic abnormalities in pediatric multiple sclerosis patients and their pathological correlates according to the tissue compartment explored.*

Tissue compartment	**Thalamic abnormalities in pediatric multiple sclerosis patients**	**Pathological correlates**
Whole thalamus	FA increase (Thalamic band 2, 9,10,12,13,14) MD decrease (Thalamic band 2)	- Microglial activation and subsequent morphological changes (Davalos *et al.*, 2005) - Metabolic changes leading to mitochondrial dysfunction and cell swelling (Hannoun *et al*, 2012; Vidaurre *et al.*, 2014) - Dendritic attenuation due to loss of afferent and efferent connections leading to a de-differentiation of synaptic spines (Ciccarelli *et al.*, 2001; Mukherjee *et al.*, 2002)
	T_1/T_2 reduction (Thalamic band 2)	- Reduction of myelin content (Glasser & Van Essen, 2011) - Inflammation-related iron deposition (Grydeland *et al.*, 2013) - Reduction of dendrite density (Righart *et al.*, 2017)
Thalamic WM	FA decrease (Thalamic band 12,13,14)	- Fiber density reduction (Kipp *et al.*, 2015)
	MD increase (Thalamic band 2,3,4)	- Axonal loss and myelin content reduction (Kolasinski *et al.*, 2012)

Abbreviations: WM = white matter; FA = fractional anisotropy; MD = mean diffusivity.

Figure 3.3.1. *Thalamic segmentation according to geodesic distance from CSF.*

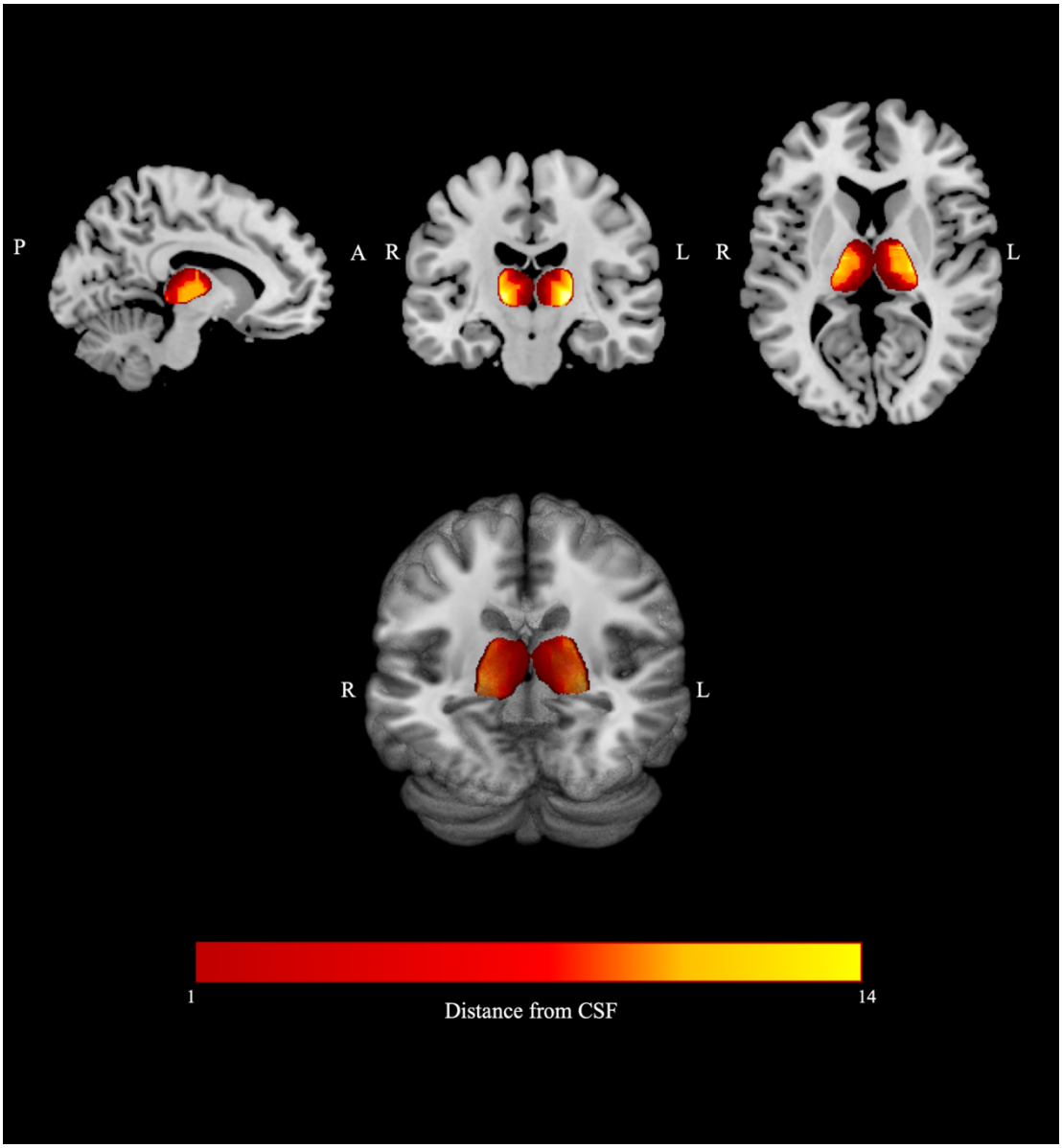

An example of thalamic segmentation obtained in a healthy subject is provided for a sagittal, coronal and axial slice, respectively (first row). A 3D representation of the same thalamic segmentation is also provided (second row). The red-yellow scale shows the different thalamic bands according to the geodesic distance from the CSF (De Meo et al., 2020b).
Abbreviations: A=anterior; P=posterior; R=right; L=left.

Figure 3.3.2. *Quantitative MRI metrics in the whole thalamus and thalamic white matter according to the distance from CSF.*

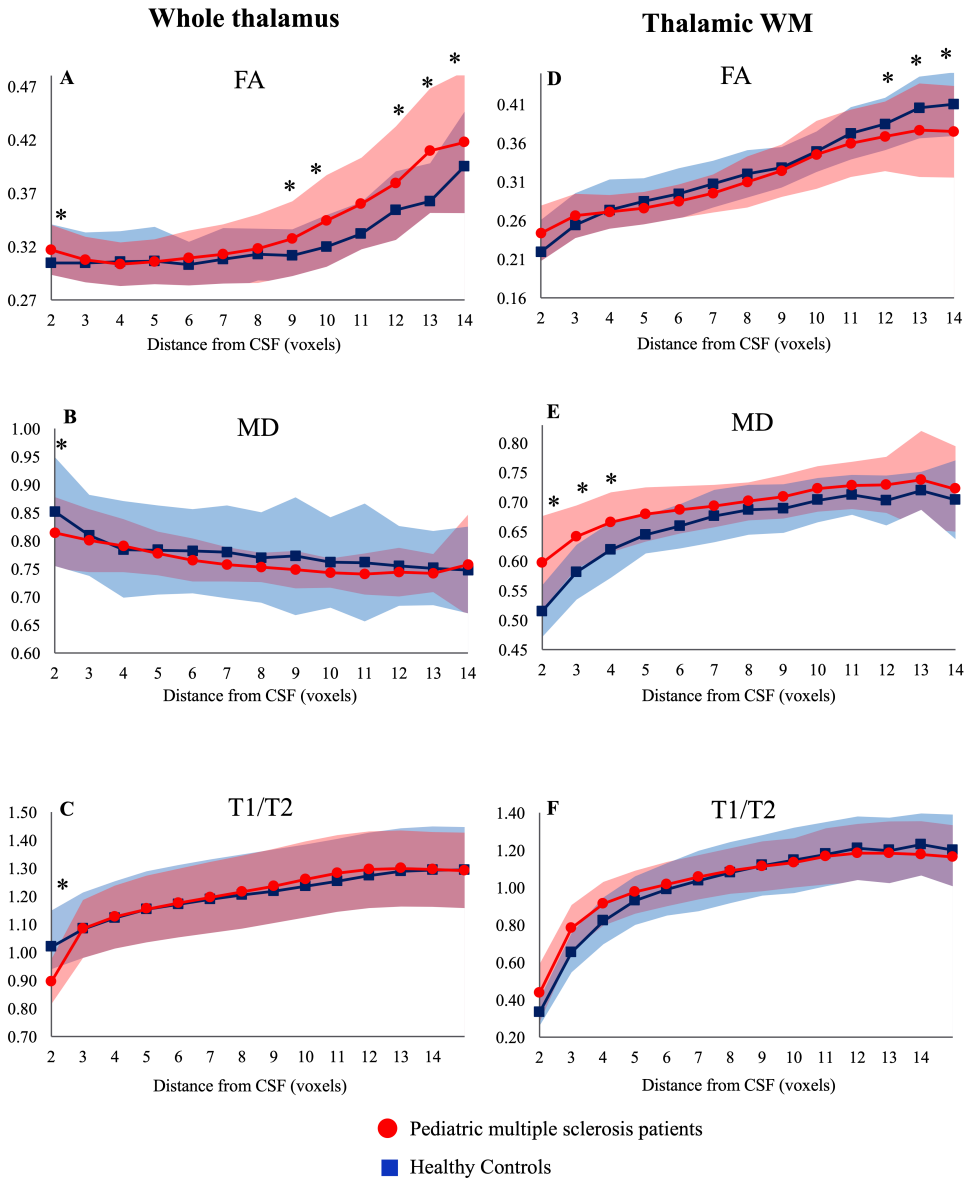

(*A) Fractional anisotropy (FA), (B) mean diffusivity (MD) and (C) T1/T2 ratio values in thalamic concentric bands obtained as a function of their geodesic distance from CSF are expressed as mean (solid lines) ± standard deviation (shaded area). (D) FA, (E) MD and (F) T1/T2 ratio values in thalamic white matter concentric bands obtained as a function of their geodesic distance from CSF are expressed as mean (solid lines) ± standard deviation (shaded area). Pediatric multiple sclerosis patients are represented in red and healthy controls in blue. Multivariate analysis adjusted for age, sex and thalamic volume was performed to compare thalamic quantitative MRI measures within each concentric band originating from CSF/thalamus-interface. For all analyses, statistically significant threshold was set at p-value <0.05, corrected for multiple comparisons (Bonferroni correction was applied). An asterisk (*) individuates the thalamic bands where metrics are significantly different between pediatric multiple sclerosis patients and healthy controls (De Meo et al., 2020b).*
Abbreviations: WM=white matter; FA=fractional anisotropy; MD=mean diffusivity.

Figure 3.3.3. *T_2 hyperintense thalamic lesion volume distribution within the thalamus.*

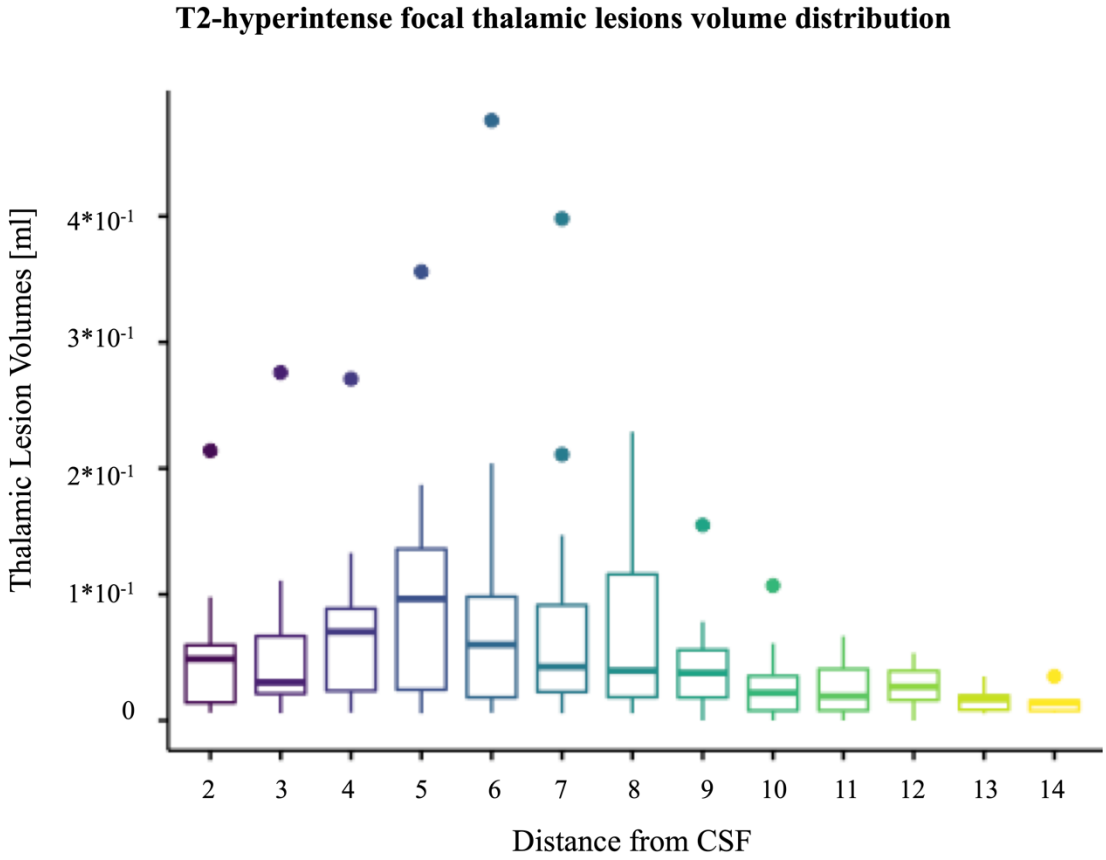

Boxplots show hyperintense focal thalamic lesions volume normalized for thalamic volume [ml] for each thalamic concentric band originating from the CSF/thalamus-interface. Each boxplot includes: the minimum (represented by the lowest data point excluding the outliers), the maximum (represented by the largest data point excluding the outliers), the sample median (the solid line within the box), and the first (the lower extremity of the box) and third quartiles (the upper extremity of the box). Outliers are represented as single dot (De Meo et al., 2020b).

Figure 3.3.4. *Mechanisms of thalamic damage at CSF/thalamus interface and thalamus/WM interface in pediatric patients with multiple sclerosis.*

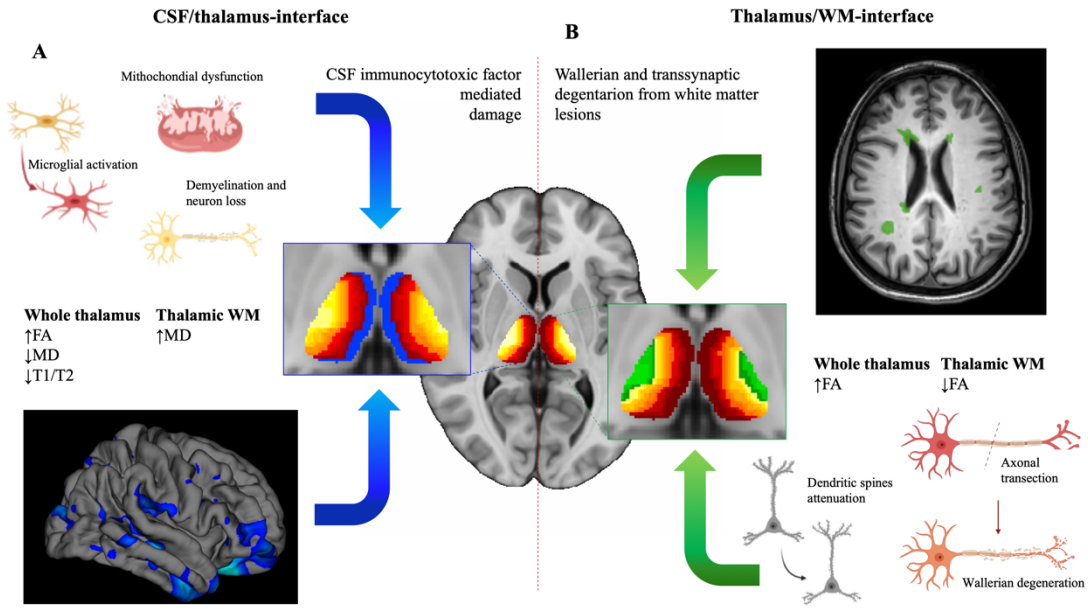

(A) Mechanisms underlying thalamic damage at CSF/thalamus interface are represented as well as significant changes in quantitative MRI metrics observed at CSF/thalamus interface. In the picture, at the bottom is shown cortical thinning in pediatric multiple sclerosis patients that was associated with abnormalities in quantitative thalamic MRI metrics observed at CSF/thalamus interface (highlighted in blue). (B) Mechanisms of thalamic damage occurring at thalamus/WM interface are represented in green. In the MRI image at the top, WM lesions detected in a pediatric MS patient, which were associated with abnormalities of quantitative MRI metrics at thalamus/WM interface, are green filled for exemplificative purpose. At the bottom, pathological changes likely to underlay the MRI abnormalities detected are graphically represented (De Meo et al., 2020b).
Abbreviations: WM = white matter; FA = fractional anisotropy; MD = mean diffusivity.

4. Assessment of clinical and MRI predictors of long-term disease course in pediatric MS

4.1 Early predictors of 9-year disability in pediatric multiple sclerosis

The following data have been published (De Meo *et al.*, 2021a).

RESEARCH ARTICLE

Early Predictors of 9-Year Disability in Pediatric Multiple Sclerosis

Ermelinda De Meo, MD,[1,2] Raffaello Bonacchi, MD,[1,3] Lucia Moiola, MD,[3] Bruno Colombo, MD,[3] Francesca Sangalli, MD,[3] Chiara Zanetta, MD,[3] Maria Pia Amato, MD,[4,5] Vittorio Martinelli, MD,[3] Maria Assunta Rocca, MD,[1,2,3] and Massimo Filippi, MD[1,2,3,6,7]

Objective: The purpose of this study was to assess early predictors of 9-year disability in pediatric patients with multiple sclerosis.
Methods: Clinical and magnetic resonance imaging (MRI) assessments of 123 pediatric patients with multiple sclerosis were obtained at disease onset and after 1 and 2 years. A 9-year clinical follow-up was also performed. Cox proportional hazard and multivariable regression models were used to assess independent predictors of time to first relapse and 9-year outcomes.
Results: Time to first relapse was predicted by optic nerve lesions (hazard ratio [HR] = 2.10, $p = 0.02$) and high-efficacy treatment exposure (HR = 0.31, $p = 0.005$). Predictors of annualized relapse rate were: at baseline, presence of cerebellar ($\beta = -0.15$, $p < 0.001$), cervical cord lesions ($\beta = 0.16$, $p = 0.003$), and high-efficacy treatment exposure ($\beta = -0.14$, $p = 0.01$); considering also 1-year variables, number of relapses ($\beta = 0.14$, $p = 0.002$), and the previous baseline predictors; considering 2-year variables, time to first relapse (2-year: $\beta = -0.12$, $p = 0.01$) entered, whereas high-efficacy treatment exposure exited the model. Predictors of 9-year disability worsening were: at baseline, presence of optic nerve lesions (odds ratio [OR] = 6.45, $p = 0.01$); considering 1-year and 2-year variables, Expanded Disability Status Scale (EDSS) changes (1-year: OR = 26.05, $p < 0.001$; 2-year: OR = 16.38, $p = 0.02$), and ≥ 2 new T2-lesions in 2 years (2-year: OR = 4.91, $p = 0.02$). Predictors of higher 9-year EDSS score were: at baseline, EDSS score ($\beta = 0.58$, $p < 0.001$), presence of brainstem lesions ($\beta = 0.31$, $p = 0.04$), and number of cervical cord lesions ($\beta = 0.22$, $p = 0.05$); considering 1-year and 2-year variables, EDSS changes (1-year: $\beta = 0.79$, $p < 0.001$; 2-year: $\beta = 0.55$, $p < 0.001$), and ≥ 2 new T2-lesions (1-year: $\beta = 0.28$, $p = 0.03$; 2-year: $\beta = 0.35$, $p = 0.01$).
Interpretation: A complete baseline MRI assessment and an accurate clinical and MRI monitoring during the first 2 years of disease contribute to predict 9-year prognosis in pediatric patients with multiple sclerosis.

ANN NEUROL 2021;89:1011–1022

Introduction

During the last decades, pediatric MS (i.e., clinical onset before age 18) has been increasingly recognized, representing from 3 to 10% of the total MS population (Banwell *et al.*, 2007a; Mikaeloff *et al.*, 2004a; Renoux *et al.*, 2007). However, only a few longitudinal studies (Iaffaldano *et al*, 2017; Mikaeloff *et al*, 2006) have been conducted in these patients.

A higher clinical activity, with higher relapse rate especially during the first years from disease onset (Benson *et al*, 2014; Gorman *et al.*, 2009), paralleled by a higher MRI activity (Waubant *et al.*, 2009), was reported for pediatric-onset compared to adult-onset MS patients. In details, MS patients with disease onset in childhood or adolescence not only experienced more frequent involvement of infratentorial regions on MRI, but also had higher lesion burden both at disease onset and on follow-up (Waubant *et al.*, 2009). However, little is known about how these early clinical and MRI features may influence the long-term clinical outcome of these patients.

In pediatric patients with a clinically isolated syndrome (CIS) some clinical factors contributed to predict the conversion to clinically defined MS (Iaffaldano *et al.*, 2017). In particular, multifocal onset and female sex were associated with a higher risk of a short-term second clinical attack, while exposure to disease modifying treatments (DMT) was protective (Iaffaldano *et al.*, 2017). In the same cohort, the occurrence of a relapse after MS diagnosis was the only significant predictor of Expanded Disability Status Scale (EDSS) worsening after 10 years (Iaffaldano *et al.*, 2017).

In adult patients with MS, MRI has a fundamental role not only in disease monitoring but also in predicting clinical course, but data are lacking for pediatric patients. For adult patients at their first demyelinating attack, asymptomatic infratentorial (Minneboo *et al*, 2004; Swanton *et al*, 2009; Tintore *et al*, 2010), spinal cord (Arrambide *et al*, 2018; Brownlee *et al*, 2017; Swanton *et al.*, 2009) and gadolinium-enhancing (Gd)-lesions (Di Filippo *et al*, 2010; Swanton *et al.*, 2009) were associated with the development of clinical disability (measured using the EDSS) over the first 5-7 years after a first clinical attack.

Considering the paucity of approved DMT in pediatric MS patients as well as safety concerns about new highly-active drugs, it appears extremely relevant to identify risk factors for disease progression in these patients.

Against this background, the aim of this study was to identify early (at disease onset and within the first 2 years of disease) clinical and MRI predictors of disease course in pediatric MS patients, by studying a large cohort of these patients. Easily obtainable and reproducible MRI measures were investigated (number and distribution of T_2-hyperintense lesions, number and distribution of Gd-lesions, including the cervical cord; presence of tumefactive lesions, number of black holes), in order to guarantee immediate clinical applicability.

Methods

Ethics committee approval. Approval was received from the local ethical standards committee on human experimentation, and written informed consent was obtained from all participants and their parents prior to study enrollment.

Subjects. A cohort of 123 pediatric patients with relapsing-remitting MS (Krupp *et al.*, 2013; Polman *et al.*, 2011; Thompson *et al.*, 2018), followed at San Raffaele Hospital, Milan, Unit of Neurology, was analyzed. We included pediatric MS patients at their first demyelinating attack with an available neurological evaluation and 1.5 Tesla brain and cervical cord MRI scan within 3 months from disease onset. Exclusion criteria were: clinical presentation with symptoms of encephalopathy referable to acute disseminated encephalomyelitis according to published operational criteria (Krupp *et al.*, 2013) and a history of other neurological/medical disorders in addition to MS.

Clinical assessment. Neurological evaluations (with EDSS score rating) at disease onset and after 1 and 2 years were collected, together with the last available clinical visit (median follow-up duration 9.4 years, interquartile range 6.9 – 12.9 years). DMT exposure and relapses during the whole follow-up period were recorded. DMT were grouped into moderate- (any preparation of interferon-beta and glatiramer acetate) and high-efficacy (natalizumab and immunosuppressants) treatments. Disability worsening was classified as a confirmed (at a following visit 12 months apart) (Kalincik *et al*, 2015) EDSS increase of at least 1.5, 1.0, and 0.5 points for baseline EDSS scores of 0, 1.0 to 5.0, and more than 5.5, respectively.

MRI assessment. Brain (n=123) and cervical cord (n=115) 1.5 Tesla MRI scans obtained in a clinical setting for diagnostic and follow-up purposes were evaluated by an experienced neurologist. In particular, the MRI scan performed at disease onset

(baseline), and – when available – yearly brain MRI scans at 1 and 2 years, were analyzed. The number, distribution and feature (tumefactive *vs* non-tumefactive appearance) of T_2-hyperintense lesions were recorded on baseline images, together with the number of new lesions on 1- and 2-year scans. For this purpose, multi-planar fluid attenuation inversion recovery (FLAIR) and T_2-weighted images of the brain, and short tau inversion recovery (STIR) and/or T_2-weighted images of the cervical cord were used. The number of black holes at baseline, and the number and distribution of Gd-lesions on baseline, 1- and 2-year-scans were measured on post-contrast, turbo-spin echo T_1-weighted scans. Regarding the distribution of lesions, the involvement of the following CNS regions was evaluated (**Figure 4.1.1**): periventricular WM (two cut-offs were used: at least one, and three or more lesions according to the better accuracy observed of three or more lesions in identifying MS patients) (Barkhof *et al*, 1997; Ruet *et al*, 2014), deep GM, cortical/juxtacortical GM/WM, brainstem, cerebellum, optic nerve (as evaluable in conventional T2-weighted sequences), and cervical cord.

Statistical analysis. Chi-squared and Mann-Whitney U tests were used as appropriate to investigate differences in demographic, clinical and MRI measures at baseline, 1- and 2-years, between patients who had worsened and those who had not at last follow-up. The same comparison was also performed for clinical measures at last follow-up. Differences in demographic, clinical and MRI measure between patients who dropped out and those who remained through-out the follow up period, as well as between patients starting moderate- and high-efficacy DMT, were also analyzed.

Stepwise Cox proportional hazard models were used to identify the independent predictors of time to first relapse. Multivariable linear regression models were used to identify independent predictors of annualized relapse rate (ARR) and of EDSS score at last follow-up. Multivariable logistic regression models were used to investigate independent predictors of disability worsening at last follow-up. Separate models were built using clinical and MRI data available at each of the follow-up time points. Baseline EDSS, age at onset, sex and the exact interval in years between onset and the last follow-up visit were included in the models as potential confounders. A stepwise variable selection procedure was used. This procedure is a combination of forward and backward selection where in each step, every variable is considered for addition to or subtraction from the set of covariates based on an F-test with a *p*-value for inclusion of 0.15.

In summary, three different models were constructed for each outcome variable:

- baseline model (n=123): baseline clinical and MRI (brain and cervical cord) variables were included. MRI measures were number, location and feature of T2-lesions, number and distribution of Gd-lesions, and number of black holes;
- 1-year model (n=115): baseline predictors plus the number of relapses and time to first relapse within the first year, and the change in EDSS score and brain MRI variables (new T2- and Gd-lesions) after 1 year were included in the model;
- 2-year model (n=105): baseline and 1-year predictors, plus the number of relapses and time to first relapse within the first 2 years, and the change in EDSS score and brain MRI variables (new T2- and Gd-lesions) after 2 years were included;

For each multivariable linear regression model R^2 is reported, as the proportion of the variance of dependent variable determined by the independent variable(s) included in the model. For multivariable logistic regression models, the model fit is reported using model C-statistic and accuracy. Statistical analysis was performed with R software (version 3.6.1). Statistical significance is reported as $p < 0.05$.

Data availability. The dataset used and analyzed during the current study is available from the corresponding author on reasonable request.

Results

Clinical features and course. One-hundred and twenty-three (89 females, 34 males) pediatric MS patients with baseline clinical and MRI evaluations were included. Of them, 115 underwent clinical and MRI follow-up evaluations exclusively after 1 year, 105 after 1 and 2 years. No significant differences in demographic, clinical and MRI features were observed between patients who dropped out and those who remained in the follow-up period (data not shown). Over the 9-year follow-up period, 13/123 (11%) pediatric patients experienced disability worsening and one of them developed SP MS, while no significant EDSS changes were observed in the whole group (EDSS at last follow-up 1.0, range: 0.0 - 7.0, p=0.89). **Figure 4.1.2** summarizes EDSS scores in patients worsened and not worsened at last clinical follow-up.

Baseline clinical and MRI features. Baseline clinical and MRI features of the study cohort are summarized in **Table 4.1.1**. Optic nerve involvement was observed in 15/19 (74%) patients experiencing clinically-manifest optic neuritis and in 10/104 (10%) patients asymptomatic for optic neuritis. No significant differences were found between patients worsened and not-worsened at follow-up except for the mean number of cervical cord Gd-lesions. Table 4.1.2 summarizes the main clinical and MRI changes occurring after 1 and 2 years of follow-up. All the patients enrolled started a DMT at diagnosis (63% interferon-beta; 13% glatiramer acetate; 19% natalizumab; 5% immunosuppressant). Compared to pediatric MS patients starting moderate efficacy DMT, patients starting high efficacy DMT were older (p=0.01), had higher EDSS score (p=0.006) and more extensive brain and cervical cord MRI involvement (p ranging from <0.001 to 0.04) (See **Table e-4.1.1** in Supplementary materials for all comparisons). Four patients switched from moderate to high efficacy DMT during the first 2-year follow-up period. During the 9-year follow-up period 30/123 (24%) patients switched to higher efficacy treatment, of which five worsened clinically.

1-year clinical and MRI features. During the first year from the disease onset (n=115), 31 patients (27%) had at least one clinical relapse, five patients (4%) disability worsening, 51 (44%) at least one new T2-lesion and 29 (25%) at least one Gd-lesion, on brain MRI.

2-year clinical and MRI features. During the second year from the disease onset (n=105), 24 patients (23%) had at least one clinical relapse, five patients (5%) disability worsening, 53 (50%) at least one new T2-lesion and 30 (29%) at least one Gd-lesion, on brain MRI. Totally, during the first 2 years from the disease onset (n=105), 38 patients (36%) had at least one clinical relapse, 10 patients (10%) disability worsening, 53 (50%) at least one new T2-lesion and 30 (29%) at least one Gd-lesion on brain MRI.

Worsened patients at 9-year follow-up had a higher number of new brain T2-lesions and greater EDSS change at 1 and 2 years compared to not worsened ones. No significant differences were found in terms of relapses. See **Table 4.1.2** for all comparisons.

Early predictors of time to first relapse and ARR. The median time from disease onset to first relapse was 1.7 years (range 0.2-13.7). Optic nerve involvement (hazard ratio [HR]=2.10, 95%-confidence interval [CI]=1.12–3.91, p=0.02) and high efficacy

DMT exposure (HR=0.31, 95%CI=0.12-0.72, p=0.005) were the independent predictors of time to first relapse (**Figure 4.1.3**). Among patients with MRI optic nerve involvement but asymptomatic for optic neuritis, only 1/10 (10%) patients experienced clinically-manifest optic neuritis as first relapse. At baseline, the presence of cerebellar lesions and the exposure to high efficacy DMT predicted lower ARR, while that of cervical cord lesions was associated with higher ARR. In the 1-year model, the same baseline variables were confirmed as predictors of ARR. Furthermore, a positive association between the number of relapses during the first year of disease and ARR was observed. In the 2-year model, the time to first relapse and the number of relapses during the first 2 years were the independent predictors of ARR, together with the baseline predictors except for high efficacy DMT exposure. **Table 4.1.3** summarizes the results of ARR models.

Early predictors of 9-year disability worsening (**Table 4.1.4**). At baseline, the presence of lesions in optic nerve and brainstem was associated with a higher probability of 9-year EDSS worsening. In the 1-year model, EDSS change during the first year of disease was the only independent predictor of 9-year disability worsening. In the 2-year model, EDSS change during the first 2 years of disease as well as the detection of at least two new brain T2-lesions during the same period were the independent predictors of 9-year disability worsening.

Early predictors of EDSS score at 9-year follow-up (**Table 4.1.5**). At baseline, EDSS score, the presence of brainstem lesions, and the number of cervical cord lesions predicted a higher 9-year EDSS score; while the presence of brain or cervical cord Gd-lesions was associated with a lower 9-year disability. In the 1-year model, baseline EDSS score, brainstem and brain Gd lesions (these last ones, although not-reaching statistical significance) confirmed their role. Furthermore, 1-year EDSS change and detection of at least two new brain T_2-lesions were associated with higher EDSS score at 9 years. In the 2-year model, the EDSS change at two years joined the one-year model predictors.

Discussion

This longitudinal study was aimed to assess the relevance of specific early clinical and MRI features for 9-year clinical outcomes in pediatric MS patients. The purpose was to aid in the definition of prognosis and in the selection of a personalized treatment plan as soon as possible.

Time to first relapse was selected as the first outcome measure, considering the existing differences between pediatric and adult MS patients: in particular, the higher disease activity as well as the longer time to clinical worsening in pediatric MS patients (Renoux *et al.*, 2007). In the present study, optic nerve involvement on brain MRI was the only independent predictor of a shorter time to first relapse. Apparently, this result may contrast with previous findings that CIS patients presenting with optic neuritis have a lower number of asymptomatic brain lesions on MRI, and thus a better prognosis, compared to other CIS presentations (Tintoré *et al*, 2005; Tintore *et al*, 2015). However, our finding has a number of explanations. First, we only included patients with a diagnosis of MS, and by consequence an abnormal brain MRI scan. Indeed, in the previous studies, the benign prognosis of patients presenting with optic neuritis was driven by the subgroup without significant brain MRI lesions, which was not obviously represented in our study (Fisniku *et al*, 2008; Tintore *et al.*, 2015). Second, optic nerve involvement on MRI may have different implications, compared to clinically-manifest optic neuritis (Davion *et al*, 2020; London *et al*, 2019). Importantly, this results does not seem to be affected by selection bias, given only one patient (out of 10) with MRI optic nerve involvement but asymptomatic for optic neuritis experienced clinically-manifest optic neuritis as the first relapse (Zimmermann *et al*, 2018). Finally, optic nerve involvement on MRI at the time of diagnosis may be associated with a shorter asymptomatic period, because the lesion is usually clinically manifest, and earliest phases of disease have been associated with a higher clinical activity in pediatric MS patients (Gorman *et al.*, 2009).

The exposure to high efficacy DMT was the only independent predictor of longer time to first relapse. This is not surprising given the differences in efficacy profile and time needed to obtain clinical and MRI benefits reported for the distinct DMT classes (Davis *et al*, 2017; Ghezzi *et al*, 2019; Killestein & Polman, 2011). This result is also particularly encouraging given these patients had more severe clinical and MRI disease parameters at onset, compared to patients receiving moderate efficacy DMT.

The second outcome variable, ARR over the first 9 years of disease, was in part predicted by baseline lesion distribution. In details, cerebellar lesions were associated with lower ARR, while cervical cord lesions with higher ARR. These associations remained also significant when short-term follow-up variables were included in the multivariable models. Considering the typical involvement of infratentorial regions and

higher ARR of pediatric compared to adult MS patients (Absinta *et al.*, 2010), the association of lesions in cerebellum with lower ARR may be puzzling. However, recent studies demonstrated that the cerebellum differentiates itself from other infratentorial structures in MS, by showing similar lesions frequencies compared to supratentorial regions (Weier *et al.*, 2016). This finding, considering the preferential lesion location in pediatric MS patients in those regions with more complete myelin maturational processes (Absinta *et al.*, 2010), could be attributed to a later cerebellar maturation (compared to the remaining infratentorial structures) occurring during late childhood and adolescence (De Meo *et al.*, 2019; Simmonds *et al*, 2014; Weier *et al.*, 2016). In this perspective, it is tempting to speculate that the relationship between cerebellar lesions and lower ARR could be due to later myelination in the cerebellum (Weier *et al.*, 2016). Indeed, the later myelination may protect this region at younger ages, which have been associated with a higher ARR compared to adolescence, when brain maturation is more advanced, and disease features become more similar to adults (e.g., lower ARR). The association between spinal cord lesions and ARR confirms the results of previous studies in adult patients with MS, in which the presence of asymptomatic spinal cord lesions was significantly predictive of an increased risk of future relapse (Zecca *et al*, 2016). Furthermore, the presence of asymptomatic spinal cord lesions was previously found to be a significant predictor of a first clinical attack in radiologically isolated syndrome (Okuda *et al*, 2011; Okuda *et al*, 2014; Sombekke *et al*, 2013) and of conversion to clinically defined MS in CIS patients (Sombekke *et al.*, 2013).

In addition, some short-term follow-up measures significantly contributed to explain 9-year ARR. We found a consistent association between the number of relapses over the first 2 years and time to first relapse with ARR. These data suggest the persistence of inflammatory activity over the first years of disease in spite of DMT be highly indicative of a more active disease, with a higher ARR over 9 years. In light of these findings, close observation of clinical and radiological disease activity during the first 2 years of disease helps in the definition of an early personalized therapeutic strategy, considering long-term benefits and risks ratio (Freedman, 2008). Once again, a protective role was found for high efficacy DMT exposure over the first year of disease. However, this effect was lost in the 2-year model, underscoring the existence of an early critical window in which the biology of disease can be modified for longer-term benefit (Harding

et al, 2019). Moreover, the protective role of high efficacy DMT exposure might partially be conveyed by the number of relapses in the first two years of disease.

With the aim of exploring disability accrual, we investigated 9-year EDSS worsening and score According to recent data suggesting disability regression post progression is quite frequent among younger MS patients (Kalincik *et al.*, 2015), we considered 12-month confirmed disability in order to reduce a potential overestimation of disability accrual. Our results confirmed the predictive role of baseline EDSS score and of clinically-eloquent site involvement (such as optic nerve, brainstem and spinal cord) for these 9-year outcomes. Regarding the former, the notion that higher baseline EDSS scores are associated with a higher risk of subsequent clinical worsening has also been reported for adult MS patients (Cree *et al*, 2016). Regarding the latter, different explanations may be valid for each CNS regions. For the optic nerve, there are no previous studies aimed at directly exploring the prognostic value of MRI abnormalities of this compartment. Nevertheless, both symptomatic and asymptomatic lesions of the optic nerve were associated with retinal neuro-axonal loss on optical coherence tomography in CIS patients (London *et al.*, 2019). In turn, different optical coherence tomography metrics have been associated with long-term clinical disability (Martinez-Lapiscina *et al*, 2016; Rothman *et al*, 2019). Accordingly, our results provided an evidence of a direct association of MRI lesions in this clinically-eloquent area with long-term disability, underscoring the role of neuroaxonal degeneration in clinically-eloquent areas of the CNS as an important driver of disability in MS (Ferguson *et al*, 1997; Minneboo *et al*, 2009; Saidha *et al*, 2015; Trapp *et al*, 1998). In line with this hypothesis, we found an association between 9-year disability worsening and baseline brainstem (presence of lesions) and spinal cord (number of not-enhancing lesions) involvement, which contain long-distance WM pathways critical for balance and locomotion. Although there are no available longitudinal studies in pediatric patients, a significant association was found between lesions in the brainstem and spinal cord with short-term (Arrambide *et al.*, 2018; Brownlee *et al.*, 2017; Brownlee *et al*, 2019; Minneboo *et al.*, 2004; Swanton *et al.*, 2009; Tintore *et al.*, 2010) and long-term EDSS changes in adult CIS patients.

In the opposite direction, we found that Gd-lesions on baseline MRI have a protective role against 9-year disability in pediatric-onset MS patients. This result, in line with recent long-term studies (Cree *et al.*, 2016; Goodin *et al*, 2012), contrasts with

findings observed in adult MS patients, in whom Gd-lesions were a negative prognostic factor for long-term clinical disability (Brownlee *et al.*, 2019). However, pediatric MS patients are known to have more frequent Gd-lesions than adults (Waubant *et al.*, 2009), with a frequency that reduces with age (Filippi *et al*, 2001). This trend is paralleled by a decrease in remyelination capability with age (Brown *et al*, 2014; Ghassemi *et al*, 2015b; Ghassemi *et al.*, 2015c), which underlays the shorter time needed to reach clinical disability in adult compared to pediatric patients (Renoux *et al.*, 2007). Indeed, a more severe acute inflammatory activity at disease onset could stimulate myelin repair and delay chronic inflammation processes typical of the progressive phase of disease (Mahad *et al*, 2015). As a matter of fact, increased levels of neural growth factors and increased regulatory T lymphocyte levels (Steinman, 2014) have been found during relapses. In this perspective, our findings underscore once again the pathophysiological differences between pediatric and adult MS patients. In addition, they point at the existence of an early critical window, in which treatment strategies need to be optimized as soon as possible, in order to protect patients' brain from the establishment of chronic neuroinflammatory processes, which probably represent the main determinant of disability accrual.

Finally, we also explored the role of a short-term follow-up in the prediction of 9-year clinical disability. As we could expect, same as for baseline EDSS, also its short-term increase provided a significant contribution in determining 9-year outcome. These results, together with the association found between 9-year clinical disability and the detection of at least two new T2-lesions at 2 years, underscore the relevance of clinical and MRI monitoring during the first years of disease in predicting long-term disease evolution (Rotstein *et al*, 2015). It is interesting to observe that, opposite to data in adult MS patients, there was no association between high efficacy DMT exposure and 9-year disability in pediatric MS patients. This finding underscores the existence of distinctive pathophysiological mechanisms of damage and repair in pediatric MS, which likely explain the more favorable clinical course in spite of higher disease activity.

This study has a few limitations. First, an inherent limitation to all longitudinal observational studies is drop-out of subjects over time, although relatively low in the present study. The second one is represented by the absence of a standardized MRI protocol, which did not allow us to quantify brain and spinal cord atrophy, known to play

an important role in determining clinical disability. In addition, optic nerve lesion assessment was performed on conventional brain MRI sequences, which have suboptimal sensitivity despite their common use for this purpose in a real-world setting. Third, we have no cognitive data for our cohort. Further long-term longitudinal studies, including cognitive data, should improve the identification of early prognostic predictors, given the paramount importance of long-term cognitive outcomes for pediatric MS patients.

In conclusion, by using clinical and easy obtainable MRI measures, we identified early predictors of 9-year disease course. High efficacy DMT exposure over the first year of disease reduced disease activity over the 9-year follow-up. Baseline cervical cord, brainstem and optic nerve involvement by lesions have a major role in predicting 9-year outcomes, both in term of disease activity and disability worsening, underscoring the need for complete CNS MRI assessment at baseline. In addition, an accurate clinical and MRI monitoring during the first 2 years of disease has proven to represent a powerful tool for counseling patients about long-term prognosis and personalizing treatment strategies.

Table 4.1.1. *Main baseline clinical and MRI features of the study cohort grouped by clinical status at 9 years follow-up.*

	All pediatric multiple sclerosis patients	**Pediatric multiple sclerosis patients not-worsened at FU**	**Pediatric multiple sclerosis patients worsened at FU**	***p* values**
Number of patients	123	110	13	-
Girls/Boys	89/34	78/32	11/2	0.47
Mean age (range) [years]	14.4 (7.3-17.9)	14.4 (7.3-17.9)	14.3 (9.8-17.0)	0.91
Median EDSS (range)	1.5 (0.0-6.0)	1.5 (1.0-4.0)	1.0 (0.0-6.0)	0.15
Treatment n (%) IFN/GA/NAT/IS	77(63)/16(13)/ 23(19)/7(5)	68(62)/13(12)/ 23(21)/6(5)	9(69)/3(23)/ 0(0)/1(8)	0.26
Clinical Presentation n (%)				
Polyfocal	35 (28)	30 (29)	5 (38)	0.88
Visual	14 (11)	10 (9)	4 (31)	0.12
Brainstem	32 (26)	31 (29)	1 (8)	0.13
Sensitive	30 (24)	28 (25)	2 (15)	0.92
Pyramidal	9 (7)	8 (6)	1 (8)	0.67
Cerebellar	2 (2)	2 (2)	0 (0)	1.00
Mean number of brain T2-lesions (range)	30.5 (3-180)	29.5 (3-167)	42.0 (3-180)	0.55
T2-lesion location n (%)				
Optic nerve	25 (20)	20 (18)	5 (38)	0.10
Periventricular (1 lesion)	99 (80)	89 (81)	10 (77)	1.00
Periventricular (>=3 lesions)	84 (68)	75 (68)	9 (69)	0.70
Cortical/juxtacortical	69 (56)	62 (56)	7 (54)	1.00
Deep gray matter	38 (31)	34 (31)	4 (31)	1.00
Cerebellum	63 (51)	54 (49)	9 (69)	0.13
Brainstem	68 (55)	59 (54)	9 (69)	0.21
Cervical spinal cord	67 (63)	61 (55)	6 (46)	0.80
Presence of black holes n (%)	51 (41)	47 (43)	4 (31)	0.66

Mean number of black holes (range)	3.2 (0-35)	3.1 (0-35)	4.1(0-21)	0.66
Presence of tumefactive lesions n (%)	25 (20)	23 (21)	2 (15)	1.00
Presence of brain Gd+ lesions n (%)	71 (58)	65 (59)	6 (46)	0.78
Mean number of brain Gd+ lesions (range)	3.0 (0 - 23)	3.0 (0 - 23)	5.5 (0 - 20)	0.87
Presence of cervical spinal cord Gd+ lesions n (%)	24 (21)	24 (23)	0 (0)	0.17
Mean number of cervical spinal cord lesions (range)	1.1 (0-6)	1.0 (0-5)	1.4 (0-6)	0.55
Mean number of Gd+ cervical spinal cord lesions (range)	0.2 (0 - 3)	0.3 (0 - 3)	0 (NA)	0.05

Abbreviations: EDSS=Expanded Disability Status Scale; Gd+=gadolinium enhancing; IFN=interferon; GA=glatiramer acetate; NAT=natalizumab; IS=immunosuppressant.

Table 4.1.2. *Main clinical and brain MRI changes over the follow-up period grouped by clinical status at 9 years.*

	All pediatric multiple sclerosis patients	**Pediatric multiple sclerosis patients not-worsened at FU**	**Pediatric multiple sclerosis patients worsened at FU**	***p* values**
Median follow-up duration (IQR) [years]	9.4 (6.9-12.9)	8.3 (6.8-13.6)	10.0 (8.1-10.7)	0.32
Mean time to first relapse (SD) [years]	2.3 (2.5)	2.3 (2.5)	2.2 (2.4)	0.23
Annualized relapse rate (SD)	0.3 (0.4)	0.3 (0.4)	0.3 (0.3)	0.75
Median EDSS at follow-up (range)	1.0 (0.0 - 7.0)	1.0 (0.0 - 4.0)	2.5(1.0 - 7.0)	<0.001
Mean number of 1-year new T2 lesions (range)	1.4 (0 - 15)	1.3 (0 - 15)	2.0 (0 - 6)	0.05
Mean number of 1-year new Gd+ lesions (range)	0.6 (0 - 10)	0.5 (0 - 5)	1.3 (0 - 10)	0.54
Mean number of 1-year relapses (range)	0.3 (0 - 3)	0.3 (0 - 3)	0.5 (0 - 2)	0.33
1-year EDSS change (range)	-0.3 (-3 - 2)	-0.4 (-3 - 1.5)	0.4 (-1 - 2)	<0.001
Mean number of 2-year new T2 lesions (range)	2.0 (0 - 15)	1.9 (0 - 15)	3.1 (0 - 7)	0.01
Mean number of 2-year new Gd+ lesions (range)	0.8 (0 - 13)	0.7 (0 - 8)	2.1 (0 - 13)	0.38
Mean number of 2-year relapses (range)	0.7 (0 - 6)	0.7 (0 - 6)	0.9 (0 - 2)	0.10
2-year EDSS change (range)	-0.2 (-2.5 - 2)	-0.4 (-2.5 - 1)	0.7 (-0.5 - 2)	<0.001

Abbreviations: SD=standard deviation; EDSS=Expanded Disability Status Scale; Gd+=gadolinium enhancing.

Table 4.1.3. *Multivariable linear regression models investigating early clinical and MRI predictors of annualized relapse rate (ARR) in pediatric multiple sclerosis patients.*

	Coefficient	**95% CI**	***p* values**	**R^2 (adjusted R^2)**
Baseline (n=123)				0.17 (0.15)
Presence of cerebellar lesions	-0.15	-0.25, - 0.05	<0.001	
Presence of cervical spinal cord lesions	0.16	0.05, 0.26	0.003	
High vs moderate efficacy DMT	-0.14	-0.25, -0.03	0.01	
Baseline – 1 year (n=115)				0.26 (0.22)
Number of 1-year relapses	0.14	0.05, 0.23	0.002	
Presence of cerebellar lesions*	-0.16	-0.26, -0.06	0.002	
Presence of cervical spinal cord lesions*	0.15	0.05, 0.25	0.004	
High vs moderate efficacy DMT	-0.12	-0.23, 0.01	0.04	
Baseline - 2 year (n=105)				0.26 (0.22)
Time to first relapse	-0.12	-0.20, -0.02	0.01	
Number of 2-year relapses	0.06	0.01, 0.12	0.02	
Presence of cerebellar lesions*	-0.12	-0.22, -0.01	0.03	
Presence of cervical spinal cord lesions*	0.10	0.00, 0.21	0.04	

*Abbreviations: CI=confidence interval; Gd+=gadolinium enhancing; DMT=disease modifying treatments; *at baseline.*

Table 4.1.4. *Multivariable logistic regression models investigating early clinical and MRI predictors of EDSS worsening after 9 years.*

	Odds ratio	**95% CI**	***p* values**	**C-statistic**	**Accuracy**
Baseline (n=123)				0.79	91%
Presence of optic nerve lesions	6.45	1.48, 30.49	0.01		
Presence of brainstem lesions	6.17	0.97, 122.48	0.10		
Baseline - 1 year (n=115)				0.90	93%
1-year EDSS change	13.40	3.27, 96.81	<0.001		
Baseline - 2 year (n=105)				0.96	90%
1-year EDSS change	26.05	4.32, 345.76	<0.001		
2-year EDSS change	16.38	1.99, 228.36	0.02		
>=2 new T2 lesions in 2 years	4.91	0.73, 46.58	0.02		

Abbreviations: EDSS: Expanded Disability Status Scale; CI=confidence interval.

Table 4.1.5. *Multivariable linear regression models investigating early clinical and MRI predictors of EDSS score at 9 years.*

	Coefficient	**95% CI**	***p* values**	**R^2 (adjusted R^2)**
Baseline (n=123)				0.42 (0.39)
Baseline EDSS	0.58	0.41, 0.75	<0.001	
Presence of brainstem lesions	0.31	0.01, 0.61	0.04	
Number of cervical spinal cord lesions	0.22	-0.02, 0.46	0.05	
Number of Gd+ cervical spinal cord lesions	-0.41	-0.77, -0.05	0.02	
Presence of brain Gd+lesions	-0.29	-0.60, 0.01	0.05	
Baseline - 1 year (n=115)				0.66 (0.64)
Baseline EDSS	0.96	0.80, 1.12	<0.001	
1-year EDSS change	0.71	0.54, 0.89	<0.001	
>=2 new T2 lesions in 1 year	0.28	0.03, 0.52	0.03	
Presence of brain Gd+lesions*	-0.22	-0.46, 0.03	0.08	
Brainstem lesions*	0.17	-0.07, 0.41	0.15	
Baseline - 2 year (n=105)				0.73 (0.71)
Baseline EDSS	0.97	0.83, 1.13	<0.001	
1-year EDSS change	0.79	0.62, 0.96	<0.001	
2-years EDSS change	0.55	0.21, 0.88	<0.001	
>=2 new T2 lesions in 2 years	0.35	0.11, 0.60	0.01	
Presence of brain Gd+lesions*	-0.19	-0.44, 0.06	0.13	

*Abbreviations: EDSS: Expanded Disability Status Scale; CI=confidence interval; Gd+=gadolinium enhancing; *at baseline.*

Figure 4.1.1. *Lesion distribution.*

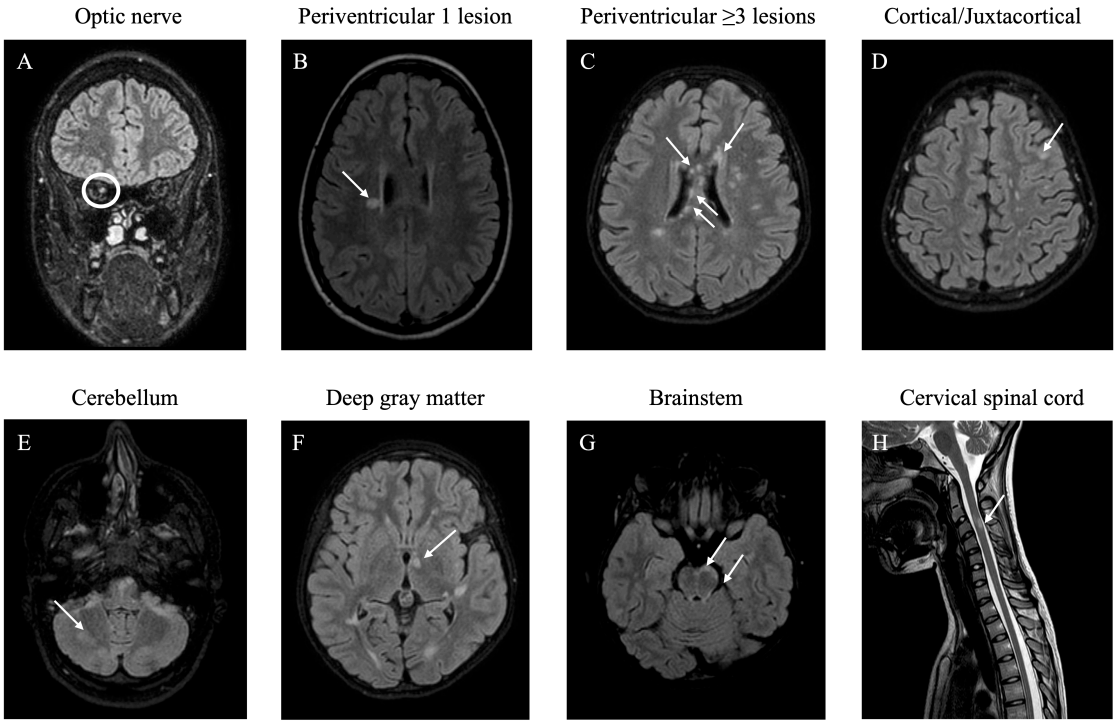

The pictures are representative of the seven brain regions considered in the study. Lesions located in the following compartments (highlighted by white circles and arrows) could be detected on FLAIR MRI sequences: (A) optic nerve; (B) periventricular region (one lesion); (C) periventricular region (three or more); (D) cortical/juxtacortical region; (E) cerebellum; (F) deep gray matter; (G) brainstem; (H) cervical cord (De Meo et al., 2021a).

Figure 4.1.2. *EDSS score at longest follow-up in pediatric multiple sclerosis patients.*

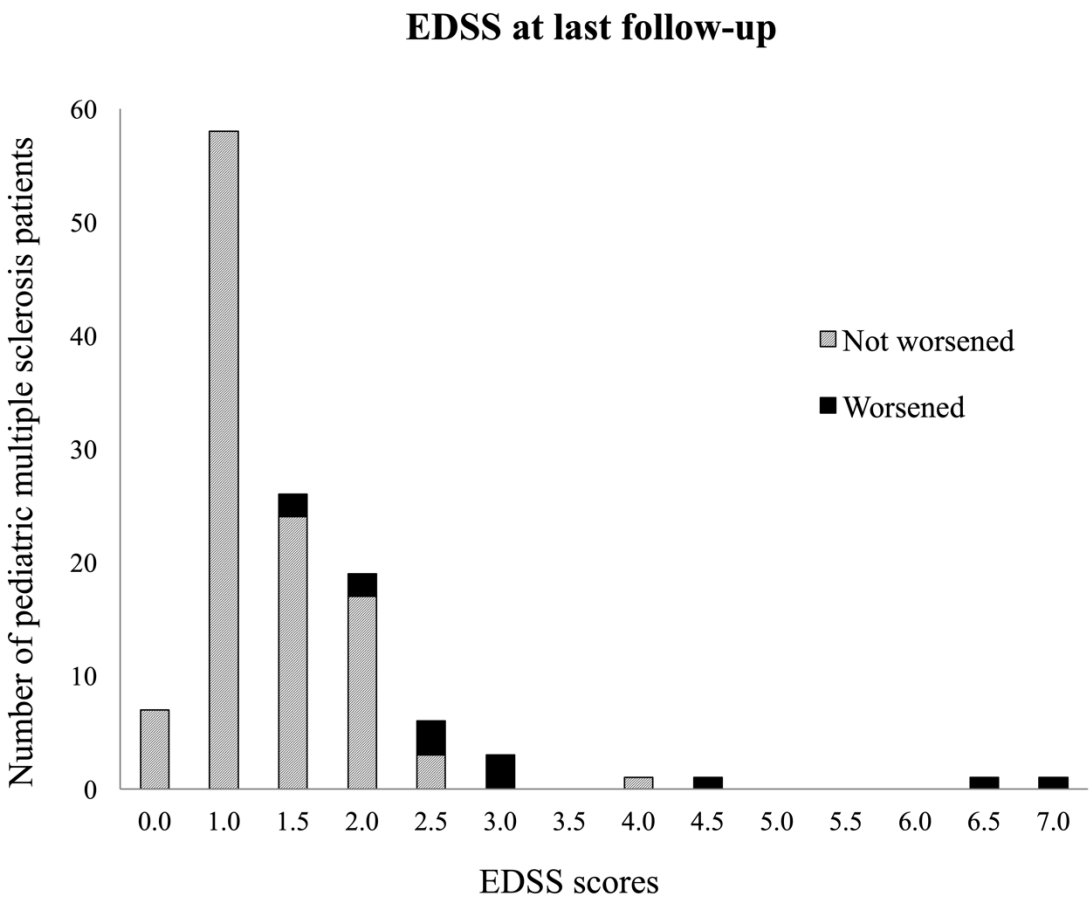

Pediatric multiple sclerosis patients not worsened at last follow-up are represented in histograms with gray filling, while those worsened at follow-up are represented in histograms with black filling (De Meo et al., 2021a).
Abbreviations: EDSS = Expanded Disability Status Scale.

Figure 4.1.3. *Risk of a first relapse in pediatric multiple sclerosis patients with and without optic nerve lesions.*

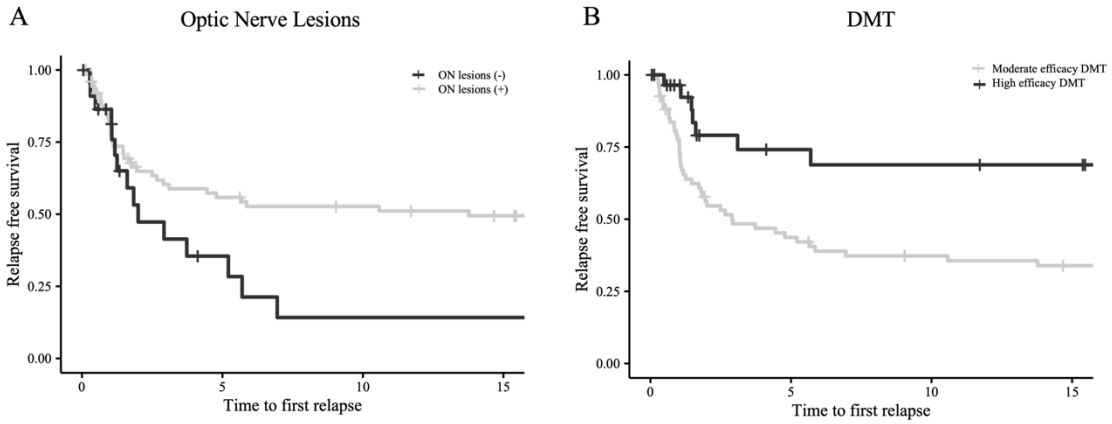

(A) Survival curves of time from disease onset to first relapse in pediatric multiple sclerosis patients with and without optic nerve lesions. Pediatric multiple sclerosis patients with optic nerve lesions are represented in black while patients without optic nerve lesions are represented light gray. (B) Survival curves of time from disease onset to first relapse in pediatric multiple sclerosis patients on moderate and high efficacy disease modifying treatments (DMT). Pediatric multiple sclerosis patients on moderate efficacy DMT are represented in light gray, while patients on high efficacy DMT are represented in black (De Meo et al., 2021a).
Abbreviations: ON=optic nerve; DMT= disease modifying treatments.

Supplementary materials

Table e-4.1.1. *Main clinical and MRI features of the study cohort grouped by exposure to moderate vs high efficacy disease modifying treatments.*

	Pediatric multiple sclerosis patients on moderate efficacy DMT	**Pediatric multiple sclerosis patients on high efficacy DMT**	***p* values**
Number of patients	93	30	-
Girls/Boys	67/26	22/8	1.00
Mean age (range) [years]	14.1 (7.3-17.9)	15.4 (10.9-17.9)	0.01
Median EDSS at baseline (range)	1.5 (0.0-6.0)	2.0 (1.0-4.0)	0.006
Median EDSS at 9-year follow-up (range)	1.0 (0.0-7.0)	1.5 (1.0-4.0)	0.21
Clinical Presentation n (%)			
Polyfocal	23 (25)	12 (40)	0.16
Visual	12 (13)	2 (7)	0.54
Brainstem	26 (28)	6 (20)	0.53
Sensitive	22 (24)	8 (26)	0.92
Pyramidal	7 (8)	2 (7)	1.00
Cerebellar	2 (2)	0 (0)	1.00
Mean number of brain T2-lesions (range)	22.9 (1-81)	52.9 (3-180)	0.008
T2-lesion location n (%)			
Optic nerve	15 (16)	10 (33)	0.07
Periventricular (1 lesion)	69 (74)	30 (100)	0.004
Periventricular (>=3 lesions)	56 (60)	28 (93)	0.006
Cortical/juxtacortical	46 (49)	23 (77)	0.02
Deep gray matter	26 (28)	12 (40)	0.31
Cerebellum	42 (45)	21 (70)	0.03
Brainstem	46 (49)	22 (73)	0.04
Cervical spinal cord	45 (48)	22 (73)	0.04
Presence of black holes n (%)	31 (33)	20 (67)	0.003
Mean number of black holes (range)	1.3 (0 - 21)	6.7 (0 - 35)	0.001
Presence of tumefactive lesions n (%)	13 (14)	12 (40)	0.005

Presence of brain Gd+ lesions n (%)	45 (48)	26 (87)	0.001
Mean number of brain Gd+ lesions (range)	1.7 (0 - 15)	6.4 (0 - 23)	<0.001
Presence of cervical spinal cord Gd+ lesions n (%)	12 (13)	12(40)	0.006
Mean number of cervical spinal cord lesions (range)	0.8 (0 - 6)	1.6 (0 - 5)	0.02
Mean number of Gd+ cervical spinal cord lesions (range)	0.2 (0 - 2)	0.5 (0 - 3)	0.002

Abbreviations: EDSS=Expanded Disability Status Scale; Gd+=gadolinium enhancing; DMT=disease modifying treatments.

4.2 Comparing natural history of pre- and post-pubertal onset multiple sclerosis

Part of the following data have been published (De Meo, 2021).

Abstract

Objectives. To describe and compare disease course and prognosis of early (i.e., disease onset before age 11 years) and late (i.e., disease onset after age 11 years) onset pediatric MS.

Methods. Prospectively-collected clinical information from the Italian Multiple Sclerosis Register of 1993 pediatric MS patients, of whom 172 with early onset, was analyzed. Cox models adjusted for sex, baseline Expanded Disability Status Scale score and disease-modifying treatments exposure were used to assess the risk of reaching irreversible Expanded Disability Status Scale scores of 3, 4, and 6, and conversion to SP phenotype in early vs late onset pediatric patients. Prognostic factors were also evaluated.

Results. A greater proportion of males, isolated brainstem involvement, and longer time interval between first and second clinical episode was observed in early vs late onset pediatric patients. Compared to late onset, early onset pediatric patients took longer time from disease onset to convert to SP phenotype and to reach all three disability milestones. Recovery from first demyelinating event, time to first relapse, annualized relapse rate during the first 3 years of disease and disease-modifying treatments exposure were independent predictors for long-term disability in early onset pediatric patients. In late onset pediatric patients, isolated optic neuritis, brainstem symptoms or progressive course at disease onset were additional predictors for long-term disability.

Interpretation. These findings may point towards the existence of specific pathophysiological mechanisms, as well as towards a greater neurorepair capacity to counteract damage, in early onset pediatric MS patients.

Introduction

Pediatric MS (MS), with disease onset before 18 years of age, represents 3-10% of all MS cases (Renoux *et al.*, 2007). MS onset before puberty (i.e,, by convention, before age 11 years) is, however, extremely rare, as it occurs in 0.2-0.6% of all cases (Chabas *et al.*, 2008). Only a few studies were conducted in this specific population, all suggesting epidemiological (Renoux *et al.*, 2007), clinical (Ruggieri *et al*, 1999) and MRI (Weygandt *et al*, 2015) differences between pediatric MS with onset before and after puberty. In this study, we are going to define the two groups as "early" and "late" onset pediatric MS, respectively.

Sex distribution was reported to be even (Huppke *et al.*, 2014) or to show male predominance (Ruggieri *et al.*, 1999) in early onset pediatric MS patients, as opposed to female preponderance in late onset ones. However, according to other studies, the female:male ratio might be similar in early vs late onset pediatric MS (Renoux *et al.*, 2007). Type of onset is also different in early onset pediatric MS patients, with a higher likelihood of brainstem involvement (Ghassemi *et al.*, 2008; Huppke *et al.*, 2014; Renoux *et al.*, 2007), polyfocal deficits and encephalopathy compared to older patients (Banwell *et al*, 2009). Particularly, this last feature is likely to delay MS diagnosis in this population, as long as ADEM needs to be excluded for applying MS diagnostic criteria (Wong *et al.*, 2018). The 2017 McDonald criteria for MS diagnosis (Thompson *et al.*, 2018) can be used for early onset pediatric MS patients, albeit with reduced sensitivity (Fadda *et al*, 2018a; Hacohen *et al.*, 2019; McLaughlin *et al*, 2009). A relapsing-remitting disease course was reported in more than 98% of pediatric MS cases (Waldman *et al.*, 2016). Moreover, compared to adults, pediatric MS patients have a higher relapse rate, significantly associated with younger age at disease onset (Benson *et al.*, 2014; Gorman *et al.*, 2009).

Compared to late onset, early onset pediatric MS patients show several MRI differences, likely reflecting different pathological substrates (Chabas *et al.*, 2008). In very young patients, initial T_2-hyperintense lesions are usually ill-defined and tend to vanish on follow-up imaging (Chabas *et al.*, 2008). Furthermore, a higher rate of deep GM involvement and fewer enhancing lesions are reported (Waubant *et al.*, 2011; Weygandt *et al.*, 2015). Different cerebrospinal fluid (CSF) profiles may indicate some differences in pathogenic mechanisms. Neutrophilic pleocytosis, a higher percentage of

monocytes and the absence of intrathecal immunoglobulin-G synthesis was more frequently found in early onset pediatric MS, suggesting a prominent involvement of the innate immune system; while lymphocytic pleocytosis and elevated CSF immunoglobulin-G were observed in late onset pediatric and adult onset MS, suggesting prominent activation of the adaptive immune system (Chabas *et al.*, 2010).

Although several differences were described between early and late onset pediatric MS, there is still limited information deriving from long-term, longitudinal studies in early onset pediatric MS. The main aims of the present study were to describe and compare the natural history of the disease and to determine prognostic factors for long-term disability in a large cohort of early onset and late onset pediatric MS patients.

Methods

Ethics committee approval. The Italian iMedWeb network was approved by the Policlinico of Bari Ethics Committee and by the local ethics committees in all participating centers. Written informed consent was obtained from all participants and their parents prior to inclusion in the Italian MS Register (Trojano *et al*, 2019).

Population and definition of cases. Registered cases of definite MS with disease onset between January 1st, 1961, and April 30th, 2018, were included, maintaining a sufficient follow-up time before the study end date of May 15, 2021. Pediatric onset cases were defined as disease onset before the age of 18 years, in accordance with the definition proposed by the International Pediatric MS Study Group (Krupp *et al.*, 2013). Patients with fewer than 3 EDSS measurements, with missing MS diagnosis or onset date, or crucial errors in records were excluded. **Figure 4.2.1** shows study flow-chart. According to these criteria from 3332 pediatric onset (i.e., before age 18 years) (Krupp *et al.*, 2013) MS patients, a cohort of 1993 pediatric onset MS patients was selected from the Italian MS Register (Trojano *et al.*, 2019). Patients were divided into early and late onset subgroups, based on disease onset before or after/equal age 11 years, respectively (Chabas *et al.*, 2008; Chabas *et al.*, 2010).

Data collection. Baseline clinical information reported in the Italian MS Register included sex, date of MS onset and symptoms manifested, date of diagnosis, clinical course and geographical region of residence. The date of MS onset was defined as the date of first recorded clinical manifestation of MS, and the diagnosis was performed by a

neurologist based on the prevailing diagnostic criteria at the time of diagnosis (Polman *et al.*, 2011; Polman *et al.*, 2005; Thompson *et al.*, 2018). Detailed information on disease phenotype, EDSS score, relapses (date and degree of remission [complete/incomplete clinical recovery within 6 months or no remission]) and disease-modifying treatments (DMT) use (product name, starting and stopping dates and reasons for stopping) were recorded by the treating neurologist every 3 or 6 months, and on occasions of clinical relapse evaluations. EDSS recorded within 30 days from a clinical relapse were excluded to avoid artificial increase of EDSS score changes over time. DMT were grouped into moderate- (any preparation of interferon-beta, glatiramer acetate, dimethyl fumarate, teriflunomide) and high-efficacy (natalizumab, fingolimod, rituximab, ocrelizumab, alemtuzumab, immunosuppressants [cyclophosphamide, mitoxantrone] and autologous hematopoietic stem cell transplantation) treatments. Data are centrally monitored in order to check the quality of collected information.

Assessment of outcomes. Focus was placed on four distinct endpoints: time to irreversible EDSS 3 (moderate disability, though fully ambulatory), EDSS 4 (limited walking ability, but able to walk more than 500 m without aid or rest), and EDSS 6 (ability to walk no more than 100 meters without rest or necessity of unilateral support), and to conversion to SP MS (Lublin *et al*, 2014). Disability was defined as irreversible when a given EDSS score persisted for at least 12 months, with all subsequent EDSS scores being either equal to this score or greater, thus excluding transient worsening of disability related to relapses (Kalincik *et al.*, 2015). Conversion to SP MS was based on the subjective decision made by the neurologists according to the Lublin criteria for secondary progression (Lublin *et al.*, 2014).

Prognostic factors. We assessed the following potential prognostic factors in predicting the three selected disability milestones: sex, initial disease course (relapse-onset vs progressive), initial symptoms, remission from first demyelinating event (complete vs incomplete/no remission), time to first relapse, ARR during the first 3 years of the disease (as over this period pediatric MS patients are known to experience higher ARR compared to their adult counterpart) and DMT exposure.

Statistical analysis. Demographic and clinical features were compared between early and late onset pediatric MS patients using chi-square and Fisher's exact tests for categorical variables and Student's t-test and Wilcoxon test for continuous variables, as

appropriate. Normal distribution was assessed by visual inspection and Kolmogorov-Smirnov test.

Kaplan-Meier and Cox proportional hazards regression models were used to assess the risk of reaching irreversible EDSS 3, 4 and 6, and of conversion to SP MS in early and late onset pediatric MS. Cox models were adjusted for sex, disease course and EDSS at the onset, and DMT exposure as a time-varying covariate. Univariate and multivariate Cox proportional hazards regression models were used to identify predictors of reaching the disability milestones. For the multivariate analysis, a stepwise variable selection procedure was used. This procedure is a combination of forward and backward selection, in which, at each step, every variable is considered for addition to or subtraction from the set of covariates based on an F-test with a p-value for inclusion of 0.15.

Given the time period of data collection spans decades of innovation in the management of MS, we performed a sensitivity analysis, re-running above steps on a subgroup of patients diagnosed before 2014 and adjusting for diagnosis epoch, as defined by Baroncini and colleagues (Baroncini *et al*, 2021) in addition to the above specified covariates.

Statistical significance was defined by $p<0.05$. Statistical analysis was performed with R software (version 4.0.2).

Data availability. The dataset used and analyzed during the current study is available from the corresponding author on reasonable request.

Results

Demographic and clinical features. Of 1993 pediatric MS cases selected for the final analysis, 172 (9%) were classified as early onset pediatric MS. **Table 4.2.1** summarizes the main clinical and demographic features of the study cohort grouped by age at disease onset. A lower female:male ratio was observed in early vs late onset pediatric MS patients (1.3:1 *vs* 2.3:1, p=0.001).

Disease onset. Compared to late onset, early onset pediatric MS patients more frequently experienced isolated brainstem symptoms (37% *vs* 24%, p<0.001) and less frequently optic neuritis (16% *vs* 25%, p=0.02) or long-tract symptoms (8% *vs* 15%, *p*=0.02) at disease onset. Only one early onset pediatric MS patient had a clinical picture consistent with ADEM at disease onset and was subsequently diagnosed with MS. The

majority of cases had a relapse-onset disease course (99%), without significant differences between the two groups. First EDSS score was similar, and no differences in the degree of remission from the first demyelinating were observed between early and late onset pediatric MS patients.

Disease course. Almost all enrolled subjects received a DMT (94%) at some point during the disease course. However, a higher percentage of never treated patients (13% *vs* 6%, $p<0.001$) and a longer time to DMT start (10.7 *vs* 7.1 years, $p<0.001$) was observed in early vs late onset pediatric MS patients. Compared to late onset, early onset pediatric MS patients showed a longer median time to first relapse (5.1 *vs* 2.6 years, $p=0.001$), while they experienced a similar ARR during the first 3 years of disease. Eleven of the 171 (6%) early onset and 234 of 1796 (13%) late onset pediatric MS patients with relapse-onset converted to SP MS during follow-up. Similar time from birth and longer time from disease onset to conversion to SP MS was observed in early vs late onset pediatric MS patients (**Table 4.2.2**). Estimation of median time for conversion to SP MS was not feasible for early onset pediatric MS patients due to the low number (n=11) of converting patients.

Time to develop irreversible disability. Similar time from birth to reach all the three disability milestones was found for early and late onset pediatric MS patients. Instead, longer time from MS onset to reach all three disability milestones was observed for early onset compared to late onset pediatric MS patients (**Table 4.2.2** and **Figure 4.2.2**). From MS onset, the median time to reach EDSS 3 (31.2 *vs* 23.7 years, $p<0.001$), 4 (36.9 *vs* 26.2 years, $p<0.001$) and 6 (40.7 *vs* 33.0 years, $p<0.001$) was longer in early compared with late onset cases.

Prognostic factors for disability milestones: univariate analysis. In early onset pediatric MS patients, shorter time to first relapse, higher ARR during the first 3 years of disease and exposure to both moderate- and high-efficacy DMT were associated with a higher risk of reaching EDSS 3 and 4. As converse, isolated optic neuritis was related to lower risk of reaching EDSS 3. Furthermore, an incomplete remission from the first demyelinating event was associated with higher risk of reaching EDSS 4 and 6 (**Table 4.2.3**).

In late onset pediatric MS patients, multifocal symptoms at onset, progressive onset, incomplete remission from the first demyelinating event, shorter time to first

relapse, higher ARR during the first 3 years of disease, and exposure to high-efficacy DMT predicted a higher risk of reaching EDSS 3 and 4. Furthermore, the exposure to moderate-efficacy DMT was associated with a higher risk of reaching EDSS 3. Age at disease onset, progressive onset, incomplete recovery from the first demyelinating event and shorter time to first relapse predicted higher risk of reaching EDSS 6. Onset with isolated optic neuritis predicted lower risk of reaching EDSS 3, 4 and 6. Exposure to moderate-efficacy DMT predicted lower risk of reaching EDSS 6 (**Table 4.2.3**).

Prognostic factors for disability milestones: multivariate analysis. In the multivariate analysis, higher ARR during the first 3 years of disease and exposure to both moderate- and high-efficacy DMT were independent predictors of higher risk of reaching EDSS 3 in early onset pediatric MS patients. Furthermore, in this cohort, the exposure to high-efficacy DMT and incomplete remission from the first demyelinating event resulted as independent predictors of higher risk of reaching EDSS 4 and 6, respectively (**Table 4.2.4**).

In late onset pediatric MS patients, multifocal symptoms at onset, incomplete remission from the first demyelinating event, shorter time to first relapse, higher ARR during the first 3 years of disease and exposure to high-efficacy DMT were associated with a higher risk of reaching EDSS 3 and 4. Furthermore, in this cohort, the exposure to moderate-efficacy DMT and a progressive onset were independent predictors of higher risk of reaching EDSS 3 and 4, respectively. Higher risk of reaching EDSS 6 was predicted by progressive onset, incomplete remission from first demyelinating event and shorter time to first relapse, while isolated optic neuritis at disease onset and exposure to moderate efficacy DMT were associated with lower risk of reaching EDSS 6 (**Table 4.2.4**).

Sensitivity analysis. A cohort of 1664 pediatric MS patients, including 146 (9%) early onset pediatric MS patients was selected for sensitivity analysis. This cohort did not differ from the entire study cohort in terms of demographic and clinical variables (data not shown). Sensitivity analysis confirmed the above reported findings. Detailed information is available in **Supplementary Material 4.2.1**.

Discussion

Comparing the natural history of early and late onset pediatric MS in a large, real life cohort of patients, this study identified several specific features of early onset pediatric MS.

In line with previous studies (Huppke *et al.*, 2014; Tintoré & Arrambide, 2009), we found a lower female:male ratio in patients with early vs late onset pediatric MS, thus supporting a role of puberty and sex hormones in determining MS onset (Bove & Chitnis, 2014). Also in line with previous studies (Banwell *et al.*, 2009; Huppke *et al.*, 2014), we observed a prominent brainstem involvement in early onset pediatric MS patients, while isolated optic neuritis or isolated spinal cord involvement prevailed later. However, we did not observe a predominance of polyfocal onset in early onset pediatric MS patients. The preferential brainstem involvement in early onset pediatric MS might be attributed to the myelination state of this structure, as long as MS lesions mainly affect myelin-rich regions. Given myelination proceeds along a caudo-rostral gradient in the encephalon (Paus, 2005), the brainstem myelinates earlier than supratentorial brain. The caudo-rostral spread of myelin occurs faster in males than in females (De Bellis *et al.*, 2001), consistently with the higher percentage of males in early vs late onset pediatric MS. In the spinal cord, myelination shows a steep increase at age 12-14 years (Geertsen *et al*, 2017; Yeo *et al*, 2014) followed by a gradual increase until the adulthood (Yeo *et al.*, 2014), which may explain the preferential spinal cord involvement in late onset pediatric MS. The more frequent onset with isolated optic neuritis in late onset vs early onset pediatric MS might be related to an effect of gender or sex hormones, as optic neuritis was found to be more frequent in females (Banwell *et al.*, 2009). Another possible explanation may be an under-report of visual difficulties in younger patients, especially those in pre-scholar age.

No difference was observed in recovery from first demyelinating between early and late onset pediatric MS patients. Complete recovery was reported in 82% early onset and 79% late onset patients, which highlights efficient repair mechanisms against brain damage during childhood and adolescence (Chitnis *et al.*, 2020). Interestingly, although several studies suggested an inverse relationship between age and relapse rate (Benson *et al.*, 2014; Gorman *et al.*, 2009), we found a significantly shorter time to first relapse in late compared to early onset pediatric MS patients. This finding is in line with the hypothesis that hormonal and metabolic changes occurring during puberty are responsible

for a higher risk of relapses in both males and females (Lulu *et al*, 2015). Although we had no data on hormone levels, growth charts or Tanner stages, age below 11 years is usually associated to pre-pubertal stage (Huppke *et al.*, 2014; Lulu *et al.*, 2015; Young *et al*, 2019), thus most probably puberty was included in our late onset group. Furthermore, we found similar ARR over the first 3 years of disease in early onset vs late onset pediatric MS patients, in line with previous studies observing no difference in pre- and post-pubertal relapse rate (Bove & Chitnis, 2014; Lulu *et al.*, 2015; Young *et al.*, 2019). In conclusion, the highest risk of relapse might be limited to the peripubertal period. As a possible biological explanation, leptin levels reach a peak at around puberty onset (Lulu *et al.*, 2015; Mantzoros *et al*, 1997). Leptin was identified as a promoter of pro-inflammatory cytokine secretion and Th1 differentiation and increased leptin secretion was observed in several autoimmune diseases (Matarese *et al*, 2008).

Early onset pediatric MS patients took a longer time from disease onset to shift to SP MS and to reach EDSS 3, 4 and 6. As a confirmation of the better prognosis of early vs late onset pediatric MS, we did not find any differences in the time from birth to reach EDSS 3, 4 and 6. While we are the first to report long-term outcomes for early onset pediatric MS patients, data for late onset pediatric patients was similar to that reported in previous studies (McKay *et al.*, 2019; Renoux *et al.*, 2007) comparing the natural history of pediatric vs adult onset MS. This suggests the present results could be generalized to other populations.

Our results support different pathophysiology between pre-and post-pubertal onset MS. These differences could be related to the developmental changes occurring in both immune system and CNS during the pubertal age. As suggested by the CSF findings (Chabas *et al.*, 2010), a prominent activation of innate immune system is likely to exist in early onset pediatric MS patients. It is possible to speculate that the preferential activation of innate immunity rather than adaptive immunity could be protective against neurodegenerative processes and delay the establishment of chronic neuroinflammation. Furthermore, the peri-pubertal period is probably key for GM and WM maturation dependent on sex (De Meo *et al.*, 2019) and sex hormone levels (Chitnis, 2013). This suggests that brain damage occurring before the hormonal boost to developmental trajectories might benefit from the highest repair capabilities, proper of younger subjects (Ghassemi *et al.*, 2015c), and might less affect GM and WM development.

In the present study, we also identified several predictors of reaching confirmed disability in both early and late onset pediatric MS patient. Sound evidence (Chitnis *et al.*, 2020; Confavreux *et al*, 2003) supports a role of relapses and incomplete recovery from relapses as contributors to disability accrual in MS. Accordingly, we observed an incomplete recovery from the first demyelinating event was associated with higher risk of reaching EDSS 6 in early onset pediatric MS patients, and EDSS 3, 4, and 6 in late onset patients. As matter of fact, relapse severity and related recovery are likely to follow a similar pattern at individual level (Mowry *et al*, 2009), thus allowing to identify those patients at higher risk to experience severe disability. Unfortunately, genetic, biologic or environmental factors underlying individual repair capability are still under investigation.

In line with previous studies (McKay *et al.*, 2019; Renoux *et al.*, 2007; Tremlett *et al*, 2009), early disease activity significantly affected long-term disability accrual in our cohort. Shorter time to first relapse was associated with higher risk of reaching EDSS 3 in early onset pediatric MS patients, and EDSS 3, 4 and 6 in late onset patients. Moreover, in both early and late onset pediatric MS patients, a higher ARR over the first 3 years of disease was associated with higher risk of reaching EDSS 3 and 4. These findings show that repeated demyelinating attacks, especially during the earliest stages of disease (Tremlett *et al.*, 2009), may increase the risk of reaching long-term irreversible disability and underscore the critical importance of early treatment also in pediatric patients (Jokubaitis *et al*, 2016).

Confirming previous findings (McKay *et al.*, 2019), we observed the exposure to moderate- and high-efficacy DMT, compared to no treatment, was associated with higher risk of confirmed disability accrual in both early and late onset pediatric MS groups. Apparently surprising, this finding is likely to reflect an "indication bias", as those with more aggressive course are more likely to be treated. In evaluating this finding, moreover, we should also consider the delayed introduction of DMT in the pediatric MS population. Indeed, in our cohort, the average time to introduction of the first DMT was 10.7 and 7.4 years from disease onset for early onset and late onset patients, respectively. It is likely that both moderate- and high-efficacy DMT might have been introduced only in face of persistent disease activity or clinical worsening, due to limited availability of approved DMT, as well as safety concerns in the pediatric patients, especially those younger than 11 years. Furthermore, the strength of the association between DMT exposure and the

risk of disability accrual became lower or not significant for EDSS 4, and, in late onset pediatric patients, it reverted by showing protection against the risk of reaching EDSS 6, a more robust disability milestone.

Lastly, the location of the first demyelinating event and a progressive course at disease onset were associated with the risk of disability accrual in late onset pediatric MS patients only. Consistently with previous findings in the adult MS population (Brownlee *et al.*, 2019), also in our cohort brainstem symptoms and polyfocal involvement were associated with a poorer prognostic outcome, whereas isolated optic neuritis at onset was associated with a better outcome (Confavreux *et al.*, 2003). The negative prognostic role of progressive onset is also well established in the literature.

This study is not without limitations. We were not able to include in our analysis MRI data, being it unfortunately available for a minority of our patients. Furthermore, although cognitive impairment can represent a relevant disease manifestation of pediatric MS (Amato *et al.*, 2016), which is not easily captured by the EDSS score, cognitive data in this population was not systematically collected in the Italian MS Register. In addition, only a small percentage of our early onset MS patients converted to SP MS, not allowing an estimate of the median time to reach this stage. Lastly, given the rarity of MS onset before age 11, disease onset of enrolled MS patient spanned over almost 60 years. Nonetheless, sensitivity analysis with diagnosis epoch (Baroncini *et al.*, 2021) as an additional covariate reassures on the validity and generalizability of study results.

Despite the above considerations, our comparative analysis on a large, real life cohort of pediatric patients, highlighting some differences in the natural history of early vs late onset pediatric MS, provides some support to the hypothesis of different pathophysiological mechanisms occurring in the prepubertal age. The study also points to the critical importance of early treatment in this population and it adds relevant prognostic information to improve the clinical management of pediatric MS patients.

Table 4.2.1. *Main clinical and demographic features of the study cohort grouped by age at the disease onset.*

	All pediatric MS patients	**Early onset (<11 years) pediatric MS patients**	**Late onset (≥11 years) pediatric MS patients**	***p* values**
Number of patients	1993	172	1821	
Male/female	631/1362	74/98	557/1264	0.001
Mean disease duration at last follow-up (SD) [years]	18.0 (11.3)	21.1 (10.9)	17.7 (11.3)	<0.001
Mean age at disease onset (SD) [years]	15.0 (2.6)	8.8 (2.0)	15.6 (1.8)	<0.001
First EDSS recorded median (IQR)	2.0 (1.0-3.0)	2.0 (1.0 – 3.0)	2.0(1.0 – 3.0)	0.62
Initial symptoms n (%)				
Isolated optic neuritis	458 (24%)	27 (16%)	431 (25%)	0.02
Isolated brainstem symptoms	485 (25%)	62 (37%)	423 (24%)	<0.001
Isolated long-tract symptoms	280 (15%)	14 (8%)	266 (15%)	0.02
Combination of symptoms	692 (37%)	63 (38%)	629 (37%)	0.65
ADEM	1 (0%)	1 (1%)	0 (0%)	0.41
Initial disease course n (%)				0.28
Relapse-onset	1967 (99%)	171 (99%)	1796 (99%)	
Primary progressive	26 (1%)	1 (1%)	25 (1%)	
Unknown	10 (1%)	0 (0%)	10 (1%)	
Mean time to DMT start (SD) [years]	7.4 (8.5)	10.7 (9.7)	7.1 (8.3)	<0.001
DMT exposure n (%)				
Never-treated	129 (6%)	22 (13%)	107 (6%)	<0.001
Moderate efficacy DMT only	781 (39%)	64 (37%)	717 (39%)	0.64
High efficacy DMT only	274 (14%)	21 (12%)	253 (14%)	0.61
Switched from moderate to high efficacy	805 (40%)	64 (37%)	741 (41%)	0.41

Degree of remission at first relapse n (%)				
Complete	661 (80%)	61 (82%)	600 (79%)	0.78
Partial	154 (19%)	12 (17%)	142 (19%)	0.67
None	16 (2%)	1 (1%)	15 (2%)	1.00
Median time to first relapse (IQR)	2.7 (0.9 - 7.6)	5.1 (1.0 -11.9)	2.6(0.9 - 7.0)	0.001
Mean ARR in the first 3 years (SD)	0.2 (0.4)	0.2 (0.4)	0.2 (0.5)	0.08

Abbreviations: MS = multiple sclerosis; SD = standard deviation; EDSS = Expanded Disability Status Scale; IQR = interquartile range; DMT = disease modifying treatments.

Table 4.2.2. *Cox models of time to EDSS 3, 4, and 6, and conversion to secondary progressive MS from birth or MS onset, comparing early vs late onset pediatric MS patients (the latter as reference group).*

Risk of reaching disability milestone in early vs late onset pediatric MS patients	**HR**	**95% CI**	**p values**	**Adjusted§ HR**	**95% CI**	**p values**
From birth to:						
EDSS 3	0.96	0.71, 1.52	0.83	1.06	0.72, 1.56	0.76
EDSS 4	0.92	0.58, 1.45	0.72	0.91	0.57, 1.43	0.68
EDSS 6	0.83	0.48, 1.44	0.51	0.84	0.49, 1.47	0.55
Conversion to SPMS*	0.61	0.33, 1.11	0.11	0.54	1.22, 1.30	0.16
From MS onset to:						
EDSS 3	0.51	0.38, 0.74	<0.001	0.51	0.35, 0.73	<0.001
EDSS 4	0.42	0.26, 0.66	<0.001	0.42	0.28, 0.65	<0.001
EDSS 6	0.39	0.23, 0.67	<0.001	0.40	0.23, 0.69	<0.001
Conversion to SPMS*	0.34	0.18, 0.67	0.001	0.41	0.18, 0.97	0.04

**Analysis performed on relapse-onset pediatric MS patients only (171 early onset and 1786 late onset patients).*

§Adjusted for sex, disease course at onset (primary progressive or relapse-onset), EDSS score at the onset, and disease-modifying therapy exposure (no treatment, moderate- or high-efficacy) as a time-varying covariate.

Abbreviations: HR = hazard ratio; CI = confidence interval; MS = multiple sclerosis; EDSS = Expanded Disability Status Scale.

Table 4.2.3. *Univariate Cox models of time from MS onset to EDSS 3, 4, and 6 early and late onset pediatric multiple sclerosis patients.*

Early onset pediatric MS	**EDSS 3**			**EDSS 4**			**EDSS 6**		
	HR	**95%CI**	***p* values**	**HR**	**95%CI**	***p* values**	**HR**	**95%CI**	***p* values**
Isolated optic neuritis*	0.37	0.14, 0.95	0.04						
Complete remission from first demyelinating event (ref)	-	-	-	1.00			1.00		
Incomplete remission from first demyelinating event	-	-	-	3.38	1.31, 8.74	0.01	8.58	2.23, 32.95	0.002
Time to first relapse	0.93	0.88, 0.97	0.03	0.95	0.90, 1.00	0.05	-	-	-
ARR in the first 3 years	4.30	2.20, 8.60	<0.001	2.15	1.5, 2.99	<0.001	-	-	-
No DMT exposure (ref)	1.00			1.00			-	-	-
Moderate efficacy DMT	5.91	2.63, 13.25	<0.001	2.70	1.14, 6.32	0.02	-	-	-
High efficacy DMT	7.25	2.83, 18.60	<0.001	3.59	1.36, 9.46	0.01	-	-	-
Late onset pediatric MS	**EDSS 3**			**EDSS 4**			**EDSS 6**		
	HR	**95%CI**	***p* values**	**HR**	**95%CI**	***p* values**	**HR**	**95%CI**	***p* values**
Age at onset	-	-	-	-	-	-	1.07	1.01, 1.14	0.03
Isolated optic neuritis*	0.74	0.60, 0.91	0.006	0.71	0.57, 0.90	0.004	0.67	0.51, 0.89	0.005
Combination of symptoms*	1.50	1.20, 1.90	0.001	1.69	1.32, 2.15	<0.001	-	-	-
Relapsing onset (ref)				1.00			1.00		
Progressive onset	2.70	1.30, 5.40	0.006	2.94	1.79, 4.81	<0.001	2.56	1.50, 4.40	<0.001

Complete remission from demyelinating event (ref)	-	-	-	1.00			1.00		
Incomplete remission from first demyelinating event	1.81	1.29, 2.54	<0.001	2.5	1.26, 5.05	0.001	1.67	1.12, 2.48	0.01
Time to first relapse	0.96	0.94, 0.98	<0.001	0.97	0.95, 0.98	<0.001	0.97	0.95, 0.98	<0.001
ARR in the first 3 years	1.60	1.40, 1.90	<0.001	1.64	1.39, 1.94	<0.001	-	-	-
No DMT exposure (ref)	1.00			1.00			1.00		
Moderate efficacy DMT	2.24	1.78, 2.83	<0.001	-	-	-	0.50	0.38, 0.64	<0.001
High efficacy DMT	2.48	1.87, 3.29	<0.001	1.92	1.49, 2.48	<0.001	-	-	-

**at disease onset*

Abbreviations: HR = hazard ratio; CI = confidence interval; MS = multiple sclerosis; EDSS = Expanded Disability Status Scale; DMT = disease modifying treatment; ref = reference level.

Table 4.2.4. *Multivariable Cox regression models of prognostic factors of time from disease onset to reach disability milestones (EDSS 3, 4 and 6) in early and late onset pediatric multiple sclerosis patients.*

Early onset pediatric MS	**EDSS 3**			**EDSS 4**			**EDSS 6**		
	HR	**95%CI**	***p* values**	**HR**	**95%CI**	***p* values**	**HR**	**95%CI**	***p* values**
Complete remission from first demyelinating event (ref)	-	-	-	-	-	-	1.00		
Incomplete remission from first demyelinating event	-	-	-	-	-	-	8.67	1.78, 42.24	0.007
ARR in the first 3 years	2.85	1.13, 7.19	0.02				-	-	-
No DMT exposure (ref)	1.00			1.00			-	-	-
Moderate efficacy DMT	9.75	1.92, 49.56	0.006				-	-	-
High efficacy DMT	7.26	1.17, 45.16	0.03	3.43	1.22, 9.67	0.02	-	-	-
Late onset pediatric MS	**EDSS 3**			**EDSS 4**			**EDSS 6**		
	HR	**95%CI**	***p* values**	**HR**	**95%CI**	***p* values**	**HR**	**95%CI**	***p* values**
Isolated optic neuritis*	-	-	-	-	-	-	0.69	0.51, 0.95	0.02
Combination of symptoms*	1.51	1.04, 2.20	0.03	1.59	1.23, 2.04	<0.001	-	-	-
Relapsing onset (ref)	-	-	-	1.00			1.00		
Progressive onset	-	-	-	3.25	1.76, 6.01	<0.001	1.89	0.93, 3.56	0.008
Complete remission from demyelinating event (ref)	1.00			1.00			1.00		

Incomplete remission from first demyelinating event	1.77	1.05, 3.01	0.03	3.45	1.39, 8.57	<0.001	1.71	1.08, 2.70	0.02
Time to first relapse	0.98	0.96, 1.00	0.07	0.96	0.94, 0.97	<0.001	0.96	0.94, 0.97	<0.001
ARR in the first 3 years	1.34	1.04, 1.71	0.02	1.26	1.03, 1.55	0.03	-	-	-
No DMT exposure (ref)	1.00			1.00			1.00		
Moderate efficacy DMT	2.81	1.89, 4.18	<0.001	-	-	-	0.49	0.37, 0.66	<0.001
High efficacy DMT	2.97	1.88, 4.69	<0.001	1.56	1.18, 2.07	0.002	-	-	-

**at disease onset*

Abbreviations: HR = hazard ratio; CI = confidence interval; MS = multiple sclerosis; EDSS = Expanded Disability Status Scale; DMT = disease modifying treatment; ref = reference level.

Figure 4.2.1. *Study flow-chart.*

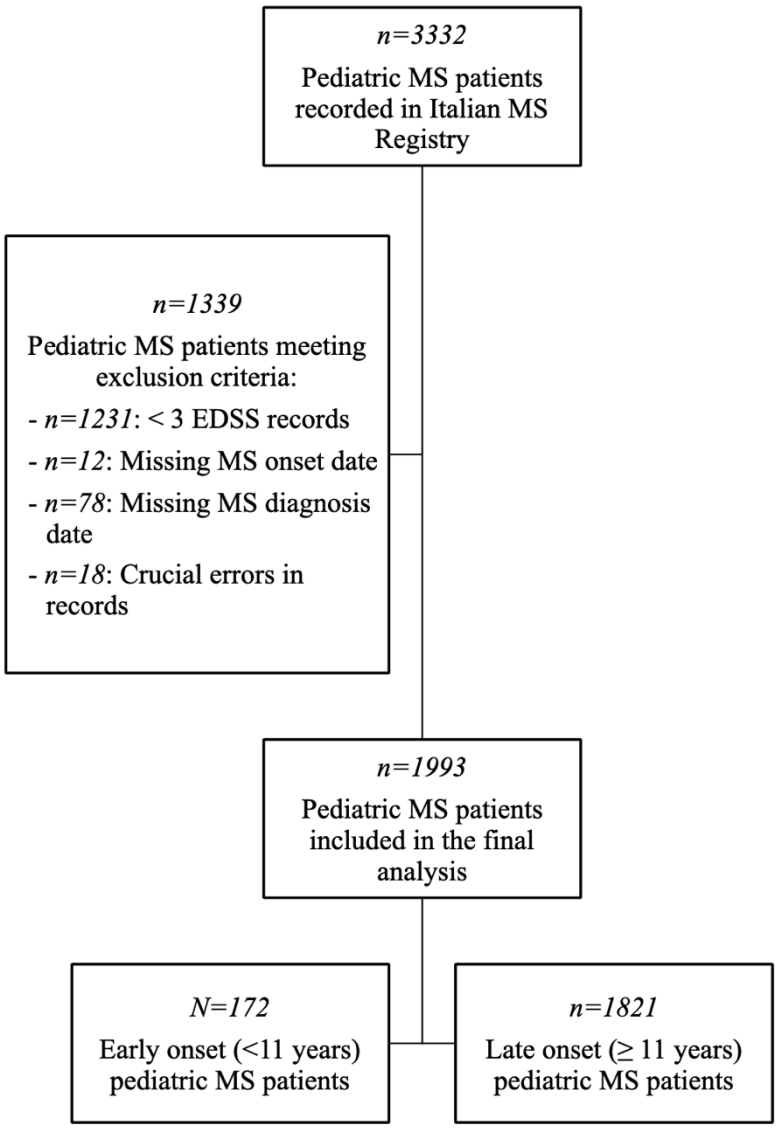

The diagram illustrates patients' selection to obtain the final dataset.
Abbreviations: EDSS = Expanded Disability Status Scale; MS = multiple sclerosis.

Figure 4.2.2. *Kaplan–Meier estimates of the time to reach disability milestones from birth or disease onset in early vs late onset pediatric MS patients.*

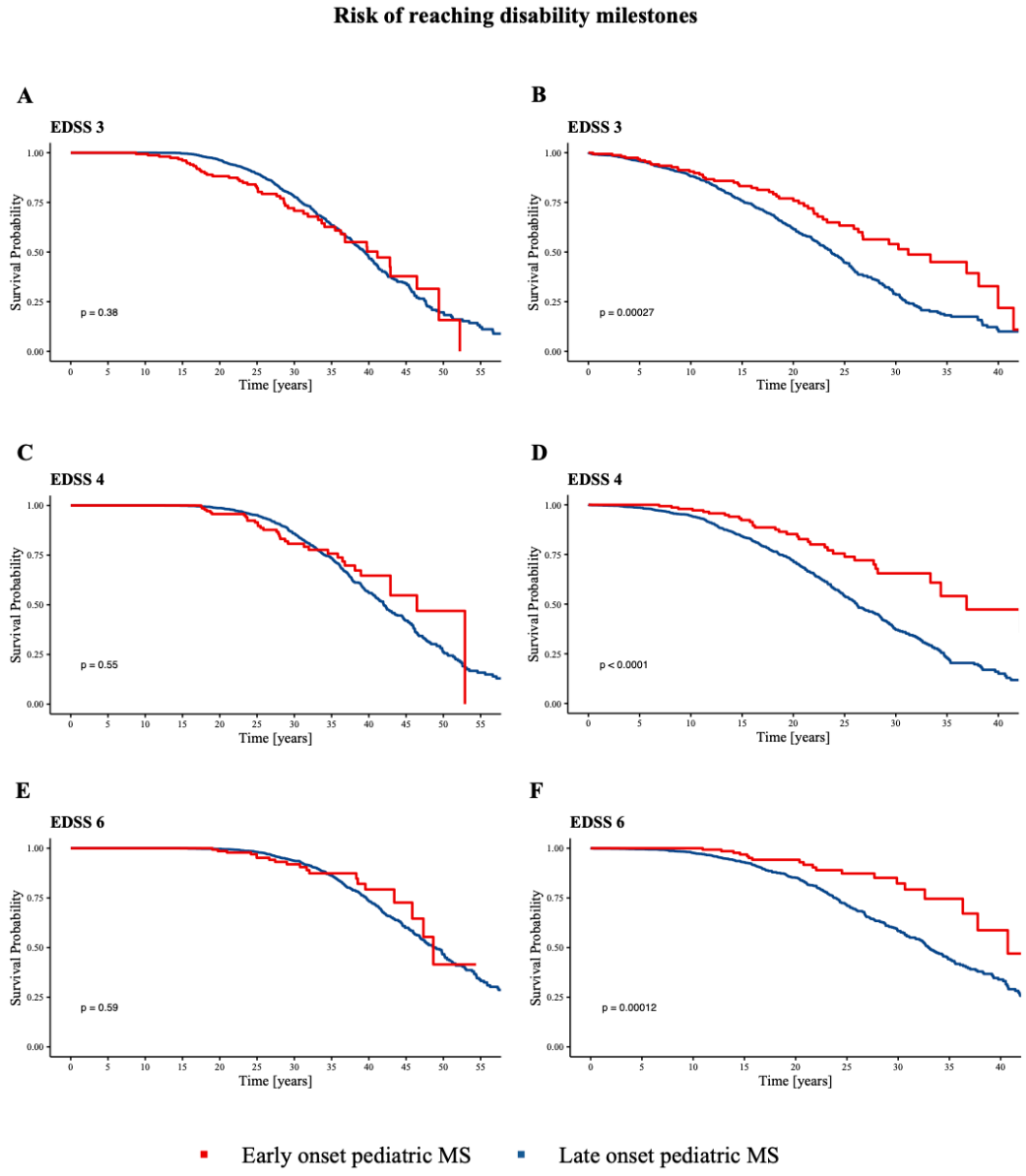

Panels on the left represent Kaplan-Meier estimates of time to reach disability milestones (EDSS 3 in A, EDSS 4 in C and EDSS 6 in E) measured from birth. Panels on the right represent Kaplan-Meier estimates of time to reach disability milestones (EDSS 3 in B, EDSS 4 in D and EDSS 6 in F) measured from MS onset.
Abbreviations: EDSS = Expanded Disability Status Scale; MS = multiple sclerosis.

Supplementary material 4.2.1

Sensitivity analysis

Table e-4.2.1. *Cox models of time to EDSS 3, 4, and 6, and to conversion to secondary progressive MS from birth or MS onset, comparing early vs late onset pediatric MS patients (the latter as reference group).*

Risk of reaching disability milestone in early vs late onset pediatric MS patients	**HR**	**95% CI**	***p* values**	**Adjusted§ HR**	**95% CI**	***p* values**
From birth to:						
EDSS 3	1.07	0.78, 1.46	0.68	1.13	0.82, 1.55	0.45
EDSS 4	0.97	0.66, 1.42	0.86	0.95	0.64, 1.41	0.79
EDSS 6	0.95	0.59, 1.52	0.83	1.00	0.62, 1.61	0.98
Conversion to SPMS*	0.68	0.37, 1.24	0.21	0.64	0.35, 1.18	0.15
From MS onset to:						
EDSS 3	0.61	0.45, 0.83	<0.001	0.69	0.50, 0.94	0.01
EDSS 4	0.50	0.35, 0.72	<0.001	0.50	0.34, 0.73	<0.001
EDSS 6	0.46	0.29, 0.74	<0.001	0.47	0.30, 0.75	<0.001
Conversion to SPMS*	0.40	0.22, 0.74	0.003	0.38	0.21, 0.70	0.001

**Analysis performed on relapse-onset pediatric MS patients only.*

§Adjusted for diagnosis epoch, sex, disease course at onset (primary progressive or relapse-onset), EDSS score at the onset, and disease-modifying therapy exposure (no treatment, moderate- or high-efficacy) as a time-varying covariate.

Abbreviations: HR = hazard ratio; CI = confidence interval; MS = multiple sclerosis; EDSS = Expanded Disability Status Scale.

Table e-4.2.2. *Univariate Cox models of time from MS onset to EDSS 3, 4, and 6 early and late onset pediatric multiple sclerosis patients.*

Early onset pediatric MS	**EDSS 3**			**EDSS 4**			**EDSS 6**		
	HR	**95%CI**	***p* values**	**HR**	**95%CI**	***p* values**	**HR**	**95%CI**	***p* values**
Isolated optic neuritis*	0.35	0.12, 0.99	0.05						
Complete remission from first demyelinating event (ref)	-	-	-	1.00			1.00		
Incomplete remission from first demyelinating event	-	-	-	4.79	1.35, 16.99	0.02	28.73	2.53, 32.95	0.002
Time to first relapse	0.91	0.85, 0.97	0.003	-	-	-		-	-
ARR in the first 3 years	5.07	2.28, 11.29	<0.001	-	-	-	-	-	-
No DMT exposure (ref)	1.00			1.00			-	-	-
Moderate efficacy DMT	6.43	2.52, 16.46	<0.001	2.48	1.03, 6.22	0.05	-	-	-
High efficacy DMT	7.43	2.29, 24.11	<0.001	4.00	1.33, 12.04	0.02	-	-	-
Late onset pediatric MS	**EDSS 3**			**EDSS 4**			**EDSS 6**		
	HR	**95%CI**	***p* values**	**HR**	**95%CI**	***p* values**	**HR**	**95%CI**	***p* values**
Age at onset	-	-	-	-	-	-	-	-	-
Isolated optic neuritis*	-	-	-	0.71	0.55, 0.92	0.009	-	-	-
Combination of symptoms*	1.39	1.04, 1.86	0.02	1.68	1.39, 2.19	<0.001	-	-	-
Relapsing onset (ref)				1.00			1.00		
Progressive onset	2.44	1.15, 5.17	0.02	2.82	1.55, 5.16	<0.001	2.16	1.24, 3.79	0.007
Complete remission from demyelinating event (ref)	1.00			1.00			1.00		

Incomplete remission from first demyelinating event	1.72	1.14, 2.59	0.01	1.95	1.32, 2.90	<0.001	1.12	1.03, 1.23	0.01
Time to first relapse	0.96	0.95, 0.98	<0.001	0.96	0.95, 0.98	<0.001	0.97	0.95, 0.98	<0.001
ARR in the first 3 years	1.59	1.32, 1.91	<0.001	1.65	1.37, 1.98	<0.001	-	-	-
No DMT exposure (ref)	1.00			1.00			1.00		
Moderate efficacy DMT	2.21	1.70, 2.88	<0.001	-	-	-	0.51	0.39, 0.69	<0.001
High efficacy DMT	2.59	1.88, 3.56	<0.001	2.14	1.64, 2.80	<0.001	-	-	-

**at disease onset*

Abbreviations: HR = hazard ratio; CI = confidence interval; MS = multiple sclerosis; EDSS = Expanded Disability Status Scale; DMT = disease modifying treatment; ref = reference level;

Table e-4.2.3. *Multivariable Cox regression models of prognostic factors of time from disease onset to reach disability milestones (EDSS 3, 4 and 6) in early and late onset pediatric multiple sclerosis patients.*

Early onset pediatric MS	**EDSS 3**			**EDSS 4**			**EDSS 6**		
	HR	**95%CI**	***p* values**	**HR**	**95%CI**	***p* values**	**HR**	**95%CI**	***p* values**
Complete remission from first demyelinating event (ref)	-	-	-	-	-	-	1.00		
Incomplete remission from first demyelinating event	-	-	-	-	-	-	28.53	3.01, 42.24	0.003
Time to first relapse	-	-	-	-	-	-	-	-	-
ARR in the first 3 years	2.82	1.23, 6.46	0.01	1.69	0.82, 3.50	0.15	-	-	-
No DMT exposure (ref)	1.00			1.00			-	-	-
Moderate efficacy DMT	5.42	1.92, 15.31	0.001	2.16	0.87, 5.32	0.09	-	-	-
High efficacy DMT	5.97	1.70, 20.95	0.005	3.43	1.22, 9.67	0.02	-	-	-
Late onset pediatric MS	**EDSS 3**			**EDSS 4**			**EDSS 6**		
	HR	**95%CI**	***p* values**	**HR**	**95%CI**	***p* values**	**HR**	**95%CI**	***p* values**
Isolated optic neuritis*	-	-	-	-	-	-	-	-	-
Isolated brainstem symptoms*	-	-	-	-	-	-	-	-	-
Combination of symptoms*	-	-	-	1.59	1.20, 2.11	0.001	-	-	-
Relapsing onset (ref)	-	-	-	1.00			-	-	-
Progressive onset	-	-	-	3.44	1.80, 6.59	<0.001	-	-	-
Complete remission from demyelinating event (ref)	1.00			1.00			-	-	-

Incomplete remission from first demyelinating event	2.40	1.54, 3.75	<0.001	2.62	1.70, 4.05	<0.001	-	-	-
Time to first relapse	-	-	-	0.96	0.94, 0.98	<0.001	0.96	0.94, 0.97	<0.001
ARR in the first 3 years	1.34	1.04, 1.71	0.02	1.27	1.02, 1.58	0.03	-	-	-
No DMT exposure (ref)	1.00			1.00			1.00		
Moderate efficacy DMT	1.93	1.43, 2.62	<0.001	-	-	-	0.51	0.37, 0.69	<0.001
High efficacy DMT	1.96	1.36, 2.85	<0.001	1.80	1.33, 2.45	<0.001	-	-	-

**at disease onset*

Abbreviations: HR = hazard ratio; CI = confidence interval; MS = multiple sclerosis; EDSS = Expanded Disability Status Scale; DMT = disease modifying treatment; ref = reference level;

5. Discussion

5.1 Characterization of pediatric MS by using advanced MRI techniques in cross-sectional and longitudinal setting

During the last decade, the application of advanced MRI techniques allowed a more precise characterization of the neuroanatomical substrates of clinical and neuropsychological features of MS patients.

However, the application of these techniques to pediatric MS patients is limited to a few studies. In Section 3 a series of experiments was performed by applying structural and functional MRI, identifying potential neuroanatomical substrates of disease-related clinical manifestations, as well as pathogenetic mechanisms underlying brain tissue damage in MS.

The thalamus confirmed its central role in determining clinical and cognitive functioning in pediatric MS patients. An increased functional recruitment of this structure was observed in pediatric MS patients with preserved cognitive performance, thus suggesting this increased activation as a compensatory mechanism against brain damage. Further supporting this hypothesis, a correlation between thalamic recruitment and GM atrophy was identified.

We explored the determinants of GM atrophy in pediatric MS patients in longitudinal settings, resulting from both failure of age-expected GM maturation and development of tissue loss. In this context, we observed significant associations between thalamic atrophy and clinical disability.

Starting from these observations as well as from the demonstration of early thalamic involvement during MS course (Eshaghi *et al.*, 2018b), we focused on the thalamus to provide *in vivo* additional insights into pathogenetic mechanisms underlying disease-related tissue damage. We described several microstructural changes, occurring before atrophy could be detectable, involving both thalamic interfaces (with WM and CSF). Significant associations were observed between microstructural abnormalities at CSF/thalamus interface with cortical damage as well as between thalamus/WM interface and WM lesions. These findings support the hypothesis of heterogeneous pathological processes, including retrograde degeneration from WM lesions and CSF-mediated

damage, leading to thalamic microstructural abnormalities, likely preceding macroscopic tissue loss.

In ***Section 3.1*** (***MRI substrates of sustained attention system and cognitive impairment in pediatric MS patients***) by using fMRI during a sustained attention task (CCPT) the relationship between cognitive impairment and sustained attention system recruitment abnormalities was investigated. A similar pattern of recruitment of the sustained attention system was observed between pediatric MS patients and HC resembling that described by previous studies in HC and patients with other neurological diseases using a similar fMRI paradigm (Strazzer *et al.*, 2015; Tana *et al.*, 2010). However, with increasing sustained attention task demand, compared to HC, pediatric MS patients showed an increased activation of the left thalamus, anterior insula and ACC. They also experienced an increased deactivation of the precuneus.

On one hand, these findings suggested the achievement of the age-expected level of functional maturation of the attentional network in pediatric MS patients, in terms of ability to activate and deactivate the main regions of the network and topographical representation of these regions. On the other, with increasing task demand, several abnormalities were detected, highlighting the adaptive and maladaptive mechanisms occurring during the earliest stages of disease to compensate brain structural damage.

This high-demanding cognitive condition allowed us to individuate the specific fMRI abnormalities underlying the cognitive performance of pediatric MS patients. In details, increased recruitment of anterior insula and ACC was observed in CP MS patients. These are among the key regions of the 'salience' network, which has a critical function in identifying the most relevant among several internal and extra-personal stimuli to guide behaviour (Seeley *et al.*, 2007). Network-analysis studies have consistently demonstrated that these two regions are involved in switching between brain networks (particularly the executive control and DMN) across task paradigms (Chen *et al.*, 2016; Menon & Uddin, 2010). Furthermore, decreased deactivation of right precuneus was observed in CP pediatric MS patients, while a more extended pattern of deactivation (involving the precuneus and SFG) was detected in CI pediatric MS patients. These results suggest that an initial increased deactivation of the precuneus together with a reduced deactivation of the ACC, as experienced in CP MS patients, may represent a compensatory mechanism allowing the patients to maintain an adequate cognitive profile.

The broader pattern of deactivation, significantly associated with structural damage, observed in CI MS patients may represent a maladaptive mechanism of cortical reorganization, characterized by an alteration of the shift from RS condition to sustained attention task performance.

Overall, the results obtained in this experiment, in line with previous studies (Akbar *et al.*, 2016b; Rocca *et al.*, 2014a), confirmed the crucial role of abnormalities in DMN posterior node centered in the precuneus, in determining cognitive dysfunction in pediatric MS patients. Moreover, a reduced capability to modulate DMN deactivation with increasing task complexity has been also demonstrated by studies in adult patients with MS (Morgen *et al.*, 2007; Rocca *et al.*, 2014c).

Interestingly, looking at the brain as a complex dynamic network, cognitive impairment in pediatric MS could be attributed to abnormalities of interaction over time between the posterior core of the DMN and fronto-parietal and subcortical networks, in particular the salience network (Bonnelle *et al.*, 2012; Chen *et al.*, 2016; Leech & Sharp, 2014; Menon & Uddin, 2010). Finally, the correlation observed between functional abnormalities of DMN and salience network with disruption of structural integrity of critical WM tracts within the networks (in particular the tract connecting the left anterior insula to the ACC) supports the hypothesis that in pediatric MS patients, the accumulation of disease-related structural damage might cause a disconnection syndrome resulting in functional and clinical abnormalities.

In ***Section 3.2*** (***Dynamic gray matter volume changes in pediatric multiple sclerosis: a 3.5 year MRI study***) we analyzed, in a longitudinal setting, the complex interplay between brain growth and disease-related pathology on regional trajectories of GM maturation in pediatric MS patients.

To these aims, we first estimated physiological variations of GM volume trajectories during development from a large cohort of pediatric HC, including participants studied on the same scanner as the MS patients as well as those from the Pediatric MRI Data Repository created by the NIH MRI Study of Normal Brain Development. In line with previous studies (Wierenga *et al.*, 2014), we detected a heterochronic (Gogtay *et al.*, 2004; Sowell *et al.*, 2001) and sexually dimorphic (Aubert-Broche *et al.*, 2014a; Lenroot *et al.*, 2007) process of maturation. Moreover, we confirmed the dynamic progression of development of GM regions, in which higher-order

association areas mature after lower-order sensorimotor regions, following a functional order and a phylogenetically based principle according to which evolutionarily older cortical areas mature first (Gogtay *et al.*, 2004).

In pediatric MS patients we observed a failure from the sex- and age-expected GM developmental trajectories in several cortical regions belonging to the frontal, temporal, parietal, occipital lobes and cerebellum, as well as subcortical regions comprising the thalamus and caudate nucleus. Failure of sex- and age-expected GM maturation of highly interconnected regions as the basal ganglia (Cavanna & Trimble, 2006), and late developing areas, such as anterior fronto-temporal regions (Ziegler *et al.*, 2017) was found to be significantly associated with the presence of focal WM lesions and the prolonged exposure to disease-related processes (as reflected by the correlation with disease duration). However failure of GM maturation was also observed in other brain regions thus suggesting the existence of other pathogenetic mechanisms, not strictly related to the presence of focal inflammatory-demyelinating lesions in the WM, leading to GM alterations in the early stages of the disease.

Exploring the evolution of GM volume abnormalities over a 3.5 year follow-up, continued deviations from the expected maturation trajectories were observed in the majority of GM areas, including several cortical and subcortical regions. Again, only for some of these regions (the thalamus and a few regions located in the precentral and postcentral gyri), maturational trajectory deviation was significantly associated with increased lesion burden.

Overall, these findings suggest the existence of at least two mechanisms explaining GM damage: the first, more related to the inflammatory WM lesion-dependent component of the disease, mainly occurring at the earliest stages of the disease and involving highly-connected regions, while the second characterized by a primary involvement of the GM.

In line with previous studies (Azevedo *et al.*, 2018; Eshaghi *et al.*, 2018b), failure of GM development in key brain regions, such as the thalamus, caudate nucleus, precuneus and frontal regions, was associated with the severity of clinical disability. Moreover, greater cognitive reserve, represented in pediatric MS patients by higher IQ, resulted protective against tissue loss in the cingulate cortex, precuneus, and several regions located in the frontal and temporal lobes and the cerebellum. These findings could

be attributed to GM pruning which selectively eliminates GM that does not effectively contribute to cognition, as suggested by a study in healthy children (Wilke *et al.*, 2003).

Overall these results suggest that although pediatric MS patients are provided with greater resilience and repair potential against brain tissue damage (Ghassemi *et al.*, 2015a), these are not sufficient to prevent GM atrophy.

In ***Section 3.3*** (***In vivo gradients of thalamic damage in pediatric multiple sclerosis: a window into pathology***), by applying a multiparametric MRI approach, we quantified in vivo the different processes involving the thalamus in term of focal lesions, microstructural damage and atrophy in pediatric MS patients.

To provide additional insights into the mechanisms associated with thalamic damage, we integrated the whole thalamic with a laminar analysis, by studying thalamic quantitative MRI metrics according to their geodesic distance from the CSF/thalamus-interface. The analysis of the whole thalamus showed that pediatric MS patients experienced a trend towards a reduction of thalamic volume and significant abnormalities in quantitative MRI metrics compared to HC, thus supporting the hypothesis that microstructural damage is likely to precede atrophy in MS (Deppe *et al.*, 2016).

At laminar analysis, supporting the hypothesis of a CSF immune-cytotoxic factor-mediated mechanism (Liu *et al.*, 2015; Louapre *et al.*, 2017), we found a dependency of thalamic T2 LV from the distance from CSF and a disruption of microstructural integrity together with evidence of demyelination in the same regions. Thalamic abnormalities in the bands nearest to CSF/thalamus interface significantly correlated with cortical thinning, suggesting a shared mechanism of damage for subpial and subependymal pathology, likely coming from the CSF. Furthermore, we also observed microstructural abnormalities in thalamic bands nearest to thalamus/WM interface that correlated with brain T2 LV, supporting the hypothesis of thalamic WM lesion-related Wallerian degeneration.

Overall, these results pointed towards the existence of heterogeneous pathogenetic mechanisms involving the thalamus in pediatric MS related to both CSF immune cytotoxic factors and WM lesions. Considering that thalamic microstructural damage occurs during the earliest stages of disease, before thalamic atrophy could be detectable, monitoring thalamic abnormalities could represent an early biomarker for diffuse damage and an ideal MRI outcome in clinical trials, especially in pediatric MS patients.

5.2 Assessment of clinical and MRI predictors of long-term disease course in pediatric MS

To date, only a few longitudinal studies (Iaffaldano *et al.*, 2017; Mikaeloff *et al.*, 2006) have been conducted in pediatric MS patients. A higher clinical activity, with higher relapse rate especially during the first years from disease onset (Benson *et al.*, 2014; Gorman *et al.*, 2009), paralleled by a higher MRI activity (Waubant *et al.*, 2009), were reported for pediatric-onset compared to adult-onset MS patients. However, little is known about how these early clinical and MRI features may influence the long-term clinical outcome of these patients.

In ***Section 4.1*** (***Early predictors of 9-year disability in pediatric multiple sclerosis***), we assessed the relevance of specific early clinical and MRI features for 9-year clinical outcomes in pediatric MS patients. As first outcome, considering its specific relevance for pediatric population (Renoux *et al.*, 2007), we selected time to first relapse. Optic nerve involvement on brain MRI resulted as the only independent predictor of a shorter time to first relapse, underscoring the different clinical implications of optic nerve involvement on MRI, compared to clinically-manifest optic neuritis (Davion *et al.*, 2020; London *et al.*, 2019). Moreover, optic nerve involvement on MRI at the time of diagnosis is likely to be associated with a shorter asymptomatic period, and earliest phases of disease have been associated with higher clinical activity in this population (Gorman *et al.*, 2009). Less surprisingly, the exposure to high efficacy DMT resulted the only independent predictor of longer time to first relapse.

The second outcome variable, ARR over the first 9 years of disease, was in part predicted by baseline lesion distribution. In details, cerebellar lesions were associated with lower ARR, while cervical cord lesions with higher ARR. A possible explanation is that cerebellum, characterized by later myelination (Weier *et al.*, 2016), could be involved later in the disease course, when disease features become more similar to adults (e.g., lower ARR). The association between spinal cord lesions and ARR confirms the results of previous studies in adult patients with MS, in which the presence of asymptomatic spinal cord lesions was significantly predictive of an increased risk of future relapse (Zecca *et al.*, 2016).

In addition, some short-term follow-up measures significantly contributed to explain 9-year ARR. We found a consistent association between the number of relapses over the first 2 years and time to first relapse with ARR, suggesting that the persistence of inflammatory activity over the first years of disease in spite of DMT exposure could be highly indicative of a more active disease. Once again, a protective role was found for high efficacy DMT exposure over the first year of disease. However, this effect was lost in the 2-year model, underscoring the existence of an early critical window in which the biology of disease can be modified for longer-term benefit (Harding *et al.*, 2019).

With the aim of exploring disability accrual, we investigated 9-year EDSS worsening and score, confirming the predictive role of baseline EDSS score and of clinically-eloquent site involvement (such as optic nerve, brainstem and spinal cord) for these 9-year outcomes. These findings highlighted the role of neuroaxonal degeneration in clinically-eloquent areas of the CNS, containing long-distance WM pathways critical for balance and locomotion as an important driver of disability in MS (Ferguson *et al.*, 1997; Minneboo *et al.*, 2009; Saidha *et al.*, 2015; Trapp *et al.*, 1998).

Interestingly, we observed that Gd-lesions on baseline MRI have a protective role against 9-year disability in pediatric MS patients. Considering that pediatric MS patients are known to have more frequent Gd-lesions than adults (Waubant *et al.*, 2009), with a frequency that reduces with age and that this trend is paralleled by a decrease in remyelination capability with age (Brown *et al.*, 2014; Ghassemi *et al.*, 2015b; Ghassemi *et al.*, 2015c), these findings suggest that a more severe acute inflammatory activity at disease onset could stimulate myelin repair and delay chronic inflammation processes typical of the progressive phase of disease (Mahad *et al.*, 2015).

Short-term follow-up also contributed to the prediction of 9-year clinical disability. Baseline EDSS and its short-term increase and the detection of at least two new T2-lesions at 2 years showed significant association with 9-year clinical disability, underscoring the relevance of clinical and MRI monitoring during the first years of disease in predicting long-term disease evolution (Rotstein *et al.*, 2015).

In ***Section 4.2*** (***Comparing natural history of pre- and post-pubertal onset multiple sclerosis***), we compared disease course and prognosis in pre- (early) and post-pubertal (late) onset MS patients identifying several specific features of early onset pediatric MS. In line with previous studies (Huppke *et al.*, 2014; Tintoré & Arrambide,

2009), we found a lower female:male ratio in patients with early vs late onset pediatric MS, thus supporting a role of puberty and sex hormones in determining MS onset (Bove & Chitnis, 2014). Again confirming previous studies (Banwell *et al.*, 2009; Huppke *et al.*, 2014), a prominent brainstem involvement was observed in early onset pediatric MS patients, while isolated optic neuritis or isolated spinal cord involvement prevailed later. These differences could be largely attributed to myelination processes proceeding along a caudo-rostral gradient in the encephalon (Paus, 2005). Moreover, also in the spinal cord, a gradual increase of myelination is described until the adulthood (Yeo *et al.*, 2014).

While no differences were observed in recovery from first demyelinating event and in ARR over the first 3 years of disease between early and late onset pediatric MS patients, surprisingly we found a significantly shorter time to first relapse in late compared to early onset pediatric MS patients. It is possible to attribute these findings to the hypothesis that hormonal and metabolic changes occurring during puberty are responsible for a higher risk of relapses in both males (Young *et al.*, 2019) and females (Lulu *et al.*, 2015). Indeed, although we had no data on hormone levels, growth charts or Tanner stages, age below 11 years is usually associated to pre-pubertal stage (Huppke *et al.*, 2014; Lulu *et al.*, 2015; Young *et al.*, 2019), thus most probably puberty was included in our late onset group.

Early onset pediatric MS patients took a longer time from disease onset to shift to SPMS and to reach EDSS 3, 4 and 6. As a confirmation of the better prognosis of early vs late onset pediatric MS, we found no differences in the time from birth to reach EDSS 3, 4 and 6. While we are the first to report long-term outcomes for early onset pediatric MS patients, data for late onset pediatric patients was similar to that reported in previous studies (McKay *et al.*, 2019; Renoux *et al.*, 2007) comparing the natural history of pediatric vs adult onset MS.

We also identified several predictors of reaching confirmed disability in both early and late onset pediatric MS patient. Disease activity in term of time to first relapse and ARR over the first 3 years of disease together with recovery from first demyelinating event significantly contributed to long-term disability in both groups. These findings underscore that repeated demyelinating attacks, especially during the earliest stages of the disease (Tremlett *et al.*, 2009), may increase the risk of reaching long-term irreversible disability.

Overall these results provide additional support to the hypothesis of different pathophysiological mechanisms occurring in the prepubertal age, also highlighting the critical relevance of early treatment also in pediatric patients.

6. Conclusions and future directions

During the present PhD we focused on pediatric MS addressing the main unsolved questions in the field. Overall, we demonstrated that the application of advanced MRI techniques could provide additional insights in the understanding of neuroanatomical basis of clinical features and in disease-related pathogenetic mechanisms. In details, fMRI provided in-vivo evidences of brain plasticity adaptive and maladaptive changes underlying cognitive status of pediatric MS patients. By exploring GM maturational trajectories at voxel-level, we were able to assess the impact of disease on GM development also identifying a crucial role for cognitive reserve in preventing failure of age-expected brain growth. The application of quantitative MRI metrics to the thalamus allowed us to assess microstructural changes occurring before than atrophy could be detectable, also identifying potential pathogenetic mechanisms of disease.

The analysis of longitudinal cohorts of pediatric MS patients allowed us to identify prognostic factors able to predict disease course and prognosis at disease onset. Moreover, by analyzing data from Italian MS Register we were able describe the natural history of pediatric MS occurring before puberty pointing towards different pathogenetic mechanisms occurring in very young patients.

Future research in this field should be aimed to the application of advanced MRI technique in longitudinal setting. To this aim, more pediatric MS patients and HC will be acquired in a 3.0 Tesla scanner. Also, in both pediatric MS patients and HC, a complete neurological evaluation will be obtained together with a complete neuropsychological assessment. Advanced MRI structural and functional MRI techniques will be applied in a longitudinal setting to analyze the cohort of subjects newly acquired. Correlations with clinical and neuropsychological data will be performed with the ultimate aim to provide a deeper understanding of the neuroanatomical bases of clinical manifestations.

7. Other studies

7.1 Identifying the Distinct Cognitive Phenotypes in Multiple Sclerosis

The following data have been published (De Meo *et al.*, 2021c).

Research

JAMA Neurology | Original Investigation

Identifying the Distinct Cognitive Phenotypes in Multiple Sclerosis

Ermelinda De Meo, MD; Emilio Portaccio, MD; Antonio Giorgio, MD; Luis Ruano, MD; Benedetta Goretti, MSc; Claudia Niccolai, MSc; Francesco Patti, MD; Clara Grazia Chisari, MSc; Paolo Gallo, MD; Paola Grossi, MSc; Angelo Ghezzi, MD; Marco Roscio, MSc; Flavia Mattioli, MD; Chiara Stampatori, MSc; Marta Simone, MD; Rosa Gemma Viterbo, MSc; Raffaello Bonacchi, MD; Maria A. Rocca, MD; Nicola De Stefano, MD; Massimo Filippi, MD; Maria Pia Amato, MD

IMPORTANCE Cognitive impairment is a common and disabling feature of multiple sclerosis (MS), but a precise characterization of cognitive phenotypes in patients with MS is lacking.

OBJECTIVES To identify cognitive phenotypes in a clinical cohort of patients with MS and to characterize their clinical and magnetic resonance imaging (MRI) features.

DESIGN, SETTING, AND PARTICIPANTS This multicenter cross-sectional study consecutively screened clinically stable patients with MS and healthy control individuals at 8 MS centers in Italy from January 1, 2010, to October 31, 2019. Patients with MS and healthy control individuals who were not using psychoactive drugs and had no history of other neurological or medical disorders, learning disability, severe head trauma, and alcohol or drug abuse were enrolled.

MAIN OUTCOMES AND MEASURES Participants underwent a neurological examination and a cognitive evaluation with the Rao Brief Repeatable Battery and Stroop Color and Word Test. A subgroup of participants also underwent a brain MRI examination. Latent profile analysis was used on cognitive test *z* scores to identify cognitive phenotypes. Linear regression and mixed-effects models were used to define clinical and MRI features of each phenotype.

RESULTS A total of 1212 patients with MS (mean [SD] age, 41.1 [11.1] years; 784 women [64.7%]) and 196 healthy control individuals (mean [SD] age, 40.4 [8.6] years; 130 women [66.3%]) were analyzed in this study. Five cognitive phenotypes were identified: preserved cognition (n = 235 patients [19.4%]), mild–verbal memory/semantic fluency (n = 362 patients [29.9%]), mild–multidomain (n = 236 patients [19.5%]), severe–executive/attention (n = 167 patients [13.8%]), and severe–multidomain (n = 212 patients [17.5%]) involvement. Patients with preserved cognition and mild–verbal memory/semantic fluency were younger (mean [SD] age, 36.5 [9.8] years and 38.2 [11.1] years) and had shorter disease duration (mean [SD] 8.0 [7.3] years and 8.3 [7.6] years) compared with patients with mild–multidomain (mean [SD] age, 42.6 [11.2] years; mean [SD] disease duration, 12.8 [9.6] years; $P < .001$), severe–executive/attention (mean [SD] age, 42.9 [11.7] years; mean [SD] disease duration, 12.2 [9.5] years; $P < .001$), and severe–multidomain (mean [SD] age, 44.0 [11.0] years; mean [SD] disease duration, 13.3 [10.2] years; $P < .001$) phenotypes. Severe cognitive phenotypes prevailed in patients with progressive MS. At MRI evaluation, compared with those with preserved cognition, patients with mild–verbal memory/semantic fluency exhibited decreased mean (SE) hippocampal volume (5.42 [0.68] mL vs 5.13 [0.68] mL; $P = .04$), patients with the mild–multidomain phenotype had decreased mean (SE) cortical gray matter volume (687.69 [35.40] mL vs 662.59 [35.48] mL; $P = .02$), patients with severe–executive/attention had higher mean (SE) T2-hyperintense lesion volume (51.33 [31.15] mL vs 99.69 [34.07] mL; $P = .04$), and patients with the severe–multidomain phenotype had extensive brain damage, with decreased volume in all the brain structures explored, except for nucleus pallidus, amygdala and caudate nucleus.

CONCLUSIONS AND RELEVANCE This study found that by defining homogeneous and clinically meaningful phenotypes, the limitations of the traditional dichotomous classification in MS can be overcome. These phenotypes can represent a more meaningful measure of the cognitive status of patients with MS and can help define clinical disability, support clinicians in treatment choices, and tailor cognitive rehabilitation strategies.

JAMA Neurol. 2021;78(4):414-425. doi:10.1001/jamaneurol.2020.4920
Published online January 4, 2021.

Supplemental content

Author Affiliations: Author affiliations are listed at the end of this article.

Corresponding Author: Ermelinda De Meo, MD, Neuroimaging Research Unit, Division of Neuroscience, IRCCS San Raffaele Scientific Institute, Via Olgettina 60, Milan 20132, Italy (demeo.ermelinda@hsr.it).

jamaneurology.com

Introduction

Cognitive impairment is a common and disabling manifestation of MS, affecting patients' performance in everyday activities, behavior and quality of life. It may be detected in the earliest stages of disease, such as clinically-(Zipoli *et al*, 2010) and radiologically-isolated syndrome (Labiano-Fontcuberta *et al*, 2016).

Numerous MRI studies aimed at exploring the pathophysiology of cognitive impairment in MS. The earliest ones linked cognitive deficits to higher brain lesion load,(Rao *et al*, 1989) while subsequent work highlighted the importance of lesion location in strategic WM regions (Kincses *et al*, 2011), WM microstructural damage (Preziosa *et al*, 2016), GM lesions (Calabrese *et al.*, 2009), cortical (Steenwijk *et al*, 2016) and deep (Damjanovic *et al*, 2017) GM atrophy (Preziosa *et al.*, 2016), and abnormal patterns of cerebral activation (Benedict *et al*, 2020).

However, most clinical and MRI studies were based on a dichotomous classification of cognitive functioning, namely "preserved *vs* impaired" cognition. The inevitable consequence in published studies was the inclusion of heterogeneous groups of patients with variable cognitive profiles, preventing a clear assessment of neuroanatomical substrates and personalized rehabilitation strategies.

A promising approach was introduced by Leavitt et al. (Leavitt *et al*, 2018), who identified three cognitively homogeneous subgroups of MS patients, defined as "cognitive phenotypes": isolated memory impairment, isolated information processing speed impairment, and combined deficits in processing speed and memory. Nevertheless, deficits in other cognitive domains are reported in MS (Chiaravalloti & DeLuca, 2008; Leavitt *et al*, 2011), and this classification was based on dichotomous definition of impairment for each domain, not considering patients with mildly reduced cognitive performance (Sumowski *et al*, 2011).

The definition of cognitive phenotypes may represent a step forward towards personalized treatment approaches and towards improving our understanding of the pathophysiology of MS-related cognitive changes.

Against this background, we aimed (i) to identify cognitive phenotypes in a clinical cohort of MS patients including the whole spectrum of disease subtypes, and (ii) to characterize their clinical and MRI features. We used an unbiased data-driven approach

on neuropsychological data, by applying latent-profile analysis (LPA) (Miettunen *et al*, 2016). For the characterization of MRI features, we selected highly reproducible and well-validated MRI metrics of MS-related brain damage.

Methods

Ethics committee approval. Approval was received from local ethical standards committees on human experimentation, and written informed consent was obtained from all participants prior to study enrollment.

Study subjects. Out of 1370 MS patients and 200 HC consecutively screened from eight Italian MS Centers from January 2010 to October 2019, we enrolled 1212 patients and 196 HC not using psychoactive drugs and without any history of other neurological/medical disorders, learning disability, severe head trauma, alcohol/drug abuse. We excluded MS patients with relapses or corticosteroid use within four weeks preceding neuropsychological assessment (Leavitt *et al.*, 2018).

Neuropsychological evaluation. All study participants underwent neuropsychological evaluation with the Rao's Brief Repeatable Battery (BRB) -and Stroop Color and Word Test (SCWT). The BRB evaluates the most frequently impaired cognitive domains in MS, incorporating tests of verbal learning and memory [SRT including Long-Term Storage (SRT-LTS), Consistent Long-Term Retrieval (SRT-CLTR) and delayed recall (SRT-D)]; visual/spatial learning and memory [10/36 SPART and its delayed recall (SPART-D)]; complex attention and information processing speed [Paced Auditory Serial Addition Test (PASAT) and SDMT]; and verbal fluency on semantic stimulus [Word List Generation (WLG)]. The SCWT (Stroop, 1935) evaluates complex attention and aspects of executive functioning, such as cognitive interference inhibition.

The neuropsychologists involved in the study participated in a common training session, in which test administration and scoring procedures were clarified and agreed upon. Corrected scores for age, sex and education according to normative values (Amato *et al*, 2006) were standardized based on HC, obtaining z-scores for each cognitive test. Fatigue was assessed on the Fatigue Severity Scale (FSS) (Krupp *et al.*, 2013) and depression on the Montgomery-Asberg Depression Scale (MADRS) (Montgomery & Asberg, 1979).

Neurological assessment. All patients underwent same-day neurological examination with rating of the EDSS score (Kurtzke, 1983) and definition of clinical subtype (Lublin *et al.*, 2014). Given the high number of relapsing-remitting MS patients, we classified them into early (disease duration < 5 years) and late (disease duration ≥ 5 years) groups (Debernard *et al*, 2014).

MRI data acquisition. Two of the eight involved centers (San Raffaele Hospital in Milan and Quantitative Neuroimaging Laboratory of the University of Siena) also performed brain MRI examination at the time of neuropsychological evaluation, in 172 MS patients and 50 HC. By using a 3T scanner 3DT1-weighted and dual-echo sequences were acquired. The complete acquisition protocol is available in **e-Methods 7.1.1** in the **Supplementary Material 7.1.1**.

MRI data analysis. T2-hyperintense lesion volumes were measured on proton density images, using a local thresholding semi-automated segmentation technique (Jim 8, Xinapse Systems, Colchester, United Kingdom). Normalized brain (NBV), WM (NWMV), GM (NGMV) and cortical GM (NcGMV) volumes were measured on lesion-filled (Chard *et al.*, 2010) 3DT1-weighted images using SIENAx software. Automated segmentation of thalamus, caudate, putamen, pallidum, hippocampus, amygdala, and nucleus accumbens was performed on lesion-filled (Chard *et al.*, 2010) 3DT1-weighted images with FMRIB Integrated Registration and Segmentation Tool (FIRST; http://fsl.fmrib.ox.ac.uk/fsl/fslwiki/FIRST) software (Patenaude *et al*, 2011). The volume of these structures was multiplied by the head-normalization factor derived from SIENAx. Given the symmetry of right and left deep GM nuclei, corresponding volumes were averaged across hemispheres before statistical analysis (Damjanovic *et al.*, 2017).

Statistical analysis. In order to identify cognitive phenotypes, we performed LPA (Miettunen *et al.*, 2016; Oberski, 2016) on cognitive test z-scores. LPA is a flexible, person-centered, and model-based clustering technique. We used it for the data-driven probabilistic identification of neuropsychologically homogeneous MS patients' subgroups, which we defined as *cognitive phenotypes*. LPA is based on specific mixture models that analyze the joint distribution of a set of continuous observed variables (in our study, neuropsychological test z-scores) as a function of a finite and mutually exclusive and exhaustive number of unobserved components—mixtures—using a latent

categorical variable (or *profile*) (Blanken *et al*, 2020; Iqbal *et al*, 2005). Here, the latent variable represents a profile of cognitive functioning in MS patients. LPA does not necessitate any *a priori* categorization of the observed variables (or *indicators*), thus facilitating a more granular examination of heterogeneity within and between latent-level groupings (Oberski, 2016; Spurk *et al*, 2020). A major advantage is the possibility to estimate profile-specific means, variances, and covariances of the observed variables (Spurk *et al.*, 2020). An important step of LPA is the selection of the best fitting model. Models with one to six profiles were run. For the optimal number of classes, Bootstrapped Likelihood Ratio Test, Bayesian Information Criterion and Integrated Completed Likelihood were inspected, in line with Nylund et al. and Scrucca et al.(Scrucca *et al*, 2016). After the selection of the best fitting model, each MS patient was classified into one of the cognitive phenotypes (*latent profiles*) based upon phenotype membership probabilities estimated directly from the model (Berlin *et al*, 2014; Nagin & Nagin, 2005; Oberski, 2016; Woo *et al*, 2018). In order to test the accuracy of the probabilistic predictions in attributing a cognitive phenotype to each patient, we performed a 10-fold cross-validation.

Cognitive phenotypes were named based on tests where patient performance was significantly lower compared to that of HC and on current knowledge about test interpretation: names we used to label different cognitive phenotypes are amenable to changes depending on future developments. A threshold of mean z-score <-1.5 was used to distinguish “severely” and “mildly” reduced performance.

Between-group comparisons of demographic and clinical parameters were performed using age- and sex-adjusted linear regression models or non-parametric tests, as appropriate (normal distribution was assessed by visual inspection and Kolmogorov-Smirnov test). Patients with and without MRI assessment were also compared with each other in terms of demographic, clinical and neuropsychological variables, for assessing representativeness of the entire study cohort. In order to characterize MRI features of each cognitive phenotype, we adopted linear mixed effects models.

Statistical significance was corrected for multiple comparisons (Bonferroni method), and threshold for significance was set at corrected $p<0.05$. To provide a measure of effect size for the comparisons performed, we also estimated Cohen’s d (d), Cliff’s

delta and Cramer's V as appropriate. Statistical analysis was performed by using R software 3.6.1, with packages "mclust", "tidyLPA" and "lme4".

Results

Demographic, clinical and neuropsychological measures. **Table 7.1.1** summarizes the main demographic and clinical features of study subjects. Compared to HC, MS patients did not differ in age, sex and education. Clinical subtypes of the 1212 MS patients were: 396 early relapsing-remitting, 652 late relapsing-remitting, 108 SP and 56 primary progressive.

Cognitive phenotypes. Using latent-profile analysis, a five-profile model was the best-fitting one (**Table e-7.1.1** in **Supplementary Material 7.1.1**). A Brier score of 0.05 was obtained at the 10-fold cross-validation analysis. Five cognitive phenotypes (**Figure e-7.1.1** in **Supplementary Material 7.1.1**) were identified:

1. "Preserved-cognition" (n=235, 19%) showing no significant difference compared to HC;
2. "Mild-verbal memory/semantic fluency" (n=362, 30%), showing only mildly reduced performance in SRT (d=-0.69, 95%CI -0.89 to -0.50, p<0.001) and WLG (d=-1.41, 95%CI -1.89 to -1.39; p<0.001) compared to HC;
3. "Mild-multi-domain" (n=236, 19%), showing mildly reduced performance in SRT (d=-1.68, 95%CI -1.92 to -1.44, p<0.001), SDMT (d=-0.96, 95%CI -1.18 to -0.74, p<0.001), SCWT (d=-0.68, 95%CI -0.90 to -0.47, p<0.001) and PASAT (d=-0.56 95%CI -0.77 to -0.35 p<0.001) compared to HC;
4. "Severe-executive/attention" (n=167, 14%), showing severely reduced performance in SCWT (d=-1.72, 95%CI -1.95 to -1.48, p<0.001) and PASAT (d=-1.83, 95%CI -2.10 to -1.57, p<0.001) and mildly reduced performance in SRT (d=-1.17, 95%CI -1.41 to -0.93, p<0.001), SPART (d=-0.29, 95%CI -0.51 to -0.07, p=.03), SDMT (d=-1.02, 95%CI -1.25 to 0.78, p<0.001) and WLG (d=-0.90, 95%CI -1.13 to 0.66, p<0.001) compared to HC;
5. "Severe-multi-domain" (n=212, 18%), showing severely reduced performance in SRT (d=-1.36 95%CI -1.60 to -1.13, p<.001, SCWT (d=-1.10, 95%CI -1.32 to -0.87, p<.001), SDMT (d=-2.06, 95%CI -2.31 to 1.80, p<0.001), PASAT (d=-2.48, 95%CI -2.75 to -2.20, p<0.001) and WLG (d=-2.40, 95%CI

-2.67 to -2.12, p<0.001) and mildly reduced performance in SPART (d=-1.71 95%CI -1.95 to -1.46, p<0.001) compared to HC.

Table 7.1.2 summarizes the neuropsychological features of each cognitive phenotype.

Clinical features of cognitive phenotypes. Significant differences were found when comparing clinical and demographic features among cognitive phenotypes, as summarized in **Figure 7.1.1** and **eTable 7.1.2** in the **Supplementary Material 7.1.1**. In particular, "preserved cognition" and "mild-verbal memory/semantic fluency" patients had similar age and disease duration, while they were younger and had a shorter disease duration compared to the other phenotypes. "Severe-multi-domain" patients had more severe physical disability compared to the other groups, while "mild-verbal memory/semantic fluency", "mild-multi-domain" and "severe-executive/attention" patients showed more severe disability compared to "preserved cognition". Regarding years of education, a difference was only found between "mild-multi-domain" and "severe-executive/attention" phenotypes. "Severe-executive/attention" patients had higher FSS scores compared to the other phenotypes. Higher MADRS scores were found in "severe-multi-domain" compared to "preserved cognition" and "severe-executive/attention" phenotypes and in "mild-verbal memory/semantic fluency" compared to "preserved cognition" phenotype. Intersecting cognitive phenotypes and clinical subtypes, we observed a progressive reduction of the relative frequencies of "preserved cognition" and "mild-verbal memory/semantic fluency" phenotypes from early relapsing-remitting to late relapsing-remitting and then to SP MS. At the same time, we found a parallel increase of the relative frequencies of "mild-multi-domain", "severe-executive/attention" and "severe-multi-domain" phenotypes. Primary progressive MS patients showed a distinct distribution of cognitive phenotypes, with higher prevalence of "mild-verbal memory/semantic fluency" followed by "severe-multi-domain", "severe-executive/attention" and "mild-multi-domain" phenotypes, and only a small percentage of "preserved cognition" patients.

MRI features of cognitive phenotypes. Subjects undergoing MRI did not differ from the entire study cohort in terms of demographic, clinical and neuropsychological variables (data not shown). **Table 7.1.3** and **Figure 7.1.2** summarize MRI features of each cognitive phenotype. Compared to HC, "preserved cognition" patients showed

significantly lower thalamic volume. A shared pattern of damage was observed when comparing “mild-verbal memory/semantic fluency”, “mild-multi-domain” and “severe-executive/attention” patients to HC, with lower NBV, NGMV, NcGMV, thalamic and putamen volumes. In addition, compared to HC, “mild-verbal memory/semantic fluency” patients were characterized by lower nucleus accumbens and hippocampal volume, “severe-executive/attention” patients by lower hippocampal volume, and “mild-multi-domain” patients by lower caudate nucleus volume. Compared to “preserved cognition”, “mild-verbal memory/semantic fluency” patients only showed significantly lower hippocampal volume; “mild-multi-domain” patients were characterized by lower NcGMV, while “severe-executive/attention” patients by higher T2 lesion volume. Patients belonging to “severe-multi-domain” phenotype had an extensive and severe brain damage. Indeed, compared to HC, they showed lower volumes in all the analyzed brain structures, except for nucleus pallidus and amygdala. Compared to “preserved cognition” patients, they showed the same differences, except for caudate nucleus.

Discussion

In this study, we propose a classification of cognitive functions in patients with MS, based on the identification of distinct cognitive phenotypes. We applied LPA on neuropsychological data from a large cohort of MS patients, obtained by using well-validated assessment tools. This approach allowed us to identify latent variables replacing single test measures, which can be affected by multiple cognitive functions, and to capture the shared variance across cognitive tests, likely reflecting purer measures of cognitive domains. Moreover, by using z-scores rather than a dichotomous classification, cognitive function was more properly represented as a continuum.

In order to improve the readability of the study and the interpretation of results, cognitive phenotypes were named based on patient’s performance at neuropsychological tests. Although current knowledge does not allow us to gain a complete understanding of these phenotypes’ meaning, their definition certainly represents a starting point for future studies.

By using MRI, we were able to identify neuroanatomical substrates for each phenotype, substantiating data-driven cognitive findings with a biological basis. Given volume loss in a specific GM region reflects demyelination and loss of neurons, synaptic

trees and supporting cells (Filippi *et al*, 2019a), the finding of reduced volume of a region with known functional relevance (Benedict *et al.*, 2020; Rocca *et al*, 2015a) in a given phenotype can represent an important biological validation of the data-driven classification.

We identified a first phenotype (named as "preserved cognition"), characterized by preserved functioning in all cognitive tests. This phenotype, prevailing in the early stages of the disease, included patients with shorter disease duration and less severe disability compared to other phenotypes. As for MRI features, patients in this group only showed lower thalamic volume compared to HC. Given the well-known thalamic involvement in cognitive functioning (Minagar *et al.*, 2013), we may hypothesize a few explanations for our findings. Real-world cognitive deficits not assessed in our neuropsychological battery (e.g. multitasking and word-finding tasks), may account for reduced thalamic volume. Otherwise, patients with higher cognitive reserve may be clustered in this phenotype, thus exhibiting normal cognitive performance despite mild thalamic damage (Sumowski & Leavitt, 2013). Future research on MS patients evaluating real-world cognitive abilities and their cognitive reserve, employing advanced MRI techniques for thalamic analysis and segmentation (Johansen-Berg *et al*, 2005; Louapre *et al.*, 2017) could help clarify the role of thalamic damage in cognitively preserved patients. In our study, we did not assess the premorbid intelligence quotient as a proxy of the subject cognitive reserve.

A second phenotype (named as "mild-verbal memory/semantic fluency") was characterized by mildly reduced performance in SRT and WLG. The data-driven co-segregation of decreased performance in verbal learning and memory and in semantic fluency (Rao *et al*, 1991), is likely due to impaired common semantic clustering strategies (Costa *et al*, 2019; Pitteri *et al*, 2019) and lexical access modalities (Kavé & Sapir-Yogev, 2020). In line with this explanation, our MRI data showed hippocampal atrophy as a potential pathological substrate. Indeed, hippocampal damage (both in terms of atrophy and abnormal functional connectivity) (Kern *et al*, 2012; van Geest *et al*, 2018) was associated with reduced performance in verbal learning and memory (Kern *et al.*, 2012; Rocca *et al*, 2018) and in semantic fluency (Catheline *et al*, 2015; Sheldon & Moscovitch, 2012). In future studies, detailed examination of cognitive functions (Beatty, 2004; Whiteside *et al*, 2016) together with MRI analysis of hippocampal subfields (Hrybouski

et al, 2019) and connections (Llufriu *et al*, 2019), may better characterize the neural basis of this phenotype. On the other hand, the lack of processing speed impairment in these patients seems to challenge the notion that slowed processing speed can always underlie memory difficulties in MS (Costa *et al*, 2017).

A third phenotype (named as "mild-multi-domain") showed mildly reduced cognitive performance in SRT, SCWT, SDMT and PASAT. These tests can recruit different cortically-oriented cognitive functions, which may be interconnected with each other. Cortical atrophy turned out to be the distinctive MRI feature of this phenotype, in line with previous findings of reduced neocortical volumes in MS patients with mild cognitive impairment. Moreover, reduced neocortical volume was associated with a poorer performance on tests of verbal memory, attention/concentration, and verbal fluency in MS (Amato *et al*, 2004; Benedict *et al*, 2006). The relative frequency of "mild-multi-domain" phenotype increased from early to late relapsing-remitting and SP MS, and was also high in primary progressive patients. These results are consistent with previous evidences on cortical atrophy in progressive MS (Eijlers *et al*, 2019; Eijlers *et al*, 2018). Future MRI studies should focus on cortical thickness estimation at vertex-level (Mainero *et al.*, 2015) and on cerebral activation (Rocca *et al.*, 2015a), in order to assess precise patterns of cortical damage, possibly corresponding to specific cognitive networks.

A fourth phenotype (named as "severe-executive/attention") was characterized by decreased performance in all tests, with more severe involvement in the PASAT and SCWT. These patients are likely to have a severe impairment of attention and aspects of executive functions, such as cognitive interference inhibition. This impairment may also justify, at least in part, the reduced performance in the remaining tests (Sarter *et al.*, 2001). Notably, this phenotype was characterized by higher fatigue scores compared to all other groups. Fatigue was previously associated to lower performance in attentive and executive tasks (Holtzer & Foley, 2009). At MRI assessment, "severe-executive/attention" compared to "preserved cognition" patients had a higher WM lesion load. Given the preferential location close to the ventricles of MS WM lesions, a high lesion burden may play a major role in causing both impaired cognition (Meijer *et al*, 2020) and higher fatigue levels (Sepulcre *et al*, 2009; Tedeschi *et al*, 2007) by disrupting long-range WM connections, also located close to the ventricles (Haider *et al*, 2016; Liu

et al., 2015). Long-range connections are determinant for efficient attention and executive functioning (Foong *et al*, 1997; Pujol *et al*, 2001), and higher lesion burden was associated with worse performance at SCWT and PASAT in MS patients (Arnett *et al*, 1994; Camp *et al*, 2005; Foong *et al.*, 1997; Nocentini *et al*, 2001; Pujol *et al.*, 2001; Sperling *et al*, 2001). Long-range connections are also involved in the pathophysiology of MS-related fatigue (Filippi *et al*, 2002; Sepulcre *et al.*, 2009; Tedeschi *et al.*, 2007), and higher lesion burden was linked to higher fatigue levels in MS (Sepulcre *et al.*, 2009; Tedeschi *et al.*, 2007). Future studies should further investigate the role of regional WM microstructural integrity as a possible neural substrate of this cognitive phenotype.

A fifth phenotype (named as "severe-multi-domain") was characterized by severely reduced performance in all cognitive tests. This phenotype was more frequent in the late stages of MS, corresponding to end-stage cognitive failure in our population. However, it was also represented in patients with short disease duration and low physical disability, underscoring the importance of cognitive assessment of MS patients from the early disease stages. These patients had severe brain atrophy on MRI, involving all explored tissue compartments, which mirrored the extensive cognitive impairment. "Severe-multi-domain" patients also experienced severe depressive symptoms, which is consistent with the association between depression and difficulties in working memory (Arnett *et al*, 1999), executive functioning (Arnett *et al*, 2001) and information processing speed (Patel & Feinstein, 2019).

Our findings may have several implications for clinical management and decision-making. This categorization of cognitive features could help plan rehabilitative strategies (Amato *et al*, 2014b; Charvet *et al*, 2017; Chiaravalloti *et al*, 2020; Fink *et al*, 2010; Hanssen *et al*, 2015; Hubacher *et al*, 2015; Pedullà *et al*, 2016) tailored to cognitively homogeneous patients' subgroups. This could be particularly relevant in patients with mildly impaired profiles who may represent the ideal candidates for rehabilitative treatments, as they may have higher brain plasticity resources (Enzinger *et al*, 2016; Filippi & Rocca, 2013; Forn *et al*, 2006; Forn *et al*, 2007). Moreover, a recent metanalysis provided some evidence supporting the potential benefit of disease modifying drugs also for the patient cognitive outcome (Amato & Krupp, 2020; Landmeyer *et al*, 2020). The patient transition to a more severe phenotype may contribute to support clinical decisions

on switches in the pharmacological treatment (Amato, 2018; Mollison *et al*, 2017; Weinstock-Guttman *et al*, 2018).

The employment of these cognitive phenotypes can also represent a step forward in research, allowing a better selection of candidates for cognitive rehabilitation trials, as well as fostering future studies on pathophysiology of cognitive changes in MS by using more advanced MRI techniques and deep learning approaches.

This study is not without limitations. The cross-sectional design did not allow us to describe the time-dependent relationships and evolution of phenotypes over time. The study was based on a clinical sample, which may not be entirely representative of the general MS population. Moreover, although commonly used in MS clinical and research settings, the BRB and SCWT do not provide a finer-grained assessment of cognitive functions. Finally, only a subgroup of subjects underwent MRI examination at the time of neuropsychological evaluation.

Despite the above considerations, provided with validation in an independent cohort of patients, our data-driven cognitive phenotypes can overcome the limitations of the traditional dichotomous classification and have the potential to represent a more meaningful measure of the cognitive status of MS patients.

Table 7.1.1. *Main demographic and clinical characteristics of healthy controls and patients with multiple sclerosis enrolled in the study.*

	Healthy controls	**Multiple sclerosis patients**	***p* values**
No.	196	1212	-
Mean age (SD) [range] [years]	40.4 (8.6) [20.2 – 60.9]	41.1 (11.1) [18.0 – 77.2]	0.38
Female/Male	130/66	784/428	0.87
Median EDSS (range)	-	2.0 (0.0 – 8.5)	-
Mean disease duration (SD) [range] [years]	-	10.5 (9.0) [0.20 - 55.2]	-
Mean age of onset (SD) [range] [years]	-	29.8 (9.9) [7·0 - 68·9]	-
Education (SD) [range] [years]	12.5 (3.4) [5.0-19.0]	12.2 (3.8) [5.0-24.0]	0.38
Mean FSS score (SD) [range]	-	14.9 (17.4) [1.0 – 63.0]	-
Mean MADRS score (SD) [range]	-	10.1 (9.3) [0.0 – 59.0]	-

Abbreviations: EDSS=Expanded Disability Status Scale; SD=standard deviation; FSS=Fatigue Severity Scale; MADRS=Montgomery-Asberg Depression Rating Scale.

Table 7.1.2. *Mean z-scores and standard deviations (SD) of cognitive tests defining each cognitive phenotype.*

	SRT	**SPART**	**SCWT**	**SDMT**	**PASAT**	**WLG**
Preserved Cognition	0.29 (0.58)	-0.01 (0.61)	0.02 (0.28)	0.75 (1.13)	0.22 (0.78)	0.06 (0.81)
Mild-verbal memory/ semantic fluency	-0.59 (0.85)	-0.22 (0.93)	-0.18 (0.89)	-0.14 (0.86)	-0.44 (0.99)	-1.29 (0.71)
Mild-multi-domain	-1.26 (0.72)	-0.25 (0.90)	-0.75 (1.11)	-1.01 (1.09)	-0.58 (1.11)	-0.16 (1.06)
Severe-executive/ attention	-1.10 (1.04)	-0.33 (1.30)	-2.51 (3.24)	-1.29 (1.46)	-2.19 (1.48)	-1.06 (1.32)
Severe-multi-domain	-1.55 (1.21)	-1.22 (0.52)	-1.89 (2.07)	-2.26 (1.16)	-2.51 (1.17)	-2.09 (0.77)

Abbreviations: SRT=Selective Reminding Test; SPART=Spatial Recall Test; SCWT=Stroop Color Word Test; SDMT=Symbol Digit Modalities Test; PASAT=Paced Auditory Serial Addition Test; WLG=Word List Generation.

Table 7.1.3. *Estimated marginal means and standard error (SE) of MRI features of cognitive phenotypes from linear mixed effect models. P values were adjusted for multiple comparisons (Bonferroni method).*

	HC	**Cognition Preserved**	***p* values *vs* HC**	**Mild- verbal memory/ semantic fluency**	***p* values *vs* HC (*vs* CP)**	**Mild-multi-domain**	***p* values *vs* HC (*vs* CP)**	**Severe-executive/ attention**	***p* values *vs* HC (*vs* CP)**	**Severe-multi-domain**	***p* values *vs* HC (*vs* CP)**
No	50	39	-	49	-	37	-	22	-	24	-
Mean T_2 LV (SE) [ml]	- -	51.33 (31.15)	- -	75.99 (30.49)	- (0.23)	76.29 (31.56)	- (0.15)	99.69 (34.07)	- (0.04)	133.70 (33.56)	- (<0.001)
Mean NBV (SE) [ml]	1532.61 (31.39)	1502.55 (31.27)	0.13 -	1493.63 (30.85)	0.03 (0.63)	1469.94 (31.52)	0.001 (0.11)	1479.23 (33.10)	0.03 (0.31)	1423.67 (32.77)	<0.001 (0.001)
Mean NGMV (SE) [ml]	764.07 (39.02)	749.69 (39.00)	0.25 -	733.70 (38.86)	0.01 (0.18)	715.71 (39.08)	0.002 (0.04)	725.78 (39.63)	0.01 (0.12)	703.70 (39.51)	<0.001 (0.002)
Mean NcGMV (SE) [ml]	698.93 (35.42)	687.69 (35.40)	0.36 -	672.04 (35.26)	0.02 (0.19)	662.59 (35.48)	0.005 (0.04)	665.35 (36.01)	0.02 (0.13)	646.36 (35.89)	<0.001 (0.005)
Mean NWMV (SE) [ml]	765.72 (68.22)	752.90 (68.22)	0.39 -	759.16 (68.15)	0.59 (0.59)	743.06 (68.25)	0.06 (0.51)	753.64 (68.51)	0.51 (0.94)	718.99 (68.45)	<0.001 (0.02)
Mean nThalV (SE) [ml]	1.39 (0.28)	9.69 (0.28)	0.005 -	9.62 (0.27)	0.001 (0.78)	9.31 (0.28)	<0.001 (0.13)	9.35 (0.31)	0.001 (0.22)	8.72 (0.30)	<0.001 (0.001)

Mean nCaudV (SE) [ml]	5.39 (0.81)	5.14 (0.81)	0.15 -	5.17 (0.81)	0.15 (0.95)	5.06 (0.81)	0.05 (0.65)	5.16 (0.81)	0.24 (0.95)	4.87 (0.81)	0.004 (0.15)
Mean nPutaV (SE) [ml]	6.39 (0.25)	6.08 (0.25)	0.09 -	6.00 (0.25)	0.03 (0.70)	5.95 (0.25)	0.01 (0.54)	5.94 (0.27)	0.04 (0.54)	5.68 (0.26)	<0.001 (0.05)
Mean nPallV (SE) [ml]	2.23 (0.08)	2.23 (0.08)	0.97 -	2.27 (0.08)	0.78 (0.78)	2.20 (0.08)	0.78 (0.78)	2.17 (0.09)	0.78 (0.78)	2.05 (0.09)	0.17 (0.17)
Mean nAmygV (SE) [ml]	1.84 (0.10)	1.74 (0.10)	0.33 -	1.82 (0.09)	0.96 (0.41)	1.82 (0.10)	0.96 (0.41)	1.82 (0.10)	0.96 (0.43)	1.69 (0.10)	0.27 (0.73)
Mean nAccuV (SE) [ml]	0.74 (0.16)	0.69 (0.16)	0.22 -	0.66 (0.16)	0.04 (0.54)	0.67 (0.16)	0.10 (0.82)	0.67 (0.17)	0.17 (0.83)	0.55 (0.16)	<0.001 (0.009)
Mean nHippV (SE) [ml]	5.58 (0.68)	5.42 (0.68)	0.25 -	5.13 (0.68)	0.03 (0.02)	5.32 (0.68)	0.06 (0.51)	5.10 (0.69)	0.006 (0.06)	5.09 (0.69)	0.002 0.05

Abbreviations: HC=healthy controls; CP=cognition preserved; SE=Standard error; LV=lesion volume; NBV=normalized brain volume; NGMV=normalized gray matter volume; NcGMV=normalized cortical gray matter volume; NWMV=normalized white matter volume; nThalV=normalized thalamic volume; nCaudV= normalized caudate volume; nPutaV=normalized putamen volume; nPallV=normalized pallidum volume; nAmygV= normalized amygdala volume; nAccuV=normalized accumbens volume; nHippV= normalized hippocampal volume.

Figure 7.1.1. *Clinical and Demographic Features of Cognitive Phenotypes.*

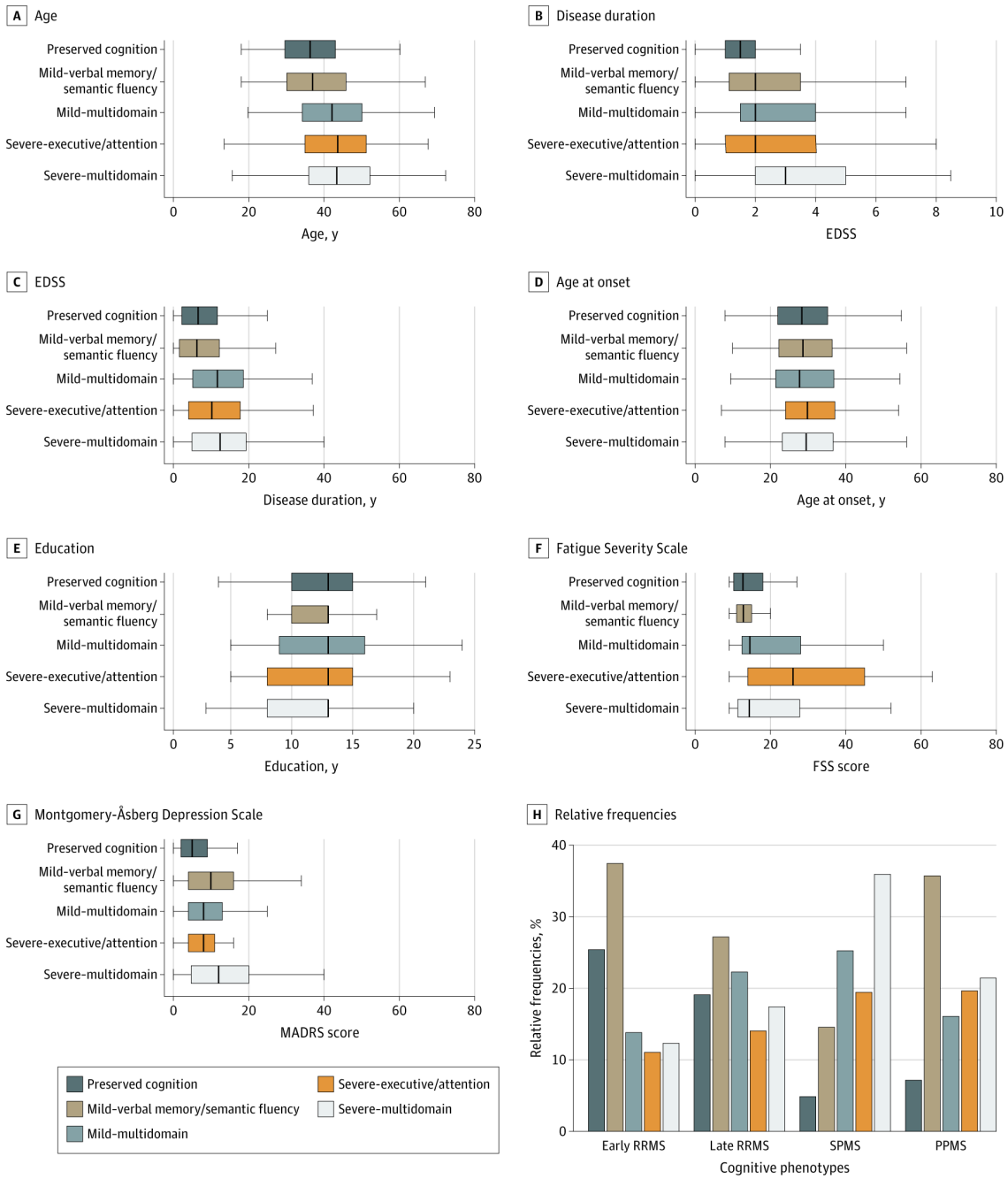

A-G, Boxplots are represented for each phenotype. H, The histograms show the relative frequencies as percentages of cognitive phenotype within clinical phenotypes from left to right: early relapsing-remitting multiple sclerosis (RRMS), late RRMS, secondary progressive multiple sclerosis (SPMS), and primary progressive multiple sclerosis (PPMS). EDSS indicates Expanded Disability Status Scale (De Meo et al, 2020a).

Figure 7.1.2. *Magnetic Resonance Imaging Features of Cognitive Phenotypes*

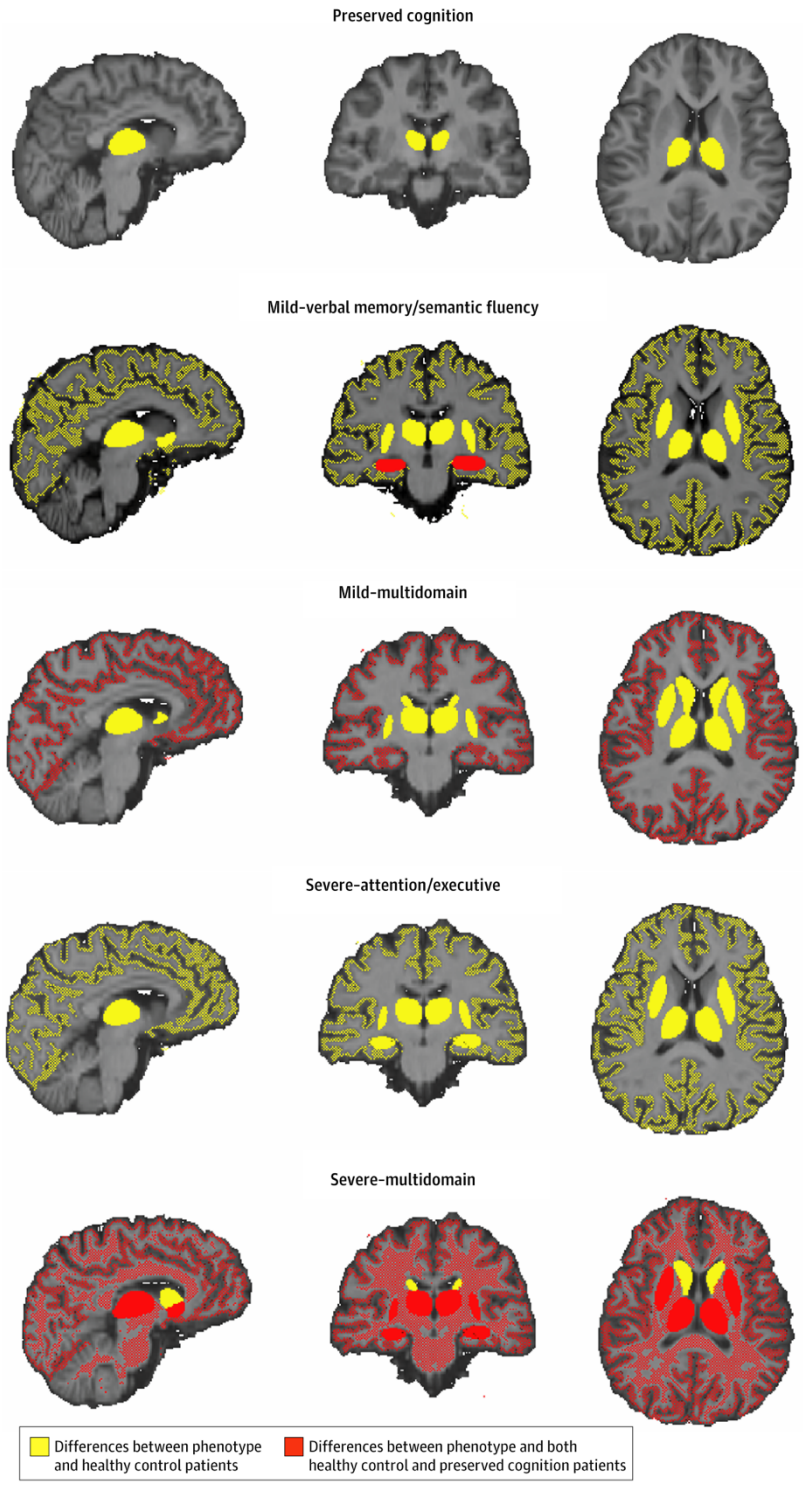

Brain structures showing differences between each phenotype and healthy controls are yellow-colored, while those showing differences between each phenotype and both healthy controls and "preserved cognition" patients are red-colored (De Meo et al., 2021c).

Supplementary Materials e-7.1.1

MRI acquisition protocol.

For both centers, a 3.0 Tesla Philips Intera MR scanner with 8-channel head coil (Philips Medical System, Best, The Netherlands) was used for MRI acquisition. The following MRI sequences of the brain were acquired from all subjects during a single session: a) 3DT1-weighted turbo field echo (repetition/echo time=25/4.6 ms; echo train length=1; flip angle=30°; matrix size=256x256; field-of-view=230x230mm^2; 220 contiguous, axial slices with voxel size=1x1x1 mm); b) dual-echo turbo spin echo yielding proton density (PD) and T2-weighted images (repetition/echo time=2599/16.80 ms, echo train length=6; flip angle=90º, matrix size=256x256, field-of-view=240x240 mm^2, 44 axial 3mm-thick slices). For all sequences, slices were positioned to run parallel to a line joining the most infero-anterior and infero-posterior margins of the corpus callosum.

Table e-7.1.1. *Fit indices of latent profile analysis models with 1 – 6 profiles.*

Number of Classes	AIC	BIC	ICL	BLRT
1	23104	23242	-23242	-
2	22713	22993	-23382	0.009
3	22763	23187	-23893	0.009
4	22593	23159	-23768	0.009
5	22497	23206	-23903	0.009
6	22627	23479	-24227	0.089

Abbreviations: AIC = Akaike Information Criterion; BIC = Bayesian Information Criterion; ICL = Integrated Completed Likelihood, BLRT=Bootstrap Likelihood Ratio Test.

Table e-7.1.2. *Main clinical and demographic features of cognitive phenotypes.*

Variables			***vs*** **Mild-verbal memory/semantic fluency**		***vs*** **Mild-multi-domain**		***vs*** **Severe-executive/attention**		***vs*** **Severe-multi-domain**	
		Mean (SD)	Effect size (95% CI)[a]	*p*	Effect size (95% CI)[a]	*p*	Effect size (95% CI)[a]	*p*	Effect size (95% CI)[a]	*p*
Age	Preserved Cognition	36.5 (9.8)	-0.16 (-0.33, -0.002)	0.98	-0.56 (-0.75, -0.38)	<0.001	-0.58 (-0.79, -0.37)	<0.001	-0.72 (-0.91, -0.53)	<0.001
	Mild-verbal memory/semantic fluency	38.2 (11.1)			-0.38 (-0.55, -0.21)	<0.001	-0.41 (-0.60, -0.22)	<0.001	-0.53 (- 0.71, -0.35)	<0.001
	Mild-multi-domain	42.6 (11.2)					-0.04 (-0.23, 0.16)	>0.99	-0.14 (-0.33, 0.04)	>0.99
	Severe-executive/attention	42.9 (11.7)							-0.10 (-0.31, -0.09)	>0.99
	Severe-multi-domain	44.0 (11.0)								
		Female/male	Effect size (95% CI)[b]	*p*	Effect size (95% CI)[b]	*p*	Effect size (95% CI)[b]	*p*	Effect size (95% CI)[b]	*p*
Sex	Preserved Cognition	155/80	0.01 (0.00, 0.08)	>0.99	0.10 (0.00, 0.19)	0.06	0.01 (0.00, 0.09)	>0.99	0.01 (0.00, 0.09)	>0.99

	Mild-verbal memory/semantic fluency	242/120			0.11 (0.03, 0.19)	0.03	0.00 (0.00, 0.04)	>0.99	0.00 (0.00, 0.01)	>0.99
	Mild-multi-domain	133/103					0.11 (0.00, 0.21)	0.05	0.11 (0.01, 0.20)	0.04
	Severe-executive/attention	112/55							0.00 (0.00, 0.01)	>.099
	Severe-multi-domain	142/70								
		Median (range)	Effect size (95% CI)[c]	*p*	Effect size (95% CI)[c]	*p*	Effect size (95% CI)[c]	*p*	Effect size (95% CI)[c]	*p*
EDSS	Preserved Cognition	1.5 (0.0 – 7.0)	-0.25 (-0.34, -0.16)	<0.001	-0.21 (-0.32, -0.11)	<.001	-0.17 (-0.29, -0.05)	.001	-0.39 (-0.49, -0.29)	<.001
	Mild-verbal memory/semantic fluency	2.0 (0.0 – 7.5)			-0.05 (-0.14, 0.05)	>.99	-0.02 (-0.14, 0.09)	>.99	-0.24 (-0.33, -0.14)	<.001
	Mild-multi-domain	2.0 (0.0 – 8.0)					0.06 (-0.05, 0.18)	>.99	-0.14 (-0.25, 0.03)	.001
	Severe-executive/attention	2.0 (0.0 – 8.0)							-0.17 (-0.29, -0.04)	.001
	Severe-multi-domain	3.0 (0.0 – 8.5)								
Disease duration		Mean (SD)	Effect size (95% CI)[a]	*p*	Effect size (95% CI)[a]	*p*	Effect size (95% CI)[a]	*p*	Effect size (95% CI)[a]	*p*

	Preserved Cognition	8.0 (7.3)	-0.04 (-0.31,0.24)	>0.99	-0.56 (-0.84, -0.27)	<0.001	-0.48 (-0.77, -0.20)	<0.001	-0.90 (-0.61, -0.32)	<0.001
	Mild-verbal memory/semantic fluency	8.3 (7.6)			-0.81 (-0.52, -0.23)	<0.001	-0.73 (-0.45, -0.16)	<0.001	-0.87 (-0.58, -0.29)	<0.001
	Mild-multi-domain	12.8 (9.6)					0.07 (-0.21, 0.35)	0.95	-0.05 (-0.33, 0.22)	0.97
	Severe-executive/attention	12.2 (9.5)							-0.13 (-0.41, 0.15)	0.72
	Severe-multi-domain	13.3 (10.2)								
Age at onset		Mean (SD)	Effect size (95% CI)[a]	*p*	Effect size (95% CI)[a]	*p*	Effect size (95% CI)[a]	*p*	Effect size (95% CI)[a]	*p*
	Preserved Cognition	28.6 (8.8)	-0.14 (-0.41, 0.14)	>0.99	-0.10 (-0.38, 0.17)	>0.99	-0.20 (-0.48, 0.08)	0.50	-0.21 (-0.49, 0.07)	0.21
	Mild-verbal memory/semantic fluency	30.0 (10.0)			0.03 (-0.24, 0.31)	>0.99	-0.06 (-0.34, 0.22)	>0.99	-0.08 (-0.35, 0.20)	>0.99
	Mild-multi-domain	29.6 (10.3)					-0.09 (-0.37, 0.18)	>0.99	-0.11 (-0.39, 0.17)	>0.99
	Severe-executive/attention	30.6 (10.0)							-0.02 (-0.29, 0.26)	>0.99
	Severe-multi-domain	30.7 (10.6)								
Education		Mean	Effect size	*p*	Effect size	*p*	Effect size	*p*	Effect size	*p*

		(SD)	(95% CI)[a]		(95% CI)[a]		(95% CI)[a]		(95% CI)[a]	
	Preserved Cognition	12.5 (3.4)	0.002 (-0.27, 0.28)	>0.99	-0.16 (-0.44, 0.12)	0.48	0.14 (-0.14, 0.41)	0.71	0.05 (-0.23, 0.32)	0.99
	Mild-verbal memory/semantic fluency	12.4 (3.3)			-0.16 (-0.44, 0.12)	0.34	0.13 (-0.14, 0.41)	0.65	0.04 (-0.23, 0.32)	0.99
	Mild-multi-domain	12.6 (3.9)					0.30 (0.02, 0.58)	0.04	0.21 (-0.07, 0.48)	0.21
	Severe-executive/attention	11.5 (4.2)							-0.09 (-0.37, 0.19)	0.91
	Severe-multi-domain	11.8 (3.9)								
FSS		Mean (SD)	Effect size (95% CI)[a]	*p*	Effect size (95% CI)[a]	*p*	Effect size (95% CI)[a]	*p*	Effect size (95% CI)[a]	*p*
	Preserved Cognition	14.2 (15.3)	0.18 (-0.10, 0.46)	0.12	-0.17 (-0.45, 0.11)	0.18	-0.48 (-0.76, -0.19)	0.002	-0.08 (-0.36, 0.20)	0.52
	Mild-verbal memory/semantic fluency	11.1 (15.5)			-0.35 (-0.63, -0.07)	0.03	-0.66 (-0.95, -0.37)	<0.001	-0.26 (-0.54, 0.02)	0.22
	Mild-multi-domain	17.2 (18.5)					-0.30 (-0.59, 0.03)	0.05	0.09 (-0.18, 0.37)	0.50
	Severe-executive/attention	22.4 (19.4)							0.40 (0.12, 0.68)	0.01
	Severe-multi-domain	15.5 (18.7)								
MADRS		Mean	Effect size	*p*	Effect size	*p*	Effect size	*p*	Effect size	*p*

		(SD)	(95% CI)[a]		(95% CI)[a]		(95% CI)[a]		(95% CI)[a]	
	Preserved Cognition	7.7 (9.5)	-0.45 (-0.74, -0.17)	0.04	-0.20 (-0.48, 0.08)	>0.99	-0.01 (-0.28, 0.27)	>0.99	-0.59 (-0.87, -0.30)	0.01
	Mild-verbal memory/semantic fluency	11.9 (10.0)			0.25 (-0.03, 0.53)	>0.99	0.44 (0.16, 0.73)	0.08	-0.13 (-0.41, 0.14)	>0.99
	Mild-multi-domain	10.0 (8.9)					0.20 (-0.08, 0.47)	>0.99	-0.38 (-0.66, -0.10)	0.36
	Severe-executive/attention	8.3 (5.5)							-0.58 (-0.87, 0.29)	0.02
	Severe-multi-domain	13.8 (11.0)								
Cognitive phenotype distribution			**vs Late RRMS**		**vs SPMS**		**vs PPMS**			
		Preserved Cognition/ Mild-verbal memory/semantic fluency/ Mild-multi-domain/ Severe-executive/attention/ Severe-multi-domain	Effect size (95% CI)[b]	*p*	Effect size (95% CI)[b]	*p*	Effect size (95% CI)[b]	*p*		

	Early RRMS	101/149/55/44/49	0.16 (0.09, 0.22)	<0.001	0.37 (0.27, 0.45)	<0.001	0.17 (0.04, 0.25)	0.01		
	Late RRMS	125/178/146/92/114			0.21 (0.13, 0.27)	<0.001	0.11 (0.00, 0.16)	0.09		
	SPMS	5/15/26/20/37					0.27 (0.03, 0.40)	0.02		
	PPMS	4/20/9/11/12								

[a] *Cohen's d effect size*
[b] *Cramer's V effect size*
[c] *Cliff's delta effect size*
Abbreviations: EDSS=Expanded Disability Status Scale; SD=standard deviation; FSS=Fatigue Severity Scale; MADRS=Montgomery Asberg Depression Rating Scale

Figure e-7.1.1. *Latent Profile Analysis results*

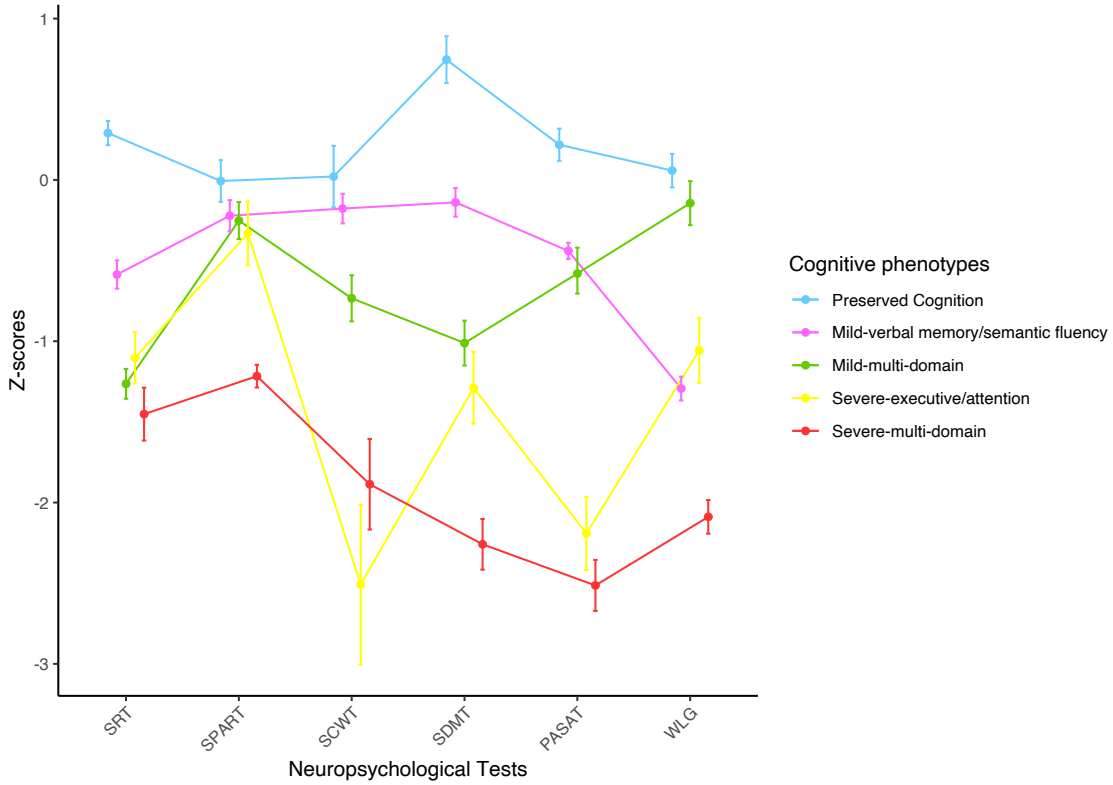

The figure represents the cognitive performance of each phenotype: points indicate mean z-scores obtained at each neuropsychological test and error bars reflect the 95% confidence interval. "Preserved cognition" phenotype is represented in cyan blue, "mild-verbal memory/semantic fluency" in purple, "mild-multi-domain" in green, "severe-attention/executive" in yellow and "severe-multi-domain" in red (De Meo et al, 2021b).
Abbreviations: SRT=Selective Reminding Test; SPART=Spatial Recall Test; SCWT=Stroop Color Word Test; SDMT=Symbol Digit Modalities Test; PASAT=Paced Auditory Serial Addition Test; WLG=Word List Generation.

7.2 Effect of BDNF Val66Met polymorphism on hippocampal subfields in multiple sclerosis patients

The following data have been published (De Meo *et al.*, 2021d).

Molecular Psychiatry www.nature.com/mp

ARTICLE

Check for updates

Effect of BDNF Val66Met polymorphism on hippocampal subfields in multiple sclerosis patients

Ermelinda De Meo[1,2✉], Emilio Portaccio[3,4], Elio Prestipino[3], Benedetta Nacmias[3,4], Silvia Bagnoli[3], Lorenzo Razzolini[5], Luisa Pastò[5], Claudia Niccolai[4], Benedetta Goretti[3], Angelo Bellinvia[5], Mattia Fonderico[5], Antonio Giorgio[6], Maria Laura Stromillo[6], Massimo Filippi[1,2,7,8], Sandro Sorbi[3,4], Nicola De Stefano[6] and Maria Pia Amato[3,4]

Brain-derived neurotrophic factor (BDNF) Val66Met polymorphism was shown to strongly affect BDNF function, but its role in modulating gray matter damage in multiple sclerosis (MS) patients is still not clear. Given BDNF relevance on the hippocampus, we aimed to explore BDNF Val66Met polymorphism effect on hippocampal subfield volumes and its role in cognitive functioning in MS patients. Using a 3T scanner, we obtained dual-echo and 3DT1-weighted sequences from 50 MS patients and 15 healthy controls (HC) consecutively enrolled. MS patients also underwent genotype analysis of BDNF, neurological and neuropsychological evaluation. Hippocampal subfields were segmented by using Freesurfer. The BDNF Val66Met polymorphism was found in 22 MS patients (44%). Compared to HC, MS patients had lower volume in: bilateral hippocampus-amygdala transition area (HATA); cornus ammonis (CA)1, granule cell layer of dentate gyrus (GCL-DG), CA4 and CA3 of the left hippocampal head; molecular layer (ML) of the left hippocampal body; presubiculum of right hippocampal body and right fimbria. Compared to BDNF Val66Val, Val66Met MS patients had higher volume in bilateral hippocampal tail; CA1, ML, CA3, CA4, and GCL-DG of left hippocampal head; CA1, ML, and CA3 of the left hippocampal body; left HATA and presubiculum of the right hippocampal head. In MS patients, higher lesion burden was associated with lower volume of presubiculum of right hippocampal body; lower volume of left hippocampal tail was associated with worse visuospatial memory performance; lower volume of left hippocampal head with worse performance in semantic fluency. Our findings suggest the BNDF Val66Met polymorphism may have a protective role in MS patients against both hippocampal atrophy and cognitive impairment. BDNF genotype might be a potential biomarker for predicting cognitive prognosis, and an interesting target to study for neuroprotective strategies.

Molecular Psychiatry; https://doi.org/10.1038/s41380-021-01345-1

Introduction

During the last decade, brain plasticity was intensively studied for its critical role in overcoming brain damage, explaining the discrepancy between clinical and neuroradiological features in MS patients (Benedict *et al.*, 2020; Rocca *et al*, 2016a). However, there are strong interindividual differences among MS patients in their capacity to compensate for brain damage, which points to the role of genetic factors.

The brain derived neurotrophic factor (BDNF) is known as the most relevant neurotrophic factor involved in brain plasticity. BDNF is secreted from dendrites to axons and from axons to dendrites, in autocrine loops, and across long distances through neural circuits (Hartmann *et al*, 2001; Murer *et al*, 2001). It may play a role in the refinement of active neural pathways through activity-dependent strengthening of co-active synapse terminals and elimination of inactive terminals (Park & Poo, 2013). The human BDNF gene has only one frequent, non-conservative polymorphism (dbSNP number rs6265): a single nucleotide polymorphism (SNP) at nucleotide 196 (G/A) resulting in an amino acid substitution (valine to methionine) at codon 66 (hence named Val66Met). The Val66Met polymorphism was shown to interfere with the intracellular trafficking and the activity-dependent secretion of BDNF (Chen *et al*, 2004; Egan *et al*, 2003).

The anatomical effect of Val66Met polymorphism on healthy individuals is most apparent on hippocampal formation and prefrontal cortex. These brain regions are involved in learning and memory, which require neuroplasticity, hence they show abundant expression of BDNF (Bimonte-Nelson *et al*, 2003; Egan *et al.*, 2003; Hariri *et al*, 2003). Moreover, the Val66Met polymorphism was associated with reduced volume of these structures in HC (Hajek *et al*, 2012).

To the opposite, previous studies on MS patients have shown contrasting effects of the BDNF Val66Met polymorphism on GM volume, also including protective effects (Liguori *et al*, 2007; Ramasamy *et al*, 2011; Stadelmann *et al*, 2002; Zivadinov *et al*, 2007). Indeed, while earlier studies (Liguori *et al.*, 2007) suggested Val66Met polymorphism might be a risk factor for GM atrophy, more recent studies demonstrated a protective role against GM damage (Dinacci *et al*, 2011; Ramasamy *et al.*, 2011; Zivadinov *et al.*, 2007). This peculiar effect of BDNF Val66Met polymorphism is

probably related to the secretion of BDNF by immune cells and to interactions of its polymorphism with the dysregulated immune system of patients with MS.

Within the hippocampal formation, regions with different vulnerability to MS-related damage have been individuated (Geurts *et al*, 2007), as well as regions prominently involved in neurogenesis, synaptic plasticity and long-term potentiation (LTP) likely to be more susceptible to BDNF effects.

Against this background, we aimed to assess the effect of the BDNF Val66Met polymorphism on the volume of hippocampal subfields in MS patients, and to investigate the potential association of hippocampal changes with cognitive functioning.

Methods

Ethics committee approval. Approval was received from Ethics Committee on human experimentation of the University of Florence, and written informed consent was obtained from all participants prior to study enrollment.

Subjects. We recruited 50 consecutive right-handed adult MS patients (42 relapsing-remitting and 8 progressive) (Lublin *et al.*, 2014; Thompson *et al.*, 2018) followed at Careggi University Hospital, Florence, division of Neurology. Exclusion criteria were: history of other neurological/medical disorders in addition to MS, use of antidepressants or other psychoactive drugs, history of learning disability, severe head trauma, alcohol or drug abuse, and relapse or corticosteroid use within 4 weeks preceding neuropsychological and MRI assessment.

Fifteen right-handed healthy subjects (HC) with no previous history of neurological dysfunction and a normal neurological examination were also consecutively enrolled as a control group.

Clinical assessment. Neurological evaluations - including ongoing treatments, relapses and disability level assessed every three months on the EDSS - were collected from the disease onset to the time of study enrollment. In addition, a complete neurological evaluation with EDSS score rating was performed at the time of MRI. In order to assess disease progression, the progression index (PI) was calculated as the difference between the last EDSS and the baseline EDSS scores, divided by the disease duration.

Neuropsychological evaluation. A complete neuropsychological evaluation(Amato *et al.*, 2006) was performed in MS patients through the administration of BRB (Amato *et al.*, 2006) and the SCWT (Stroop, 1935). The BRB assesses the most frequently impaired cognitive domains in MS (Amato *et al.*, 2006), incorporating tests of: verbal learning and memory [SRT including Long-Term Storage (SRT-LTS), Consistent Long-Term Retrieval (SRT-CLTR) and delayed recall (SRT-D)]; visual/spatial learning and memory (10/36 SPART and SPART-D); complex attention and information processing speed (PASAT and SDMT); and verbal fluency on semantic stimulus (WLG). The SCWT (Stroop, 1935) assesses complex attention and aspects of executive functioning such as the ability to inhibit cognitive interference, thus integrating (Amato *et al.*, 2006) the BRB. Corrected scores for age, sex and education according to normative values (Amato *et al.*, 2006) were calculated for each test. Finally, based on a population of age- and gender-matched HC (n=90, females=69, mean age [standard deviation]=41.6 [10.4] years), z-scores for each cognitive test were calculated. A threshold of mean z-score <-1.5 was used to distinguish "severely" and "mildly" reduced performance at each test (De Meo *et al.*, 2021c).

The Fatigue Severity Scale (FSS) (Krupp *et al.*, 1989) and the Montgomery and Asberg Depression Scale (MADRS) (Montgomery & Asberg, 1979) were also administered during the evaluation, in order to assess fatigue and depression.

Genetic analysis: genotyping of BDNF. Blood samples were obtained from MS patients at the time of study enrollment. As previously described (Bagnoli *et al*, 2004), the presence of the BDNF Val66Met polymorphism was determined by polymerase chain reaction (PCR), amplifying the DNA obtained from patients' leukocytes. Subjects' DNA was isolated from peripheral blood using the automatic standardized method (QIAcube, QIAGEN). The G→A nucleotide substitution, identifying the Val→Met amino acid change, was assayed by the High Resolution Melting Analysis (HRMA). PCR primers were 5′-ACTCTGGAGAGCGTGAATGG-3' and 5′-ACTACTGAGCATCACCCTGGA-3′. Genotypes were identified by sequencing (310 ABI PRISM Genetic Analyzer, Applied Biosystem).

MRI acquisition. A 3.0 Tesla Philips Intera MR scanner with dedicated head coil (Philips Medical System, Best, The Netherlands) was used for MRI acquisition. The following MRI sequences of the brain were acquired from all subjects during a single

session: a) 3DT1-weighted turbo field echo (repetition/echo time=25/4.6 ms; echo train length=1; flip angle=30°; matrix size=256x256; field-of-view=230x230mm2; 220 contiguous, axial slices with voxel size=1x1x1 mm); b) dual-echo turbo spin echo yielding proton density and T2-weighted images (repetition/echo time=2599/16.80 ms, echo train length=6; flip angle=90º, matrix size=256x256, field-of-view=240x240 mm2, 44 axial 3mm-thick slices). For all sequences, the slices were positioned to run parallel to a line that joined the most infero-anterior and infero-posterior margins of the corpus callosum. MRI scans were visually assessed and repeated in case of artifacts.

MRI analysis. T2-hyperintense lesion volumes were measured on proton density images, using a semi-automated local thresholding segmentation technique (Jim 8, Xinapse Systems, Colchester, United Kingdom). Normalized brain (NBV), WM (NWMV) and GM (NGMV) volumes were measured on lesion-filled 3DT1-weighted images using SIENAx software.

Hippocampal segmentation. The hippocampal module(Iglesias *et al*, 2015) of the FreeSurfer software, version 7.1.1 (http://surfer.nmr.mgh.harvard.edu), was applied to lesion-filled 3DT1- weighted images according the cross-sectional(Fischl, 2012) standard pipeline (**Figure 1**). Global hippocampal volume and volumes of hippocampal subfields were estimated and normalized for total intracranial volume. We followed the proposed quality control procedure guidelines for the FreeSurfer-based segmentation of the hippocampal subregions designed for the Enhancing Neuro Imaging Genetics through Meta-Analysis (ENIGMA) consortium (Samann *et al*, 2020).

Statistical Analysis. Between-group comparisons of demographic, clinical, neuropsychological and conventional MRI variables were performed with Fischer exact test for categorical variables, and Mann-Whitney, t test or age-, sex-, disease duration- and phenotype-adjusted (for MS patients) linear models for continuous variables, as appropriate according to normality distribution assessed by visual inspection and Shapiro-Wilk test.

Volumes of the hippocampi and their subfields were compared between MS patients and HC, between MS patients grouped by BDNF polymorphism and HC, and between MS patients with and without BDNF Val66Met polymorphism by using age-, sex-, disease duration- and phenotype-adjusted (for MS patients) linear models.

Age-, sex-, disease duration- and phenotype-adjusted linear models were also used

to explore the relationship of hippocampal subfield volumes showing significant abnormalities in MS patients *vs* HC with clinical, conventional MRI and neuropsychological features. Multivariate regression models, including EDSS, NBV, NWMV and NGMV in addition to hippocampal subfield volumes and the above-specified covariates, were adopted to assess the role of hippocampal subfield volumes as independent predictors of cognitive performance. A stepwise variable selection procedure was used ($p = 0.15$ for entry and $p = 0.05$ to remain in the model). Finally, we performed a regression analysis exploring the role of the BDNF polymorphism on neuropsychological variables, while assessing the role of hippocampal subfield volumes as mediators.

False-discovery-rate (Benjamini-Hochberg procedure) correction was separately applied to account for the overall number of each group of pairwise comparisons and pairwise contrasts, in between-group comparisons and regression analysis, respectively. For all analysis, statistical threshold was set at p-value < 0.05. Statistical analysis was performed with the R software, version 4.0.2.

Data availability. The dataset used and analyzed during the current study is available from the corresponding Author on reasonable request.

Results

Clinical and conventional MRI measures. **Table 7.2.1** summarizes the main demographic, clinical and conventional MRI features of the study cohort. Compared to HC, MS patients were well matched in terms of age distribution, although they had a preponderance of female subjects (p=0.02). They had brain (p=0.04) and WM (p=0.03) atrophy, but no significant NGMV reduction. Compared to HC, MS patients showed a trend towards left (p=0.08) and right (p=0.09) normalized hippocampal volume reduction. Twenty-two (44%) MS patients were carriers of the BDNF Val66Met polymorphism. Compared to Val66Val, Val66Met MS patients included a greater proportion of male subjects (p=0.02), while no significant differences were observed in terms of age, disability, disease duration, phenotype and disease modifying treatment. Compared to HC, Val66Val MS patients showed lower left (p=0.02) and right (p=0.05) normalized hippocampal volume, but no significant differences in NBV, NGMV, NWMV. Compared to HC, Val66Met patients showed no significant difference in

normalized hippocampal volume as well as in NBV, NGMV, NWMV. Compared to Val66Val, Val66Met MS patients showed higher left (p=0.01) and right (p=0.05) normalized hippocampal volume, but no significant differences in NBV, NGMV, NWMV.

Neuropsychological measures. **Table 7.2.2** summarizes the main neuropsychological features of MS patients. MS patients showed mildly reduced cognitive performance in all cognitive tests, compared to HC. No difference in education was observed between Val66Val and Val66Met MS patients. Only in SPART-D, BDNF Val66Val MS patients showed severely reduced performance compared to HC, and Val66Met MS patients showed better performance compared to Val66Val MS patients (p=0.02). No significant differences were observed between Val66Val and Val66Met MS patients in the remaining cognitive tests, as well as in fatigue and depression scores.

Hippocampal subfields. Compared to HC, MS patients had lower volumes in: left (p=0.04) and right (p=0.04) hippocampus-amygdala transition area (HATA); cornus ammonis (CA)1 (p=0.04), granule cell layer of dentate gyrus (GCL-DG) (p=0.04), CA4 (p=0.05) and CA3 (p=0.05) of left hippocampal head; molecular layer (ML) (p=0.05) of left hippocampal body; presubiculum (p=0.05) of right hippocampal body and right fimbria (p=0.03). Compared to HC, BDNF Val66Val MS patients had lower volume in: left (p=0.01) and right (p=0.01) HATA; left (p=0.05) and right (p=0.05) hippocampal tail; CA1 (p=0.04), GCL-DG (p=0.04), CA4 (p=0.05), CA3 (p=0.01) of left hippocampal head; ML (p=0.05) of left hippocampal body; CA3 (p=0.05) of right hippocampal head, presubiculum (p=0.02) of right hippocampal body, and right fimbria (p=0.05). Compared to HC, BDNF Val66Met MS patients had lower volume in: left (p=0.02) and right (p=0.01) HATA; left CA3 (p=0.04) of hippocampal head; and presubiculum of right hippocampal body (p=0.01).

Compared to BDNF Val66Val, Val66Met MS patients had higher volume in: left (p=0.03) and right (p=0.01) hippocampal tail; CA1 (p=0.01), ML (p=0.01), CA3 (p=0.02), CA4 (p=0.01) and GCL-DG (p=0.02) of left hippocampal head; CA1 (p=0.02), ML (p=0.01) and CA3 (p=0.01) of left hippocampal body, left HATA (p=0.01) and presubiculum of right hippocampal head (p=0.05) (**Table 7.2.3**).

Correlation analysis. No significant associations were found between hippocampal subfield abnormalities with clinical and conventional MRI variables, except

for T2 lesion volume, which was associated with lower volume of presubiculum of right hippocampal body (β=-3.76; *p*=0.05). **Table 7.2.4** summarizes significant associations between hippocampal subfield volumes and neuropsychological variables. Significant associations were found between :

- Worse SPART-D performance with lower left hippocampal tail volume (β=0.39; *p*=0.04);
- Worse WLG performance with lower volume of GCL-DG (β=0.39; *p*=0.04), CA3 (β=0.40; *p*=0.04) and CA4 (β=0.43; *p*=0.02) belonging to left hippocampal head.

Multivariate analysis confirmed the role of left hippocampal tail as an independent predictor of SPART-D performance (β=0.44, 95%CI=0.45-0.47; *p*=0.05) and CA4 of left hippocampal head as an independent predictor of WLG performance (β=0.62; 95%CI=0.59-0.65; *p*=0.006).

Left hippocampal tail volume resulted as mediator of BDNF polymorphism effect on SPART-D performance: introducing left hippocampal tail volume as covariate, BDNF polymorphism had no significant effect on SPART-D performance (*p*=0.10).

Discussion

In this study, we explored the impact of the BDNF Val66Met polymorphism on hippocampal formation in MS patients, and its clinical and neuropsychological correlates. The analysis was separately performed for each hippocampal subfield, considering both their different susceptibility to MS-related damage (Cacciaguerra *et al*, 2019; Geurts *et al.*, 2007; Sicotte *et al*, 2008) and their functional specialization. These features, together with the evidence of plasticity occurring in this structure, make the analysis of hippocampal subfields a powerful tool to *in-vivo* explore disease-related changes, including neuronal loss, neurogenesis and functional reorganization, and the impact of the BDNF Val66Met polymorphism on these processes (Rocca *et al.*, 2018).

Compared to HC, we observed reduced volumes of several left hippocampal subfields, including CA1, GCL-DG, CA4 and CA3. These results are in line with previous findings highlighting the prominent vulnerability of CA1(Longoni *et al*, 2015; Sicotte *et al.*, 2008) and of CA3/CA4/DG(Gold *et al*, 2010) in MS. In details, CA1 is the most affected hippocampal region in a variety of neurological disorders, and especially in MS. Neurons within the CA1 region are highly susceptible to ischemia and glutamate-

mediated excitotoxicity (Wang *et al*, 2005), implicated in MS-related CNS damage (Vallejo-Illarramendi *et al*, 2006). In MS, pathological studies reported reduction of neuronal count and size (Papadopoulos *et al*, 2009), decreased dendritic density and the presence of demyelinating lesions in this area (Geurts *et al.*, 2007; Papadopoulos *et al.*, 2009), which translate into CA1 volume loss. Despite the relevance of CA1 volume loss in MS, a recent study demonstrated that the CA3/CA4/DG subfield of the hippocampus is the first region to become atrophic in MS, from the stage of clinically-isolated syndrome (Planche *et al*, 2018). Moreover, CA4/DG atrophy at the stage of clinically-isolated syndrome was found to predict the atrophy of CA1 one year later, thus suggesting a possible pattern of hippocampal damage spreading. According to this hypothesis a gradient of infiltrating immune cells and cytokines might diffuse progressively from CSF to DG, then to CA1, and finally to the whole medial temporal lobe (Planche *et al.*, 2018).

Beyond previous studies, we also showed atrophy of left ML, right presubiculum, right fimbria and bilateral HATA in MS patients compared to HC. These results may partly be due to the adoption of an advanced hippocampal subfield segmentation technique, with heightened sensitivity. The ML contains interneurons and the apical dendrites of hippocampal pyramidal cells, thus representing an input region to hippocampal subfields, which receive a great flow of information (Duvernoy *et al*, 2013; Iglesias *et al.*, 2015). The decreased volume observed in this subfield could be due to both reduced intra- and extra-hippocampal connectivity and neuron loss in subiculum and CA fields (Haukvik *et al*, 2020). Previous studies have already described subiculum involvement in MS, defining “subiculum” as the so-called “subicular complex”, which included presubiculum, subiculum and post-subiculum. It is the cytoarchitectonic organization of presubicular cortex [comprising six-layers (Ishihara & Fukuda, 2016; O'Mara *et al*, 2001) and the dense plexus formed by afferent axons] which distinguishes the presubiculum from the neighboring subiculum and post-subiculum. Given the density of afferent axons to the presubiculum, which plays prominent roles in intrahippocampal and cortico-hippocampal pathways, it is not surprising that our study demonstrated a specific atrophy of the right presubiculum within the subicular complex. The association found between reduced right presubiculum volume and higher T2 lesion burden supports the hypothesis of Wallerian degeneration originating from the damage to connecting fibers by MS WM lesions. Moreover, although not assessed in the present study,

intracortical and leukocortical demyelinating lesions are frequent in the presubiculum (Geurts *et al.*, 2007; Papadopoulos *et al.*, 2009), and may contribute to its morphologic alterations.

The HATA is part of the hippocampus-amygdala circuitry. The CA1 projects to the amygdala, which in turn projects to the HATA (Fudge *et al*, 2012; Kishi *et al*, 2006). Thus, this region mediates the hippocampus-amygdala interactions involved in visuospatial function and object discrimination. The fimbria, a WM structure forming part of the fornix and projecting to the amygdala (Iglesias *et al.*, 2015), is also involved in such cognitive functions. Damage to these areas might be due to MS lesions along the fornix or in the hippocampus-amygdala circuitry, which were not specifically assessed in our study. Given the polysynaptic projection of the CA1 back to the HATA, we might further speculate damage to the HATA may be partially secondary to neuronal loss in the CA1.

Looking at the effect of BDNF Val66Met polymorphism onto the hippocampal formation in MS, we found higher volumes of several hippocampal subfields in Val66Met carriers, thus suggesting a protective role of this polymorphism in MS. We investigated this polymorphism given the central role of BDNF in neurogenesis, neuronal maturation, circuit formation and activity-dependent forms of plasticity, such as long-term potentiation (LTP) of synaptic transmission (Toda *et al*, 2019). In details, the BDNF was shown to stimulate proliferation of neural progenitor cells and to promote long-term survival of their progeny (Katoh-Semba *et al*, 2002; Kuipers *et al*, 2009; Sairanen *et al*, 2005), and intra-hippocampal infusion of BDNF stimulated hippocampal neurogenesis (Scharfman *et al*, 2005; Schmidt & Duman, 2010; Shirayama *et al*, 2002). Nevertheless, the main function of BDNF is to enhance synaptic transmission, facilitate synaptic plasticity and promote synaptic growth (Lu *et al*, 2013). The BDNF Val66Met polymorphism has been proven to result in impaired dendritic trafficking and synaptic localization of the protein and, most importantly, an 18–30% reduction in activity-dependent BDNF secretion (Chen *et al*, 2006; Egan *et al.*, 2003). Indeed, the BNDF Val66Met polymorphism is generally linked to lower brain and hippocampal volumes and to worse cognitive performance in neurodegenerative disorders. However, the results of our and previous studies in MS contrast with these findings in neurodegenerative disorders, showing a protective role of the BNDF Val66Met polymorphism.

A first study by Liguori et al.(Liguori *et al.*, 2007) showed that the Met66 allele was associated with lower GM volume in a group of Italian RRMS patients. Conversely, in line with our findings, subsequent studies on larger cohorts of MS patients highlighted a protective effect of the BDNF Val66Met polymorphism on GM volume (Ramasamy *et al.*, 2011; Zivadinov *et al*, 2013). These results suggest an interplay between BDNF functioning and the inflammatory microenvironment. As a matter of fact, BDNF is also secreted by immune cells to promote neuronal and axonal survival or repair in the context of inflammation. In RRMS patients, higher levels of BDNF are secreted by lymphocytes during relapses (2.6-fold higher) and during the subsequent recovery phase (2-fold higher), compared with a stable remission period (Sarchielli *et al*, 2002). Moreover, the inflammatory microenvironment might exert epigenetic effects on BDNF secretion. Indeed, MS patients with a more severe inflammation showed de-methylation of its gene, leading to a higher secretion of BDNF (Nociti *et al*, 2018).

On the other hand, the increased secretion of BDNF in MS also is likely to have negative consequences. LTP induced by BDNF facilitates glutamatergic synaptic transmission (Black, 1999; Narisawa-Saito *et al*, 2002) and, hence, glutamate-excitotoxicity with loss of oligodendrocytes and neurons. Furthermore, the overproduction of BNDF might lead to a faster exploitation of brain reserve (for instance, in terms of progenitor cells and synapses), thus leading to a more severe brain damage over the long-term. Against this background, a reduced secretion of BDNF due to the presence of the Val66Met polymorphism may have a protective function in MS. An intriguing hypothesis is that chronically elevated levels of BDNF released by immune cells reduce the signal/noise ratio of neurally-secreted BDNF in MS, thus reducing activity-dependent function of BDNF. Another hypothesis suggests that BDNF Val66Met polymorphism, especially in inflammatory context, is likely to alter the proportions of the proapoptotic proBDNF and the antiapoptotic mature BDNF, enhancing the levels of the latter (Lee *et al*, 2001).

In line with the notion that Val66Met polymorphism only affects the BDNF activity-dependent pathways (Egan *et al.*, 2003), in our study we found higher volumes in Val66Met *vs* Val66Val patients in those hippocampal subfields where BDNF is most likely to exert its function (directly or indirectly), namely the GCL-DG, CA1 and CA3. In details, compared to HC, while Val66Met patients had reduced volume in the

previously mentioned subfields, Val66Val patients had reduced volume in CA3 only, supporting the hypothesis of a protective role of the BDNF Val66Met polymorphism on these subfields. Indeed, as previously specified, BDNF plays a major role in adult neurogenesis, which is typically localized in the GCL-DG. Furthermore, this region, together with CA1 and CA3, is part of the tri-synaptic loop (Hasselmo & McClelland, 1999; Naber *et al*, 2000), the main substrate of LTP, playing a fundamental role in learning and memory information.

The hippocampal tail and the presubiculum of hippocampal body are two well-connected areas of the hippocampus (especially with the prefrontal cortex), and also substrates of LTP. Although we did not find significant differences when comparing MS *vs* HC in left and right hippocampal tail volume, we observed that Val66Val – but not Val66Met – MS patients had reduced volume in this region, compared to HC. Moreover, we found higher volumes in Val66Met *vs* Val66Val patients in such regions, further suggesting a protective role of the BDNF Val66Met polymorphism on hippocampal subfields with high synaptic plasticity.

It is interesting to underscore the differential involvement of left and right hippocampi in our study, providing an *in-vivo* evidence of left–right asymmetry in synaptic function and MS-related damage (El-Gaby *et al*, 2015). We might speculate the higher plasticity of left hippocampus make it more vulnerable to glutamate-mediated excitotoxicity and remodeling phenomena secondary to disease-related damage. As converse, the right hippocampus harbors more stable synapses. Thus, it might be more likely to suffer from damage due to Wallerian degeneration, caused by axonal transection from WM lesions. In line with this hypothesis, we found a broader pattern of damage involving the left hippocampus in MS patients compared to HC, especially in areas with a high synaptic density. These results are in line with existing literature reporting a preferential left-sided lateralization of atrophy in MS (Prinster *et al*, 2006). Instead, in our study the right hippocampus showed a more selective involvement of the output component and areas involved in the amygdala–hippocampus interaction. In our patients, the connection to WM lesions was supported by the association of right presubiculum volume with brain T2 lesion burden.

In line with previous studies (Ramasamy *et al.*, 2011; Zivadinov *et al.*, 2007), we found significant associations between lower hippocampal subfield volume and worse

performance on specific neuropsychological tests in MS patients, thus pointing towards a protective role of the BDNF Val66Met polymorphism. We found a significant association between better visuospatial memory performance (SPART-D) and left hippocampal tail volume. Moreover, left hippocampal tail volume resulted as mediator of BDNF polymorphism effect on visuospatial memory performance. Although it is widely known that posterior hippocampal regions are related to visuospatial navigation (Burgess *et al*, 2002; Doeller *et al*, 2008; Maguire *et al*, 1998; Spiers *et al*, 2001; Wolbers *et al*, 2014), visuospatial performance is generally lateralized to the right. However, recent evidence reported bilateral hippocampal involvement in visuospatial memory, with complementary roles of left and right formations. In details, left hippocampus mediates spatiotemporal associations between the multiple elements of episodic memory (Eichenbaum, 2004; Spiers *et al.*, 2001) underlying the planning of complex routes in humans (Ghaem *et al*, 1997; Hartley *et al*, 2003). Moreover, fMRI studies reported left hippocampus activation when a novel sensory stimulus is spatially or temporally different from a previously encountered input (Kumaran & Maguire, 2007). As converse, right hippocampal activation was seen only in cases when there was a complete match between novel and previously encountered inputs (Kumaran & Maguire, 2007). Therefore, the left hippocampus might be preferentially involved in updating internal representations in response to changes in sensory experience, thus showing more intense brain plasticity phenomena.

In line with the localization of semantic processing in anterior hippocampal regions, we found significant associations between subfields belonging to left hippocampal head and semantic fluency performance on the WLG. In detail, the anterior hippocampus is involved in the integration of distinct informational elements around a central conceptual node, relating a set of ideas or experiences to a common theme, as it happens in autobiographical memory (Nielson *et al*, 2015; Zeidman *et al*, 2015). This anterior distribution for semantic retrieval is likely to be subserved by anterior hippocampus connections with anterior medial temporal lobes and anterior portion of lateral temporal lobes (Moscovitch *et al*, 2016; Persson *et al*, 2014; Suzuki & Amaral, 1994).

This study is not without limitations. The main limitation is the small numerosity of our cohort. Also, we could not obtain BDNF genotyping on HC. There were some sex-

related differences between study groups, which were accounted for by specific adjustment during statistical analysis. Only few patients had hippocampal lesions, so we could not consider hippocampal lesion load as a marker of damage. Finally, the cross-sectional study design did not allow us to assess whether the BDNF Val66Met polymorphism is actually neuroprotective, slowing down MS-related hippocampal atrophy. The alternative hypothesis is that Val66Met MS patients may start off with a greater hippocampal volume, thus masking – in a cross-sectional setting – a similar rate of hippocampal atrophy as Val66Val MS patients. We address to future longitudinal studies to resolve the matter.

In conclusion, by adopting an advanced MRI technique combined with genetic analysis, we suggest the BDNF Val66Met polymorphism might play a protective role in MS patients, limiting hippocampal damage and possibly preventing disease-related cognitive decline. This pilot study can pave the way to longitudinal studies on the effect of the BDNF Val66Met polymorphism in MS. In future, BDNF genotyping may prove to be helpful to predict patient long-term prognosis. The study of the molecular mechanisms underlying the protective effect of Val66Met polymorphism in MS might help individuate new targets for neuroprotective therapeutic strategies.

Table 7.2.1. *Main clinical, demographic and conventional MRI features of healthy controls and multiple sclerosis patients.*

	Healthy controls	**MS patients**	***p* values**	**BDNF Val66Val MS patients**	**BDNF Val66Met MS patients**	***p* values**
Number of participants	15	50	-	22	28	-
Mean age (SD) [years]	40.6 (9.9)	41.5 (10.8)	0.83	41.8 (10.6)	41.0 (9.4)	0.89
Female/Male	8/7	40/8	0.02	26/2	15/7	0.02
Median EDSS (IQR)	-	1.5 (1.0-2.5)	-	1.0 (1.0-2.5)	1.5 (1.0-3.0)	0.15
Phenotype (RRMS/PMS)	-	42/8	-	25/3	17/5	0.46
Mean PI (SD)	-	0.04 (0.12)	-	0.04 (0.13)	0.03 (0.11)	0.63
Median disease duration (IQR) [years]	-	10.2 (4.8-19.3)	-	9.1 (4.7-16.4)	15.4 (5.2-21.2)	0.33
Ongoing DMT (none/moderate/high efficacy) *	-	4/31/15	-	2/17/9	2/14/6	0.91
Median T2 LV (IQR) [mL]	-	2.2 (1.3-6.7)	-	1.8 (0.9-6.7)	2.4 (1.9-5.8)	0.43
Mean NBV (SD) [mL]	1456 (70)	1415 (71)	0.04	1428 (65)	1398 (76)	0.23
Mean NGMV (SD) [mL]	760 (48)	741 (45)	0.21	752 (40)	725 (48)	0.22
Mean NWMV (SD) [mL]	696 (30)	673 (35)	0.03	675.0 (33)	672.4 (38)	0.58
Mean normalized left hippocampal volume (SD) [mL]	2.5 (0.3)	2.4 (0.2)	0.08	2.4 (0.2)	2.5 (0.2)	0.01
Mean normalized right hippocampal (SD) [mL]	2.5 (0.3)	2.4 (0.2)	0.09	2.4 (0.2)	2.5 (0.2)	0.03

**moderate efficacy: any interferon-beta preparation, glatiramer acetate, teriflunomide, dymethilfumarte; high efficacy: fingolimod, natalizumab, ocrelizumab.*

Abbreviations: MS = multiple sclerosis; SD = standard deviation; EDSS = Expanded Disability Status Scale; PI=Progression Index; IQR = interquartile range; LV=lesion volumes; NBV = normalized brain volume; NGMV = normalized gray matter volume; NWMV = normalized white matter volume.

Table 7.2.2. *Neuropsychological variables, reported as z-scores, in the whole group of multiple sclerosis (MS) patients and in MS patients grouped according to the presence of brain derived neurotrophic factor (BDNF) Val66Met polymorphism.*

	All MS patients	**BDNF Val66Val MS patients**	**BDNF Val66Met MS patients**	***p* value***
Education [years]	13.0 (2.8)	13.8 (2.8)	12.1 (2.5)	0.14
FSS	4.0 (2.1)	3.8 (2.1)	4.2 (2.3)	0.75
MADRS	5.3 (3.7)	4.9 (2.2)	5.8 (5.1)	0.54
Verbal Learning				
SRT-LTS	-0.57 (0.84)	-0.69 (0.87)	-0.41 (0.82)	0.56
SRT-CLTR	-0.56 (0.79)	-0.46 (0.76)	-0.69 (0.83)	0.76
SRT-D	-0.19 (0.97)	-0.27 (1.03)	-0.09 (0.06)	0.74
Visuo-spatial Learning				
SPART	-0.46 (1.09)	-0.68 (1.09)	-0.17 (1.05)	0.26
SPART-D	-1.02 (0.96)	-1.52 (0.95)	-0.55 (0.78)	0.03
Attention and Information Processing speed				
SDMT	-0.27 (1.30)	-0.36 (1.53)	-0.16 (0.98)	0.91
PASAT3	-0.70 (1.37)	-0.77 (1.31)	-0.62 (1.48)	0.76
PASAT2	-0.82 (1.83)	-1.21 (2.08)	-0.30 (1.37)	0.13
Language				
WLG	-0.39 (0.76)	-0.35 (0.71)	-0.41 (0.85)	0.99
Executive functions				
SCWT	-0.33 (1.25)	-0.51 (0.82)	-0.12 (1.63)	0.42

**adjusted for disease duration and phenotype and false-discovery-rate corrected.*

Abbreviations: MS = multiple sclerosis; BDNF = brain derived neurotrophic factor; FSS = Fatigue Severity Scale; MADRS= Montgomery-Asberg Depression Scale; SRT=Selective Reminding Test; LTS = Long-Term Storage; CLTR = Consistent Long-Term Retrieval; D = delayed recall; SPART = Spatial Recall Test; PASAT = Paced Auditory Serial Addition Test; SDMT = Symbol Digit Modalities Test; WLG = Word List Generation; SCWT = Stroop Color Word Test.

Table 7.2.3. *Mean and standard deviations of left and right hippocampal subfield volumes are reported for multiple sclerosis (MS) patients and healthy controls as well as for MS patients grouped according to the presence of BDNF Val66Met polymorphism.*

Left Hippocampus	**HC**	**MS patients**	***p* value *vs* HC**	**BDNF Val66Val MS patients**	***p* value *vs* HC**	**BDNF Val66Met MS patients**	***p* value *vs* HC**	**Val66Met *vs* Val66Val *p* value**
Hippocampal tail [mL]	0.41 (0.07)	0.39 (0.05)	0.73	0.38 (0.04)	**0.05**	0.40 (0.05)	0.75	**0.03**
Subiculum body [mL]	0.17 (0.02)	0.17 (0.02)	0.96	0.17 (0.02)	0.82	0.16 (0.02)	0.88	0.35
CA1 body [mL]	0.10 (0.01)	0.09 (0.01)	0.24	0.09 (0.01)	0.12	0.10 (0.01)	0.46	**0.02**
Subiculum head [mL]	0.12 (0.02)	0.13 (0.01)	0.90	0.13 (0.01)	0.85	0.13 (0.01)	0.69	0.48
Presubiculum head [mL]	0.09 (0.01)	0.09 (0.01)	0.54	0.09 (0.01)	0.26	0.09 (0.01)	0.43	0.15
CA1 head [mL]	0.39 (0.06)	0.37 (0.04)	**0.04**	0.36 (0.04)	**0.04**	0.38 (0.04)	0.18	**0.01**
Presubiculum body [mL]	0.11 (0.02)	0.10 (0.02)	0.11	0.10 (0.02)	0.26	0.10 (0.01)	0.09	0.62
Parasubiculum [mL]	0.04 (0.01)	0.04 (0.01)	0.97	0.04 (0.01)	0.89	0.05 (0.01)	0.96	0.34
Molecular layer head [mL]	0.24 (0.04)	0.23 (0.02)	0.28	0.23 (0.02)	0.10	0.24 (0.02)	0.29	**0.01**
Molecular layer body [mL]	0.17 (0.02)	0.16 (0.02)	**0.05**	0.16 (0.02)	**0.05**	0.17 (0.02)	0.27	**0.01**
Granule cell layer of DG head [mL]	0.12 (0.02)	0.11 (0.01)	**0.04**	0.11 (0.01)	**0.04**	0.12 (0.02)	0.13	**0.02**
CA3 body [mL]	0.07 (0.01)	0.07 (0.01)	0.70	0.07 (0.01)	0.20	0.08 (0.01)	0.76	**0.01**
Granule cell layer of DG body [mL]	0.10 (0.01)	0.10 (0.01)	0.72	0.10 (0.01)	0.38	0.10 (0.01)	0.91	0.15
CA4 head [mL]	0.10 (0.01)	0.09 (0.01)	**0.05**	0.09 (0.01)	**0.05**	0.10 (0.01)	0.23	**0.01**

CA4 body [mL]	0.09 (0.01)	0.09 (0.01)	0.95	0.09 (0.01)	0.52	0.09 (0.01)	0.68	0.13
Fimbria [mL]	0.05 (0.01)	0.05 (0.01)	0.43	0.05 (0.01)	0.14	0.05 (0.01)	0.15	0.34
CA3 head [mL]	0.10 (0.02)	0.09 (0.01)	**0.05**	0.09 (0.01)	**0.01**	0.10 (0.01)	**0.04**	**0.02**
HATA [mL]	0.05 (0.01)	0.04 (0.01)	**0.04**	0.04 (0.01)	**0.01**	0.05 (0.01)	**0.02**	**0.01**
Right Hippocampus	**HC**	**MS patients**	***p* value *vs* HC**	**BDNF Val66Val MS patients**	***p* value *vs* HC**	**BDNF Val66Met MS patients**	***p* value *vs* HC**	**Val66Met *vs* Val66Val *p* value**
Hippocampal tail [mL]	0.42 (0.07)	0.39 (0.04)	0.24	0.38 (0.04)	**0.05**	0.40 (0.04)	0.15	**0.01**
Subiculum body [mL]	0.17 (0.02)	0.17 (0.02)	0.89	0.17 (0.02)	0.54	0.17 (0.02)	0.93	0.35
CA1 body [mL]	0.10 (0.01)	0.10 (0.01)	0.87	0.10 (0.02)	0.46	0.10 (0.01)	0.81	0.54
Subiculum head [mL]	0.13 (0.02)	0.13 (0.02)	0.96	0.13 (0.02)	0.76	0.13 (0.01)	0.80	0.34
Presubiculum head [mL]	0.09 (0.01)	0.09 (0.01)	0.55	0.09 (0.01)	0.28	0.09 (0.01)	0.67	**0.05**
CA1 head [mL]	0.37 (0.06)	0.35 (0.03)	0.43	0.35 (0.03)	0.21	0.36 (0.03)	0.36	0.20
Presubiculum body [mL]	0.11 (0.02)	0.10 (0.02)	**0.05**	0.10 (0.02)	**0.02**	0.10 (0.02)	**0.01**	0.72
Parasubiculum [mL]	0.04 (0.01)	0.04 (0.01)	0.75	0.04 (0.01)	0.72	0.05 (0.01)	0.41	0.37
Molecular layer head [mL]	0.24 (0.03)	0.23 (0.02)	0.60	0.23 (0.02)	0.36	0.23 (0.02)	0.62	0.15
Molecular layer body [mL]	0.17 (0.03)	0.16 (0.02)	0.43	0.16 (0.02)	0.19	0.16 (0.02)	0.33	0.41
Granule cell layer of DG head [mL]	0.11 (0.02)	0.11 (0.01)	0.55	0.11 (0.01)	0.11	0.11 (0.01)	0.46	0.30
CA3 body [mL]	0.07 (0.01)	0.07 (0.01)	0.95	0.07 (0.01)	0.44	0.07 (0.01)	0.54	0.20

Granule cell layer of DG body [mL]	0.10 (0.02)	0.10 (0.01)	0.73	0.10 (0.01)	0.16	0.10 (0.01)	0.77	0.41
CA4 head [mL]	0.09 (0.02)	0.09 (0.01)	0.69	0.09 (0.01)	0.16	0.09 (0.01)	0.64	0.23
CA4 body [mL]	0.09 (0.01)	0.09 (0.01)	0.96	0.09 (0.01)	0.30	0.09 (0.01)	0.86	0.41
Fimbria [mL]	0.06 (0.01)	0.05 (0.01)	**0.03**	0.05 (0.01)	**0.05**	0.05 (0.01)	0.13	0.41
CA3 head [mL]	0.09 (0.02)	0.09 (0.01)	0.47	0.09 (0.01)	**0.05**	0.09 (0.01)	0.33	0.41
HATA [mL]	0.05 (0.01)	0.04 (0.01)	**0.04**	0.04 (0.01)	**0.01**	0.04 (0.01)	**0.01**	0.94

Abbreviations: BDNF=brain derived neurotrophic factor; HC=healthy controls; MS=multiple sclerosis; CA=cornus ammonis; DG= dentate gyrus; HATA=hippocampus amygdala transitional area.

Table 7.2.4. *Results of age-, sex-, phenotype- and disease duration-adjusted linear regression models for the effect of hippocampal subfields on neuropsychological variables.*

	Hippocampal subfield	**β**	**95% CI**	***p values***
SPART-D	Left hippocampal tail	0.39	0.38, 0.40	0.04
WLG	Left granule cell layer of DG	0.39	0.37, 0.41	0.04
	Left CA4 head	0.43	0.41, 0.46	0.02
	Left CA3 head	0.40	0.38, 0.42	0.04

Abbreviations: CI= confidence interval; DG= dentate gyrus; CA= cornus ammonis; SPART-D = Spatial Recall Test delayed recall; WLG = Word List Generation.

Figure 7.2.1. Graphical representation of hippocampal subfields segmentation.

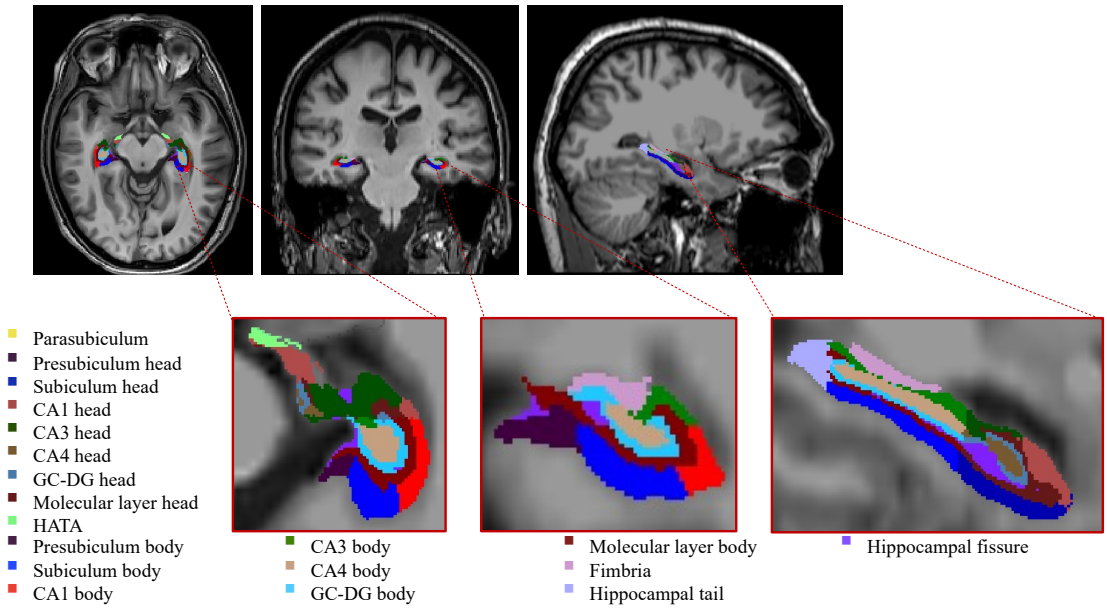

Axial, coronal and sagittal views of hippocampal subfields obtained in a healthy subject enrolled in the study. Hippocampal subfields are overlaid on the corresponding T1-weighted image by using FreeView visualization tool (https://surfer.nmr.mgh.harvard.edu/fswiki/FreeviewGuide/(De Meo et al., 2021d)). Abbreviations: CA=cornus ammonis; GC-DG=granule cell layer of dentate gyrus; HATA=hippocampus-amygdala transitional area.

8. References

Abelev B, Adam J, Adamova D, Aggarwal MM, Aglieri Rinella G, Agnello M, Agostinelli A, Agrawal N, Ahammed Z, Ahmad N *et al* (2014) Exclusive J/psi photoproduction off protons in ultraperipheral p-Pb collisions at radical(s(NN))=5.02 TeV. *Phys Rev Lett* 113: 232504

Absinta M, Rocca MA, Moiola L, Copetti M, Milani N, Falini A, Comi G, Filippi M (2011) Cortical lesions in children with multiple sclerosis. *Neurology* 76: 910-913

Absinta M, Rocca MA, Moiola L, Ghezzi A, Milani N, Veggiotti P, Comi G, Filippi M (2010) Brain macro- and microscopic damage in patients with paediatric MS. *J Neurol Neurosurg Psychiatry* 81: 1357-1362

Absoud M, Cummins C, Desai N, Gika A, McSweeney N, Munot P, Hemingway C, Lim M, Nischal KK, Wassmer E (2011) Childhood optic neuritis clinical features and outcome. *Arch Dis Child* 96: 860-862

Akbar N, Banwell B, Sled JG, Binns MA, Doesburg SM, Rypma B, Lysenko M, Till C (2016a) Brain activation patterns and cognitive processing speed in patients with pediatric-onset multiple sclerosis. *Journal of clinical and experimental neuropsychology* 38: 393-403

Akbar N, Giorgio A, Till C, Sled JG, Doesburg SM, De Stefano N, Banwell B (2016b) Alterations in Functional and Structural Connectivity in Pediatric-Onset Multiple Sclerosis. *PloS one* 11: e0145906

Akbar N, Till C, Sled JG, Binns MA, Doesburg SM, Aubert-Broche B, Collins DL, Araujo D, Narayanan S, Arnold DL *et al* (2016c) Altered resting-state functional connectivity in cognitively preserved pediatric-onset MS patients and relationship to structural damage and cognitive performance. *Multiple Sclerosis Journal* 22: 792-800

Aktas O, Hartung HP (2019) CSI: Multiple sclerosis. Tracing optic nerve involvement by standardized optical coherence tomography. *Ann Neurol* 85: 615-617

Alroughani R, Das R, Penner N, Pultz J, Taylor C, Eraly S (2018) Safety and Efficacy of Delayed-Release Dimethyl Fumarate in Pediatric Patients With Relapsing Multiple Sclerosis (FOCUS). *Pediatr Neurol* 83: 19-24

Alroughani R, Huppke P, Mazurkiewicz-Beldzinska M, Blaschek A, Valis M, Aaen G, Pultz J, Peng X, Beynon V (2021) Delayed-Release Dimethyl Fumarate Safety and Efficacy in Pediatric Patients With Relapsing-Remitting Multiple Sclerosis. *Frontiers in Neurology* 11: 1731

Amato MP (2018) A decline in cognitive function should lead to a change in disease-modifying therapy - Commentary. *Mult Scler* 24: 1685-1686

Amato MP, Bartolozzi ML, Zipoli V, Portaccio E, Mortilla M, Guidi L, Siracusa G, Sorbi S, Federico A, De Stefano N (2004) Neocortical volume decrease in relapsing-remitting MS patients with mild cognitive impairment. *Neurology* 63: 89-93

Amato MP, Goretti B, Ghezzi A, Hakiki B, Niccolai C, Lori S, Moiola L, Falautano M, Viterbo RG, Patti F *et al* (2014a) Neuropsychological features in childhood and juvenile multiple sclerosis: five-year follow-up. *Neurology* 83: 1432-1438

Amato MP, Goretti B, Ghezzi A, Lori S, Zipoli V, Moiola L, Falautano M, De Caro MF, Viterbo R, Patti F *et al* (2010) Cognitive and psychosocial features in childhood and juvenile MS: two-year follow-up. *Neurology* 75: 1134-1140

Amato MP, Goretti B, Ghezzi A, Lori S, Zipoli V, Portaccio E, Moiola L, Falautano M, De Caro MF, Lopez M *et al* (2008) Cognitive and psychosocial features of childhood and juvenile MS. *Neurology* 70: 1891-1897

Amato MP, Goretti B, Viterbo RG, Portaccio E, Niccolai C, Hakiki B, Iaffaldano P, Trojano M (2014b) Computer-assisted rehabilitation of attention in patients with multiple sclerosis: results of a randomized, double-blind trial. *Mult Scler* 20: 91-98

Amato MP, Krupp LB (2020) Disease-modifying therapy aids cognition in multiple sclerosis. *Nat Rev Neurol*

Amato MP, Krupp LB, Charvet LE, Penner I, Till C (2016) Pediatric multiple sclerosis: Cognition and mood. *Neurology* 87: S82-87

Amato MP, Portaccio E, Goretti B, Zipoli V, Ricchiuti L, De Caro MF, Patti F, Vecchio R, Sorbi S, Trojano M (2006) The Rao's Brief Repeatable Battery and Stroop Test: normative values with age, education and gender corrections in an Italian population. *Mult Scler* 12: 787-793

Arnett PA, Higginson CI, Randolph JJ (2001) Depression in multiple sclerosis: relationship to planning ability. *J Int Neuropsychol Soc* 7: 665-674

Arnett PA, Higginson CI, Voss WD, Bender WI, Wurst JM, Tippin JM (1999) Depression in multiple sclerosis: relationship to working memory capacity. *Neuropsychology* 13: 546-556

Arnett PA, Rao SM, Bernardin L, Grafman J, Yetkin FZ, Lobeck L (1994) Relationship between frontal lobe lesions and Wisconsin Card Sorting Test performance in patients with multiple sclerosis. *Neurology* 44: 420-425

Arnold DL, Matthews PM, Francis GS, O'Connor J, Antel JP (1992) Proton magnetic resonance spectroscopic imaging for metabolic characterization of demyelinating plaques. *Annals of Neurology* 31: 235-241

Aron AR, Behrens TE, Smith S, Frank MJ, Poldrack RA (2007) Triangulating a cognitive control network using diffusion-weighted magnetic resonance imaging (MRI) and functional MRI. *J Neurosci* 27: 3743-3752

Arrambide G, Rovira A, Sastre-Garriga J, Tur C, Castilló J, Río J, Vidal-Jordana A, Galán I, Rodríguez-Acevedo B, Midaglia L *et al* (2018) Spinal cord lesions: A modest contributor to diagnosis in clinically isolated syndromes but a relevant prognostic factor. *Mult Scler* 24: 301-312

Ashburner J (2007) A fast diffeomorphic image registration algorithm. *Neuroimage* 38: 95-113

Ashburner J, Friston KJ (2005) Unified segmentation. *Neuroimage* 26: 839-851

Ashburner J, Ridgway GR (2012) Symmetric diffeomorphic modeling of longitudinal structural MRI. *Front Neurosci* 6: 197

Aubert-Broche B, Fonov V, Ghassemi R, Narayanan S, Arnold DL, Banwell B, Sled JG, Collins DL (2011) Regional brain atrophy in children with multiple sclerosis. *Neuroimage* 58: 409-415

Aubert-Broche B, Fonov V, Narayanan S, Arnold DL, Araujo D, Fetco D, Till C, Sled JG, Banwell B, Collins DL *et al* (2014a) Onset of multiple sclerosis before adulthood leads to failure of age-expected brain growth. *Neurology* 83: 2140-2146

Aubert-Broche B, Fonov V, Narayanan S, Arnold DL, Araujo D, Fetco D, Till C, Sled JG, Banwell B, Collins DL *et al* (2014b) Onset of multiple sclerosis before adulthood leads to failure of age-expected brain growth. *Neurology* 83: 2140-2146

Aubert-Broche B, Weier K, Longoni G, Fonov VS, Bar-Or A, Marrie RA, Yeh EA, Narayanan S, Arnold DL, Verhey LH *et al* (2017) Monophasic demyelination reduces brain growth in children. *Neurology* 88: 1744-1750

Azevedo CJ, Cen SY, Khadka S, Liu S, Kornak J, Shi Y, Zheng L, Hauser SL, Pelletier D (2018) Thalamic atrophy in multiple sclerosis: A magnetic resonance imaging marker of neurodegeneration throughout disease. *Ann Neurol* 83: 223-234

Bagnoli S, Nacmias B, Tedde A, Guarnieri BM, Cellini E, Petruzzi C, Bartoli A, Ortenzi L, Sorbi S (2004) Brain-derived neurotrophic factor genetic variants are not susceptibility factors to Alzheimer's disease in Italy. *Ann Neurol* 55: 447-448

Balint B, Haas J, Schwarz A, Jarius S, Furwentsches A, Engelhardt K, Bussmann C, Ebinger F, Fritzsching B, Paul F *et al* (2013) T-cell homeostasis in pediatric multiple sclerosis: old cells in young patients. *Neurology* 81: 784-792

Banwell B, Arnold DL, Tillema JM, Rocca MA, Filippi M, Weinstock-Guttman B, Zivadinov R, Sormani MP (2016) MRI in the evaluation of pediatric multiple sclerosis. *Neurology* 87: S88-96

Banwell B, Bar-Or A, Arnold DL, Sadovnick D, Narayanan S, McGowan M, O'Mahony J, Magalhaes S, Hanwell H, Vieth R *et al* (2011) Clinical, environmental, and genetic determinants of multiple sclerosis in children with acute demyelination: a prospective national cohort study. *The Lancet Neurology* 10: 436-445

Banwell B, Ghezzi A, Bar-Or A, Mikaeloff Y, Tardieu M (2007a) Multiple sclerosis in children: clinical diagnosis, therapeutic strategies, and future directions. *Lancet neurology* 6: 887-902

Banwell B, Kennedy J, Sadovnick D, Arnold DL, Magalhaes S, Wambera K, Connolly MB, Yager J, Mah JK, Shah N *et al* (2009) Incidence of acquired demyelination of the CNS in Canadian children. *Neurology* 72: 232-239

Banwell B, Krupp L, Kennedy J, Tellier R, Tenembaum S, Ness J, Belman A, Boiko A, Bykova O, Waubant E *et al* (2007b) Clinical features and viral serologies in children with multiple sclerosis: a multinational observational study. *Lancet Neurol* 6: 773-781

Banwell B, Reder AT, Krupp L, Tenembaum S, Eraksoy M, Alexey B, Pohl D, Freedman M, Schelensky L, Antonijevic I (2006) Safety and tolerability of interferon beta-1b in pediatric multiple sclerosis. *Neurology* 66: 472-476

Banwell B, Shroff M, Ness JM, Jeffery D, Schwid S, Weinstock-Guttman B, International Pediatric MSSG (2007c) MRI features of pediatric multiple sclerosis. *Neurology* 68: S46-53

Banwell BL (2013) Pediatric multiple sclerosis. *Handb Clin Neurol* 112: 1263-1274

Bar-Or A (2008) The immunology of multiple sclerosis. *Semin Neurol* 28: 29-45

Bar-Or A, Hintzen RQ, Dale RC, Rostasy K, Brück W, Chitnis T (2016) Immunopathophysiology of pediatric CNS inflammatory demyelinating diseases. *Neurology* 87: S12

Barkhof F, Filippi M, Miller DH, Scheltens P, Campi A, Polman CH, Comi G, Ader HJ, Losseff N, Valk J (1997) Comparison of MRI criteria at first presentation to predict

conversion to clinically definite multiple sclerosis. *Brain : a journal of neurology* 120 (Pt 11): 2059-2069

Barlow-Krelina E, Turner GR, Akbar N, Banwell B, Lysenko M, Yeh EA, Narayanan S, Collins DL, Aubert-Broche B, Till C (2019) Enhanced Recruitment During Executive Control Processing in Cognitively Preserved Patients With Pediatric-Onset MS. *J Int Neuropsychol Soc* 25: 432-442

Baroncini D, Simone M, Iaffaldano P, Brescia Morra V, Lanzillo R, Filippi M, Romeo M, Patti F, Chisari CG, Cocco E *et al* (2021) Risk of Persistent Disability in Patients With Pediatric-Onset Multiple Sclerosis. *JAMA Neurol*

Barraza G, Deiva K, Husson B, Adamsbaum C (2021) Imaging in Pediatric Multiple Sclerosis : An Iconographic Review. *Clin Neuroradiol* 31: 61-71

Basser PJ, Mattiello J, LeBihan D (1994) MR diffusion tensor spectroscopy and imaging. *Biophys J* 66: 259-267

Beatty WW (2004) RBANS analysis of verbal memory in multiple sclerosis. *Arch Clin Neuropsychol* 19: 825-834

Ben Sira L, Miller E, Artzi M, Fattal-Valevski A, Constantini S, Ben Bashat D (2010) 1H-MRS for the diagnosis of acute disseminated encephalomyelitis: insight into the acute-disease stage. *Pediatric radiology* 40: 106-113

Benedict RH, Bruce JM, Dwyer MG, Abdelrahman N, Hussein S, Weinstock-Guttman B, Garg N, Munschauer F, Zivadinov R (2006) Neocortical atrophy, third ventricular width, and cognitive dysfunction in multiple sclerosis. *Arch Neurol* 63: 1301-1306

Benedict RH, Hulst HE, Bergsland N, Schoonheim MM, Dwyer MG, Weinstock-Guttman B, Geurts JJ, Zivadinov R (2013) Clinical significance of atrophy and white matter mean diffusivity within the thalamus of multiple sclerosis patients. *Mult Scler* 19: 1478-1484

Benedict RHB, Amato MP, DeLuca J, Geurts JJG (2020) Cognitive impairment in multiple sclerosis: clinical management, MRI, and therapeutic avenues. *The Lancet Neurology* 19: 860-871

Benson LA, Healy BC, Gorman MP, Baruch NF, Gholipour T, Musallam A, Chitnis T (2014) Elevated relapse rates in pediatric compared to adult MS persist for at least 6 years. *Mult Scler Relat Disord* 3: 186-193

Beres SJ, Graves J, Waubant E (2014) Rituximab Use in Pediatric Central Demyelinating Disease. *Pediatr Neurol*

Bergamaschi R, Rezzani C, Minguzzi S, Amato MP, Patti F, Marrosu MG, Bonavita S, Grasso MG, Ghezzi A, Rottoli M *et al* (2009) Validation of the DYMUS questionnaire for the assessment of dysphagia in multiple sclerosis. *Functional neurology* 24: 159-162

Bergsland N, Schweser F, Dwyer MG, Weinstock-Guttman B, Benedict RHB, Zivadinov R (2018) Thalamic white matter in multiple sclerosis: A combined diffusion-tensor imaging and quantitative susceptibility mapping study. *Hum Brain Mapp* 39: 4007-4017

Berlin KS, Williams NA, Parra GR (2014) An Introduction to Latent Variable Mixture Modeling (Part 1): Overview and Cross-Sectional Latent Class and Latent Profile Analyses. *Journal of Pediatric Psychology* 39: 174-187

Bigi S, Banwell B, Yeh EA (2014) Outcomes After Early Administration of Plasma Exchange in Pediatric Central Nervous System Inflammatory Demyelination. *Journal of Child Neurology* 30: 874-880

Bimonte-Nelson HA, Hunter CL, Nelson ME, Granholm AC (2003) Frontal cortex BDNF levels correlate with working memory in an animal model of Down syndrome. *Behav Brain Res* 139: 47-57

Bisecco A, Rocca MA, Pagani E, Mancini L, Enzinger C, Gallo A, Vrenken H, Stromillo ML, Copetti M, Thomas DL *et al* (2015) Connectivity-based parcellation of the thalamus in multiple sclerosis and its implications for cognitive impairment: A multicenter study. *Hum Brain Mapp* 36: 2809-2825

Black IB (1999) Trophic regulation of synaptic plasticity. *J Neurobiol* 41: 108-118

Blanken AE, Jang JY, Ho JK, Edmonds EC, Han SD, Bangen KJ, Nation DA (2020) Distilling Heterogeneity of Mild Cognitive Impairment in the National Alzheimer Coordinating Center Database Using Latent Profile Analysis. *JAMA Netw Open* 3: e200413

Bo L, Geurts JJ, van der Valk P, Polman C, Barkhof F (2007) Lack of correlation between cortical demyelination and white matter pathologic changes in multiple sclerosis. *Arch Neurol* 64: 76-80

Boiko A, Vorobeychik G, Paty D, Devonshire V, Sadovnick D, University of British Columbia MSCN (2002) Early onset multiple sclerosis: a longitudinal study. *Neurology* 59: 1006-1010

Bonavita S, Gallo A, Sacco R, Corte MD, Bisecco A, Docimo R, Lavorgna L, Corbo D, Costanzo AD, Tortora F *et al* (2011) Distributed changes in default-mode resting-state connectivity in multiple sclerosis. *Mult Scler* 17: 411-422

Bonnelle V, Ham TE, Leech R, Kinnunen KM, Mehta MA, Greenwood RJ, Sharp DJ (2012) Salience network integrity predicts default mode network function after traumatic brain injury. *Proceedings of the National Academy of Sciences of the United States of America* 109: 4690-4695

Bove R, Chitnis T (2014) The role of gender and sex hormones in determining the onset and outcome of multiple sclerosis. *Multiple Sclerosis Journal* 20: 520-526

Brex PA, Ciccarelli O, O'Riordan JI, Sailer M, Thompson AJ, Miller DH (2002) A longitudinal study of abnormalities on MRI and disability from multiple sclerosis. *The New England journal of medicine* 346: 158-164

Brown JW, Pardini M, Brownlee WJ, Fernando K, Samson RS, Prados Carrasco F, Ourselin S, Gandini Wheeler-Kingshott CA, Miller DH, Chard DT (2017) An abnormal periventricular magnetization transfer ratio gradient occurs early in multiple sclerosis. *Brain* 140: 387-398

Brown RA, Narayanan S, Arnold DL (2014) Imaging of repeated episodes of demyelination and remyelination in multiple sclerosis. *Neuroimage Clin* 6: 20-25

Brownlee WJ, Altmann DR, Alves Da Mota P, Swanton JK, Miszkiel KA, Wheeler-Kingshott CG, Ciccarelli O, Miller DH (2017) Association of asymptomatic spinal cord lesions and atrophy with disability 5 years after a clinically isolated syndrome. *Mult Scler* 23: 665-674

Brownlee WJ, Altmann DR, Prados F, Miszkiel KA, Eshaghi A, Gandini Wheeler-Kingshott CAM, Barkhof F, Ciccarelli O (2019) Early imaging predictors of long-term outcomes in relapse-onset multiple sclerosis. *Brain : a journal of neurology* 142: 2276-2287

Bruhn H, Frahm J, Merboldt KD, Hanicke W, Hanefeld F, Christen HJ, Kruse B, Bauer HJ (1992a) Multiple sclerosis in children: cerebral metabolic alterations monitored by localized proton magnetic resonance spectroscopy in vivo. *Annals of neurology* 32: 140-150

Bruhn H, Frahm J, Merboldt KD, Hanicke W, Hanefeld F, Christen HJ, Kruse B, Bauer HJ (1992b) Multiple sclerosis in children: Cerebral metabolic alterations monitored by localized proton magnetic resonance spectroscopy in vivo. *Annals of Neurology* 32: 140-150

Burgess N, Maguire EA, O'Keefe J (2002) The Human Hippocampus and Spatial and Episodic Memory. *Neuron* 35: 625-641

Cacciaguerra L, Pagani E, Mesaros S, Dackovic J, Dujmovic-Basuroski I, Drulovic J, Valsasina P, Filippi M, Rocca MA (2019) Dynamic volumetric changes of hippocampal subfields in clinically isolated syndrome patients: A 2-year MRI study. *Mult Scler* 25: 1232-1242

Calabrese M, Agosta F, Rinaldi F, Mattisi I, Grossi P, Favaretto A, Atzori M, Bernardi V, Barachino L, Rinaldi L *et al* (2009) Cortical lesions and atrophy associated with cognitive impairment in relapsing-remitting multiple sclerosis. *Arch Neurol* 66: 1144-1150

Calabrese M, Seppi D, Romualdi C, Rinaldi F, Alessio S, Perini P, Gallo P (2012) Gray Matter Pathology in MS: A 3-Year Longitudinal Study in a Pediatric Population. *American Journal of Neuroradiology* 33: 1507-1511

Callen DJ, Shroff MM, Branson HM, Li DK, Lotze T, Stephens D, Banwell BL (2009) Role of MRI in the differentiation of ADEM from MS in children. *Neurology* 72: 968-973

Camp SJ, Stevenson VL, Thompson AJ, Ingle GT, Miller DH, Borras C, Brochet B, Dousset V, Falautano M, Filippi M *et al* (2005) A longitudinal study of cognition in primary progressive multiple sclerosis. *Brain* 128: 2891-2898

Cappellani R, Bergsland N, Weinstock-Guttman B, Kennedy C, Carl E, Ramasamy DP, Hagemeier J, Dwyer MG, Patti F, Zivadinov R (2014) Diffusion tensor MRI alterations of subcortical deep gray matter in clinically isolated syndrome. *J Neurol Sci* 338: 128-134

Caramanos Z, DiMaio S, Narayanan S, Lapierre Y, Arnold DL (2009) (1)H-MRSI evidence for cortical gray matter pathology that is independent of cerebral white matter lesion load in patients with secondary progressive multiple sclerosis. *Journal of the neurological sciences* 282: 72-79

Catheline G, Amieva H, Dilharreguy B, Bernard C, Duperron MG, Helmer C, Dartigues JF, Allard M (2015) Semantic retrieval over time in the aging brain: Structural evidence of hippocampal contribution. *Hippocampus* 25: 1008-1016

Cavanna AE, Trimble MR (2006) The precuneus: a review of its functional anatomy and behavioural correlates. *Brain* 129: 564-583

Ceccarelli A, Rocca MA, Pagani E, Colombo B, Martinelli V, Comi G, Filippi M (2008) A voxel-based morphometry study of grey matter loss in MS patients with different clinical phenotypes. *Neuroimage* 42: 315-322

Ceccarelli A, Rocca MA, Perego E, Moiola L, Ghezzi A, Martinelli V, Comi G, Filippi M (2011) Deep grey matter T2 hypo-intensity in patients with paediatric multiple sclerosis. *Mult Scler* 17: 702-707

Chabas D, Castillo-Trivino T, Mowry EM, Strober JB, Glenn OA, Waubant E (2008) Vanishing MS T2-bright lesions before puberty: a distinct MRI phenotype? *Neurology* 71: 1090-1093

Chabas D, Ness J, Belman A, Yeh EA, Kuntz N, Gorman MP, Strober JB, De Kouchkovsky I, McCulloch C, Chitnis T *et al* (2010) Younger children with MS have a distinct CSF inflammatory profile at disease onset. *Neurology* 74: 399-405

Chard DT, Jackson JS, Miller DH, Wheeler-Kingshott CA (2010) Reducing the impact of white matter lesions on automated measures of brain gray and white matter volumes. *Journal of magnetic resonance imaging : JMRI* 32: 223-228

Charvet LE, O'Donnell EH, Belman AL, Chitnis T, Ness JM, Parrish J, Patterson M, Rodriguez M, Waubant E, Weinstock-Guttman B *et al* (2014) Longitudinal evaluation of cognitive functioning in pediatric multiple sclerosis: report from the US Pediatric Multiple Sclerosis Network. *Mult Scler* 20: 1502-1510

Charvet LE, Yang J, Shaw MT, Sherman K, Haider L, Xu J, Krupp LB (2017) Cognitive function in multiple sclerosis improves with telerehabilitation: Results from a randomized controlled trial. *PLoS One* 12: e0177177

Chen CH, Fiecas M, Gutierrez ED, Panizzon MS, Eyler LT, Vuoksimaa E, Thompson WK, Fennema-Notestine C, Hagler DJ, Jr., Jernigan TL *et al* (2013) Genetic topography of brain morphology. *Proc Natl Acad Sci U S A* 110: 17089-17094

Chen T, Cai W, Ryali S, Supekar K, Menon V (2016) Distinct Global Brain Dynamics and Spatiotemporal Organization of the Salience Network. *PLoS Biol* 14: e1002469

Chen ZY, Jing D, Bath KG, Ieraci A, Khan T, Siao CJ, Herrera DG, Toth M, Yang C, McEwen BS *et al* (2006) Genetic variant BDNF (Val66Met) polymorphism alters anxiety-related behavior. *Science* 314: 140-143

Chen ZY, Patel PD, Sant G, Meng CX, Teng KK, Hempstead BL, Lee FS (2004) Variant brain-derived neurotrophic factor (BDNF) (Met66) alters the intracellular trafficking and activity-dependent secretion of wild-type BDNF in neurosecretory cells and cortical neurons. *J Neurosci* 24: 4401-4411

Chenevert TL, Malyarenko DI, Newitt D, Li X, Jayatilake M, Tudorica A, Fedorov A, Kikinis R, Liu TT, Muzi M *et al* (2014) Errors in Quantitative Image Analysis due to Platform-Dependent Image Scaling. *Transl Oncol* 7: 65-71

Chenn A, Walsh CA (2002) Regulation of cerebral cortical size by control of cell cycle exit in neural precursors. *Science* 297: 365-369

Chiaravalloti ND, DeLuca J (2008) Cognitive impairment in multiple sclerosis. *Lancet Neurol* 7: 1139-1151

Chiaravalloti ND, Moore NB, DeLuca J (2020) The efficacy of the modified Story Memory Technique in progressive MS. *Mult Scler* 26: 354-362

Chitnis T (2007) The role of CD4 T cells in the pathogenesis of multiple sclerosis. *Int Rev Neurobiol* 79: 43-72

Chitnis T (2013) Role of puberty in multiple sclerosis risk and course. *Clinical Immunology* 149: 192-200

Chitnis T, Aaen G, Belman A, Benson L, Gorman M, Goyal MS, Graves JS, Harris Y, Krupp L, Lotze T *et al* (2020) Improved relapse recovery in paediatric compared to adult multiple sclerosis. *Brain* 143: 2733-2741

Chitnis T, Arnold DL, Banwell B, Brück W, Ghezzi A, Giovannoni G, Greenberg B, Krupp L, Rostásy K, Tardieu M *et al* (2018) Trial of Fingolimod versus Interferon Beta-1a in Pediatric Multiple Sclerosis. *N Engl J Med* 379: 1017-1027

Chitnis T, Banwell B, Krupp L, Arnold DL, Bar-Or A, Brück W, Giovannoni G, Greenberg B, Ghezzi A, Waubant E *et al* (2021) Temporal profile of lymphocyte counts and relationship with infections with fingolimod therapy in paediatric patients with multiple sclerosis: Results from the PARADIGMS study. *Mult Scler* 27: 922-932

Chitnis T, Ghezzi A, Bajer-Kornek B, Boyko A, Giovannoni G, Pohl D (2016) Pediatric multiple sclerosis: Escalation and emerging treatments. *Neurology* 87: S103-109

Chitnis T, Glanz B, Jaffin S, Healy B (2009) Demographics of pediatric-onset multiple sclerosis in an MS center population from the Northeastern United States. *Mult Scler* 15: 627-631

Chitnis T, Krupp L, Yeh A, Rubin J, Kuntz N, Strober JB, Chabas D, Weinstock-Guttmann B, Ness J, Rodriguez M *et al* (2011) Pediatric Multiple Sclerosis. *Neurologic Clinics* 29: 481-505

Chitnis T, Tenembaum S, Banwell B, Krupp L, Pohl D, Rostasy K, Yeh EA, Bykova O, Wassmer E, Tardieu M *et al* (2012) Consensus statement: evaluation of new and existing therapeutics for pediatric multiple sclerosis. *Mult Scler* 18: 116-127

Ciccarelli O, Werring DJ, Wheeler-Kingshott CA, Barker GJ, Parker GJ, Thompson AJ, Miller DH (2001) Investigation of MS normal-appearing brain using diffusion tensor MRI with clinical correlations. *Neurology* 56: 926-933

Cirillo S, Rocca MA, Ghezzi A, Valsasina P, Moiola L, Veggiotti P, Amato MP, Comi G, Falini A, Filippi M (2015) Abnormal cerebellar functional MRI connectivity in patients with paediatric multiple sclerosis. *Multiple Sclerosis Journal* 22: 292-301

Cohen JA, Coles AJ, Arnold DL, Confavreux C, Fox EJ, Hartung HP, Havrdova E, Selmaj KW, Weiner HL, Fisher E *et al* (2012) Alemtuzumab versus interferon beta 1a as first-line treatment for patients with relapsing-remitting multiple sclerosis: a randomised controlled phase 3 trial. *Lancet* 380: 1819-1828

Coles AJ, Twyman CL, Arnold DL, Cohen JA, Confavreux C, Fox EJ, Hartung HP, Havrdova E, Selmaj KW, Weiner HL *et al* (2012) Alemtuzumab for patients with relapsing multiple sclerosis after disease-modifying therapy: a randomised controlled phase 3 trial. *Lancet* 380: 1829-1839

Comi G, Martinelli V, Medaglini S, Locatelli T, Filippi M, Canal N, Triulzi F, DelMaschio A (1989) Correlation between multimodal evoked potentials and magnetic resonance imaging in multiple sclerosis. *Journal of Neurology* 236: 4-8

Confavreux C, O'Connor P, Comi G, Freedman MS, Miller AE, Olsson TP, Wolinsky JS, Bagulho T, Delhay JL, Dukovic D *et al* (2014) Oral teriflunomide for patients with

relapsing multiple sclerosis (TOWER): a randomised, double-blind, placebo-controlled, phase 3 trial. *Lancet Neurol* 13: 247-256

Confavreux C, Vukusic S, Adeleine P (2003) Early clinical predictors and progression of irreversible disability in multiple sclerosis: an amnesic process. *Brain* 126: 770-782

Cook DG, Mendall MA, Whincup PH, Carey IM, Ballam L, Morris JE, Miller GJ, Strachan DP (2000) C-reactive protein concentration in children: relationship to adiposity and other cardiovascular risk factors. *Atherosclerosis* 149: 139-150

Costa SL, DeLuca J, Costanza K, Chiaravalloti ND (2019) Comparing the Open Trial - Selective Reminding Test results with the California Learning Verbal Test II in multiple sclerosis. *Appl Neuropsychol Adult* 26: 488-496

Costa SL, Genova HM, DeLuca J, Chiaravalloti ND (2017) Information processing speed in multiple sclerosis: Past, present, and future. *Mult Scler* 23: 772-789

Cree BA, Gourraud PA, Oksenberg JR, Bevan C, Crabtree-Hartman E, Gelfand JM, Goodin DS, Graves J, Green AJ, Mowry E *et al* (2016) Long-term evolution of multiple sclerosis disability in the treatment era. *Ann Neurol* 80: 499-510

Dale RC, de Sousa C, Chong WK, Cox TC, Harding B, Neville BG (2000) Acute disseminated encephalomyelitis, multiphasic disseminated encephalomyelitis and multiple sclerosis in children. *Brain* 123 Pt 12: 2407-2422

Damjanovic D, Valsasina P, Rocca MA, Stromillo ML, Gallo A, Enzinger C, Hulst HE, Rovira A, Muhlert N, De Stefano N *et al* (2017) Hippocampal and Deep Gray Matter Nuclei Atrophy Is Relevant for Explaining Cognitive Impairment in MS: A Multicenter Study. *AJNR Am J Neuroradiol* 38: 18-24

Das B, Dimas V, Guleserian K, Lacelle C, Anton K, Moore L, Morrow R (2017) Alemtuzumab (Campath-1H) therapy for refractory rejections in pediatric heart transplant recipients. *Pediatr Transplant* 21

Datta R, Sethi V, Ly S, Waldman AT, Narula S, Dewey BE, Sati P, Reich D, Banwell B (2017) 7T MRI Visualization of Cortical Lesions in Adolescents and Young Adults with

Pediatric-Onset Multiple Sclerosis. *Journal of neuroimaging : official journal of the American Society of Neuroimaging* 27: 447-452

Davalos D, Grutzendler J, Yang G, Kim JV, Zuo Y, Jung S, Littman DR, Dustin ML, Gan W-B (2005) ATP mediates rapid microglial response to local brain injury in vivo. *Nature Neuroscience* 8: 752-758

Davion JB, Lopes R, Drumez É, Labreuche J, Hadhoum N, Lannoy J, Vermersch P, Pruvo JP, Leclerc X, Zéphir H *et al* (2020) Asymptomatic optic nerve lesions: An underestimated cause of silent retinal atrophy in MS. *Neurology* 94: e2468-e2478

Davis MD, Ashtamker N, Steinerman JR, Knappertz V (2017) Time course of glatiramer acetate efficacy in patients with RRMS in the GALA study. *Neurology(R) neuroimmunology & neuroinflammation* 4: e327-e327

De Bellis MD, Keshavan MS, Beers SR, Hall J, Frustaci K, Masalehdan A, Noll J, Boring AM (2001) Sex differences in brain maturation during childhood and adolescence. *Cereb Cortex* 11: 552-557

De Meo E (2021) ECTRIMS 2021 – Oral Presentations. *Multiple Sclerosis Journal* 27: 3-133

De Meo E, Bonacchi R, Moiola L, Colombo B, Sangalli F, Zanetta C, Amato MP, Martinelli V, Rocca MA, Filippi M (2021a) Early Predictors of 9-Year Disability in Pediatric Multiple Sclerosis. *Ann Neurol*

De Meo E, Meani A, Moiola L, Ghezzi A, Veggiotti P, Filippi M, Rocca MA (2019) Dynamic gray matter volume changes in pediatric multiple sclerosis: A 3.5 year MRI study. *Neurology* 92: e1709-e1723

De Meo E, Moiola L, Ghezzi A, Veggiotti P, Capra R, Amato MP, Pagani E, Fiorino A, Pippolo L, Pera MC *et al* (2017) MRI substrates of sustained attention system and cognitive impairment in pediatric MS patients. *Neurology* 89: 1265-1273

De Meo E, Portaccio E, Giorgio A, Ruano L, Goretti B, Niccolai C, Patti F, Chisari CG, Gallo P, Grossi P *et al* (2021b) Identifying the Distinct Cognitive Phenotypes in Multiple Sclerosis. *JAMA Neurol* 78: 414-425

De Meo E, Portaccio E, Giorgio A, Ruano L, Goretti B, Niccolai C, Patti F, Chisari CG, Gallo P, Grossi P *et al* (2021c) Identifying the Distinct Cognitive Phenotypes in Multiple Sclerosis. *JAMA Neurol*

De Meo E, Portaccio E, Prestipino E, Nacmias B, Bagnoli S, Razzolini L, Pastò L, Niccolai C, Goretti B, Bellinvia A *et al* (2021d) Effect of BDNF Val66Met polymorphism on hippocampal subfields in multiple sclerosis patients. *Molecular Psychiatry*

De Meo E, Ruano L, Goretti B, Niccolai C, Patti F, Chiasari C, Gallo P, Grossi P, Ghezzi A, Roscio M *et al* (2020a) Identifying distinct cognitive phenotypes in multiple sclerosis. *European Journal of Neurology*: 78

De Meo E, Storelli L, Moiola L, Ghezzi A, Veggiotti P, Filippi M, Rocca MA (2020b) In vivo gradients of thalamic damage in paediatric multiple sclerosis: a window into pathology. *Brain*

De Stefano N, Matthews PM, Arnold DL (1995) Reversible decreases in N-acetylaspartate after acute brain injury. *Magnetic resonance in medicine : official journal of the Society of Magnetic Resonance in Medicine / Society of Magnetic Resonance in Medicine* 34: 721-727

Deary IJ, Penke L, Johnson W (2010) The neuroscience of human intelligence differences. *Nat Rev Neurosci* 11: 201-211

Debernard L, Melzer TR, Van Stockum S, Graham C, Wheeler-Kingshott CA, Dalrymple-Alford JC, Miller DH, Mason DF (2014) Reduced grey matter perfusion without volume loss in early relapsing-remitting multiple sclerosis. *J Neurol Neurosurg Psychiatry* 85: 544-551

Deiva K, Mahlaoui N, Beaudonnet F, de Saint Basile G, Caridade G, Moshous D, Mikaeloff Y, Blanche S, Fischer A, Tardieu M (2012) CNS involvement at the onset of primary hemophagocytic lymphohistiocytosis. *Neurology* 78: 1150-1156

Deppe M, Krämer J, Tenberge JG, Marinell J, Schwindt W, Deppe K, Groppa S, Wiendl H, Meuth SG (2016) Early silent microstructural degeneration and atrophy of the thalamocortical network in multiple sclerosis. *Hum Brain Mapp* 37: 1866-1879

Dhaunchak AS, Becker C, Schulman H, De Faria O, Jr., Rajasekharan S, Banwell B, Colman DR, Bar-Or A, Canadian Pediatric Demyelinating Disease G (2012) Implication of perturbed axoglial apparatus in early pediatric multiple sclerosis. *Ann Neurol* 71: 601-613

Di Filippo M, Anderson VM, Altmann DR, Swanton JK, Plant GT, Thompson AJ, Miller DH (2010) Brain atrophy and lesion load measures over 1 year relate to clinical status after 6 years in patients with clinically isolated syndromes. *J Neurol Neurosurg Psychiatry* 81: 204-208

Dinacci D, Tessitore A, Russo A, De Bonis ML, Lavorgna L, Picconi O, Sacco R, Bonavita S, Gallo A, Servillo G *et al* (2011) BDNF Val66Met polymorphism and brain volumes in multiple sclerosis. *Neurological Sciences* 32: 117-123

Doeller CF, King JA, Burgess N (2008) Parallel striatal and hippocampal systems for landmarks and boundaries in spatial memory. *Proceedings of the National Academy of Sciences* 105: 5915

Donohue K, Cox JL, Dwyer MG, Aliotta R, Corwin M, Weinstock-Guttman B, Ann Yeh E, Zivadinov R (2014) No Regional Gray Matter Atrophy Differences between Pediatric- and Adult-Onset Relapsing-Remitting Multiple Sclerosis. *Journal of Neuroimaging* 24: 63-67

Dosenbach NU, Fair DA, Miezin FM, Cohen AL, Wenger KK, Dosenbach RA, Fox MD, Snyder AZ, Vincent JL, Raichle ME *et al* (2007) Distinct brain networks for adaptive and stable task control in humans. *Proceedings of the National Academy of Sciences of the United States of America* 104: 11073-11078

Duquette P, Murray TJ, Pleines J, Ebers GC, Sadovnick D, Weldon P, Warren S, Paty DW, Upton A, Hader W *et al* (1987) Multiple sclerosis in childhood: Clinical profile in 125 patients. *Journal of Pediatrics* 111: 359-363

Duvernoy H, Cattin F, Risold P-Y (2013) Anatomy. In: *The Human Hippocampus: Functional Anatomy, Vascularization and Serial Sections with MRI*, Duvernoy H.M., Cattin F., Risold P.-Y. (eds.) pp. 39-68. Springer Berlin Heidelberg: Berlin, Heidelberg

Egan MF, Kojima M, Callicott JH, Goldberg TE, Kolachana BS, Bertolino A, Zaitsev E, Gold B, Goldman D, Dean M *et al* (2003) The BDNF val66met polymorphism affects activity-dependent secretion of BDNF and human memory and hippocampal function. *Cell* 112: 257-269

Egeland J, Kovalik-Gran I (2010) Measuring several aspects of attention in one test: the factor structure of conners's continuous performance test. *J Atten Disord* 13: 339-346

Eichenbaum H (2004) Hippocampus: cognitive processes and neural representations that underlie declarative memory. *Neuron* 44: 109-120

Eijlers AJC, Dekker I, Steenwijk MD, Meijer KA, Hulst HE, Pouwels PJW, Uitdehaag BMJ, Barkhof F, Vrenken H, Schoonheim MM *et al* (2019) Cortical atrophy accelerates as cognitive decline worsens in multiple sclerosis. *Neurology* 93: e1348-e1359

Eijlers AJC, van Geest Q, Dekker I, Steenwijk MD, Meijer KA, Hulst HE, Barkhof F, Uitdehaag BMJ, Schoonheim MM, Geurts JJG (2018) Predicting cognitive decline in multiple sclerosis: a 5-year follow-up study. *Brain* 141: 2605-2618

El-Gaby M, Shipton OA, Paulsen O (2015) Synaptic Plasticity and Memory: New Insights from Hippocampal Left-Right Asymmetries. *Neuroscientist* 21: 490-502

Enzinger C, Pinter D, Rocca MA, De Luca J, Sastre-Garriga J, Audoin B, Filippi M (2016) Longitudinal fMRI studies: Exploring brain plasticity and repair in MS. *Mult Scler* 22: 269-278

Eshaghi A, Marinescu RV, Young AL, Firth NC, Prados F, Jorge Cardoso M, Tur C, De Angelis F, Cawley N, Brownlee WJ *et al* (2018a) Progression of regional grey matter atrophy in multiple sclerosis. *Brain* 141: 1665-1677

Eshaghi A, Prados F, Brownlee WJ, Altmann DR, Tur C, Cardoso MJ, De Angelis F, van de Pavert SH, Cawley N, De Stefano N *et al* (2018b) Deep gray matter volume loss drives disability worsening in multiple sclerosis. *Ann Neurol* 83: 210-222

Eshaghi A, Prados F, Brownlee WJ, Altmann DR, Tur C, Cardoso MJ, De Angelis F, van de Pavert SH, Cawley N, De Stefano N *et al* (2018c) Deep gray matter volume loss drives disability worsening in multiple sclerosis. *Ann Neurol* 83: 210-222

Evangelou N, Konz D, Esiri MM, Smith S, Palace J, Matthews PM (2001) Size-selective neuronal changes in the anterior optic pathways suggest a differential susceptibility to injury in multiple sclerosis. *Brain* 124: 1813-1820

Evans AC, Brain Development Cooperative G (2006) The NIH MRI study of normal brain development. *Neuroimage* 30: 184-202

Fadda G, Armangue T, Hacohen Y, Chitnis T, Banwell B (2021) Paediatric multiple sclerosis and antibody-associated demyelination: clinical, imaging, and biological considerations for diagnosis and care. *Lancet Neurol* 20: 136-149

Fadda G, Brown RA, Longoni G, Castro DA, O'Mahony J, Verhey LH, Branson HM, Waters P, Bar-Or A, Marrie RA *et al* (2018a) MRI and laboratory features and the performance of international criteria in the diagnosis of multiple sclerosis in children and adolescents: a prospective cohort study. *Lancet Child Adolesc Health* 2: 191-204

Fadda G, Brown RA, Longoni G, Castro DA, O'Mahony J, Verhey LH, Branson HM, Waters P, Bar-Or A, Marrie RA *et al* (2018b) MRI and laboratory features and the performance of international criteria in the diagnosis of multiple sclerosis in children and adolescents: a prospective cohort study. *Lancet Child Adolesc Health* 2: 191-204

Fadda G, Brown RA, Longoni G, Castro DA, O'Mahony J, Verhey LH, Branson HM, Waters P, Bar-Or A, Marrie RA *et al* (2018c) MRI and laboratory features and the performance of international criteria in the diagnosis of multiple sclerosis in children and adolescents: a prospective cohort study. *Lancet Child Adolesc Health* 2: 191-204

Fadda G, Brown RA, Magliozzi R, Aubert-Broche B, O'Mahony J, Shinohara RT, Banwell B, Marrie RA, Yeh EA, Collins DL *et al* (2019) A surface-in gradient of thalamic damage evolves in pediatric multiple sclerosis. *Ann Neurol* 85: 340-351

Fair DA, Dosenbach NU, Church JA, Cohen AL, Brahmbhatt S, Miezin FM, Barch DM, Raichle ME, Petersen SE, Schlaggar BL (2007) Development of distinct control networks through segregation and integration. *Proc Natl Acad Sci U S A* 104: 13507-13512

Fan J, Hof PR, Guise KG, Fossella JA, Posner MI (2008) The functional integration of the anterior cingulate cortex during conflict processing. *Cerebral cortex (New York, NY : 1991)* 18: 796-805

Ferguson B, Matyszak MK, Esiri MM, Perry VH (1997) Axonal damage in acute multiple sclerosis lesions. *Brain : a journal of neurology* 120 (Pt 3): 393-399

Filippi M (2014) MRI measures of neurodegeneration in multiple sclerosis: implications for disability, disease monitoring, and treatment. *Journal of Neurology*: 1-6

Filippi M, Bar-Or A, Piehl F, Preziosa P, Solari A, Vukusic S, Rocca MA (2018) Multiple sclerosis. *Nat Rev Dis Primers* 4: 43

Filippi M, Brück W, Chard D, Fazekas F, Geurts JJG, Enzinger C, Hametner S, Kuhlmann T, Preziosa P, Rovira À *et al* (2019a) Association between pathological and MRI findings in multiple sclerosis. *Lancet Neurol* 18: 198-210

Filippi M, Bruck W, Chard D, Fazekas F, Geurts JJG, Enzinger C, Hametner S, Kuhlmann T, Preziosa P, Rovira A *et al* (2019b) Association between pathological and MRI findings in multiple sclerosis. *Lancet Neurol* 18: 198-210

Filippi M, Preziosa P, Copetti M, Riccitelli G, Horsfield MA, Martinelli V, Comi G, Rocca MA (2013) Gray matter damage predicts the accumulation of disability 13 years later. *Neurology* 81: 1759-1767

Filippi M, Rocca MA (2004) Magnetization transfer magnetic resonance imaging in the assessment of neurological diseases. *Journal of neuroimaging : official journal of the American Society of Neuroimaging* 14: 303-313

Filippi M, Rocca MA (2013) Present and future of fMRI in multiple sclerosis. *Expert Rev Neurother* 13: 27-31

Filippi M, Rocca MA, Barkhof F, Bruck W, Chen JT, Comi G, DeLuca G, De Stefano N, Erickson BJ, Evangelou N *et al* (2012) Association between pathological and MRI findings in multiple sclerosis. *Lancet Neurol* 11: 349-360

Filippi M, Rocca MA, Ciccarelli O, De Stefano N, Evangelou N, Kappos L, Rovira A, Sastre-Garriga J, Tintore M, Frederiksen JL *et al* (2016) MRI criteria for the diagnosis of multiple sclerosis: MAGNIMS consensus guidelines. *Lancet Neurol* 15: 292-303

Filippi M, Rocca MA, Colombo B, Falini A, Codella M, Scotti G, Comi G (2002) Functional magnetic resonance imaging correlates of fatigue in multiple sclerosis. *Neuroimage* 15: 559-567

Filippi M, Rocca MA, Comi G (2003) The use of quantitative magnetic-resonance-based techniques to monitor the evolution of multiple sclerosis. *Lancet Neurol* 2: 337-346

Filippi M, Wolinsky JS, Sormani MP, Comi G, Group ECGAS (2001) Enhancement frequency decreases with increasing age in relapsing-remitting multiple sclerosis. *Neurology* 56: 422-423

Fink F, Rischkau E, Butt M, Klein J, Eling P, Hildebrandt H (2010) Efficacy of an executive function intervention programme in MS: a placebo-controlled and pseudo-randomized trial. *Mult Scler* 16: 1148-1151

Fischl B (2012) FreeSurfer. *NeuroImage* 62: 774-781

Fisniku LK, Brex PA, Altmann DR, Miszkiel KA, Benton CE, Lanyon R, Thompson AJ, Miller DH (2008) Disability and T2 MRI lesions: a 20-year follow-up of patients with relapse onset of multiple sclerosis. *Brain : a journal of neurology* 131: 808-817

Foong J, Rozewicz L, Quaghebeur G, Davie CA, Kartsounis LD, Thompson AJ, Miller DH, Ron MA (1997) Executive function in multiple sclerosis. The role of frontal lobe pathology. *Brain* 120 (Pt 1): 15-26

Forn C, Barros-Loscertales A, Escudero J, Belloch V, Campos S, Parcet MA, Avila C (2006) Cortical reorganization during PASAT task in MS patients with preserved working memory functions. *Neuroimage* 31: 686-691

Forn C, Barros-Loscertales A, Escudero J, Benlloch V, Campos S, Antonia Parcet M, Avila C (2007) Compensatory activations in patients with multiple sclerosis during preserved performance on the auditory N-back task. *Hum Brain Mapp* 28: 424-430

Fortenbaugh FC, DeGutis J, Esterman M (2017) Recent theoretical, neural, and clinical advances in sustained attention research. *Annals of the New York Academy of Sciences*: n/a-n/a

Freedman MS (2008) Induction vs. escalation of therapy for relapsing multiple sclerosis: the evidence. *Neurol Sci* 29 Suppl 2: S250-252

Friston KJ, Frith CD, Frackowiak RS, Turner R (1995a) Characterizing dynamic brain responses with fMRI: a multivariate approach. *NeuroImage* 2: 166-172

Friston KJ, Holmes AP, Poline JB, Grasby PJ, Williams SC, Frackowiak RS, Turner R (1995b) Analysis of fMRI time-series revisited. *NeuroImage* 2: 45-53

Fu L, Matthews PM, De Stefano N, Worsley KJ, Narayanan S, Francis GS, Antel JP, Wolfson C, Arnold DL (1998) Imaging axonal damage of normal-appearing white matter in multiple sclerosis. *Brain* 121: 103-113

Fudge JL, deCampo DM, Becoats KT (2012) Revisiting the hippocampal–amygdala pathway in primates: Association with immature-appearing neurons. *Neuroscience* 212: 104-119

Fuentes A, Collins DL, Garcia-Lorenzo D, Sled JG, Narayanan S, Arnold DL, Banwell BL, Till C (2012) Memory performance and normalized regional brain volumes in patients with pediatric-onset multiple sclerosis. *Journal of the International Neuropsychological Society : JINS* 18: 471-480

Ganzetti M, Wenderoth N, Mantini D (2014) Whole brain myelin mapping using T1- and T2-weighted MR imaging data. *Front Hum Neurosci* 8: 671

Geertsen SS, Willerslev-Olsen M, Lorentzen J, Nielsen JB (2017) Development and aging of human spinal cord circuitries. *Journal of neurophysiology* 118: 1133-1140

Gennatas ED, Avants BB, Wolf DH, Satterthwaite TD, Ruparel K, Ciric R, Hakonarson H, Gur RE, Gur RC (2017) Age-Related Effects and Sex Differences in Gray Matter Density, Volume, Mass, and Cortical Thickness from Childhood to Young Adulthood. *J Neurosci* 37: 5065-5073

Geschwind DH, Rakic P (2013) Cortical evolution: judge the brain by its cover. *Neuron* 80: 633-647

Geurts JJ, Bö L, Roosendaal SD, Hazes T, Daniëls R, Barkhof F, Witter MP, Huitinga I, van der Valk P (2007) Extensive hippocampal demyelination in multiple sclerosis. *J Neuropathol Exp Neurol* 66: 819-827

Geurts JJ, Pouwels PJ, Uitdehaag BM, Polman CH, Barkhof F, Castelijns JA (2005) Intracortical lesions in multiple sclerosis: improved detection with 3D double inversion-recovery MR imaging. *Radiology* 236: 254-260

Ghaem O, Mellet E, Crivello F, Tzourio N, Mazoyer B, Berthoz A, Denis M (1997) Mental navigation along memorized routes activates the hippocampus, precuneus, and insula. *Neuroreport* 8: 739-744

Ghassemi R, Antel SB, Narayanan S, Francis SJ, Bar-Or A, Sadovnick AD, Banwell B, Arnold DL (2008) Lesion distribution in children with clinically isolated syndromes. *Ann Neurol* 63: 401-405

Ghassemi R, Brown R, Banwell B, Narayanan S, Arnold DL, Canadian Pediatric Demyelinating Disease Study G (2015a) Quantitative Measurement of tissue damage and recovery within new T2w lesions in pediatric- and adult-onset multiple sclerosis. *Mult Scler* 21: 718-725

Ghassemi R, Brown R, Banwell B, Narayanan S, Arnold DL, Group CPDDS (2015b) Quantitative Measurement of tissue damage and recovery within new T2w lesions in pediatric- and adult-onset multiple sclerosis. *Mult Scler* 21: 718-725

Ghassemi R, Brown R, Narayanan S, Banwell B, Nakamura K, Arnold DL (2015c) Normalization of white matter intensity on T1-weighted images of patients with acquired central nervous system demyelination. *J Neuroimaging* 25: 184-190

Ghassemi R, Narayanan S, Banwell B, Sled JG, Shroff M, Arnold DL (2014) Quantitative determination of regional lesion volume and distribution in children and adults with relapsing-remitting multiple sclerosis. *PloS one* 9: e85741

Ghezzi A, Amato M, Annovazzi P, Capobianco M, Gallo P, La Mantia L, Marrosu M, Martinelli V, Milani N, Moiola L *et al* (2009) Long-term results of immunomodulatory treatment in children and adolescents with multiple sclerosis: the Italian experience. *Neurol Sci* 30: 193-199

Ghezzi A, Amato MP, Capobianco M, Gallo P, Marrosu G, Martinelli V, Milani N, Milanese C, Moiola L, Patti F *et al* (2005) Disease-modifying drugs in childhood-juvenile multiple sclerosis: results of an Italian co-operative study. *Mult Scler* 11: 420-424

Ghezzi A, Amato MP, Makhani N, Shreiner T, Gartner J, Tenembaum S (2016) Pediatric multiple sclerosis: Conventional first-line treatment and general management. *Neurology* 87: S97-S102

Ghezzi A, Banwell B, Boyko A, Amato MP, Anlar B, Blinkenberg M, Boon M, Filippi M, Jozwiak S, Ketelslegers I *et al* (2010) Meeting Review: The management of multiple sclerosis in children: a European view. *Multiple Sclerosis* 16: 1258-1267

Ghezzi A, Comi G, Grimaldi LM, Moiola L, Pozzilli C, Fantaccini S, Gallo P (2019) Pharmacokinetics and pharmacodynamics of natalizumab in pediatric patients with RRMS. *Neurol Neuroimmunol Neuroinflamm* 6: e591

Ghezzi A, Pozzilli C, Liguori M, Marrosu MG, Milani N, Milanese C, Simone I, Zaffaroni M (2002) Prospective study of multiple sclerosis with early onset. *Multiple Sclerosis* 8: 115-118

Gianfrancesco MA, Stridh P, Rhead B, Shao X, Xu E, Graves JS, Chitnis T, Waldman A, Lotze T, Schreiner T *et al* (2017) Evidence for a causal relationship between low vitamin D, high BMI, and pediatric-onset MS. *Neurology* 88: 1623-1629

Giedd JN (2004) Structural magnetic resonance imaging of the adolescent brain. *Ann N Y Acad Sci* 1021: 77-85

Gilmore CP, Donaldson I, Bö L, Owens T, Lowe J, Evangelou N (2009) Regional variations in the extent and pattern of grey matter demyelination in multiple sclerosis: a comparison between the cerebral cortex, cerebellar cortex, deep grey matter nuclei and the spinal cord. *J Neurol Neurosurg Psychiatry* 80: 182-187

Ginsberg JP (2010) An experimental protocol for fertility preservation in prepubertal boys recently diagnosed with cancer: a report of acceptability and safety. *Hum Reprod* 25: 37-41

Giorgio A, Stromillo ML, Rossi F, Battaglini M, Hakiki B, Portaccio E, Federico A, Amato MP, De Stefano N (2011) Cortical lesions in radiologically isolated syndrome. *Neurology* 77: 1896-1899

Giorgio A, Watkins KE, Chadwick M, James S, Winmill L, Douaud G, De Stefano N, Matthews PM, Smith SM, Johansen-Berg H *et al* (2010) Longitudinal changes in grey and white matter during adolescence. *Neuroimage* 49: 94-103

Giovannoni G, Comi G, Cook S, Rammohan K, Rieckmann P, Soelberg Sorensen P, Vermersch P, Chang P, Hamlett A, Musch B *et al* (2010) A placebo-controlled trial of oral cladribine for relapsing multiple sclerosis. *The New England journal of medicine* 362: 416-426

Glasser MF, Coalson TS, Robinson EC, Hacker CD, Harwell J, Yacoub E, Ugurbil K, Andersson J, Beckmann CF, Jenkinson M *et al* (2016) A multi-modal parcellation of human cerebral cortex. *Nature* 536: 171-178

Glasser MF, Goyal MS, Preuss TM, Raichle ME, Van Essen DC (2014) Trends and properties of human cerebral cortex: correlations with cortical myelin content. *Neuroimage* 93 Pt 2: 165-175

Glasser MF, Van Essen DC (2011) Mapping human cortical areas in vivo based on myelin content as revealed by T1- and T2-weighted MRI. *J Neurosci* 31: 11597-11616

Gogtay N, Giedd JN, Lusk L, Hayashi KM, Greenstein D, Vaituzis AC, Nugent TF, 3rd, Herman DH, Clasen LS, Toga AW *et al* (2004) Dynamic mapping of human cortical development during childhood through early adulthood. *Proc Natl Acad Sci U S A* 101: 8174-8179

Gold SM, Kern KC, O'Connor MF, Montag MJ, Kim A, Yoo YS, Giesser BS, Sicotte NL (2010) Smaller cornu ammonis 2-3/dentate gyrus volumes and elevated cortisol in multiple sclerosis patients with depressive symptoms. *Biol Psychiatry* 68: 553-559

Goodin DS, Traboulsee A, Knappertz V, Reder AT, Li D, Langdon D, Wolf C, Beckmann K, Konieczny A, Ebers GC *et al* (2012) Relationship between early clinical characteristics and long term disability outcomes: 16 year cohort study (follow-up) of the pivotal interferon β-1b trial in multiple sclerosis. *J Neurol Neurosurg Psychiatry* 83: 282-287

Goretti B, Portaccio E, Ghezzi A, Lori S, Moiola L, Falautano M, Viterbo R, Patti F, Vecchio R, Pozzilli C *et al* (2012) Fatigue and its relationships with cognitive functioning and depression in paediatric multiple sclerosis. *Mult Scler* 18: 329-334

Gorman MP, Healy BC, Polgar-Turcsanyi M, Chitnis T (2009) Increased relapse rate in pediatric-onset compared with adult-onset multiple sclerosis. *Archives of Neurology* 66: 54-59

Graves JS, Chitnis T, Weinstock-Guttman B, Rubin J, Zelikovitch AS, Nourbakhsh B, Simmons T, Waltz M, Casper TC, Waubant E *et al* (2017) Maternal and Perinatal Exposures Are Associated With Risk for Pediatric-Onset Multiple Sclerosis. *Pediatrics* 139

Green R, Adler A, Banwell BL, Fabri TL, Yeh EA, Collins DL, Sled JG, Narayanan S, Till C (2018) Involvement of the Amygdala in Memory and Psychosocial Functioning in Pediatric-Onset Multiple Sclerosis. *Dev Neuropsychol* 43: 524-534

Gronseth GS, Ashman EJ (2000) Practice parameter: The usefulness of evoked potentials in identifying clinically silent lesions in patients with suspected multiple sclerosis (an

evidence-based review): Report of the Quality Standards Subcommittee of the American Academy of Neurology. *Neurology* 54: 1720-1725

Grydeland H, Walhovd KB, Tamnes CK, Westlye LT, Fjell AM (2013) Intracortical myelin links with performance variability across the human lifespan: results from T1- and T2-weighted MRI myelin mapping and diffusion tensor imaging. *J Neurosci* 33: 18618-18630

Guillemot-Legris O, Muccioli GG (2017) Obesity-induced neuroinflammation: beyond the hypothalamus. *Trends in Neurosciences* 40: 237-253

Hacohen Y, Brownlee W, Mankad K, Chong WKK, Thompson A, Lim M, Wassmer E, Hemingway C, Barkhof F, Ciccarelli O (2019) Improved performance of the 2017 McDonald criteria for diagnosis of multiple sclerosis in children in a real-life cohort. *Multiple Sclerosis Journal* 26: 1372-1380

Hahn CD, Shroff MM, Blaser SI, Banwell BL (2004) MRI criteria for multiple sclerosis: Evaluation in a pediatric cohort. *Neurology* 62: 806-808

Haider L, Simeonidou C, Steinberger G, Hametner S, Grigoriadis N, Deretzi G, Kovacs GG, Kutzelnigg A, Lassmann H, Frischer JM (2014) Multiple sclerosis deep grey matter: the relation between demyelination, neurodegeneration, inflammation and iron. *J Neurol Neurosurg Psychiatry* 85: 1386-1395

Haider L, Zrzavy T, Hametner S, Höftberger R, Bagnato F, Grabner G, Trattnig S, Pfeifenbring S, Brück W, Lassmann H (2016) The topograpy of demyelination and neurodegeneration in the multiple sclerosis brain. *Brain* 139: 807-815

Hajek T, Kopecek M, Höschl C (2012) Reduced hippocampal volumes in healthy carriers of brain-derived neurotrophic factor Val66Met polymorphism: meta-analysis. *World J Biol Psychiatry* 13: 178-187

Hanninen K, Viitala M, Paavilainen T, Karhu JO, Rinne J, Koikkalainen J, Lotjonen J, Soilu-Hanninen M (2019) Thalamic Atrophy Without Whole Brain Atrophy Is Associated With Absence of 2-Year NEDA in Multiple Sclerosis. *Front Neurol* 10: 459

Hannoun S, Durand-Dubief F, Confavreux C, Ibarrola D, Streichenberger N, Cotton F, Guttmann CR, Sappey-Marinier D (2012) Diffusion tensor-MRI evidence for extra-axonal neuronal degeneration in caudate and thalamic nuclei of patients with multiple sclerosis. *AJNR Am J Neuroradiol* 33: 1363-1368

Hanssen KT, Saltytė Benth J, Beiske AG, Landrø NI, Hessen E (2015) Goal attainment in cognitive rehabilitation in MS patients. *Neuropsychol Rehabil* 25: 137-154

Harding K, Williams O, Willis M, Hrastelj J, Rimmer A, Joseph F, Tomassini V, Wardle M, Pickersgill T, Robertson N *et al* (2019) Clinical Outcomes of Escalation vs Early Intensive Disease-Modifying Therapy in Patients With Multiple Sclerosis. *JAMA neurology* 76: 536-541

Harding KE, Liang K, Cossburn MD, Ingram G, Hirst CL, Pickersgill TP, Te Water Naude J, Wardle M, Ben-Shlomo Y, Robertson NP (2013) Long-term outcome of paediatric-onset multiple sclerosis: a population-based study. *J Neurol Neurosurg Psychiatry* 84: 141-147

Hariri AR, Goldberg TE, Mattay VS, Kolachana BS, Callicott JH, Egan MF, Weinberger DR (2003) Brain-derived neurotrophic factor val66met polymorphism affects human memory-related hippocampal activity and predicts memory performance. *J Neurosci* 23: 6690-6694

Hartley T, Maguire EA, Spiers HJ, Burgess N (2003) The well-worn route and the path less traveled: distinct neural bases of route following and wayfinding in humans. *Neuron* 37: 877-888

Hartmann M, Heumann R, Lessmann V (2001) Synaptic secretion of BDNF after high-frequency stimulation of glutamatergic synapses. *EMBO J* 20: 5887-5897

Hasselmo ME, McClelland JL (1999) Neural models of memory. *Curr Opin Neurobiol* 9: 184-188

Haukvik UK, Gurholt TP, Nerland S, Elvsåshagen T, Akudjedu TN, Alda M, Alnæs D, Alonso-Lana S, Bauer J, Baune BT *et al* (2020) In vivo hippocampal subfield volumes in

bipolar disorder—A mega-analysis from The Enhancing Neuro Imaging Genetics through Meta-Analysis Bipolar Disorder Working Group. *Human Brain Mapping* n/a

Hauser SL, Waubant E, Arnold DL, Vollmer T, Antel J, Fox RJ, Bar-Or A, Panzara M, Sarkar N, Agarwal S *et al* (2008) B-cell depletion with rituximab in relapsing-remitting multiple sclerosis. *The New England journal of medicine* 358: 676-688

Hedstrom AK, Olsson T, Alfredsson L (2012) High body mass index before age 20 is associated with increased risk for multiple sclerosis in both men and women. *Mult Scler* 18: 1334-1336

Hennes EM, Baumann M, Schanda K, Anlar B, Bajer-Kornek B, Blaschek A, Brantner-Inthaler S, Diepold K, Eisenkolbl A, Gotwald T *et al* (2017) Prognostic relevance of MOG antibodies in children with an acquired demyelinating syndrome. *Neurology* 89: 900-908

Herranz E, Gianni C, Louapre C, Treaba CA, Govindarajan ST, Ouellette R, Loggia ML, Sloane JA, Madigan N, Izquierdo-Garcia D *et al* (2016) Neuroinflammatory component of gray matter pathology in multiple sclerosis. *Ann Neurol* 80: 776-790

Herting MM, Sowell ER (2017) Puberty and structural brain development in humans. *Front Neuroendocrinol* 44: 122-137

Hesselink JR (2006) Differential diagnostic approach to MR imaging of white matter diseases. . *Top Magn Reson Imaging* 17: 243-263

Hintzen RQ, Dale RC, Neuteboom RF, Mar S, Banwell B (2016) Pediatric acquired CNS demyelinating syndromes: Features associated with multiple sclerosis. *Neurology* 87: S67-73

Holtzer R, Foley F (2009) The relationship between subjective reports of fatigue and executive control in multiple sclerosis. *J Neurol Sci* 281: 46-50

Homack S, Riccio CA (2006) Conners' Continuous Performance Test (2nd ed.; CCPT-II). *J Atten Disord* 9: 556-558

Horton MK, McCauley K, Fadrosh D, Fujimura K, Graves J, Ness J, Wheeler Y, Gorman MP, Benson LA, Weinstock-Guttman B *et al* (2021) Gut microbiome is associated with multiple sclerosis activity in children. *Ann Clin Transl Neurol*

Hosseini B, Flora DB, Banwell BL, Till C (2014) Age of onset as a moderator of cognitive decline in pediatric-onset multiple sclerosis. *Journal of the International Neuropsychological Society : JINS* 20: 796-804

Howell OW, Reeves CA, Nicholas R, Carassiti D, Radotra B, Gentleman SM, Serafini B, Aloisi F, Roncaroli F, Magliozzi R *et al* (2011) Meningeal inflammation is widespread and linked to cortical pathology in multiple sclerosis. *Brain* 134: 2755-2771

Hrybouski S, MacGillivray M, Huang Y, Madan CR, Carter R, Seres P, Malykhin NV (2019) Involvement of hippocampal subfields and anterior-posterior subregions in encoding and retrieval of item, spatial, and associative memories: Longitudinal versus transverse axis. *Neuroimage* 191: 568-586

Hua K, Zhang J, Wakana S, Jiang H, Li X, Reich DS, Calabresi PA, Pekar JJ, van Zijl PC, Mori S (2008) Tract probability maps in stereotaxic spaces: analyses of white matter anatomy and tract-specific quantification. *NeuroImage* 39: 336-347

Hubacher M, Kappos L, Weier K, Stöcklin M, Opwis K, Penner IK (2015) Case-Based fMRI Analysis after Cognitive Rehabilitation in MS: A Novel Approach. *Front Neurol* 6: 78

Huitema MJD, Schenk GJ (2018) Insights into the Mechanisms That May Clarify Obesity as a Risk Factor for Multiple Sclerosis. *Curr Neurol Neurosci Rep* 18: 18

Huppke B, Ellenberger D, Rosewich H, Friede T, Gartner J, Huppke P (2014) Clinical presentation of pediatric multiple sclerosis before puberty. *Eur J Neurol* 21: 441-446

Huppke P, Huppke B, Ellenberger D, Rostasy K, Hummel H, Stark W, Bruck W, Gartner J (2019) Therapy of highly active pediatric multiple sclerosis. *Mult Scler* 25: 72-80

Huppke P, Rostasy K, Karenfort M, Huppke B, Seidl R, Leiz S, Reindl M, Gartner J (2013) Acute disseminated encephalomyelitis followed by recurrent or monophasic optic neuritis in pediatric patients. *Mult Scler* 19: 941-946

Hypponen E, Laara E, Reunanen A, Jarvelin MR, Virtanen SM (2001) Intake of vitamin D and risk of type 1 diabetes: a birth-cohort study. *Lancet* 358: 1500-1503

Iaffaldano P, Simone M, Lucisano G, Ghezzi A, Coniglio G, Brescia Morra V, Salemi G, Patti F, Lugaresi A, Izquierdo G *et al* (2017) Prognostic indicators in pediatric clinically isolated syndrome. *Ann Neurol* 81: 729-739

Iglesias JE, Augustinack JC, Nguyen K, Player CM, Player A, Wright M, Roy N, Frosch MP, McKee AC, Wald LL *et al* (2015) A computational atlas of the hippocampal formation using ex vivo, ultra-high resolution MRI: Application to adaptive segmentation of in vivo MRI. *Neuroimage* 115: 117-137

Iqbal K, Flory M, Khatoon S, Soininen H, Pirttila T, Lehtovirta M, Alafuzoff I, Blennow K, Andreasen N, Vanmechelen E *et al* (2005) Subgroups of Alzheimer's disease based on cerebrospinal fluid molecular markers. *Ann Neurol* 58: 748-757

Ishihara Y, Fukuda T (2016) Immunohistochemical investigation of the internal structure of the mouse subiculum. *Neuroscience* 337: 242-266

Jacobs BM, Noyce AJ, Giovannoni G, Dobson R (2020) BMI and low vitamin D are causal factors for multiple sclerosis. *Neurology - Neuroimmunology Neuroinflammation* 7: e662

Jehna M, Pirpamer L, Khalil M, Fuchs S, Ropele S, Langkammer C, Pichler A, Stulnig F, Deutschmann H, Fazekas F *et al* (2015) Periventricular lesions correlate with cortical thinning in multiple sclerosis. *Ann Neurol* 78: 530-539

Jeong A, Oleske DM, Holman J (2019) Epidemiology of Pediatric-Onset Multiple Sclerosis: A Systematic Review of the Literature. *J Child Neurol* 34: 705-712

Johansen-Berg H, Behrens TE, Sillery E, Ciccarelli O, Thompson AJ, Smith SM, Matthews PM (2005) Functional-anatomical validation and individual variation of

diffusion tractography-based segmentation of the human thalamus. *Cereb Cortex* 15: 31-39

Jokubaitis VG, Spelman T, Kalincik T, Lorscheider J, Havrdova E, Horakova D, Duquette P, Girard M, Prat A, Izquierdo G *et al* (2016) Predictors of long-term disability accrual in relapse-onset multiple sclerosis. *Ann Neurol* 80: 89-100

Jung RE, Haier RJ (2007) The Parieto-Frontal Integration Theory (P-FIT) of intelligence: converging neuroimaging evidence. *Behav Brain Sci* 30: 135-154; discussion 154-187

Junker A, Wozniak J, Voigt D, Scheidt U, Antel J, Wegner C, Brück W, Stadelmann C (2020) Extensive subpial cortical demyelination is specific to multiple sclerosis. *Brain Pathol*

Kaabak MM, Babenko NN, Samsonov DV, Sandrikov VA, Maschan AA, Zokoev AK (2013) Alemtuzumab induction in pediatric kidney transplantation. *Pediatr Transplant* 17: 168-178

Kalincik T, Cutter G, Spelman T, Jokubaitis V, Havrdova E, Horakova D, Trojano M, Izquierdo G, Girard M, Duquette P *et al* (2015) Defining reliable disability outcomes in multiple sclerosis. *Brain* 138: 3287-3298

Kanda T, Fukusato T, Matsuda M, Toyoda K, Oba H, Kotoku J, Haruyama T, Kitajima K, Furui S (2015) Gadolinium-based Contrast Agent Accumulates in the Brain Even in Subjects without Severe Renal Dysfunction: Evaluation of Autopsy Brain Specimens with Inductively Coupled Plasma Mass Spectroscopy. *Radiology* 276: 228-232

Katoh-Semba R, Asano T, Ueda H, Morishita R, Takeuchi IK, Inaguma Y, Kato K (2002) Riluzole enhances expression of brain-derived neurotrophic factor with consequent proliferation of granule precursor cells in the rat hippocampus. *Faseb j* 16: 1328-1330

Kavé G, Sapir-Yogev S (2020) Associations between memory and verbal fluency tasks. *J Commun Disord* 83: 105968

Kennedy J, O'Connor P, Sadovnick AD, Perara M, Yee I, Banwell B (2006) Age at onset of multiple sclerosis may be influenced by place of residence during childhood rather than ancestry. *Neuroepidemiology* 26: 162-167

Kerbrat A, Aubert-Broche B, Fonov V, Narayanan S, Sled JG, Arnold DA, Banwell B, Collins DL (2012) Reduced head and brain size for age and disproportionately smaller thalami in child-onset MS. *Neurology* 78: 194-201

Kern KC, Ekstrom AD, Suthana NA, Giesser BS, Montag M, Arshanapalli A, Bookheimer SY, Sicotte NL (2012) Fornix damage limits verbal memory functional compensation in multiple sclerosis. *Neuroimage* 59: 2932-2940

Ketelslegers IA, Catsman-Berrevoets CE, Neuteboom RF, Boon M, van Dijk KG, Eikelenboom MJ, Gooskens RH, Niks EH, Overweg-Plandsoen WC, Peeters EA *et al* (2012) Incidence of acquired demyelinating syndromes of the CNS in Dutch children: a nationwide study. *J Neurol* 259: 1929-1935

Keyhanian K, Saxena S, Gombolay G, Healy BC, Misra M, Chitnis T (2019) Adipokines are associated with pediatric multiple sclerosis risk and course. *Mult Scler Relat Disord* 36: 101384

Killestein J, Polman CH (2011) Determinants of interferon β efficacy in patients with multiple sclerosis. *Nature Reviews Neurology* 7: 221-228

Kim IK, Choi J, Vo AA, Kang A, Patel M, Toyoda M, Mirocha J, Kamil ES, Cohen JL, Louie S *et al* (2017) Safety and Efficacy of Alemtuzumab Induction in Highly Sensitized Pediatric Renal Transplant Recipients. *Transplantation* 101: 883-889

Kincses ZT, Ropele S, Jenkinson M, Khalil M, Petrovic K, Loitfelder M, Langkammer C, Aspeck E, Wallner-Blazek M, Fuchs S *et al* (2011) Lesion probability mapping to explain clinical deficits and cognitive performance in multiple sclerosis. *Mult Scler* 17: 681-689

Kipp M, Wagenknecht N, Beyer C, Samer S, Wuerfel J, Nikoubashman O (2015) Thalamus pathology in multiple sclerosis: from biology to clinical application. *Cell Mol Life Sci* 72: 1127-1147

Kishi T, Tsumori T, Yokota S, Yasui Y (2006) Topographical projection from the hippocampal formation to the amygdala: A combined anterograde and retrograde tracing study in the rat. *Journal of Comparative Neurology* 496: 349-368

Kolasinski J, Stagg CJ, Chance SA, Deluca GC, Esiri MM, Chang EH, Palace JA, McNab JA, Jenkinson M, Miller KL *et al* (2012) A combined post-mortem magnetic resonance imaging and quantitative histological study of multiple sclerosis pathology. *Brain* 135: 2938-2951

Kornek B, Bernert G, Balassy C, Geldner J, Prayer D, Feucht M (2003) Glatiramer acetate treatment in patients with childhood and juvenile onset multiple sclerosis. *Neuropediatrics* 34: 120-126

Korteweg T, Tintore M, Uitdehaag B, Rovira A, Frederiksen J, Miller D, Fernando K, Filippi M, Agosta F, Rocca M *et al* (2006) MRI criteria for dissemination in space in patients with clinically isolated syndromes: a multicentre follow-up study. *Lancet Neurol* 5: 221-227

Kovacs M, Paulauskas S, Gatsonis C, Richards C (1988) Depressive disorders in childhood. III. A longitudinal study of comorbidity with and risk for conduct disorders. *J Affect Disord* 15: 205-217

Krupp LB, LaRocca NG, Muir-Nash J, Steinberg AD (1989) The fatigue severity scale. Application to patients with multiple sclerosis and systemic lupus erythematosus. *Arch Neurol* 46: 1121-1123

Krupp LB, Rintell D, Charvet LE, Milazzo M, Wassmer E (2016) Pediatric multiple sclerosis: Perspectives from adolescents and their families. *Neurology* 87: S4-7

Krupp LB, Tardieu M, Amato MP, Banwell B, Chitnis T, Dale RC, Ghezzi A, Hintzen R, Kornberg A, Pohl D *et al* (2013) International Pediatric Multiple Sclerosis Study Group criteria for pediatric multiple sclerosis and immune-mediated central nervous system demyelinating disorders: revisions to the 2007 definitions. *Mult Scler* 19: 1261-1267

Krysko KM, Graves JS, Rensel M, Weinstock-Guttman B, Rutatangwa A, Aaen G, Belman A, Benson L, Chitnis T, Gorman M (2020) Real-world effectiveness of initial disease-modifying therapies in pediatric multiple sclerosis. *Annals of neurology* 88: 42-55

Krysko KM, O'Connor P (2016) Quality of Life, Cognition and Mood in Adults with Pediatric Multiple Sclerosis. *Can J Neurol Sci* 43: 368-374

Kuipers SD, Tiron A, Soule J, Messaoudi E, Trentani A, Bramham CR (2009) Selective survival and maturation of adult-born dentate granule cells expressing the immediate early gene Arc/Arg3.1. *PLoS One* 4: e4885

Kumaran D, Maguire EA (2007) Match–mismatch processes underlie human hippocampal responses to associative novelty. *Journal of Neuroscience* 27: 8517-8524

Kurtzke JF (1983) Rating neurologic impairment in multiple sclerosis: an expanded disability status scale (EDSS). *Neurology* 33: 1444-1452

Labiano-Fontcuberta A, Martínez-Ginés ML, Aladro Y, Ayuso L, Mitchell AJ, Puertas-Martín V, Cerezo M, Higueras Y, Benito-León J (2016) A comparison study of cognitive deficits in radiologically and clinically isolated syndromes. *Mult Scler* 22: 250-253

Landmeyer NC, Bürkner PC, Wiendl H, Ruck T, Hartung HP, Holling H, Meuth SG, Johnen A (2020) Disease-modifying treatments and cognition in relapsing-remitting multiple sclerosis: A meta-analysis. *Neurology* 94: e2373-e2383

Lavery AM, Collins BN, Waldman AT, Hart CN, Bar-Or A, Marrie RA, Arnold D, O'Mahony J, Banwell B (2019) The contribution of secondhand tobacco smoke exposure to pediatric multiple sclerosis risk. *Mult Scler* 25: 515-522

Le Page E, Veillard D, Laplaud DA, Hamonic S, Wardi R, Lebrun C, Zagnoli F, Wiertlewski S, Deburghgraeve V, Coustans M (2015) Oral versus intravenous high-dose methylprednisolone for treatment of relapses in patients with multiple sclerosis (COPOUSEP): a randomised, controlled, double-blind, non-inferiority trial. *The Lancet* 386: 974-981

Leavitt VM, Lengenfelder J, Moore NB, Chiaravalloti ND, DeLuca J (2011) The relative contributions of processing speed and cognitive load to working memory accuracy in multiple sclerosis. *J Clin Exp Neuropsychol* 33: 580-586

Leavitt VM, Tosto G, Riley CS (2018) Cognitive phenotypes in multiple sclerosis. *J Neurol* 265: 562-566

Lee JY, Chitnis T (2016) Pediatric Multiple Sclerosis. *Semin Neurol* 36: 148-153

Lee R, Kermani P, Teng KK, Hempstead BL (2001) Regulation of cell survival by secreted proneurotrophins. *Science* 294: 1945-1948

Leech R, Sharp DJ (2014) The role of the posterior cingulate cortex in cognition and disease. *Brain : a journal of neurology* 137: 12-32

Leist TP, Comi G, Cree BA, Coyle PK, Freedman MS, Hartung HP, Vermersch P, Casset-Semanaz F, Scaramozza M, oral cladribine for early MSSG (2014) Effect of oral cladribine on time to conversion to clinically definite multiple sclerosis in patients with a first demyelinating event (ORACLE MS): a phase 3 randomised trial. *Lancet Neurol* 13: 257-267

Lenroot RK, Gogtay N, Greenstein DK, Wells EM, Wallace GL, Clasen LS, Blumenthal JD, Lerch J, Zijdenbos AP, Evans AC *et al* (2007) Sexual dimorphism of brain developmental trajectories during childhood and adolescence. *Neuroimage* 36: 1065-1073

Liguori M, Fera F, Gioia MC, Valentino P, Manna I, Condino F, Cerasa A, La Russa A, Clodomiro A, Paolillo A *et al* (2007) Investigating the role of brain-derived neurotrophic factor in relapsing-remitting multiple sclerosis. *Genes Brain Behav* 6: 177-183

Lisak RP, Benjamins JA, Nedelkoska L, Barger JL, Ragheb S, Fan B, Ouamara N, Johnson TA, Rajasekharan S, Bar-Or A (2012) Secretory products of multiple sclerosis B cells are cytotoxic to oligodendroglia in vitro. *J Neuroimmunol* 246: 85-95

Liu Z, Pardini M, Yaldizli Ö, Sethi V, Muhlert N, Wheeler-Kingshott CAM, Samson RS, Miller DH, Chard DT (2015) Magnetization transfer ratio measures in normal-appearing

white matter show periventricular gradient abnormalities in multiple sclerosis. *Brain* 138: 1239-1246

Llufriu S, Rocca MA, Pagani E, Riccitelli GC, Solana E, Colombo B, Rodegher M, Falini A, Comi G, Filippi M (2019) Hippocampal-related memory network in multiple sclerosis: A structural connectivity analysis. *Mult Scler* 25: 801-810

London F, Zéphir H, Drumez E, Labreuche J, Hadhoum N, Lannoy J, Hodel J, Vermersch P, Pruvo JP, Leclerc X *et al* (2019) Optical coherence tomography: a window to the optic nerve in clinically isolated syndrome. *Brain : a journal of neurology* 142: 903-915

Longoni G, Brown RA, MomayyezSiahkal P, Elliott C, Narayanan S, Bar-Or A, Marrie RA, Yeh EA, Filippi M, Banwell B *et al* (2017) White matter changes in paediatric multiple sclerosis and monophasic demyelinating disorders. *Brain* 140: 1300-1315

Longoni G, Rocca MA, Pagani E, Riccitelli GC, Colombo B, Rodegher M, Falini A, Comi G, Filippi M (2015) Deficits in memory and visuospatial learning correlate with regional hippocampal atrophy in MS. *Brain Struct Funct* 220: 435-444

Louapre C, Govindarajan ST, Giannì C, Madigan N, Sloane JA, Treaba CA, Herranz E, Kinkel RP, Mainero C (2017) Heterogeneous pathological processes account for thalamic degeneration in multiple sclerosis: Insights from 7 T imaging. *Multiple Sclerosis Journal* 24: 1433-1444

Lu B, Nagappan G, Guan X, Nathan PJ, Wren P (2013) BDNF-based synaptic repair as a disease-modifying strategy for neurodegenerative diseases. *Nature Reviews Neuroscience* 14: 401-416

Lublin FD, Reingold SC, Cohen JA, Cutter GR, Sørensen PS, Thompson AJ, Wolinsky JS, Balcer LJ, Banwell B, Barkhof F *et al* (2014) Defining the clinical course of multiple sclerosis: the 2013 revisions. *Neurology* 83: 278-286

Lucchinetti C, Bruck W, Parisi J, Scheithauer B, Rodriguez M, Lassmann H (2000) Heterogeneity of multiple sclerosis lesions: implications for the pathogenesis of demyelination. *Ann Neurol* 47: 707-717

Lulu S, Graves J, Waubant E (2015) Menarche increases relapse risk in pediatric multiple sclerosis. *Multiple Sclerosis Journal* 22: 193-200

MacAllister WS, Boyd JR, Holland NJ, Milazzo MC, Krupp LB, International Pediatric MSSG (2007a) The psychosocial consequences of pediatric multiple sclerosis. *Neurology* 68: S66-69

MacAllister WS, Christodoulou C, Milazzo M, Krupp LB (2007b) Longitudinal neuropsychological assessment in pediatric multiple sclerosis. *Dev Neuropsychol* 32: 625-644

MacAllister WS, Christodoulou C, Troxell R, Milazzo M, Block P, Preston TE, Bender HA, Belman A, Krupp LB (2009) Fatigue and quality of life in pediatric multiple sclerosis. *Multiple Sclerosis* 15: 1502-1508

Maguire EA, Burgess N, Donnett JG, Frackowiak RSJ, Frith CD, O'Keefe J (1998) Knowing where and getting there: a human navigation network. *Science* 280: 921-924

Mahad DH, Trapp BD, Lassmann H (2015) Pathological mechanisms in progressive multiple sclerosis. *Lancet neurology* 14: 183-193

Mainero C, Louapre C, Govindarajan ST, Gianni C, Nielsen AS, Cohen-Adad J, Sloane J, Kinkel RP (2015) A gradient in cortical pathology in multiple sclerosis by in vivo quantitative 7 T imaging. *Brain* 138: 932-945

Makhani N (2009) Cyclophosphamide therapy in pediatric multiple sclerosis. *Neurology* 72: 2076-2082

Manguinao M, Krysko KM, Maddike S, Rutatangwa A, Francisco C, Hart J, Chong J, Graves JS, Waubant E (2019) A retrospective cohort study of plasma exchange in central nervous system demyelinating events in children. *Mult Scler Relat Disord* 35: 50-54

Mantzoros CS, Flier JS, Rogol AD (1997) A longitudinal assessment of hormonal and physical alterations during normal puberty in boys. V. Rising leptin levels may signal the onset of puberty. *J Clin Endocrinol Metab* 82: 1066-1070

Maranzano J, Till C, Assemlal HE, Fonov V, Brown R, Araujo D, O'Mahony J, Yeh EA, Bar-Or A, Marrie RA *et al* (2019) Detection and clinical correlation of leukocortical lesions in pediatric-onset multiple sclerosis on multi-contrast MRI. *Mult Scler* 25: 980-986

Margoni M, Rinaldi F, Riccardi A, Franciotta S, Perini P, Gallo P (2019) No evidence of disease activity including cognition (NEDA-3 plus) in naive pediatric multiple sclerosis patients treated with natalizumab. *J Neurol*

Marin SE, Banwell BB, Till C (2013) Cognitive trajectories in 4 patients with pediatric-onset multiple sclerosis: serial evaluation over a decade. *J Child Neurol* 28: 1577-1586

Markowitsch HJ (1998) Differential contribution of right and left amygdala to affective information processing. *Behav Neurol* 11: 233-244

Martinez-Lapiscina EH, Arnow S, Wilson JA, Saidha S, Preiningerova JL, Oberwahrenbrock T, Brandt AU, Pablo LE, Guerrieri S, Gonzalez I *et al* (2016) Retinal thickness measured with optical coherence tomography and risk of disability worsening in multiple sclerosis: a cohort study. *Lancet neurology* 15: 574-584

Matarese G, Procaccini C, De Rosa V (2008) The intricate interface between immune and metabolic regulation: a role for leptin in the pathogenesis of multiple sclerosis? *J Leukoc Biol* 84: 893-899

McAdam LC, Blaser SI, Banwell BL (2002) Pediatric tumefactive demyelination: case series and review of the literature. *Pediatr Neurol* 26: 18-25

McDonald WI, Compston A, Edan G, Goodkin D, Hartung HP, Lublin FD, McFarland HF, Paty DW, Polman CH, Reingold SC *et al* (2001) Recommended diagnostic criteria for multiple sclerosis: Guidelines from the International Panel on the Diagnosis of Multiple Sclerosis. *Annals of Neurology* 50: 121-127

McKay KA, Hillert J, Manouchehrinia A (2019) Long-term disability progression of pediatric-onset multiple sclerosis. *Neurology* 92: e2764-e2773

McLaughlin KA, Chitnis T, Newcombe J, Franz B, Kennedy J, McArdel S, Kuhle J, Kappos L, Rostasy K, Pohl D *et al* (2009) Age-dependent B cell autoimmunity to a myelin surface antigen in pediatric multiple sclerosis. *J Immunol* 183: 4067-4076

Meijer KA, Steenwijk MD, Douw L, Schoonheim MM, Geurts JJG (2020) Long-range connections are more severely damaged and relevant for cognition in multiple sclerosis. *Brain* 143: 150-160

Menary K, Collins PF, Porter JN, Muetzel R, Olson EA, Kumar V, Steinbach M, Lim KO, Luciana M (2013) Associations between cortical thickness and general intelligence in children, adolescents and young adults. *Intelligence* 41: 597-606

Menon V, Uddin LQ (2010) Saliency, switching, attention and control: a network model of insula function. *Brain structure & function* 214: 655-667

Mesaros S, Rocca MA, Absinta M, Ghezzi A, Milani N, Moiola L, Veggiotti P, Comi G, Filippi M (2008a) Evidence of thalamic gray matter loss in pediatric multiple sclerosis. *Neurology* 70: 1107-1112

Mesaros S, Rocca MA, Pagani E, Sormani MP, Petrolini M, Comi G, Filippi M (2011) Thalamic damage predicts the evolution of primary-progressive multiple sclerosis at 5 years. *AJNR Am J Neuroradiol* 32: 1016-1020

Mesaros S, Rovaris M, Pagani E, Pulizzi A, Caputo D, Ghezzi A, Bertolotto A, Capra R, Falautano M, Martinelli V *et al* (2008b) A magnetic resonance imaging voxel-based morphometry study of regional gray matter atrophy in patients with benign multiple sclerosis. *Arch Neurol* 65: 1223-1230

Mexhitaj I, Nyirenda MH, Li R, O'Mahony J, Rezk A, Rozenberg A, Moore CS, Johnson T, Sadovnick D, Collins DL *et al* (2019) Abnormal effector and regulatory T cell subsets in paediatric-onset multiple sclerosis. *Brain* 142: 617-632

Mezzapesa DM, Rocca MA, Falini A, Rodegher ME, Ghezzi A, Comi G, Filippi M (2004a) A preliminary diffusion tensor and magnetization transfer magnetic resonance imaging study of early-onset multiple sclerosis. *Arch Neurol* 61: 366-368

Mezzapesa DM, Rocca MA, Falini A, Rodegher ME, Ghezzi A, Comi G, Filippi M (2004b) A Preliminary Diffusion Tensor and Magnetization Transfer Magnetic Resonance Imaging Study of Early-Onset Multiple Sclerosis. *Archives of Neurology* 61: 366-368

Miettunen J, Nordström T, Kaakinen M, Ahmed AO (2016) Latent variable mixture modeling in psychiatric research--a review and application. *Psychol Med* 46: 457-467

Mikaeloff Y, Adamsbaum C, Husson B, Vallee L, Ponsot G, Confavreux C, Tardieu M, Suissa S (2004a) MRI prognostic factors for relapse after acute CNS inflammatory demyelination in childhood. *Brain* 127: 1942-1947

Mikaeloff Y, Adamsbaum C, Husson B, Vallee L, Ponsot G, Confavreux C, Tardieu M, Suissa S, Radiology KSGo (2004b) MRI prognostic factors for relapse after acute CNS inflammatory demyelination in childhood. *Brain* 127: 1942-1947

Mikaeloff Y, Caridade G, Assi S, Suissa S, Tardieu M (2006) Prognostic factors for early severity in a childhood multiple sclerosis cohort. *Pediatrics* 118: 1133-1139

Mikaeloff Y, Caridade G, Tardieu M, Suissa S, group Ks (2007) Parental smoking at home and the risk of childhood-onset multiple sclerosis in children. *Brain* 130: 2589-2595

Mikaeloff Y, Moreau T, Debouverie M, Pelletier J, Lebrun C, Gout O, Pedespan J-M, Van Hulle C, Vermersch P, Ponsot G (2001) Interferon-β treatment in patients with childhood-onset multiple sclerosis. *The Journal of pediatrics* 139: 443-446

Mikaeloff Y, Suissa S, Vallee L, Lubetzki C, Ponsot G, Confavreux C, Tardieu M, Group KS (2004c) First episode of acute CNS inflammatory demyelination in childhood: prognostic factors for multiple sclerosis and disability. *The Journal of pediatrics* 144: 246-252

Miller DH, Weinshenker BG, Filippi M, Banwell BL, Cohen JA, Freedman MS, Galetta SL, Hutchinson M, Johnson RT, Kappos L *et al* (2008) Differential diagnosis of suspected multiple sclerosis: A consensus approach. *Multiple Sclerosis* 14: 1157-1174

Minagar A, Barnett MH, Benedict RH, Pelletier D, Pirko I, Sahraian MA, Frohman E, Zivadinov R (2013) The thalamus and multiple sclerosis: modern views on pathologic, imaging, and clinical aspects. *Neurology* 80: 210-219

Minneboo A, Barkhof F, Polman CH, Uitdehaag BM, Knol DL, Castelijns JA (2004) Infratentorial lesions predict long-term disability in patients with initial findings suggestive of multiple sclerosis. *Arch Neurol* 61: 217-221

Minneboo A, Uitdehaag BM, Jongen P, Vrenken H, Knol D, van Walderveen MA, Polman CH, Castelijns JA, Barkhof F (2009) Association between MRI parameters and the MS severity scale: a 12 year follow-up study. *Mult Scler* 15: 632-637

Moll NM, Rietsch AM, Thomas S, Ransohoff AJ, Lee JC, Fox R, Chang A, Ransohoff RM, Fisher E (2011) Multiple sclerosis normal-appearing white matter: pathology-imaging correlations. *Ann Neurol* 70: 764-773

Mollison D, Sellar R, Bastin M, Chandran S, Wardlaw J, Connick P (2017) The clinico-radiological paradox of cognitive function and MRI burden of white matter lesions in people with multiple sclerosis: A systematic review and meta-analysis. *PLoS One* 12: e0177727

Montgomery SA, Asberg M (1979) A new depression scale designed to be sensitive to change. *Br J Psychiatry* 134: 382-389

Morgen K, Sammer G, Courtney SM, Wolters T, Melchior H, Blecker CR, Oschmann P, Kaps M, Vaitl D (2007) Distinct mechanisms of altered brain activation in patients with multiple sclerosis. *NeuroImage* 37: 937-946

Moscovitch M, Cabeza R, Winocur G, Nadel L (2016) Episodic memory and beyond: the hippocampus and neocortex in transformation. *Annual review of psychology* 67: 105-134

Mowry EM, Krupp LB, Milazzo M, Chabas D, Strober JB, Belman AL, McDonald JC, Oksenberg JR, Bacchetti P, Waubant E (2010) Vitamin D status is associated with relapse rate in pediatric-onset multiple sclerosis. *Ann Neurol* 67: 618-624

Mowry EM, Pesic M, Grimes B, Deen S, Bacchetti P, Waubant E (2009) Demyelinating events in early multiple sclerosis have inherent severity and recovery. *Neurology* 72: 602

Mukherjee P, Miller JH, Shimony JS, Philip JV, Nehra D, Snyder AZ, Conturo TE, Neil JJ, McKinstry RC (2002) Diffusion-tensor MR imaging of gray and white matter development during normal human brain maturation. *AJNR Am J Neuroradiol* 23: 1445-1456

Murer MG, Yan Q, Raisman-Vozari R (2001) Brain-derived neurotrophic factor in the control human brain, and in Alzheimer's disease and Parkinson's disease. *Prog Neurobiol* 63: 71-124

Naber PA, Witter MP, Lopes Silva FH (2000) Networks of the hippocampal memory system of the rat. The pivotal role of the subiculum. *Ann N Y Acad Sci* 911: 392-403

Nagin DS, Nagin D (2005) *Group-based modeling of development*. Harvard University Press

Narisawa-Saito M, Iwakura Y, Kawamura M, Araki K, Kozaki S, Takei N, Nawa H (2002) Brain-derived neurotrophic factor regulates surface expression of alpha-amino-3-hydroxy-5-methyl-4-isoxazoleproprionic acid receptors by enhancing the N-ethylmaleimide-sensitive factor/GluR2 interaction in developing neocortical neurons. *J Biol Chem* 277: 40901-40910

Nielson DM, Smith TA, Sreekumar V, Dennis S, Sederberg PB (2015) Human hippocampus represents space and time during retrieval of real-world memories. *Proceedings of the National Academy of Sciences* 112: 11078-11083

Nieuwenhuys R, Broere CA (2017) A map of the human neocortex showing the estimated overall myelin content of the individual architectonic areas based on the studies of Adolf Hopf. *Brain Struct Funct* 222: 465-480

Nimmerjahn A, Kirchhoff F, Helmchen F (2005) Resting Microglial Cells Are Highly Dynamic Surveillants of Brain Parenchyma in Vivo. *Science* 308: 1314

Nocentini U, Rossini PM, Carlesimo GA, Graceffa A, Grasso MG, Lupoi D, Oliveri M, Orlacchio A, Pozzilli C, Rizzato B *et al* (2001) Patterns of cognitive impairment in secondary progressive stable phase of multiple sclerosis: correlations with MRI findings. *Eur Neurol* 45: 11-18

Nociti V, Santoro M, Quaranta D, Losavio FA, De Fino C, Giordano R, Palomba NP, Rossini PM, Guerini FR, Clerici M *et al* (2018) BDNF rs6265 polymorphism methylation in Multiple Sclerosis: A possible marker of disease progression. *PLoS One* 13: e0206140

Nyirenda MH, Fadda G, Healy LM, Mexhitaj I, Poliquin-Lasnier L, Hanwell H, Saveriano AW, Rozenberg A, Li R, Moore CS *et al* (2021) Pro-inflammatory adiponectin in pediatric-onset multiple sclerosis. *Mult Scler*: 1352458521989090

O'Connor P, Wolinsky JS, Confavreux C, Comi G, Kappos L, Olsson TP, Benzerdjeb H, Truffinet P, Wang L, Miller A *et al* (2011) Randomized trial of oral teriflunomide for relapsing multiple sclerosis. *The New England journal of medicine* 365: 1293-1303

O'Mahony J, Marrie RA, Laporte A, Bar-Or A, Yeh EA, Brown A, Dilenge ME, Banwell B, Canadian Pediatric Demyelinating Disease N (2018) Pediatric-onset multiple sclerosis is associated with reduced parental health-related quality of life and family functioning. *Mult Scler*: 1352458518796676

O'Mara SM, Commins S, Anderson M, Gigg J (2001) The subiculum: a review of form, physiology and function. *Prog Neurobiol* 64: 129-155

Oberski D (2016) Mixture Models: Latent Profile and Latent Class Analysis. In: pp. 275-287.

Oguz KK, Kurne A, Aksu AO, Karabulut E, Serdaroglu A, Teber S, Haspolat S, Senbil N, Kurul S, Anlar B (2009) Assessment of citrullinated myelin by 1H-MR spectroscopy in early-onset multiple sclerosis. *AJNR American journal of neuroradiology* 30: 716-721

Okuda DT, Mowry EM, Cree BA, Crabtree EC, Goodin DS, Waubant E, Pelletier D (2011) Asymptomatic spinal cord lesions predict disease progression in radiologically isolated syndrome. *Neurology* 76: 686-692

Okuda DT, Siva A, Kantarci O, Inglese M, Katz I, Tutuncu M, Keegan BM, Donlon S, Hua lH, Vidal-Jordana A *et al* (2014) Radiologically isolated syndrome: 5-year risk for an initial clinical event. *PLoS One* 9: e90509

Ormerod IE MD, McDonald WI, du Boulay EP, Rudge P, Kendall BE, Moseley IF, Johnson G, Tofts PS, Halliday AM et al. (1987) The role of NMR imaging in the assessment of multiple sclerosis and isolated neurological lesions. A quantitative study. *Brain* Dec: 1579-1616

Otallah S, Banwell B (2018) Pediatric Multiple Sclerosis: an Update. *Curr Neurol Neurosci Rep* 18: 76

Papadopoulos D, Dukes S, Patel R, Nicholas R, Vora A, Reynolds R (2009) Substantial archaeocortical atrophy and neuronal loss in multiple sclerosis. *Brain Pathol* 19: 238-253

Pardini M, Sudre CH, Prados F, Yaldizli O, Sethi V, Muhlert N, Samson RS, van de Pavert SH, Cardoso MJ, Ourselin S *et al* (2016) Relationship of grey and white matter abnormalities with distance from the surface of the brain in multiple sclerosis. *J Neurol Neurosurg Psychiatry* 87: 1212-1217

Park H, Poo MM (2013) Neurotrophin regulation of neural circuit development and function. *Nat Rev Neurosci* 14: 7-23

Patel VP, Feinstein A (2019) The link between depression and performance on the Symbol Digit Modalities Test: Mechanisms and clinical significance. *Mult Scler* 25: 118-121

Patenaude B, Smith SM, Kennedy DN, Jenkinson M (2011) A Bayesian model of shape and appearance for subcortical brain segmentation. *Neuroimage* 56: 907-922

Paus T (2005) Mapping brain maturation and cognitive development during adolescence. *Trends Cogn Sci* 9: 60-68

Pedullà L, Brichetto G, Tacchino A, Vassallo C, Zaratin P, Battaglia MA, Bonzano L, Bove M (2016) Adaptive vs. non-adaptive cognitive training by means of a personalized App: a randomized trial in people with multiple sclerosis. *J Neuroeng Rehabil* 13: 88

Persson J, Spreng RN, Turner G, Herlitz A, Morell A, Stening E, Wahlund LO, Wikström J, Söderlund H (2014) Sex differences in volume and structural covariance of the anterior and posterior hippocampus. *Neuroimage* 99: 215-225

Pfeifenbring S, Bunyan RF, Metz I, Röver C, Huppke P, Gärtner J, Lucchinetti CF, Brück W (2015) Extensive acute axonal damage in pediatric multiple sclerosis lesions. *Annals of Neurology* 77: 655-667

Pitteri M, Dapor C, Pisani AI, Castellaro M, DeLuca J, Chiaravalloti N, Guandalini M, Ziccardi S, Calabrese M (2019) Executive functioning affects verbal learning process in multiple sclerosis patients: Behavioural and imaging results. *J Neuropsychol*

Planche V, Koubiyr I, Romero JE, Manjon JV, Coupé P, Deloire M, Dousset V, Brochet B, Ruet A, Tourdias T (2018) Regional hippocampal vulnerability in early multiple sclerosis: Dynamic pathological spreading from dentate gyrus to CA1. *Human Brain Mapping* 39: 1814-1824

Pohl D, Alper G, Van Haren K, Kornberg AJ, Lucchinetti CF, Tenembaum S, Belman AL (2016) Acute disseminated encephalomyelitis: Updates on an inflammatory CNS syndrome. *Neurology* 87: S38-45

Pohl D, Rostasy K, Gartner J, Hanefeld F (2005) Treatment of early onset multiple sclerosis with subcutaneous interferon beta-1a. *Neurology* 64: 888-890

Pohl D, Rostasy K, Reiber H, Hanefeld F (2004) CSF characteristics in early-onset multiple sclerosis. *Neurology* 63: 1966-1967

Pohl D, Rostasy K, Treiber-Held S, Brockmann K, Gärtner J, Hanefeld F (2006) Pediatric multiple sclerosis: Detection of clinically silent lesions by multimodal evoked potentials. *The Journal of Pediatrics* 149: 125-127

Polman CH, Reingold SC, Banwell B, Clanet M, Cohen JA, Filippi M, Fujihara K, Havrdova E, Hutchinson M, Kappos L *et al* (2011) Diagnostic criteria for multiple sclerosis: 2010 Revisions to the McDonald criteria. *Ann Neurol* 69: 292-302

Polman CH, Reingold SC, Edan G, Filippi M, Hartung HP, Kappos L, Lublin FD, Metz LM, McFarland HF, O'Connor PW *et al* (2005) Diagnostic criteria for multiple sclerosis: 2005 revisions to the "McDonald Criteria". *Ann Neurol* 58: 840-846

Portaccio E, De Meo E, Bellinvia A, Amato MP (2021) Cognitive Issues in Pediatric Multiple Sclerosis. *Brain Sci* 11

Portaccio E, Goretti B, Lori S, Zipoli V, Centorrino S, Ghezzi A, Patti F, Bianchi V, Comi G, Trojano M *et al* (2009) The brief neuropsychological battery for children: a screening tool for cognitive impairment in childhood and juvenile multiple sclerosis. *Mult Scler* 15: 620-626

Poser CM, Paty DW, Scheinberg L (1983) New diagnostic criteria for multiple sclerosis: Guidelines for research protocols. *Annals of Neurology* 13: 227-231

Posner MI, Rothbart MK, Sheese BE, Tang Y (2007) The anterior cingulate gyrus and the mechanism of self-regulation. *Cognitive, affective & behavioral neuroscience* 7: 391-395

Preziosa P, Rocca MA, Pagani E, Stromillo ML, Enzinger C, Gallo A, Hulst HE, Atzori M, Pareto D, Riccitelli GC *et al* (2016) Structural MRI correlates of cognitive impairment in patients with multiple sclerosis: A Multicenter Study. *Hum Brain Mapp* 37: 1627-1644

Prinster A, Quarantelli M, Orefice G, Lanzillo R, Brunetti A, Mollica C, Salvatore E, Morra VB, Coppola G, Vacca G *et al* (2006) Grey matter loss in relapsing–remitting multiple sclerosis: A voxel-based morphometry study. *NeuroImage* 29: 859-867

Pritzker LB, Joshi S, Gowan JJ, Harauz G, Moscarello MA (2000a) Deimination of myelin basic protein. 1. Effect of deimination of arginyl residues of myelin basic protein on its structure and susceptibility to digestion by cathepsin D. *Biochemistry* 39: 5374-5381

Pritzker LB, Joshi S, Harauz G, Moscarello MA (2000b) Deimination of myelin basic protein. 2. Effect of methylation of MBP on its deimination by peptidylarginine deiminase. *Biochemistry* 39: 5382-5388

Pujol J, Vendrell P, Deus J, Junqué C, Bello J, Martí-Vilalta JL, Capdevila A (2001) The effect of medial frontal and posterior parietal demyelinating lesions on stroop interference. *Neuroimage* 13: 68-75

Raichle ME, MacLeod AM, Snyder AZ, Powers WJ, Gusnard DA, Shulman GL (2001) A default mode of brain function. *Proc Natl Acad Sci U S A* 98: 676-682

Rakic P (1995) A small step for the cell, a giant leap for mankind: a hypothesis of neocortical expansion during evolution. *Trends Neurosci* 18: 383-388

Ramasamy DP, Ramanathan M, Cox JL, Antulov R, Weinstock-Guttman B, Bergsland N, Benedict RH, Dwyer MG, Minagar A, Zivadinov R (2011) Effect of Met66 allele of the BDNF rs6265 SNP on regional gray matter volumes in patients with multiple sclerosis: A voxel-based morphometry study. *Pathophysiology* 18: 53-60

Ramsden S, Richardson FM, Josse G, Thomas MS, Ellis C, Shakeshaft C, Seghier ML, Price CJ (2011) Verbal and non-verbal intelligence changes in the teenage brain. *Nature* 479: 113-116

Rao SM, Leo GJ, Bernardin L, Unverzagt F (1991) Cognitive dysfunction in multiple sclerosis. I. Frequency, patterns, and prediction. *Neurology* 41: 685-691

Rao SM, Leo GJ, Haughton VM, St Aubin-Faubert P, Bernardin L (1989) Correlation of magnetic resonance imaging with neuropsychological testing in multiple sclerosis. *Neurology* 39: 161-166

Reich DS, Lucchinetti CF, Calabresi PA (2018) Multiple Sclerosis. *N Engl J Med* 378: 169-180

Reinhardt K, Weiss S, Rosenbauer J, Gartner J, von Kries R (2014) Multiple sclerosis in children and adolescents: incidence and clinical picture - new insights from the nationwide German surveillance (2009-2011). *Eur J Neurol* 21: 654-659

Renoux C, Vukusic S, Mikaeloff Y, Edan G, Clanet M, Dubois B, Debouverie M, Brochet B, Lebrun-Frenay C, Pelletier J *et al* (2007) Natural history of multiple sclerosis with childhood onset. *N Engl J Med* 356: 2603-2613

Rhead B, Baarnhielm M, Gianfrancesco M, Mok A, Shao X, Quach H, Shen L, Schaefer C, Link J, Gyllenberg A *et al* (2016) Mendelian randomization shows a causal effect of low vitamin D on multiple sclerosis risk. *Neurol Genet* 2: e97

Rhead B, Shao X, Graves JS, Chitnis T, Waldman AT, Lotze T, Schreiner T, Belman A, Krupp L, Greenberg BM *et al* (2019) miRNA contributions to pediatric-onset multiple sclerosis inferred from GWAS. *Ann Clin Transl Neurol* 6: 1053-1061

Righart R, Biberacher V, Jonkman LE, Klaver R, Schmidt P, Buck D, Berthele A, Kirschke JS, Zimmer C, Hemmer B *et al* (2017) Cortical pathology in multiple sclerosis detected by the T1/T2-weighted ratio from routine magnetic resonance imaging. *Ann Neurol* 82: 519-529

Rocca MA, Absinta M, Amato MP, Moiola L, Ghezzi A, Veggiotti P, Capra R, Portaccio E, Fiorino A, Pippolo L *et al* (2014a) Posterior brain damage and cognitive impairment in pediatric multiple sclerosis. *Neurology* 82: 1314-1321

Rocca MA, Absinta M, Ghezzi A, Moiola L, Comi G, Filippi M (2009) Is a preserved functional reserve a mechanism limiting clinical impairment in pediatric MS patients? *Human Brain Mapping* 30: 2844-2851

Rocca MA, Absinta M, Moiola L, Ghezzi A, Colombo B, Martinelli V, Comi G, Filippi M (2010) Functional and structural connectivity of the motor network in pediatric and adult-onset relapsing-remitting multiple sclerosis. *Radiology* 254: 541-550

Rocca MA, Amato MP, De Stefano N, Enzinger C, Geurts JJ, Penner IK, Rovira A, Sumowski JF, Valsasina P, Filippi M *et al* (2015a) Clinical and imaging assessment of cognitive dysfunction in multiple sclerosis. *Lancet Neurol* 14: 302-317

Rocca MA, Barkhof F, De Luca J, Frisén J, Geurts JJG, Hulst HE, Sastre-Garriga J, Filippi M (2018) The hippocampus in multiple sclerosis. *Lancet Neurol* 17: 918-926

Rocca MA, Battaglini M, Benedict RH, De Stefano N, Geurts JJ, Henry RG, Horsfield MA, Jenkinson M, Pagani E, Filippi M (2017) Brain MRI atrophy quantification in MS: From methods to clinical application. *Neurology* 88: 403-413

Rocca MA, De Meo E, Amato MP, Copetti M, Moiola L, Ghezzi A, Veggiotti P, Capra R, Fiorino A, Pippolo L *et al* (2015b) Cognitive impairment in paediatric multiple sclerosis patients is not related to cortical lesions. *Mult Scler* 21: 956-959

Rocca MA, De Meo E, Filippi M (2016a) Functional MRI in investigating cognitive impairment in multiple sclerosis. *Acta Neurol Scand* 134 Suppl 200: 39-46

Rocca MA, Filippi M (2006) Functional MRI to study brain plasticity in clinical neurology. *Neurol Sci* 27 Suppl 1: S24-26

Rocca MA, Filippi M (2007) Functional MRI in multiple sclerosis. *Journal of neuroimaging : official journal of the American Society of Neuroimaging* 17 Suppl 1: 36S-41S

Rocca MA, Morelli ME, Amato MP, Moiola L, Ghezzi A, Veggiotti P, Capra R, Pagani E, Portaccio E, Fiorino A *et al* (2016b) Regional hippocampal involvement and cognitive impairment in pediatric multiple sclerosis. *Mult Scler* 22: 628-640

Rocca MA, Sonkin M, Copetti M, Pagani E, Arnold DL, Narayanan S, Sled JG, Banwell B, Filippi M (2016c) Diffusion tensor magnetic resonance imaging in very early onset pediatric multiple sclerosis. *Mult Scler* 22: 620-627

Rocca MA, Valsasina P, Absinta M, Moiola L, Ghezzi A, Veggiotti P, Amato MP, Horsfield MA, Falini A, Comi G *et al* (2014b) Intranetwork and internetwork functional connectivity abnormalities in pediatric multiple sclerosis. *Human brain mapping* 35: 4180-4192

Rocca MA, Valsasina P, Hulst HE, Abdel-Aziz K, Enzinger C, Gallo A, Pareto D, Riccitelli G, Muhlert N, Ciccarelli O *et al* (2014c) Functional correlates of cognitive dysfunction in multiple sclerosis: A multicenter fMRI Study. *Hum Brain Mapp* 35: 5799-5814

Roosendaal SD, Schoonheim MM, Hulst HE, Sanz-Arigita EJ, Smith SM, Geurts JJ, Barkhof F (2010) Resting state networks change in clinically isolated syndrome. *Brain* 133: 1612-1621

Ross B, Bluml S (2001) Magnetic resonance spectroscopy of the human brain. *The Anatomical Record* 265: 54-84

Rothman A, Murphy OC, Fitzgerald KC, Button J, Gordon-Lipkin E, Ratchford JN, Newsome SD, Mowry EM, Sotirchos ES, Syc-Mazurek SB *et al* (2019) Retinal measurements predict 10-year disability in multiple sclerosis. *Ann Clin Transl Neurol* 6: 222-232

Rotstein DL, Healy BC, Malik MT, Chitnis T, Weiner HL (2015) Evaluation of no evidence of disease activity in a 7-year longitudinal multiple sclerosis cohort. *JAMA Neurol* 72: 152-158

Rubia K, Hyde Z, Halari R, Giampietro V, Smith A (2010) Effects of age and sex on developmental neural networks of visual-spatial attention allocation. *NeuroImage* 51: 817-827

Ruet A, Arrambide G, Brochet B, Auger C, Simon E, Rovira A, Montalban X, Tintore M (2014) Early predictors of multiple sclerosis after a typical clinically isolated syndrome. *Mult Scler* 20: 1721-1726

Ruggieri M, Iannetti P, Polizzi A, Pavone L, Grimaldi LM (2004) Multiple sclerosis in children under 10 years of age. *Neurol Sci* 25 Suppl 4: S326-335

Ruggieri M, Polizzi A, Pavone L, Grimaldi LM (1999) Multiple sclerosis in children under 6 years of age. *Neurology* 53: 478-484

Saidha S, Al-Louzi O, Ratchford JN, Bhargava P, Oh J, Newsome SD, Prince JL, Pham D, Roy S, van Zijl P *et al* (2015) Optical coherence tomography reflects brain atrophy in multiple sclerosis: A four-year study. *Ann Neurol* 78: 801-813

Sairanen M, Lucas G, Ernfors P, Castrén M, Castrén E (2005) Brain-derived neurotrophic factor and antidepressant drugs have different but coordinated effects on neuronal turnover, proliferation, and survival in the adult dentate gyrus. *J Neurosci* 25: 1089-1094

Samann PG, Iglesias JE, Gutman B, Grotegerd D, Leenings R, Flint C, Dannlowski U, Clarke-Rubright EK, Morey RA, van Erp TGM *et al* (2020) FreeSurfer-based

segmentation of hippocampal subfields: A review of methods and applications, with a novel quality control procedure for ENIGMA studies and other collaborative efforts. *Hum Brain Mapp*

Sarchielli P, Greco L, Stipa A, Floridi A, Gallai V (2002) Brain-derived neurotrophic factor in patients with multiple sclerosis. *J Neuroimmunol* 132: 180-188

Sarter M, Givens B, Bruno JP (2001) The cognitive neuroscience of sustained attention: where top-down meets bottom-up. *Brain research Brain research reviews* 35: 146-160

Scharfman H, Goodman J, Macleod A, Phani S, Antonelli C, Croll S (2005) Increased neurogenesis and the ectopic granule cells after intrahippocampal BDNF infusion in adult rats. *Exp Neurol* 192: 348-356

Schmidt HD, Duman RS (2010) Peripheral BDNF produces antidepressant-like effects in cellular and behavioral models. *Neuropsychopharmacology* 35: 2378-2391

Schoonheim MM, Hulst HE, Brandt RB, Strik M, Wink AM, Uitdehaag BM, Barkhof F, Geurts JJ (2015) Thalamus structure and function determine severity of cognitive impairment in multiple sclerosis. *Neurology* 84: 776-783

Schumacher GA, Beebe G, Kibler RF, Kurland LT, Kurtzke JF, McDowell F, Nagler B, Sibley WA, Tourtellotte WW, Willmon TL (1965) PROBLEMS OF EXPERIMENTAL TRIALS OF THERAPY IN MULTIPLE SCLEROSIS: REPORT BY THE PANEL ON THE EVALUATION OF EXPERIMENTAL TRIALS OF THERAPY IN MULTIPLE SCLEROSIS. *Annals of the New York Academy of Sciences* 122: 552-568

Schwartz CE, Grover SA, Powell VE, Noguera A, Mah JK, Mar S, Mednick L, Banwell BL, Alper G, Rensel M (2018) Risk factors for non-adherence to disease-modifying therapy in pediatric multiple sclerosis. *Multiple Sclerosis Journal* 24: 175-185

Schwarz A, Balint B, Korporal-Kuhnke M, Jarius S, von Engelhardt K, Furwentsches A, Bussmann C, Ebinger F, Wildemann B, Haas J (2017) B-cell populations discriminate between pediatric- and adult-onset multiple sclerosis. *Neurol Neuroimmunol Neuroinflamm* 4: e309

Scrucca L, Fop M, Murphy TB, Raftery AE (2016) mclust 5: Clustering, Classification and Density Estimation Using Gaussian Finite Mixture Models. *R J* 8: 289-317

Seeley WW, Menon V, Schatzberg AF, Keller J, Glover GH, Kenna H, Reiss AL, Greicius MD (2007) Dissociable intrinsic connectivity networks for salience processing and executive control. *J Neurosci* 27: 2349-2356

Segalowitz SJ, Santesso DL, Jetha MK (2010) Electrophysiological changes during adolescence: a review. *Brain Cogn* 72: 86-100

Sepulcre J, Masdeu JC, Goñi J, Arrondo G, Vélez de Mendizábal N, Bejarano B, Villoslada P (2009) Fatigue in multiple sclerosis is associated with the disruption of frontal and parietal pathways. *Mult Scler* 15: 337-344

Sepulcre J, Vanotti S, Hernandez R, Sandoval G, Caceres F, Garcea O, Villoslada P (2006) Cognitive impairment in patients with multiple sclerosis using the Brief Repeatable Battery-Neuropsychology test. *Multiple sclerosis* 12: 187-195

Shahar E, Andraus J, Savitzki D, Pilar G, Zelnik N (2002) Outcome of Severe Encephalomyelitis in Children: Effect of High-Dose Methylprednisolone and Immunoglobulins. *Journal of Child Neurology* 17: 810-814

Sheldon S, Moscovitch M (2012) The nature and time-course of medial temporal lobe contributions to semantic retrieval: an fMRI study on verbal fluency. *Hippocampus* 22: 1451-1466

Shirayama Y, Chen AC, Nakagawa S, Russell DS, Duman RS (2002) Brain-derived neurotrophic factor produces antidepressant effects in behavioral models of depression. *J Neurosci* 22: 3251-3261

Sicotte NL, Kern KC, Giesser BS, Arshanapalli A, Schultz A, Montag M, Wang H, Bookheimer SY (2008) Regional hippocampal atrophy in multiple sclerosis. *Brain* 131: 1134-1141

Simmonds DJ, Hallquist MN, Asato M, Luna B (2014) Developmental stages and sex differences of white matter and behavioral development through adolescence: a longitudinal diffusion tensor imaging (DTI) study. *Neuroimage* 92: 356-368

Simone IL (2002) Course and prognosis in early-onset MS: comparison with adult-onset forms. *Neurology* 59: 1922-1928

Simone IL, Carrara D, Tortorella C, Liguori M, Lepore V, Pellegrini F, Bellacosa A, Ceccarelli A, Pavone I, Livrea P (2002) Course and prognosis in early-onset MS: Comparison with adult-onset forms. *Neurology* 59: 1922-1928

Smith AB, Halari R, Giampetro V, Brammer M, Rubia K (2011) Developmental effects of reward on sustained attention networks. *NeuroImage* 56: 1693-1704

Smith SM, Jenkinson M, Johansen-Berg H, Rueckert D, Nichols TE, Mackay CE, Watkins KE, Ciccarelli O, Cader MZ, Matthews PM *et al* (2006) Tract-based spatial statistics: voxelwise analysis of multi-subject diffusion data. *Neuroimage* 31: 1487-1505

Soelberg Sorensen P, Haas J, Sellebjerg F, Olsson T, Ravnborg M, Group tTS (2004) IV immunoglobulins as add-on treatment to methylprednisolone for acute relapses in MS. *Neurology* 63: 2028-2033

Sombekke MH, Wattjes MP, Balk LJ, Nielsen JM, Vrenken H, Uitdehaag BM, Polman CH, Barkhof F (2013) Spinal cord lesions in patients with clinically isolated syndrome: a powerful tool in diagnosis and prognosis. *Neurology* 80: 69-75

Soun JE, Liu MZ, Cauley KA, Grinband J (2017) Evaluation of neonatal brain myelination using the T1- and T2-weighted MRI ratio. *J Magn Reson Imaging* 46: 690-696

Sowell ER, Thompson PM, Leonard CM, Welcome SE, Kan E, Toga AW (2004) Longitudinal mapping of cortical thickness and brain growth in normal children. *J Neurosci* 24: 8223-8231

Sowell ER, Thompson PM, Tessner KD, Toga AW (2001) Mapping continued brain growth and gray matter density reduction in dorsal frontal cortex: Inverse relationships during postadolescent brain maturation. *J Neurosci* 21: 8819-8829

Spalice A, Properzi E, Lo Faro V, Acampora B, Iannetti P (2004) Intravenous Immunoglobulin and Interferon: Successful Treatment of Optic Neuritis in Pediatric Multiple Sclerosis. *Journal of Child Neurology* 19: 623-626

Sperling RA, Guttmann CR, Hohol MJ, Warfield SK, Jakab M, Parente M, Diamond EL, Daffner KR, Olek MJ, Orav EJ *et al* (2001) Regional magnetic resonance imaging lesion burden and cognitive function in multiple sclerosis: a longitudinal study. *Arch Neurol* 58: 115-121

Spiers HJ, Burgess N, Maguire EA, Baxendale SA, Hartley T, Thompson PJ, O'Keefe J (2001) Unilateral temporal lobectomy patients show lateralized topographical and episodic memory deficits in a virtual town. *Brain* 124: 2476-2489

Spurk D, Hirschi A, Wang M, Valero D, Kauffeld S (2020) Latent profile analysis: A review and "how to" guide of its application within vocational behavior research. *Journal of Vocational Behavior* 120: 103445

Stadelmann C, Kerschensteiner M, Misgeld T, Brück W, Hohlfeld R, Lassmann H (2002) BDNF and gp145trkB in multiple sclerosis brain lesions: neuroprotective interactions between immune and neuronal cells? *Brain* 125: 75-85

Stankiewicz J, Panter SS, Neema M, Arora A, Batt CE, Bakshi R (2007) Iron in chronic brain disorders: imaging and neurotherapeutic implications. *Neurotherapeutics : the journal of the American Society for Experimental NeuroTherapeutics* 4: 371-386

Steenwijk MD, Geurts JJ, Daams M, Tijms BM, Wink AM, Balk LJ, Tewarie PK, Uitdehaag BM, Barkhof F, Vrenken H *et al* (2016) Cortical atrophy patterns in multiple sclerosis are non-random and clinically relevant. *Brain* 139: 115-126

Steinman L (2014) Immunology of relapse and remission in multiple sclerosis. *Annu Rev Immunol* 32: 257-281

Stiles J, Jernigan TL (2010) The basics of brain development. *Neuropsychol Rev* 20: 327-348

Straussberg R, Schonfeld T, Weitz R, Karmazyn B, Harel L (2001) Improvement of atypical acute disseminated encephalomyelitis with steroids and intravenous immunoglobulins. *Pediatric Neurology* 24: 139-143

Strazzer S, Rocca MA, Molteni E, De Meo E, Recla M, Valsasina P, Arrigoni F, Galbiati S, Bardoni A, Filippi M (2015) Altered Recruitment of the Attention Network Is Associated with Disability and Cognitive Impairment in Pediatric Patients with Acquired Brain Injury. *Neural plasticity* 2015: 104282

Stroop JR (1935) Studies of interference in serial verbal reactions. *Journal of experimental psychology* 18: 643

Sumowski JF, Chiaravalloti N, Erlanger D, Kaushik T, Benedict RH, DeLuca J (2011) L-amphetamine improves memory in MS patients with objective memory impairment. *Mult Scler* 17: 1141-1145

Sumowski JF, Leavitt VM (2013) Cognitive reserve in multiple sclerosis. *Multiple Sclerosis Journal* 19: 1122-1127

Supekar K, Uddin LQ, Prater K, Amin H, Greicius MD, Menon V (2010) Development of functional and structural connectivity within the default mode network in young children. *Neuroimage* 52: 290-301

Suzuki WA, Amaral DG (1994) Perirhinal and parahippocampal cortices of the macaque monkey: cortical afferents. *J Comp Neurol* 350: 497-533

Swanton JK, Fernando KT, Dalton CM, Miszkiel KA, Altmann DR, Plant GT, Thompson AJ, Miller DH (2009) Early MRI in optic neuritis: the risk for disability. *Neurology* 72: 542-550

Tana MG, Montin E, Cerutti S, Bianchi AM (2010) Exploring cortical attentional system by using fMRI during a Continuous Perfomance Test. *Computational intelligence and neuroscience*: 329213

Tedeschi G, Dinacci D, Lavorgna L, Prinster A, Savettieri G, Quattrone A, Livrea P, Messina C, Reggio A, Servillo G *et al* (2007) Correlation between fatigue and brain atrophy and lesion load in multiple sclerosis patients independent of disability. *J Neurol Sci* 263: 15-19

Tenembaum SN, Banwell B, Pohl D, Krupp LB, Boyko A, Meinel M, Lehr L, Rocak S, Cantogno EV, Moraga MS *et al* (2013) Subcutaneous interferon Beta-1a in pediatric multiple sclerosis: a retrospective study. *J Child Neurol* 28: 849-856

Tenembaum SN, Segura MJ (2006) Interferon beta-1a treatment in childhood and juvenile-onset multiple sclerosis. *Neurology* 67: 511-513

Thannhauser JE, Mah JK, Metz LM (2009) Adherence of adolescents to multiple sclerosis disease-modifying therapy. *Pediatr Neurol* 41: 119-123

Thompson AJ, Banwell BL, Barkhof F, Carroll WM, Coetzee T, Comi G, Correale J, Fazekas F, Filippi M, Freedman MS *et al* (2018) Diagnosis of multiple sclerosis: 2017 revisions of the McDonald criteria. *Lancet Neurol* 17: 162-173

Tiemeier H, Lenroot RK, Greenstein DK, Tran L, Pierson R, Giedd JN (2010) Cerebellum development during childhood and adolescence: a longitudinal morphometric MRI study. *Neuroimage* 49: 63-70

Till C, Deotto A, Tipu V, Sled JG, Bethune A, Narayanan S, Arnold DL, Banwell BL (2011a) White matter integrity and math performance in pediatric multiple sclerosis: a diffusion tensor imaging study. *Neuroreport* 22: 1005-1009

Till C, Ghassemi R, Aubert-Broche B, Kerbrat A, Collins DL, Narayanan S, Arnold DL, Desrocher M, Sled JG, Banwell BL (2011b) MRI Correlates of Cognitive Impairment in Childhood-Onset Multiple Sclerosis. *Neuropsychology* 25: 319-332

Till C, Racine N, Araujo D, Narayanan S, Collins DL, Aubert-Broche B, Arnold DL, Banwell B (2013) Changes in cognitive performance over a 1-year period in children and adolescents with multiple sclerosis. *Neuropsychology* 27: 210-219

Tintoré M, Arrambide G (2009) Early onset multiple sclerosis: The role of gender. *Journal of the Neurological Sciences* 286: 31-34

Tintore M, Rovira A, Arrambide G, Mitjana R, Río J, Auger C, Nos C, Edo MC, Castilló J, Horga A *et al* (2010) Brainstem lesions in clinically isolated syndromes. *Neurology* 75: 1933-1938

Tintoré M, Rovira A, Rio J, Nos C, Grivé E, Téllez N, Pelayo R, Comabella M, Montalban X (2005) Is optic neuritis more benign than other first attacks in multiple sclerosis? *Ann Neurol* 57: 210-215

Tintore M, Rovira À, Río J, Otero-Romero S, Arrambide G, Tur C, Comabella M, Nos C, Arévalo MJ, Negrotto L *et al* (2015) Defining high, medium and low impact prognostic factors for developing multiple sclerosis. *Brain : a journal of neurology* 138: 1863-1874

Toda T, Parylak SL, Linker SB, Gage FH (2019) The role of adult hippocampal neurogenesis in brain health and disease. *Molecular Psychiatry* 24: 67-87

Tomassini V, Matthews PM, Thompson AJ, Fuglo D, Geurts JJ, Johansen-Berg H, Jones DK, Rocca MA, Wise RG, Barkhof F *et al* (2012) Neuroplasticity and functional recovery in multiple sclerosis. *Nature reviews Neurology* 8: 635-646

Tortorella P, Rocca MA, Mezzapesa DM, Ghezzi A, Lamantia L, Comi G, Filippi M (2006) MRI quantification of gray and white matter damage in patients with early-onset multiple sclerosis. *J Neurol* 253: 903-907

Tovar-Moll F, Evangelou IE, Chiu AW, Richert ND, Ostuni JL, Ohayon JM, Auh S, Ehrmantraut M, Talagala SL, McFarland HF *et al* (2009) Thalamic involvement and its impact on clinical disability in patients with multiple sclerosis: a diffusion tensor imaging study at 3T. *AJNR Am J Neuroradiol* 30: 1380-1386

Trapp BD, Peterson J, Ransohoff RM, Rudick R, Mork S, Bo L (1998) Axonal transection in the lesions of multiple sclerosis. *N Engl J Med* 338: 278-285

Travis F (1998) Cortical and cognitive development in 4th, 8th and 12th grade students. The contribution of speed of processing and executive functioning to cognitive development. *Biol Psychol* 48: 37-56

Tremlett H, Fadrosh DW, Faruqi AA, Zhu F, Hart J, Roalstad S, Graves J, Lynch S, Waubant E, Centers USNoPM (2016) Gut microbiota in early pediatric multiple sclerosis: a case-control study. *Eur J Neurol* 23: 1308-1321

Tremlett H, Waubant E (2018a) Gut microbiome and pediatric multiple sclerosis. *Mult Scler* 24: 64-68

Tremlett H, Waubant E (2018b) The Gut Microbiota and Pediatric Multiple Sclerosis: Recent Findings. *Neurotherapeutics : the journal of the American Society for Experimental NeuroTherapeutics* 15: 102-108

Tremlett H, Yousefi M, Devonshire V, Rieckmann P, Zhao Y (2009) Impact of multiple sclerosis relapses on progression diminishes with time. *Neurology* 73: 1616

Trojano M, Bergamaschi R, Amato MP, Comi G, Ghezzi A, Lepore V, Marrosu MG, Mosconi P, Patti F, Ponzio M *et al* (2019) The Italian multiple sclerosis register. *Neurol Sci* 40: 155-165

Tustison NJ, Avants BB, Cook PA, Zheng Y, Egan A, Yushkevich PA, Gee JC (2010) N4ITK: improved N3 bias correction. *IEEE Trans Med Imaging* 29: 1310-1320

Tzourio-Mazoyer N, Landeau B, Papathanassiou D, Crivello F, Etard O, Delcroix N, Mazoyer B, Joliot M (2002) Automated anatomical labeling of activations in SPM using a macroscopic anatomical parcellation of the MNI MRI single-subject brain. *NeuroImage* 15: 273-289

Valle M, Martos R, Gascon F, Canete R, Zafra MA, Morales R (2005) Low-grade systemic inflammation, hypoadiponectinemia and a high concentration of leptin are present in very young obese children, and correlate with metabolic syndrome. *Diabetes Metab* 31: 55-62

Vallejo-Illarramendi A, Domercq M, Pérez-Cerdá F, Ravid R, Matute C (2006) Increased expression and function of glutamate transporters in multiple sclerosis. *Neurobiol Dis* 21: 154-164

van Geest Q, Hulst HE, Meijer KA, Hoyng L, Geurts JJG, Douw L (2018) The importance of hippocampal dynamic connectivity in explaining memory function in multiple sclerosis. *Brain Behav* 8: e00954

Vargas-Lowy D, Kivisakk P, Gandhi R, Raddassi K, Soltany P, Gorman MP, Khoury SJ, Chitnis T (2013) Increased Th17 response to myelin peptides in pediatric MS. *Clin Immunol* 146: 176-184

Venkateswaran S, Banwell B (2010) Pediatric multiple sclerosis. *Neurologist* 16: 92-105

Vercellino M, Masera S, Lorenzatti M, Condello C, Merola A, Mattioda A, Tribolo A, Capello E, Mancardi GL, Mutani R *et al* (2009) Demyelination, inflammation, and neurodegeneration in multiple sclerosis deep gray matter. *Journal of neuropathology and experimental neurology* 68: 489-502

Verhey LH, Branson HM, Shroff MM, Callen DJA, Sled JG, Narayanan S, Sadovnick AD, Bar-Or A, Arnold DL, Marrie RA *et al* (2011) MRI parameters for prediction of multiple sclerosis diagnosis in children with acute CNS demyelination: A prospective national cohort study. *The Lancet Neurology* 10: 1065-1073

Verhey LH, Signori A, Arnold DL, Bar-Or A, Sadovnick AD, Marrie RA, Banwell B, Sormani MP (2013) Clinical and MRI activity as determinants of sample size for pediatric multiple sclerosis trials. *Neurology* 81: 1215-1221

Verhey LH, Sled JG (2013) Advanced Magnetic Resonance Imaging in Pediatric Multiple Sclerosis. *Neuroimaging Clinics of North America* 23: 337-354

Vermersch P, Czlonkowska A, Grimaldi LM, Confavreux C, Comi G, Kappos L, Olsson TP, Benamor M, Bauer D, Truffinet P *et al* (2014) Teriflunomide versus subcutaneous interferon beta-1a in patients with relapsing multiple sclerosis: a randomised, controlled phase 3 trial. *Mult Scler* 20: 705-716

Vidaurre OG, Haines JD, Katz Sand I, Adula KP, Huynh JL, McGraw CA, Zhang F, Varghese M, Sotirchos E, Bhargava P *et al* (2014) Cerebrospinal fluid ceramides from patients with multiple sclerosis impair neuronal bioenergetics. *Brain* 137: 2271-2286

Vishwas MS, Chitnis T, Pienaar R, Healy BC, Grant PE (2010) Tract-based analysis of callosal, projection, and association pathways in pediatric patients with multiple sclerosis: a preliminary study. *AJNR American journal of neuroradiology* 31: 121-128

Waldman A, Ghezzi A, Bar-Or A, Mikaeloff Y, Tardieu M, Banwell B (2014) Multiple sclerosis in children: an update on clinical diagnosis, therapeutic strategies, and research. *Lancet Neurol* 13: 936-948

Waldman A, Ness J, Pohl D, Simone IL, Anlar B, Amato MP, Ghezzi A (2016) Pediatric multiple sclerosis: Clinical features and outcome. *Neurology* 87: S74-81

Waldman AT, Hiremath G, Avery RA, Conger A, Pineles SL, Loguidice MJ, Talman LS, Galetta KM, Shumski MJ, Wilson J *et al* (2013) Monocular and binocular low-contrast visual acuity and optical coherence tomography in pediatric multiple sclerosis. *Mult Scler Relat Disord* 3: 326-334

Wallin MT, Culpepper WJ, Nichols E, Bhutta ZA, Gebrehiwot TT, Hay SI, Khalil IA, Krohn KJ, Liang X, Naghavi M (2019) Global, regional, and national burden of multiple sclerosis 1990–2016: a systematic analysis for the Global Burden of Disease Study 2016. *The Lancet Neurology* 18: 269-285

Wang X, Pal R, Chen XW, Limpeanchob N, Kumar KN, Michaelis EK (2005) High intrinsic oxidative stress may underlie selective vulnerability of the hippocampal CA1 region. *Brain Res Mol Brain Res* 140: 120-126

Waters P, Fadda G, Woodhall M, O'Mahony J, Brown RA, Castro DA, Longoni G, Irani SR, Sun B, Yeh EA *et al* (2020) Serial Anti–Myelin Oligodendrocyte Glycoprotein Antibody Analyses and Outcomes in Children With Demyelinating Syndromes. *JAMA Neurology* 77: 82-93

Waubant E, Chabas D, Okuda DT, Glenn O, Mowry E, Henry RG, Strober JB, Soares B, Wintermark M, Pelletier D (2009) Difference in disease burden and activity in pediatric

patients on brain magnetic resonance imaging at time of multiple sclerosis onset vs adults. *Arch Neurol* 66: 967-971

Waubant E, Hietpas J, Stewart T, Dyme Z, Herbert J, Lacy J, Miller C, Rensel M, Schwid S, Goodkin D (2001) Interferon beta-1a in children with multiple sclerosis is well tolerated. *Neuropediatrics* 32: 211-213

Waubant E, Mowry EM, Krupp L, Chitnis T, Yeh EA, Kuntz N, Ness J, Chabas D, Strober J, McDonald J *et al* (2011) Common viruses associated with lower pediatric multiple sclerosis risk. *Neurology* 76: 1989-1995

Waubant E, Ponsonby A-L, Pugliatti M, Hanwell H, Mowry EM, Hintzen RQ (2016) Environmental and genetic factors in pediatric inflammatory demyelinating diseases. *Neurology* 87: S20

Waxman SG (1998) Demyelinating diseases--new pathological insights, new therapeutic targets. *N Engl J Med* 338: 323-325

Wechsler D (1974) WISC-R Manual for the Wechsler Intelligence Scale for Children-Revised. *New York, The Psychological Corporation*

Weier K, Fonov V, Aubert-Broche B, Arnold DL, Banwell B, Collins DL (2016) Impaired growth of the cerebellum in pediatric-onset acquired CNS demyelinating disease. *Mult Scler* 22: 1266-1278

Weier K, Till C, Fonov V, Yeh EA, Arnold DL, Banwell B, Collins DL (2015) Contribution of the cerebellum to cognitive performance in children and adolescents with multiple sclerosis. *Multiple Sclerosis Journal* 22: 599-607

Weiner HL, Mackin GA, Orav EJ, Hafler DA, Dawson DM, LaPierre Y, Herndon R, Lehrich JR, Hauser SL, Turel A *et al* (1993) Intermittent cyclophosphamide pulse therapy in progressive multiple sclerosis: Final report of the Northeast Cooperative Multiple Sclerosis Treatment Group. *Neurology* 43: 910

Weinstock-Guttman B, Eckert S, Benedict RH (2018) A decline in cognitive function should lead to a change in disease-modifying therapy - Yes. *Mult Scler* 24: 1681-1682

Weisbrot DM, Ettinger AB, Gadow KD, Belman AL, MacAllister WS, Milazzo M, Reed ML, Serrano D, Krupp LB (2010) Psychiatric comorbidity in pediatric patients with demyelinating disorders. *Journal of Child Neurology* 25: 192-202

Weygandt M, Hummel HM, Schregel K, Ritter K, Allefeld C, Dommes E, Huppke P, Haynes JD, Wuerfel J, Gärtner J (2015) MRI-based diagnostic biomarkers for early onset pediatric multiple sclerosis. *Neuroimage Clin* 7: 400-408

Whiteside DM, Kealey T, Semla M, Luu H, Rice L, Basso MR, Roper B (2016) Verbal Fluency: Language or Executive Function Measure? *Appl Neuropsychol Adult* 23: 29-34

Wierenga LM, Langen M, Oranje B, Durston S (2014) Unique developmental trajectories of cortical thickness and surface area. *Neuroimage* 87: 120-126

Wilbur C, Reginald YA, Longoni G, Grover SA, Wong AM, Mabbott DJ, Arnold DL, Marrie RA, Bar-Or A, Banwell B *et al* (2019) Early neuroaxonal injury is seen in the acute phase of pediatric optic neuritis. *Mult Scler Relat Disord* 36: 101387

Wilejto M, Shroff M, Buncic JR, Kennedy J, Goia C, Banwell B (2006) The clinical features, MRI findings, and outcome of optic neuritis in children. *Neurology* 67: 258-262

Wilke M, Sohn JH, Byars AW, Holland SK (2003) Bright spots: correlations of gray matter volume with IQ in a normal pediatric population. *Neuroimage* 20: 202-215

Wolbers T, Dudchenko P, Wood E (2014) Spatial memory—a unique window into healthy and pathological aging. *Frontiers in Aging Neuroscience* 6: 35

Wong YYM, Bruijstens AL, Barro C, Michalak Z, Melief MJ, Wierenga AF, van Pelt ED, Neuteboom RF, Kuhle J, Hintzen RQ (2019) Serum neurofilament light chain in pediatric MS and other acquired demyelinating syndromes. *Neurology* 93: e968-e974

Wong YYM, de Mol CL, van der Vuurst de Vries RM, van Pelt ED, Ketelslegers IA, Catsman-Berrevoets CE, Neuteboom RF, Hintzen RQ (2018) Real-world validation of the 2017 McDonald criteria for pediatric MS. *Neurology(R) neuroimmunology & neuroinflammation* 6: e528-e528

Woo SE, Jebb AT, Tay L, Parrigon S (2018) Putting the “Person” in the Center: Review and Synthesis of Person-Centered Approaches and Methods in Organizational Science. *Organizational Research Methods* 21: 814-845

Wuerfel E, Weddige A, Hagmayer Y, Jacob R, Wedekind L, Stark W, Gartner J (2018) Cognitive deficits including executive functioning in relation to clinical parameters in paediatric MS patients. *PloS one* 13: e0194873

Yan K, Balijepalli C, Desai K, Gullapalli L, Druyts E (2020) Epidemiology of pediatric multiple sclerosis: A systematic literature review and meta-analysis. *Multiple Sclerosis and Related Disorders* 44: 102260

Yeh EA, Chitnis T, Krupp L, Ness J, Chabas D, Kuntz N, Waubant E, Excellence USNoPMSCo (2009a) Pediatric multiple sclerosis. *Nature reviews Neurology* 5: 621-631

Yeh EA, Waubant E, Krupp LB, Ness J, Chitnis T, Kuntz N, Ramanathan M, Belman A, Chabas D, Gorman MP *et al* (2011) Multiple sclerosis therapies in pediatric patients with refractory multiple sclerosis. *Archives of Neurology* 68: 437-444

Yeh EA, Weinstock-Guttman B, Lincoff N, Reynolds J, Weinstock A, Madurai N, Agarwal N, Buch P, Karpinski M, Ramanathan M (2009b) Retinal nerve fiber thickness in inflammatory demyelinating diseases of childhood onset. *Mult Scler* 15: 802-810

Yeh EA, Weinstock-Guttman B, Ramanathan M, Ramasamy DP, Willis L, Cox JL, Zivadinov R (2009c) Magnetic resonance imaging characteristics of children and adults with paediatric-onset multiple sclerosis. *Brain* 132: 3392-3400

Yeo SS, Jang SH, Son SM (2014) The different maturation of the corticospinal tract and corticoreticular pathway in normal brain development: diffusion tensor imaging study. *Frontiers in Human Neuroscience* 8: 573

Young B, Waubant E, Lulu S, Graves J (2019) Puberty onset and pediatric multiple sclerosis activity in boys. *Multiple Sclerosis and Related Disorders* 27: 184-187

Zecca C, Disanto G, Sormani MP, Riccitelli GC, Cianfoni A, Del Grande F, Pravatà E, Gobbi C (2016) Relevance of asymptomatic spinal MRI lesions in patients with multiple sclerosis. *Mult Scler* 22: 782-791

Zeidman P, Mullally SL, Maguire EA (2015) Constructing, perceiving, and maintaining scenes: hippocampal activity and connectivity. *Cerebral Cortex* 25: 3836-3855

Ziegler G, Ridgway GR, Blakemore SJ, Ashburner J, Penny W (2017) Multivariate dynamical modelling of structural change during development. *Neuroimage* 147: 746-762

Zimmermann HG, Knier B, Oberwahrenbrock T, Behrens J, Pfuhl C, Aly L, Kaminski M, Hoshi M-M, Specovius S, Giess RM *et al* (2018) Association of Retinal Ganglion Cell Layer Thickness With Future Disease Activity in Patients With Clinically Isolated Syndrome. *JAMA neurology* 75: 1071-1079

Zipoli V, Goretti B, Hakiki B, Siracusa G, Sorbi S, Portaccio E, Amato MP (2010) Cognitive impairment predicts conversion to multiple sclerosis in clinically isolated syndromes. *Mult Scler* 16: 62-67

Zivadinov R, Bergsland N, Dolezal O, Hussein S, Seidl Z, Dwyer MG, Vaneckova M, Krasensky J, Potts JA, Kalincik T *et al* (2013) Evolution of cortical and thalamus atrophy and disability progression in early relapsing-remitting MS during 5 years. *AJNR Am J Neuroradiol* 34: 1931-1939

Zivadinov R, Weinstock-Guttman B, Benedict R, Tamaño-Blanco M, Hussein S, Abdelrahman N, Durfee J, Ramanathan M (2007) Preservation of gray matter volume in multiple sclerosis patients with the Met allele of the rs6265 (Val66Met) SNP of brain-derived neurotrophic factor. *Human Molecular Genetics* 16: 2659-2668